UNIVERSIDADE FEDERAL DO PARANÁ

LUCAS PIOLI REHBEIN KÜRTEN IHLENFELD

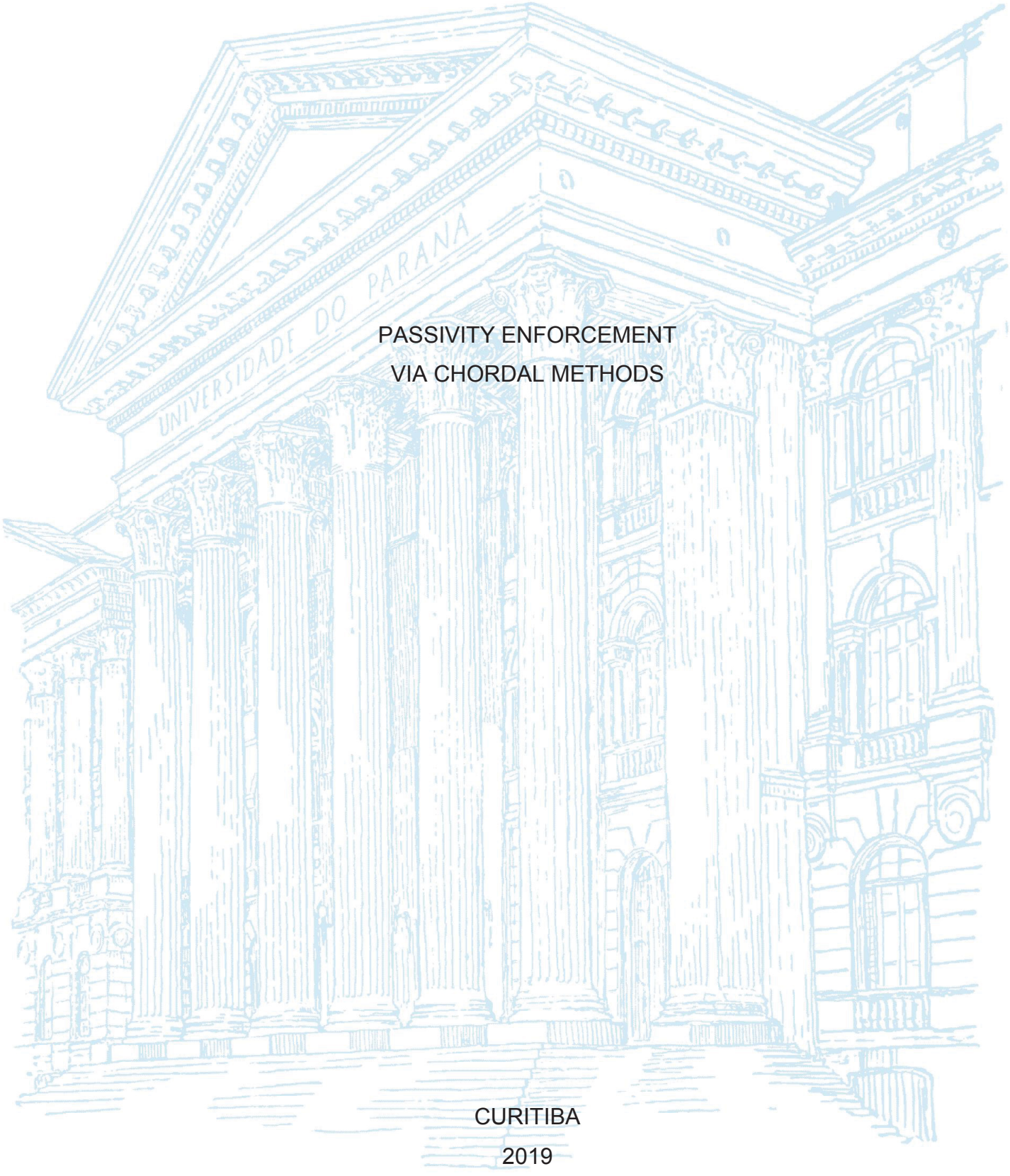

PASSIVITY ENFORCEMENT VIA CHORDAL METHODS

CURITIBA

2019

LUCAS PIOLI REHBEIN KÜRTEN IHLENFELD

PASSIVITY ENFORCEMENT VIA CHORDAL METHODS

Tese apresentada ao curso de Pós-Graduação em Engenharia Elétrica, Setor de Tecnologia, Universidade Federal do Paraná, como requisito parcial à obtenção do título de Doutor em Engenharia Elétrica.

Orientador: Prof. Dr. Gustavo Henrique da Costa Oliveira

CURITIBA

2019

Catalogação na Fonte: Sistema de Bibliotecas, UFPR
Biblioteca de Ciência e Tecnologia

I25p Ihlenfeld, Lucas Pioli Rehbein Kurten
Passivity enforcement via chordal methods [recurso eletrônico] / Lucas Pioli Rehbein Kurten Ihlenfeld– Curitiba, 2019.

Tese - Universidade Federal do Paraná, Setor de Tecnologia, Programa de Pós-graduação em Engenharia Elétrica.
Orientador: Prof. Dr. Gustavo Henrique da Costa Oliveira

1. Transformadores. 2. Álgebra linear. 3. Algoritmos. I. Universidade Federal do Paraná. II. Oliveira, Gustavo Henrique da Costa. III. Título.

CDD: 621.314

Bibliotecária: Roseny Rivelini Morciani CRB-9/1585

MINISTÉRIO DA EDUCAÇÃO
SETOR DE TECNOLOGIA
UNIVERSIDADE FEDERAL DO PARANÁ
PRÓ-REITORIA DE PESQUISA E PÓS-GRADUAÇÃO
PROGRAMA DE PÓS-GRADUAÇÃO ENGENHARIA ELÉTRICA - 40001016043P4

TERMO DE APROVAÇÃO

Os membros da Banca Examinadora designada pelo Colegiado do Programa de Pós-Graduação em ENGENHARIA ELÉTRICA da Universidade Federal do Paraná foram convocados para realizar a arguição da tese de Doutorado de **LUCAS PIOLI REHBEIN KURTEN IHLENFELD** intitulada: **PASSIVITY ENFORCEMENT VIA CHORDAL METHODS**, sob orientação do Prof. Dr. GUSTAVO HENRIQUE DA COSTA OLIVEIRA, que após após terem inquirido o aluno e realizado a avaliação do trabalho, são de parecer pela sua APROVAÇÃO no rito de defesa.

A outorga do título de doutor está sujeita à homologação pelo colegiado, ao atendimento de todas as indicações e correções solicitadas pela banca e ao pleno atendimento das demandas regimentais do Programa de Pós-Graduação.

CURITIBA, 27 de Agosto de 2019.

GUSTAVO HENRIQUE DA COSTA OLIVEIRA
Presidente da Banca Examinadora (UNIVERSIDADE FEDERAL DO PARANÁ)

SERGIO LUIS VARRICCHIO
Avaliador Externo (CENTRO DE PESQUISAS DE ENERGIA ELéTRICA - CEPEL)

ROMAN KUIAVA
Avaliador Interno (UNIVERSIDADE FEDERAL DO PARANÁ)

ALEXANDRE SANFELICE BAZANELLA
Avaliador Externo (UNIVERSIDADE FEDERAL DO RIO GRANDE DO SUL)

To Amanda,
fide et amore.

To Lineo Rehbein,
in memoriam.

ACKNOWLEDGMENTS

This is the end product of a grueling intellectual adventure and I'm deeply indebted to a number of people. First and foremost I would like to thank my advisor, Professor Dr. Gustavo H. C. Oliveira, for his continued advice, encouragement and mentorship. It has been a true privilege to be under his tutelage specially for having nurtured my academic freedom and fostering a learning culture that is dedicated to excellence.

I express my heartfelt gratitude to Amanda, my loving wife, for the unwavering encouragement and support during this, past and future endeavors. I doubt it I would have made it had I been alone along this journey: thank you, my love! I rejoice to share a life with you! Special thanks are also due to my family for supporting me through the earlier stages of my life. Should this thesis be anything it's a tribute to your unending love, support, and sacrifice.

I truly appreciate the valuable feedback from the Thesis Committee Members, Professor Dr. Alexandre Sanfelici Bazanella, Professor Dr. Roman Kuiava and Dr. Sergio Luis Varricchio, on how to improve and clarify this thesis document. Their comments have materially improved it and helped to remove obscurities from the text. Naturally, any such which remain are entirely my own fault, a responsibility that is mine alone.

It is also a pleasure to acknowledge the financial support provided by CAPES, the Brazilian Federal Agency for Support and Evaluation of Graduate Education, within the Ministry of Education of Brazil, for the greater part of my graduate studies. I am also very grateful to Energia Sustentável do Brasil (ESBR) through the research and technological development program, P&D ANEEL 06631-0006/2017, under the auspices of the Brazilian Electricity Regulatory Agency (ANEEL - Agência Nacional de Energia Elétrica), which provided financial support during the final stages of my graduate research. Special thanks are due to Diogo J. D. E. Santo, Gizele Silva and Yuri Ferreira at ESBR for welcoming me warmly at the Jirau Power Plant.

Was kann ich wissen?
Was darf ich hoffen?
(Immanuel Kant)
Wir müssen wissen,
wir werden wissen.
(David Hilbert)
Wir harren aufs Licht...
...so wandeln wir im Dunkeln.
(Jesaja 59)
Wissen ist unser Schicksal.
(Carl Sagan)
ignoramus et ignorabimus
(Emil du Bois-Reymond)
... die Wissenschaft immer als ein noch nicht ganz aufgelöstes Problem behandeln
und daher immer im Forschen bleiben...
(Wilhelm von Humboldt)

RESUMO

Neste documento são propostos três algoritmos inéditos associados aos problemas subsequentes de aferição e imposição da passividade, a qual é uma propriedade qualitativa, geral e fundamental na modelagem matemática de transitórios eletromagnéticos de sistemas elétricos passivos, como transformadores. Esses algoritmos baseiam-se numa combinação de teoria dos grafos e otimização convexa. O primeiro deles consiste na aferição de subsistemas passivos contidos num sistema não passivo, intuitivamente busca-se partes passivas contidas num todo não passivo. Já na etapa de imposição de passividade, o segundo algoritmo é consequência natural do primeiro: retendo apenas os parâmetros associados às partes passivas e descartando os demais, parte-se de um sistema passivo parcialmente especificado para se determinar novos parâmetros em substituição àqueles descartados de modo que o sistema como um todo seja passivo. A possibilidade de determinação dos novos parâmetros depende de uma propriedade topológica de um grafo associado às matrizes de parâmetros do modelo, tal propriedade é denominada cordalidade. O terceiro algoritmo aborda novamente a questão de imposição da passividade e também faz uso da cordalidade, não mais como condição de existência de solução, mas sim como uma forma de explorar a esparsidade das matrizes de parâmetros. O problema de imposição da passividade encerra dois desafios no seu processo de solução, a saber: (i) compensação de parâmetros resultando na degradação do modelo bem como (ii) longos tempos de solução. Os algoritmos ora propostos são uma resposta a essas questões e os resultados obtidos demonstraram-se comparáveis àqueles já existentes na literatura especializada, em alguns casos apresentando melhorias, seja em termos de aproximação ou tempo computacionais. Os algoritmos foram testados a partir de dados de medição de um Transformador de Potencial Indutivo bem como de um Transformador de Potência.

Palavras-chave: Macro-modelagem Passiva. Teoria de Sistemas. Álgebra Linear Aplicada. Análise de Transitórios. Transformadores.

ABSTRACT

Three novel algorithms are herein proposed to solve passivity assessment and enforcement problems. Passivity is a general, qualitative and fundamental property pertaining to the modeling associated with electromagnetic transients in passive power systems, such as transformers. These algorithms make combined use of Graph Theory and Convex Optimization. The first algorithm is concerned with passivity assesment. In particular, it searches for passive subsystems embedded into a larger nonpassive system and eventually specifies a partially specified passive system. Focusing on the subsequent step, algorithm two is a natural consequence of the preceeding one: retaining only the parameter set associated with passive subsystems as determined before, this partially specified passive system is used to further determine the remaining parameters so that the entire system be fully specified and passive. The existence condition for finding a fully specified system hinges on the fulfillment of a topological property of the graph associated the parameter matrices, namely chordality. The third algorithm also solves the passivity enforcement problem by making use of chordality, not as an existence condition, but rather by exploiting chordal sparsity patterns obtained with the parameter matrices. Solving passivity enforcement problems entails two persisting challenges, namely: (i) passivity compensations to parameters prompting increased model degradation as well as (ii) large computation times. The algorithms herein proposed tackle these issues and yield results comparable to those already in use, sometimes resulting in improved performance in terms of either approximation accuracy or runtime. These results herein reported entail data from actual measurements of an Inductive Voltage Transformer and a Power Transformer.

Keywords: Passive Macromodeling. System Theory. Applied Linear Algebra. Transient Analysis. Transformers.

LIST OF FIGURES

LIST OF TABLES

LIST OF ABBREVIATIONS AND ACRONYMS

I/O	Input/Output signals
RBF	Rational Basis Functions
OE	Output Error representation
SK	Sanathanan-Koerner iterations
EMTP	Electromagnetic Transients Program
ATP	Alternative Transients Program
PSCAD	Power Systems Computer-Aided Design
LP	Linear Programming
QP	Quadratic Programming
QCQP	Quadratically Constrained Quadratic Programming
SOCP	Second-Order Cone Programming
SDP	Semidefinite Prgramming
CP	Conic Programming
NLP	Non-linear Programming
LMI	Linear Matrix Inequality
PD	Positive Definite
PSD	Positive Semi-Definite
PDCP	Positive Definite Completion Problem
PPMPA	Partial Positive Matrix Passivity Assessment
CBPE	Completion-Based Passivity Enforcement
CDPE	Chordal Decomposition Passivity Enforcement
CT	Continuous Time
LTI	Linear Time-Invariant
LQ	Linear Quadratic

KYP	Kalman-Yakubovich-Popov
PRL	Positive-Real Lemma
BRL	Bounded-Real Lemma
RLC	Resistor-Inductor-Capacitor
KVL	Kirchhoff's Voltage Law
KCL	Kirchhoff's Current Law
SISO	Single-Input Single-Output
SIMO	Single-Input Multi-Output
MIMO	Multi-Input Multi-Output
BIBO	Bounded-Input Bounded-Output
VF	Vector Fitting
PFVF	Positive Fraction Vector Fitting
RMSE	Root-Mean Square Error
PEO	Perfect Elimination Ordering
MCS	Maximum Cardinality Search
MP	Modal Perturbation
RP	Residue Perturbation
RPD	Residue Perturbation Driver
PMAP	Principal Minor Assignment Problem
IVT	Inductive Voltage Transformer
GIS	Gas-Insulated Substation
DC	Direct-Current

CONTENTS

1 INTRODUCTION

THE pervasiveness of mathematical models in every imaginable instance of the scientific endeavor is a constant reminder of their successful history but it also prompts one to wonder whether they have realized their full potential. For the purposes of this study, a model is an abstract construction - as expressed by means of equations that can be realized computationally - devoted to representing and characterizing a particular phenomenon. Given the vast breadth and high complexity of both natural and artificial phenomena amenable to a quantitative treatment, all sorts of mathematics at different levels can be employed to obtain a suitable model. This translates into a rich variety of equations, conceptual models or *model structures* that can be effectively used in quest of the finest possible pattern description and prediction.

Nearly all observed phenomena have distinguishing dynamic features thus requiring a specialized class of mathematical models for quantities that evolve over time or whose time evolution is of central importance, namely *dynamical systems*. In the early days of dynamics the astounding accuracy achieved in celestial mechanics to describe planetary motion prompted an obsession with prediction making at the highest level of accuracy that has persisted unabated throughout time. Along this intellectual journey many fruitful ideas have flourished leaving a rich legacy of conceptual and numerical frameworks that once resided in the arcane realms of pure science and eventually spread out to a wide range of application fields such as Engineering, Biology, Economics and even Social Sciences. Unlike in the natural sciences where models generally assume an exclusive descriptive role (analysis), in Engineering they can also fulfil a prescriptive one (synthesis, design or control).

A particular instance of a dynamic phenomenon permeating all of Electrical Engineering and requiring accurate modeling techniques is that of electromagnetic transients. Their adverse impact can be felt across a broad spectrum of electrical devices from the tiniest piece of electronics to a nationwide power network. According to (GRIVET-TALOCIA; GUSTAVSEN, 2016), a system-level methodology has become the standard for the analysis of electrical interconnects as well as high-voltage power grids including their usual constituent components such as transmission lines and power transformers. The end product then is a network equivalent which encompasses all individually modeled components. This modular approach is the very essence of macromodeling.

Situated in this latter, modular context are multi-terminal network components all intricately interconnected into the ubiquitous and indispensable power grids. Earlier research extensively portrays the damaging effect electromagnetic transients can have

on network components, detailed accounts can be found in (JWG-A2/C4.39, 2014; HORI et al., 2007; SHIPP et al., 2011; JURISIC et al., 2016; AMOIRALIS; TSILI; KLADAS, 2009; BECHARA, 2010) - to mention but a few - thus providing some empirical evidence that a system-level approach must be adopted.

As the overall procedure culminating in a network equivalent entails the extraction of individual models to be subsequently interconnected, the modeling task is usually subsumed into three main categories. According to (AGUIRRE, 2007) and (LJUNG, 2010), even though the nomenclature is not unanimously standard in the literature, they are referred to as *white-box*, *black-box* and *grey-box* models:

- *White-box* models comprise those based on first principles, *i.e.* the physical laws governing the system behavior thus requiring in-depth knowledge of all intrinsic properties of the actual system such as equipment geometry, detailed specification of manufacturing materials and other manufacturer proprietary information often classified as industrial and trade secrets;
- *Black-box* models constitute an experimental data-based technique which requires little or no prior knowledge of the system being modeled that has gained preference among many modelers for it only depends on exogenous input/output measurements from well-defined external terminals;
- *Grey-box* models are conceived as an in-between strategy, neither a *Black-box* nor a *White-box* model. They are conceived to rely on auxiliary and additional information beyond the initial data; further details can be found in (LJUNG, 2010).

The real advantage of black-box techniques over the other alternatives is its relatively reduced complexity and numerical efficiency. Should further structure like linearity and time-invariance be imposed on the constitutive equations the advantages can far outweigh the disadvantages thus leading to compact and high-precision models obtained with efficient algorithms which need no further parameter tweaking and tuning. Linearity and time-invariance can be rightfully assumed for the description of phenomena associated with electromagnetic coupling or interaction with a characteristic high-frequency content; further clarification regarding this assumption can be substantiated by (JURISIC et al., 2016; AMOIRALIS; TSILI; KLADAS, 2009; GRIVET-TALOCIA; GUSTAVSEN, 2016; ANNAKKAGE et al., 2012).

All models herein discussed will be derived using black-box macromodeling via system identification from external I/O data. Two essential preliminaries include obtaining the data and defining the model structure for the subsequent data fitting. The first consists of either actual measurements (GUSTAVSEN, 2004b; JURISIC et al., 2016) or computer simulations (GRIVET-TALOCIA; GUSTAVSEN, 2016) using some commercial

field solver in either the time or frequency domains. Whichever option and domain be chosen there'll be either one or more of the following features: sampling rate, noise and band width. As for the second preliminary, there is a wealth of possible candidates ((AGUIRRE, 2007; LJUNG, 1999)) - out of which the Rational Basis Functions (RBF's), which can be considered as an alternative output-error (OE) representation, have achieved substantial prominence. The central idea is to define a basis in a function space, *i.e.* to form a sequence of functions, and determine a linear combination thereof (parameter estimation or regression) to match as accurately as possible a given data set. For a given data set one may consider several candidate choices of appropriate basis functions but they are usually chosen based on data characteristics, patterns and features. A natural choice of basis functions for the proposed context of this research are the pole-residue and the Takenaka-Malmquist orthonormal functions. There are well-known efficient algorithms employing such rational basis functions in an iterative manner (SK iterations, as in (SANATHANN; KOERNER, 1963)) based on weighted least-squares (GUSTAVSEN; SEMLYEN, 1999; DESCHRIJVER; DHAENE; HAEGEMAN, 2007; OLIVEIRA; MITCHELL, 2013; SCHUMACHER; OLIVEIRA, 2017). For a broad perspective and some illustrative case studies of black-box modeling in the frequency-domain, refer to (AKÇAY; ISLAM; NINNESS, 1998), (GUSTAVSEN; SEMLYEN, 1998), (GUSTAVSEN, 2010), (REGINATO; OLIVEIRA, 2007), (REGINATO; OLIVEIRA, 2008) , (REGINATO, 2008),(OLIVEIRA; MAESTRELLI; ROCHA, 2009), (MAESTRELLI; OLIVEIRA, 2010), (MAESTRELLI, 2010) and (OLIVEIRA; MITCHELL, 2013).

1.1 Dissipative Systems

Despite the significant strides that have been made in modeling to describe a multitude of dynamical systems, researchers cannot overlook the fact that models are often committed to translating physical reality. Even black-box models can become irredeemably dysfunctional without incorporating the right physics into the mathematical equations. *Passive Macromodeling* is a way to reconcile modeling with physics, the physics of energy balance, and concepts such as *Dissipativity* and *Passivity* consist precisely of formulating physical energy balancing constraints into the modelling problem so that energy is never really created nor destroyed, but rather transferred between interconnected entities.

In a somewhat rudimentary form, the concept of dissipativity had its genesis in (BRUNE, 1931). Brune proved that a transfer function is realizable as an impedance of a circuit containing only the interconnection of positive resistors, inductors, capacitors, and transformers provided the transfer function be rational and positive real. Subsequently, in establishing the relation between input/output and Lyapunov stability using a state-space

setting, the notion of a dissipative system emerged in the works of Willems: (WILLEMS, 1971), (WILLEMS, 1972a), (WILLEMS, 1972b) and (WILLEMS, 2007a). As will be later discussed at some length, dissipativity is a concept in its own right consisting of a generalization of Lyapunov functions to open systems, *i.e.* systems with inputs and outputs.

Dissipativity constitutes an atribute of many physical systems which can be formulated and represented within a given system representation as inequalities of some sort. Since the primary purpose of modeling is to give an accurate, full account of the system behavior, this basic empirical character must be embedded into the model. Dissipativity is widely known and used in the literature as one of its special cases, *viz.* passivity.

The whole macromodeling enterprise is bound to fail dismally should some fundamental system properties be overlooked. Even though macromodels are inherently approximate, for their construction deliberately neglects some aspects such as the detailed internal structure and topology of the actual system there exists a risk in placing undue reliance upon approximation quality metrics only. According to (TRIVERIO et al., 2007), despite being a major concern for model validation, approximation accuracy alone cannot serve as the sole criterion for the final model approval. A suitable model must also reflect every distinguishing feature of the actual system being emulated. In qualitative analysis of linear systems, the usual intrinsic properties pertaining to such systems can be enumerated as: causality, stability, passivity/dissipativity, controllability, observability *etc.* As described in (CHEN, 1999; WILLEMS, 2008; ANTOULAS, 2010; HINRICHSEN; PRITCHARD, 2013), these fundamental properties comprise a necessary condition for obtaining a consistent description (model) of the physical system.

In spite of the significant number of techniques and algorithms available for accomplishing the parameter identification task, an iterative algorithm based on least-squares rational approximation with an appropriate weighting scheme such as the Vector Fitting (GUSTAVSEN; SEMLYEN, 1999) and variations can be employed to obtain a state-space representation which is causal, stable and minimal (controllable/observable) by construction. Passivity, however, remains an unmodeled effect. Passivity has become a major concern for the macromodeling community because passive systems possess Algebraic Closure (WILLEMS, 1972a), *i.e.* the interconnection of dissipative systems leads to an overall dissipative system. This closed system algebra is definitively instrumental in building an overall complete network equivalent out of partial blocks with series/cascade and parallel connections. It was once thought that stability was endowed with algebraic closure but this myth has long been debunked and stability alone cannot guarantee numerical stability of time-domain simulations in system-level transients studies (COELHO; PHILLIPS; SILVEIRA, 2004; GUSTAVSEN; SEMLYEN,

2001; TRIVERIO et al., 2007).

This closure property explains why passivity has gained a prominent role: closure is essential for interconnection. As networks are formed by means of interconnections, all terminal variables (currents and voltages) are constrained to obey collective physical relationships, namely Kirchhoff's laws and passivity conditions. For that reason, network-level compatibility can only be *a priori* guaranteed by enforcing model compliance with passive behavior. Otherwise, nonphysical anomalies may compromise any time-domain transient simulation, *e.g.* a transient with a bounded amount of energy propagating into a network through the various interconnected terminals exhibiting current and voltage variables that grow arbitrarily unbounded. A finite energy source or stimulus cannot have its effects simply increased or amplified in an arbitrary manner. Such numerical instabilities due to passivity violations can hardly be predicted at the moment each individual model is devised for there is a complex interplay between the overall network and each of its constituent parts. Hence, it is nearly impossible to envisage what exact terminal conditions will give rise to instabilities and have a deleterious effect on the overall system simulation. Furthermore, passivity implies both causality and stability.

In summary, passivity provides an unified, integrated and consistent modeling environment where the energy exchange is correctly accounted and individual systems can be characterized and modeled independently using a different number of existing techniques to be subsequently connected together. Consequently, passivity has been broadly explored in the literature as a golden model property and has been fully incorporated as a modeling task to be used along with general-purpose time domain simulation tools, *e.g.* the Electromagnetic Transients Program (EMTP), Alternative Transients Program (ATP), PSCAD and so forth, for studying transient behavior of electrical networks ((TRANSFORMERS-SWITCHGEAR-COMMITTEE, 2010) and (JWG-A2/C4.39, 2014))). These facts have spawned active research on passivity enforcement methods.

1.2 Passivity Enforcement

In general terms, passivity enforcement comprises a set of algorithmic procedures designed to ensure that models comply with passive behaviour by satisfying passivity inequalities which are numerical representations of this qualitative structure or behavior. Essentially, algorithms involve either (*i*) parameter perturbation of existing models or (*ii*) constraining the parameter estimation during the model construction. The enforcement problem can be formulated in both non-parametric and parametric contexts: the first is specialized in excising passivity violations from the raw data whenever it is tainted with passivity violations whereas the latter tackles the problem using model parameters, but they can be jointly used as in (IHLENFELD; OLIVEIRA; SANS, 2016): one preceding the model parameter identification and the other subsequently. The

reason for two approaches is simple: either the data and/or the identified model can fail to conform to passive behaviour.

As already mentioned the ubiquitous black-box modeling technique has total reliance on I/O data for the parameter identification task. Ideally, both the data collected from a passive system and any approximation thereof should reflect that property altogether. Regrettably, conformity with passive behaviour happens to be highly volatile during both data acquisition and system identification. Incidentally, one should not be enticed into believing that passive measurements imply passive models. As pointed out by (COELHO; PHILLIPS; SILVEIRA, 2004), there is a common misconception that passive data yields a passive model by simply estimating model parameters in some given model structure that result in a sufficiently faithful approximation, however counter-intuitive this statement may seem. The fact that passive can remain unmodeled during parameter estimation is a natural consequence of inevitable processes affecting data acquisition and the underlying numerics of the estimation algorithms. Even though the data acquisition process is not in the scope of this research, it is a topic of concern for passive macromodeling. Data is inexorably subjected to corrupting factors during its acquisition process since existing technology and instrumentation are so sensitive that isolation from external disturbances is often impossible, *e.g.* , stray capacitances and inductances due to measurement cables, numerical noise, round-off error and so forth. Similar remarks apply to the inaccuracies associated with approximation algorithms. Since passivity cannot remain an unmodeled effect, a passivity enforcement procedure must be applied insofar as this characteristic feature be somehow recovered or retained.

Passivity enforcement has been assiduously investigated in the literature and the subject can be divided into two major classes of enforcement strategies, namely perturbative and non-perturbative enforcement schemes. Perturbative enforcement relies on model parameter perturbation to recover passivity when an existing model reveals passivity violations. Perturbative enforcement algorithms use different strategies to achieve the final passive behaviour, some methods are based on discrete frequency methods such that common implementations include Linear Programming (LP) in (SARASWAT; ACHAR; NAKHLA, 2004), Quadratic Programming (QP) in (GUSTAVSEN; SEMLYEN, 2001) and Second-order Cone Programming (SOCP) in (GRIVET-TALOCIA; UBOLLI, 2008). Another perturbative method uses a Hamiltonian Perturbation as in (GRIVET-TALOCIA, 2004). On the other hand, non-perturbative methods estimate parameters leading to passive behaviour. Instances of non-perturbative methods comprise those based on the positive-real lemma, namely (COELHO; PHILLIPS; SILVEIRA, 2004; OLIVEIRA; RODIER; IHLENFELD, 2016; IHLENFELD; OLIVEIRA, 2019), as well as the Positive Fraction Vector Fitting - PFVF in (TOMMASI et al., 2011). This latter class of non-perturbative enforcement schemes does not involve change any existing parameters, but rather a direct and constrained parameter estimation. Apart from

these formulations, there have been more recent variations, e.g., (PORDANJANI et al., 2011),(PORDANJANI; MAZIN; XU, 2013), (CALAFIORE; CHINEA; GRIVET-TALOCIA, 2012), (MAHMOOD et al., 2014), (KASSIS et al., 2016), (XIAO; KABIR; KHAZAKA, 2016), (SU et al., 2016), (YAMIN; ZADEHGOL, 2016), (GRIVET-TALOCIA, 2017),(HU et al., 2017), (TOMMASI; MAGNANI; MAGISTRIS, 2017), (MAHANTA; YAMIN; ZADEHGOL, 2017), (ZANCO et al., 2018) and (MORALES et al., 2018).

1.3 Chordal Methods

Most passivity enforcement methods are conceived in a way that the whole set of system parameters are adjusted while passivity is enforced. In pursuit of improved results relative to existing methods, new formulations are herein proposed which differ fundamentally from existing methods in the literature in that some parameters remain invariant while their complement set contains the free variables to enforce passive behavior. This proposed divide between fixed and free parameters also requires a special, new kind of passivity assessment. The rationale behind this novel approach is to identify and modify precisely those parameters that wreak passivity violations while preserving the remaining ones, in a somewhat divide-and-conquer strategy.

This combined novel approach is inspired by a problem called the Positive (Semi-)Definite Completion Problem, consisting of assigning some entries or blocks of a given matrix, *i.e.* specifying a partial matrix so as to obtain a completion of a certain desired type, *viz.* positive definite; a survey can be found in (JOHNSON, 1990). As introduced in the sequel, such problems are founded on Graph Theory to provide existence conditions for succesfully achieving passivity enforcement in a completion manner. Intuitively, the idea hinges on exploiting topological properties of a static structure, a particular sort of graph called chordal graphs, to make inferences about the dynamic behavior of physically realizable systems. This novel approach culminates into two algorithms: the Partial Positive Matrix Passivity Assessment (PPMPA) and the Completion-Based Passivity Enforcement (CBPE).

Surprisingly, the research into Completion-like problems revealed additional routes to further combining chordal graphs and passivity enforcement problems. Unlike the aforementioned proposed approach whereby graphs are used as an existence conditions for ensuring that a solution exists, they can also be used to exploit sparsity patterns to ease the computational burden involved in enforcement problems. A survey of chordal sparsity patterns can be found in (VANDENBERGHE; ANDERSEN, 2015). The end result of this second approach is the Chordal Decomposition Passivity Enforcement algorithm (CDPE).

All of the aforesaid discussion sets the stage for what is pursued further in this research: chordal methods for passive macromodeling employing black-box rational

models.

1.4 Objectives

1.4.1 General Objective

This research's prime objective is to propose a novel and systematic approach to the passivity enforcement problem using chordal methods as a means to achieve both reduced passivity compensation on model parameters as well as reduced runtime.

1.4.2 Specific Objectives

The aforementioned primary research objective can be divided into the following set of sub-objectives:

- To formulate and implement a novel passivity assessment algorithm to identify partial positive systems;
- To extend the Positive (semi-)definite Completion Problem to System Theory;
- To exploit chordal sparsity patterns to improve computational efficiency;

1.5 Document Outline

This first preliminary chapter provides a tour d'horizon of where the material presented in the subsequent chapters ultimately leads. Chapter (2) introduces the basics of (dissipative) system theory, network theory and system identification required to contextualize the research. While chapter (3) makes a theoretical detour to justify the mathematical methods employed in the algorithms, the upcoming Chapter (4) features many of the standard existing methods for both passivity assessment and enforcement in the literature. In Chapter (5) results of previous chapters are woven together into novel passivity assessment and enforcement algorithms which end up applied to measured system data. The subsequent Chapter (6) presents a second algorithm employing chordal methods to passivity enforcement problems. The closing Chapter (7) furnishes some concluding remarks, summarizes the results obtained and discusses further research prospects.

1.6 Notation

This Section sets the notational and typographical conventions used in this thesis. For instance, lightface lower-case x denote scalar variables whereas boldface lower **x** and upper-case **X** indicate vectors and matrices, respectively. The standard scalar inequalities $>$,$\geq$, $<$ and $\leq$ have the following symbols for their analogous generalized

inequalities $\succ$, $\succeq$, $\prec$ and $\preceq$, both for vector and matrix inequalities. The operator $vec(\cdot)$ takes as argument a matrix a converts it into a column vector by stacking the columns of the matrix on top of one another.

2 PASSIVE LINEAR SYSTEMS

This chapter contains a brief review of some basic concepts and definitions from linear systems, networks and system identification, deliberately focusing on making explicit the assumptions that underlie the ensuing exposure as well as steering the discussion to the point of view of linear systems as p-ports (p-terminals). Since the treatment is by no means encyclopedic, and is meant mostly to set out the notation, terminology and context pertaining to the research, rigorous mathematical details are omitted so as to avoid heavy notations and long derivations.

2.1 Linear System Basics

In a broader context, virtually anything that evolves over time may be deemed a dynamical system. This poses a need to define and limit the scope of this thesis *ab initio*. Therefore, throughout this document we are only concerned with lumped, linear, time-invariant systems and models described by the following set of equations:

$$\Sigma : \begin{cases} \dot{\mathbf{x}}(t) &= \mathbf{A}\mathbf{x}(t) &+ \mathbf{B}\mathbf{u}(t) \\ \mathbf{y}(t) &= \mathbf{C}\mathbf{x}(t) &+ \mathbf{D}\mathbf{u}(t) \end{cases}, \quad \mathbf{x}(0) = \mathbf{x}_0. \tag{2.1}$$

In engineering terminology, this set of equations are commonly referred to as a state-space description, a state-variable description or even an internal description of a given system. Mathematically, it consists of two different sets of equations: a set of continuous-time, constant-coefficient or autonomous, first-order, linear ordinary differential equations and a set of algebraic simultaneous equations, respectively. We also denote these equations by CT-LTI system or simply a realization. As in Figure (1), these equations provide the structure for representing the time linkages among system variables.

In standard system theory notation and terminology, the system variables $\mathbf{x}(t) \in \mathbb{R}^n$, $\mathbf{u}(t) \in \mathbb{R}^p$, $\mathbf{y}(t) \in \mathbb{R}^p$ are the state, input and output vectors or signals. Likewise, the system parameters are the following real matrices $\mathbf{A} \in \mathbb{R}^{n\times n}$, $\mathbf{B} \in \mathbb{R}^{n\times p}$, $\mathbf{C} \in \mathbb{R}^{p\times n}$, $\mathbf{D} \in \mathbb{R}^{p\times p}$.

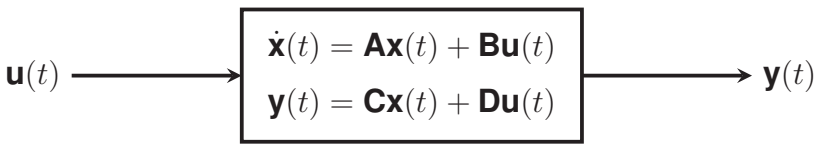

Figure 1 – System's Internal Description.

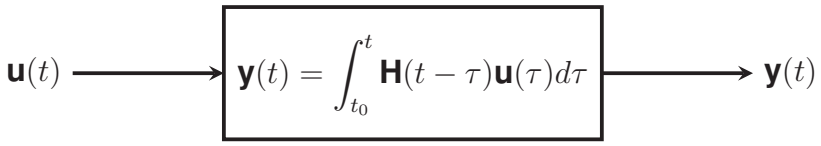

Figure 2 – System's External Description.

Alternatively, linearity and time invariance also enable the use of the convolution representation:

$$\Sigma : \left\{ \quad \mathbf{y}(t) = \int_{-\infty}^{t} \mathbf{H}(t-\tau)\mathbf{u}(\tau)d\tau \ , \right. \tag{2.2}$$

whereby the $p \times p$ matrix $\mathbf{H}(\cdot)$ is the system impulse response. Equation (2.2) is commonly called the external description owing to the fact that inputs and outputs are the only apparent systems variables; see Figure (2), nonetheless both descriptions are intimately related. Based on these two alternative descriptions, the system variables $\mathbf{u}(t)$ and $\mathbf{y}(t)$ are labelled as **external variables** whereas the system variables $\mathbf{x}(t)$ are labelled as **internal variables**[1].

Linear Systems comprise the most widely studied model class in all system theory and such models can be viewed from many alternative perspectives and serve a number of different purposes. Our concern is essentialy related to the model itself, its own structural properties or characteristics as well as the interplay between them and their implications to modeling. Despite its simplicity, CT-LTI systems are endowed with a number of properties some of which are of interest to us and we state them as definitions for further reference.

Since the material of this section is customary in system and control theory research, we only offer short summaries of the definitions concentrating on parts which are mostly relevant to weave a coherent discussion emphasizing this thesis' objectives. For a more detailed account, we refer to the references consulted, in particular (ANTOULAS, 2010), (WILLEMS, 2008), (TRIVERIO et al., 2007) and (CHEN, 1999).

Definition 1 *The **dimension** of the system Σ is defined as the dimension of its associated state-space:*

$$dim(\Sigma) = n.$$

Systems with a finite dimension number are also called finite-dimensional or lumped systems.

[1] This nomenclature treating inputs and outputs as external variables and states as internal variables is standard in System Theory.

Definition 2 *A **square system** Σ has the same number of input and output channels*[2]*:*

$$dim(\boldsymbol{u}(t)) = dim(\boldsymbol{y}(t)) = dim(\mathbb{R}^p) = p.$$

Definition 3 *The system Σ is defined to be **causal** provided that the following holds:*

$$\boldsymbol{H}(t-\tau) = 0, \quad \forall t \text{ such that } t \leq \tau$$

with τ denoting the instant the stimulus is applied to the input channels.

Definition 4 *The system Σ is defined to be **asymptotically stable** provided that $\lim_{t\to\infty} \mathbf{x}(t) = 0$ for some $\mathbf{x}(t_0) \neq 0$ and $\mathbf{u}(t) = 0$ or equivalently that all eigenvalues of system matrix **A** be located in the open left half complex-plane*[3]*.*

Definition 5 *The system Σ is **controllable***[4] *provided that the system's **controllability matrix** $\mathcal{C}(\boldsymbol{A}, \boldsymbol{B})$ be full rank:*

$$\mathcal{C}(\boldsymbol{A}, \boldsymbol{B}) = \begin{bmatrix} \boldsymbol{B} & \boldsymbol{AB} & \boldsymbol{A}^2\boldsymbol{B} & \dots & \boldsymbol{A}^{n-1}\boldsymbol{B} \end{bmatrix}$$
$$\boldsymbol{Rank}\big(\mathcal{C}(\boldsymbol{A}, \boldsymbol{B})\big) = n$$

Definition 6 *The system Σ is **observable** provided that the system's **observability matrix** $\mathcal{O}(\boldsymbol{C}, \boldsymbol{A})$ be full rank:*

$$\mathcal{O}(\boldsymbol{C}, \boldsymbol{A}) = \begin{bmatrix} \boldsymbol{C} \\ \boldsymbol{CA} \\ \boldsymbol{CA}^2 \\ \vdots \\ \boldsymbol{CA}^{n-1} \end{bmatrix}$$
$$\boldsymbol{Rank}\big(\mathcal{O}(\boldsymbol{C}, \boldsymbol{A})\big) = n$$

Definition 7 *The system Σ is **minimal** provided that its both controllable and observable.*

---

[2] Channel is System Theory terminology, later on the designation port and terminal will be introduced.
[3] If the matrix **A** possesses such property, it is also called Hurwitz.
[4] In fact, Reachability is a more general property than Controllability but for systems of the sort herein used they are equivalent. Further details in (ANTOULAS, 2010).

2.2 Dissipative CT-LTI Systems

Definition 8 *A system Σ is defined to be **dissipative** with respect to a **supply function** $\Phi : \mathbb{R}^p \times \mathbb{R}^p \to \mathbb{R}$ if there exists a **storage function** $V : \mathbb{R}^n \to \mathbb{R}$ such that the integral-form dissipation inequality*

$$V(\boldsymbol{x}(t_1)) \leq V(\boldsymbol{x}(t_0)) + \int_{t_0}^{t_1} \Phi\big(\boldsymbol{y}(\tau), \boldsymbol{u}(\tau)\big) d\tau$$

holds $\forall \tau$ in $t_0 \leq \tau \leq t_1$.

It is instructive to analyze each term in the dissipation inequality for it imparts a very clear, intuitive understanding of what it means to be dissipative. The storage function corresponds to the system's internal energy at time t and has much to do with the work pioneered by Lyapunov, for this very reason the terminology Lyapunov function is equally applicable to $V(\mathbf{x}(t))$. The supply function establishes a measure for power exchange between the system and the environment at some time t. The integral of the supply function over the bounds $t_0 \leq \tau \leq t_1$ can been understood as the energy supplied to the system over that same interval.

Since this thesis is concerned with the fulfillment of the dissipation inequality and all future developments revolve around it, a deeper discussion is in order.

2.2.1 Linear Quadratic Dissipative Systems

The natural question that arises concerns the scalar functions $V(\mathbf{x}(t))$ and $\Phi(\mathbf{y}(t), \mathbf{u}(t))$. Even though one can discuss the general properties of these functions at great length and generality, we concentrate efforts on discussing particular forms that are actually solvable. To that end, we assume both storage and supply functions to be of linear quadratic (LQ) form, thus focusing the scope on LQ-Lyapunov and LQ-dissipative systems.

As a tentative and preliminary step, let us assume Σ to be a Homogeneous CT-LTI system, *i.e.* the system is closed in the sense that it does not interact[5] with its environment. This special condition can be mathematically formalized by setting the external variables to zero for all time, namely $\mathbf{u}(t) = 0$ and $\mathbf{y}(t) = 0$. Under such conditions, the dissipation inequality takes on a special form:

$$V(\mathbf{x}(t_1)) \leq V(\mathbf{x}(t_0)) \quad \Longrightarrow \quad \Delta V(\mathbf{x}(t)) \leq 0.$$

Assuming the storage function $V : \mathbb{R}^n \to \mathbb{R}$ to be differentiable, the dissipation inequality can be written in local or differentiable-form:

[5] What is meant by the term interaction is energy exchange.

$$\dot{V}(\mathbf{x}) = \frac{d}{dt}V(\mathbf{x})|_{\dot{x}=Ax} \leq 0, \qquad \forall x,\, \forall t$$

Any storage function satisfying this inequality for all trajectories[6] $x(t)$ is called a Lyapunov Function for the autonomous system; existence of such functions is used in stability analysis. Lyapunov Stability is a research field on its own and for the purposes of this thesis we concentrate on Lyapunov Quadratic functions or LQ-Lyapunov Stability such as:

$$V(\mathbf{x}(t)) = \mathbf{x}^T\mathbf{P}\mathbf{x}, \quad \mathbf{P} = \mathbf{P}^T \succeq 0 \in \mathbb{R}^{n\times n}$$

By substituting this particular quadratic function into the differential-form dissipation inequality we get:

$$\begin{aligned}\frac{d}{dt}V(\mathbf{x}) &= \frac{d}{dt}(\mathbf{x}^T)\mathbf{P}\mathbf{x} + \mathbf{x}^T\mathbf{P}\frac{d}{dt}(\mathbf{x}) \\ &= \mathbf{x}^T \underbrace{\left[\mathbf{A}^T\mathbf{P} + \mathbf{P}\mathbf{A}\right]}_{\mathbf{Q}\preceq 0}\mathbf{x} \\ &= \mathbf{x}^T\mathbf{Q}\mathbf{x} \\ &\leq 0.\end{aligned}$$

The fact that $\mathbf{Q} \preceq 0$ is a natural consequence of **A** being a Hurwitz matrix and $\mathbf{P} \succeq 0$. Should those conditions be fully satisfied, the autonomous system is said to be internally dissipative or stable in the sense of Lyapunov. Nevertheless, systems surely do interact with their environments or equivalently they are not closed.

Therefore, stronger conditions are needed so as to ensure agreement between theoretical models and their corresponding physical systems. This has prompted the theoretical developments culminating in system dissipativity. All the subsequent discussion on formalizing open systems by means of LQ-dissipative systems is based on the seminal papers (WILLEMS, 1971), (WILLEMS, 1972a),(WILLEMS, 1972b), (WILLEMS, 2007b), (WILLEMS; TAKABA, 2007), (WILLEMS, 2007a) and book (WILLEMS, 2008) with a few adaptations to avoid clashing notation.

Since supply functions are herein constrained to be quadratic, they are differentiable and we can use the dissipation inequality in local or differentiable-form:

$$\begin{aligned}\dot{V}(\mathbf{x}(t)) &\leq \Phi(\mathbf{y}(t), \mathbf{u}(t)) \\ \frac{d}{dt}V(\mathbf{x})|_{\dot{x}=Ax+Bu} &\leq \Phi(\mathbf{y}(t), \mathbf{u}(t))\end{aligned}$$

[6] To avoid notational clutter, $x(t)$ is sometimes simply denoted x.

Note that the variation in the storage function is now dependent on the input. Since this inequality has a particular inner structure which will be of interest later on, it will be worked out once. Hence, by working out the indicated derivative, we get:

$$
\begin{aligned}
(\mathbf{Ax}+\mathbf{Bu})^T\mathbf{Px}+\mathbf{x}^T\mathbf{P}(\mathbf{Ax}+\mathbf{Bu}) &\leq \Phi(\mathbf{y}(t),\mathbf{u}(t)) \\
\begin{bmatrix} \mathbf{x}(t) \\ \mathbf{u}(t) \end{bmatrix}^T \begin{bmatrix} \mathbf{A}^T\mathbf{P}+\mathbf{PA} & \mathbf{PB} \\ \mathbf{B}^T\mathbf{P} & 0 \end{bmatrix} \begin{bmatrix} \mathbf{x}(t) \\ \mathbf{u}(t) \end{bmatrix} &\leq \Phi(\mathbf{y}(t),\mathbf{u}(t)) \\
\dot{V}(\mathbf{x}(t),\mathbf{u}(t)) &\leq \Phi(\mathbf{y}(t),\mathbf{u}(t))
\end{aligned}
$$

After having manipulated the left-hand side a little and having its structure revealed, let us keep it dormant for a while and shift the attention to the right-hand side containing the quadratic supply function.

$$
\begin{aligned}
\dot{V}(\mathbf{x}(t),\mathbf{u}(t)) &\leq \Phi(\mathbf{y}(t),\mathbf{u}(t)) \\
\Phi(\mathbf{y}(t),\mathbf{u}(t)) &= \begin{bmatrix} \mathbf{y}(t) \\ \mathbf{u}(t) \end{bmatrix}^T \begin{bmatrix} \mathbf{L} & \mathbf{W} \\ \mathbf{W}^T & \mathbf{R} \end{bmatrix} \begin{bmatrix} \mathbf{y}(t) \\ \mathbf{u}(t) \end{bmatrix} \\
&= \begin{bmatrix} \mathbf{Cx}(t)+\mathbf{Du}(t) \\ \mathbf{u}(t) \end{bmatrix}^T \begin{bmatrix} \mathbf{L} & \mathbf{W} \\ \mathbf{W}^T & \mathbf{R} \end{bmatrix} \begin{bmatrix} \mathbf{Cx}(t)+\mathbf{Du}(t) \\ \mathbf{u}(t) \end{bmatrix} \\
&= \begin{bmatrix} \mathbf{x}(t) \\ \mathbf{u}(t) \end{bmatrix}^T \begin{bmatrix} \mathbf{C}^T\mathbf{LC} & \mathbf{C}^T\mathbf{LD}+\mathbf{C}^T\mathbf{W} \\ \mathbf{D}^T\mathbf{LC}+\mathbf{W}^T\mathbf{C} & \mathbf{D}^T\mathbf{LD}+\mathbf{D}^T\mathbf{W}+\mathbf{W}^T\mathbf{D}+\mathbf{R} \end{bmatrix} \begin{bmatrix} \mathbf{x}(t) \\ \mathbf{u}(t) \end{bmatrix} \\
&= \begin{bmatrix} \mathbf{x}(t) \\ \mathbf{u}(t) \end{bmatrix}^T \begin{bmatrix} \tilde{\mathbf{L}} & \tilde{\mathbf{W}} \\ \tilde{\mathbf{W}}^T & \tilde{\mathbf{R}} \end{bmatrix} \begin{bmatrix} \mathbf{x}(t) \\ \mathbf{u}(t) \end{bmatrix} \\
&= \tilde{\Phi}(\mathbf{x}(t),\mathbf{u}(t))
\end{aligned}
$$

whereby $\mathbf{L}=\mathbf{L}^T$, $\mathbf{R}=\mathbf{R}^T$, $\mathbf{W}$ and their versions capped with tildes are all given matrices that reflect how the external variables are interconnected. Finally, the dissipation inequality attains the following form called the Kalman-Yakubovich-Popov(Anderson) Lemma (KYP(A) lemma)[7]:

$$
\begin{bmatrix} \mathbf{x}(t) \\ \mathbf{u}(t) \end{bmatrix}^T \begin{bmatrix} \mathbf{A}^T\mathbf{P}+\mathbf{PA} & \mathbf{PB} \\ \mathbf{B}^T\mathbf{P} & 0 \end{bmatrix} \begin{bmatrix} \mathbf{x}(t) \\ \mathbf{u}(t) \end{bmatrix} \leq \begin{bmatrix} \mathbf{x}(t) \\ \mathbf{u}(t) \end{bmatrix}^T \begin{bmatrix} \tilde{\mathbf{L}} & \tilde{\mathbf{W}} \\ \tilde{\mathbf{W}}^T & \tilde{\mathbf{R}} \end{bmatrix} \begin{bmatrix} \mathbf{x}(t) \\ \mathbf{u}(t) \end{bmatrix}.
$$

The KYP-lemma is in a convenient form for a few subsequent remarks concerning two special cases of dissipative systems which are of interest to applications pertaining

[7] There have been many generalizations of the KYP LMI since it first appeared in the early sixties, (ANDERSON, 1967b),(ANDERSON; VONGPANITLERD, 2006).

to electrical networks and their particular inputs and outputs, namely passive and contractive/nonexpansive systems.

Let $\Phi(\mathbf{y}(t), \mathbf{u}(t))$ be a supply function reflecting some desired input and output conditions or particular interconnections:

$$\Phi(\mathbf{y}(t), \mathbf{u}(t)) = \mathbf{u}(t)^T \mathbf{y}(t) + \mathbf{y}(t)^T \mathbf{u}(t) \tag{2.3}$$

Next, express it in matrix form:

$$\Phi(\mathbf{y}(t), \mathbf{u}(t)) = \begin{bmatrix} \mathbf{y}(t) \\ \mathbf{u}(t) \end{bmatrix}^T \begin{bmatrix} 0 & \mathbf{I} \\ \mathbf{I} & 0 \end{bmatrix} \begin{bmatrix} \mathbf{y}(t) \\ \mathbf{u}(t) \end{bmatrix}$$

$$\tilde{\Phi}(\mathbf{x}(t), \mathbf{u}(t)) = \begin{bmatrix} \mathbf{x}(t) \\ \mathbf{u}(t) \end{bmatrix}^T \begin{bmatrix} 0 & \mathbf{C}^T \\ \mathbf{C} & \mathbf{D} + \mathbf{D}^T \end{bmatrix} \begin{bmatrix} \mathbf{x}(t) \\ \mathbf{u}(t) \end{bmatrix}$$

The specific supply function of equation (2.3) establishes a particular kind of dissipative system.

Definition 9 *A system Σ is defined to be **passive** if it satifies the dissipativity inequality with the supply function $\Phi(\boldsymbol{y}(t), \boldsymbol{u}(t)) = \boldsymbol{u}(t)^T \boldsymbol{y}(t) + \boldsymbol{y}(t)^T \boldsymbol{u}(t)$:*

$$\begin{bmatrix} \boldsymbol{x}(t) \\ \boldsymbol{u}(t) \end{bmatrix}^T \left\{ \begin{bmatrix} \boldsymbol{A}^T \boldsymbol{P} + \boldsymbol{P}\boldsymbol{A} & \boldsymbol{P}\boldsymbol{B} \\ \boldsymbol{B}^T \boldsymbol{P} & 0 \end{bmatrix} - \begin{bmatrix} 0 & \boldsymbol{C}^T \\ \boldsymbol{C} & \boldsymbol{D} + \boldsymbol{D}^T \end{bmatrix} \right\} \begin{bmatrix} \boldsymbol{x}(t) \\ \boldsymbol{u}(t) \end{bmatrix} \leq 0$$

Note that the scalar passivity inequality is fulfilled provided that the following LMI is negative-semidefinite:

$$\begin{bmatrix} \mathbf{A}^T\mathbf{P} + \mathbf{P}\mathbf{A} & \mathbf{P}\mathbf{B} - \mathbf{C}^T \\ \mathbf{B}^T\mathbf{P} - \mathbf{C} & -\mathbf{D} - \mathbf{D}^T \end{bmatrix} \preceq 0,$$

or equivalently:

$$\begin{bmatrix} -\mathbf{A}^T\mathbf{P} - \mathbf{P}\mathbf{A} & -\mathbf{P}\mathbf{B} + \mathbf{C}^T \\ -\mathbf{B}^T\mathbf{P} + \mathbf{C} & \mathbf{D} + \mathbf{D}^T \end{bmatrix} \succeq 0 \tag{2.4}$$

The LMI (2.4) is called the Positive-Real Lemma[8] and it is a particular case of the KYP Lemma. Alternatively, there is yet another supply function of interest. Instead, let $\Phi(\mathbf{y}(t), \mathbf{u}(t))$ be the following supply function:

$$\Phi(\mathbf{y}(t), \mathbf{u}(t)) = \|\mathbf{u}(t)\|^2 - \|\mathbf{y}(t)\|^2 \tag{2.5}$$

[8] Sometimes abbreviated to PRL.

which is another quadratic function equally amenable to a matrix representation:

$$\Phi(\mathbf{y}(t),\mathbf{u}(t)) = \begin{bmatrix} \mathbf{y}(t) \\ \mathbf{u}(t) \end{bmatrix}^T \begin{bmatrix} -\mathbf{I} & 0 \\ 0 & \mathbf{I} \end{bmatrix} \begin{bmatrix} \mathbf{y}(t) \\ \mathbf{u}(t) \end{bmatrix}$$

$$\tilde{\Phi}(\mathbf{x}(t),\mathbf{u}(t)) = \begin{bmatrix} \mathbf{x}(t) \\ \mathbf{u}(t) \end{bmatrix}^T \begin{bmatrix} -\mathbf{C}^T\mathbf{C} & -\mathbf{C}^T\mathbf{D} \\ -\mathbf{D}^T\mathbf{C} & \mathbf{I}-\mathbf{D}\mathbf{D}^T \end{bmatrix} \begin{bmatrix} \mathbf{x}(t) \\ \mathbf{u}(t) \end{bmatrix}$$

Definition 10 *A system Σ is defined to be **contractive/nonexpansive** if it satifies the dissipativity inequality with the supply function $\Phi(\boldsymbol{y}(t),\boldsymbol{u}(t)) = \|\boldsymbol{u}(t)\|^2 - \|\boldsymbol{y}(t)\|^2$:*

$$\begin{bmatrix} \boldsymbol{x}(t) \\ \boldsymbol{u}(t) \end{bmatrix}^T \left\{ \begin{bmatrix} \boldsymbol{A}^T\boldsymbol{P}+\boldsymbol{P}\boldsymbol{A} & \boldsymbol{P}\boldsymbol{B} \\ \boldsymbol{B}^T\boldsymbol{P} & 0 \end{bmatrix} - \begin{bmatrix} -\boldsymbol{C}^T\boldsymbol{C} & -\boldsymbol{C}^T\boldsymbol{D} \\ -\boldsymbol{D}^T\boldsymbol{C} & \boldsymbol{I}-\boldsymbol{D}\boldsymbol{D}^T \end{bmatrix} \right\} \begin{bmatrix} \boldsymbol{x}(t) \\ \boldsymbol{u}(t) \end{bmatrix} \leq 0$$

This scalar contractivity or nonexpansion inequality is satisfied as long as the following LMI be negative-semidefinite:

$$\begin{bmatrix} \mathbf{A}^T\mathbf{P}+\mathbf{P}\mathbf{A}+\mathbf{C}^T\mathbf{C} & \mathbf{P}\mathbf{B}+\mathbf{C}^T\mathbf{D} \\ \mathbf{B}^T\mathbf{P}+\mathbf{D}^T\mathbf{C} & \mathbf{D}\mathbf{D}^T-\mathbf{I} \end{bmatrix} \preceq 0$$

The LMI above is the Bounded-real Lemma (BRL), nontheless it has an equivalent form which happens to be in a more convenient form for future developments. Since,

$$\begin{bmatrix} \mathbf{C}^T\mathbf{C} & \mathbf{C}^T\mathbf{D} \\ \mathbf{D}^T\mathbf{C} & \mathbf{D}\mathbf{D}^T \end{bmatrix} = \begin{bmatrix} \mathbf{C}^T \\ \mathbf{D}^T \end{bmatrix} \begin{bmatrix} \mathbf{C} & \mathbf{D} \end{bmatrix} \succeq 0,$$

use of Schur Complement allows the BRL LMI to be rewritten as:

$$\begin{bmatrix} \mathbf{A}^T\mathbf{P}+\mathbf{P}\mathbf{A} & \mathbf{P}\mathbf{B} & \mathbf{C}^T \\ \mathbf{B}^T\mathbf{P} & -\mathbf{I} & \mathbf{D}^T \\ \mathbf{C} & \mathbf{D} & -\mathbf{I} \end{bmatrix} \preceq 0 \tag{2.6}$$

Whenever we make reference to the BRL equation, we mean equation (2.6). Both the positive and bounded-real lemmas are cornerstones in system and control theories and many uses other than those made in this research are possible, some reference books on applicability of these results in general are (BOYD et al., 1994), (GHAOUI; NICULESCU, 2000).

2.2.2 Frequency Domain Dissipativity

It's well-known that CT-LTI systems can be efficiently studied by transform methods, most notoriously in engineering for simplifications in processes of differentiation and integration into simple algebraic operations. The direct unilateral Laplace Transform $H(s)$ can be defined as:

Definition 11 *$H(s)$ is the Laplace Transform of $h(t)$ provided that the following integral converges:*

$$H(s) = \mathscr{L}\{h(t)\} = \int_0^\infty e^{-st} h(t) dt$$

where $s = \sigma + j\omega$, i.e. *$s \in \mathbb{C}$.*

Existence, convergence, properties and many other extensions of this definition can be found in the vast specialized literature on this topic out of which we highlight (HOLBROOK, 1966), (SPIEGEL, 1965) and (DOETSCH, 1974). If associated with a CT-LTI system, the complex-valued function $H(s)$ possesses one particular property which is of interest for future developments when it is obtained by application of the Laplace Transform to the real-valued function $h(t)$, therefore it is stated as a definition.

Definition 12 *$H(s)$ is a **rational function** in the complex variable $s = \sigma + j\omega$ and can be expressed as a ratio of two polynomials:*

$$H(s) = \frac{N(s)}{D(s)} = \frac{b_m s^m + b_{m-1} s^{m-1} + \cdots + b_1 s + b_0}{a_n s^n + a_{n-1} s^{n-1} + \cdots + a_1 s + a_0}$$

with $b_i, i = 0, \ldots, m$ and $a_i, i = 0, \ldots, n$ all real, nonzero and $n \geq m$[9].

Definition 13 *The roots of the coprime[10] polynomials $N(s)$ and $D(s)$ are respectively called the **zeros** and **poles** of the rational function $H(s)$.*

Definition 14 *The monic polynomial[11] $D(s)$ is defined to be the **characteristic polynomial** of $H(s)$ and this polynomial is of **Hurwitz** type,* i.e. *all its roots have negative real parts.*

Evoking all previous definitions and assuming a very special initial-value problem, namely $\mathbf{x}(0) = 0$, we can apply the Laplace Transform to the system equations (2.1) as follows:

$$\mathscr{L}(\Sigma) : \begin{cases} \mathscr{L}\{\dot{\mathbf{x}}(t)\} &= \mathbf{A}\mathscr{L}\{\mathbf{x}(t)\} &+ \mathbf{B}\mathscr{L}\{\mathbf{u}(t)\} \\ \mathscr{L}\{\mathbf{y}(t)\} &= \mathbf{C}\mathscr{L}\{\mathbf{x}(t)\} &+ \mathbf{D}\mathscr{L}\{\mathbf{u}(t)\} \end{cases} \tag{2.7}$$

[9] Rational functions of this kind are commonly referred to as (strictly) proper.
[10] Coprimeness is assumed throughout and is equivalent to the absence of common factors.
[11] Meaning $a_n = 1$.

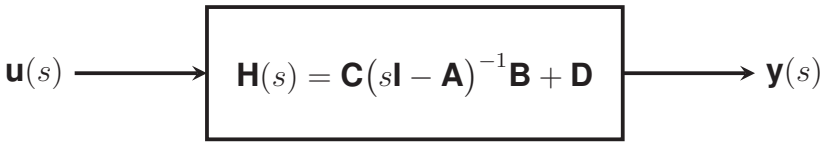

Figure 3 – Transfer Function Description.

Then, after some simple algebraic manipulation one can easily establish the following equality:

$$\mathscr{L}\{\mathbf{y}(t)\} = \underbrace{\left[\mathbf{C}(s\mathbf{I} - \mathbf{A})^{-1}\mathbf{B} + \mathbf{D}\right]}_{\mathbf{H}(s)} \mathscr{L}\{\mathbf{u}(t)\}. \tag{2.8}$$

The signal flow for Equation (2.8) is illustrated in Figure (3).

Definition 15 *The system Σ has an associated **transfer function**[12] denoted by $\boldsymbol{H}(s)$ and defined as:*

$$\boldsymbol{H}(s) = \boldsymbol{C}(s\boldsymbol{I} - \boldsymbol{A})^{-1}\boldsymbol{B} + \boldsymbol{D}$$

For finite-dimensional or lumped CT-LTI systems the transfer matrix is a rational function, a particular class of function possessing special properties.

Definition 16 *The degree of $\boldsymbol{H}(s)$ denoted deg($\boldsymbol{H}(s)$) is defined as the degree of its characteristic polynomial $D(s)$.*

Definition 17 *The system $\mathscr{L}(\Sigma)$ is defined to be **minimal** provided that:*

$$dim(\Sigma) = deg(\boldsymbol{H}(s)) = n.$$

As a result of these definitions, the transfer function is a frequency domain description of a CT-LTI system under special initial conditions. This brief summary sets the stage for the derivation of a frequency-domain dissipation inequality analogous to the time-domain dissipation inequality (8).

Equivalences between dissipativity inequalities in both the time and frequency domains are established in (WILLEMS, 1971).

Definition 18 *A system $\mathscr{L}(\Sigma)$ described by its transfer function $\boldsymbol{H}(s)$ is dissipative with respect to a supply function $\mathscr{L}(\Phi) : \mathbb{C}^p \times \mathbb{C}^p \to \mathbb{C}$ if and only if the following inequality*

[12] No distinction is made between Transfer Matrix Function and Transfer (Scalar) Function, the context should make it clear which one is meant.

$$\begin{bmatrix} \boldsymbol{H}(s) \\ \boldsymbol{I} \end{bmatrix}^H \begin{bmatrix} \Phi(s) \end{bmatrix} \begin{bmatrix} \boldsymbol{H}(s) \\ \boldsymbol{I} \end{bmatrix} \succeq 0$$ [13]

holds for all $s = i\omega$, $\omega \in \mathbb{R}$ *and det*$(s\boldsymbol{I} - \boldsymbol{A}) \neq 0$.

Based on the analysis made for the time domain, the specific supply functions of interest are:

$$\Phi(\mathbf{y}(s), \mathbf{u}(s)) = \begin{bmatrix} \mathbf{y}(s) \\ \mathbf{u}(s) \end{bmatrix}^T \begin{bmatrix} \mathbf{0} & \mathbf{I} \\ \mathbf{I} & \mathbf{0} \end{bmatrix} \begin{bmatrix} \mathbf{y}(s) \\ \mathbf{u}(s) \end{bmatrix}$$

for the passive case and

$$\Phi(\mathbf{y}(s), \mathbf{u}(s)) = \begin{bmatrix} \mathbf{y}(s) \\ \mathbf{u}(s) \end{bmatrix}^T \begin{bmatrix} -\mathbf{I} & \mathbf{0} \\ \mathbf{0} & \mathbf{I} \end{bmatrix} \begin{bmatrix} \mathbf{y}(s) \\ \mathbf{u}(s) \end{bmatrix}$$

for the contractive/nonexpansive case.

Definition 19 *A system* $\mathscr{L}(\Sigma)$ *is passive if and only if its associated transfer function* $\boldsymbol{H}(s)$ *is* ***positive real****:*

$$\begin{bmatrix} \boldsymbol{H}(s) \\ \boldsymbol{I} \end{bmatrix}^H \begin{bmatrix} \mathbf{0} & \boldsymbol{I} \\ \boldsymbol{I} & \mathbf{0} \end{bmatrix} \begin{bmatrix} \boldsymbol{H}(s) \\ \boldsymbol{I} \end{bmatrix} = \boldsymbol{H}(s) + \boldsymbol{H}^H(s) \succeq 0.$$

Definition (19) simply establishes an equivalence between passivity in the time domain and positive-realness[14] in the frequency domain.

Definition 20 *A system* $\mathscr{L}(\Sigma)$ *is contractive/nonexpansive if and only if its associated transfer function* $\boldsymbol{H}(s)$ ***bounded real****:*

$$\begin{bmatrix} \boldsymbol{H}(s) \\ \boldsymbol{I} \end{bmatrix}^H \begin{bmatrix} -\boldsymbol{I} & \mathbf{0} \\ \mathbf{0} & \boldsymbol{I} \end{bmatrix} \begin{bmatrix} \boldsymbol{H}(s) \\ \boldsymbol{I} \end{bmatrix} = \boldsymbol{I} - \boldsymbol{H}^H(s)\boldsymbol{H}(s) \succeq 0.$$

Similarly, Definition (20) establishes an equivalence between contractivity/non-expansivity in the time domain and bounded-realness in the frequency domain.

[13] The quadratic function on the left side is also called a Popov Function.

[14] The first to express the equivalence between complex-valued positive-real functions and resistive networks synthesis having only positive resistors was Otto Brune, in his Phd thesis at MIT, (BRUNE, 1931).

So far the discussion has revolved around system representations and their properties with dissipativity kept at the forefront. Emphasis is now shifted towards what kind of physical meaning is to be assigned to these constructs.

2.3 Network Theory Basics

According to (BAMBERG; STERNBERG, 1990), Network Theory can be regarded as branch of Electromagnetic Theory whereby there is a sweeping underlying assumption that the interesting phenomena can be fully described in terms of what happens along the wires and other individual lumped constituents of the network, each with its own characteristic dynamic behavior. This approximation serves a useful purpose, namely to predict how the system as a whole behaves when the components are interconnected in various ways.

In the previous section the case has been made for centering the discussion upon open system, *i.e.* those interacting with its environment. The kind of dynamic system being modeled throughout this research consists of electrical devices or equipment whose interaction with the surrounding environment is established through specific conductors[15] called terminals and they are the only means by which the system is allowed to electrically interact with its exterior[16]. Specifically, it is a terminal description of a system that is being herein sought, in other words the dynamic system explains the terminal behavior, *i.e.* it's literally a black-box[17] with terminals emerging as the sole interface. The only assumption concerning its internal architecture is that it is equivalent to a LTI RLC network whereas other system's internal details like topology and *et cetera* are not taken into account. Despite the subtlety, this is a trifle different than the usual setting for systems and control whereby systems interact via distinct, specific input and output channels[18]. The particular systems under scrutiny are not mere signal processors.

As the concern in transient simulation of electrical networks is shifted towards describing power and energy flows and their interaction with the various neighbouring components, the most natural choice of terminal variables are currents and voltages, both of them seen more as physical quantities rather than mere signals. Therefore, instead of referencing to input and output signals as well as their associated channels, reference is made to terminals in a way that voltages are defined between or across each pair of terminals and currents flow through terminals, as shown in Figure (4).

[15] Like wires or leads.
[16] This precludes the possibility of radiated energy
[17] The phrase Black-box modeling is heavily overloaded throughout this document for (i) an electrical network as described by its terminal behaviour is a black-box description (ii) system identification using input and output data (terminal data) is also denoted black-box identification.
[18] This is the standard terminology in systems and control theory.

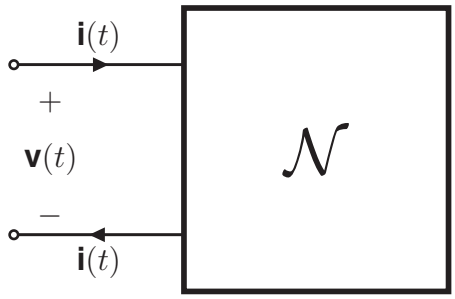

Figure 4 – The schematic of a LTI one-port.

Having currents and voltages involved requires the adoption of further conventions and definitions which are essential whenever energy and power considerations play a central role, thus ensuring that the modeling and the physics involved remain cohesive. Consequently, it is a necessity to introduce and distinguish between the notions of *terminals*, *interconnections* and *ports* for they have a special meaning in network theory which goes well beyond simple nomenclature. The ensuing discussion is a summary of the ideas found in (NEWCOMB, 1966),(KUO, 1966),(CHUA; LAM, 1973), (ALLEN, 2004),(GAWTHROP; BEVAN, 2007), (HUELSMAN, 2011), (WILLEMS, 2009) and (WILLEMS, 2010). As these references show these ideas of terminals and ports can be put in a very formal and mathematically rigorous footing.

The notion of a port involving 2 terminals is standard in the literature, but 2 terminals cannot be simply chosen at random to form a port. As a result, the grouping of terminals into ports depends on how the terminals as well as their terminations (sources and loads) are interconnected. Interconnection in its turn ought to be viewed as terminals sharing their variables as they are connected to one another, *i.e.* interconnection establishes actual physical constraints to terminal variables and not only forming a mere logical path for signal flows.

Definition 21 *A port can be defined as a pair of terminals that satisfies Kirchhoff's laws,* i.e. *in which the current into one terminal equals the one out the other terminal and is completely specified when the voltage-current relationship at the terminals of the port is given.*

Pure and isolated resistors, inductors or capacitors are trivial examples of one-ports but Figure (4) illustrates how a more general 2-terminal or one-port can be formed when driven by sinusoidal quantities, for instance. Note that whether its internal architecture comprises a single resistor or a number of interconnected LTI RLC lumped components is of little importance since it is a black-box description.

There is no reason not to consider even more terminals and generalize the discussion to multi-terminals or multi-ports, thus leading to the n-port concept. This

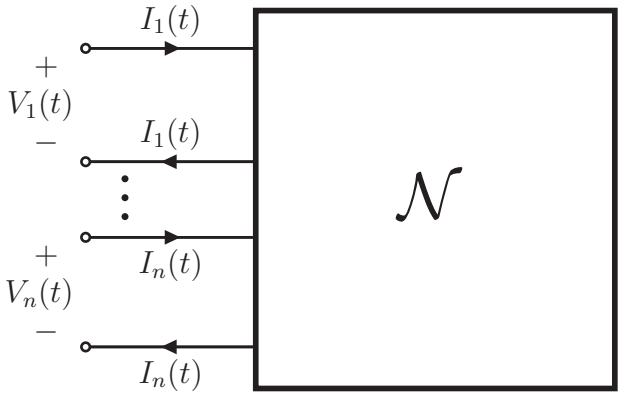

Figure 5 – The schematic of a LTI n-port.

generalization is not only of theoretical interest but also of a practical one for there exist many electrical devices requiring more than just two terminals (one-port) for their mathematical description, e.g. a power transformer. The rationale behind choosing ports lies in that the physics holds true so that both Kirchhoff's Current and Voltage laws also hold. For establishing the n-port concept, one simply builds on the former concept: instead of a single pair of terminals there are as many as n pairs, or alternatively $2n$ terminals, and their associated port variables as depicted in Figure (5). Again, each pair of terminals recursively obeying the conservation of current: the current flowing into one terminal of the pair equals the current flowing out of the other terminal.

The reason for defining ports resides in the intended interpretation for modeling in terms of power and energy which is only valid provided that the terminals can be grouped into ports. If all terminals $\{1, 2, \ldots, 2n\}$ of the general n-port illustraded in Figure (5) are grouped into n ports, then the power supplied to the n-port at time t along these terminals equals to:

$$\Phi(t) = I_1(t)V_1(t) + I_2(t)V_2(t) + \cdots + I_n(t)V_n(t).$$

Similarly, the energy $\mathcal{E}$ delivered over the time interval $[t_0, t_1]$ yields:

$$\mathcal{E}(t) = \int_{t_0}^{t_1} \big(I_1(t)V_1(t) + I_2(t)V_2(t) + \cdots + I_n(t)V_n(t)\big)dt.$$

According to (WILLEMS, 2010), this physical interpretation in terms of power and energy is legitimate only if the terminals form a port[19]. Otherwise, these expressions have the dimension of power and energy without necessarily corrresponding to physical power and energy. This is a reminder of the enlighting quote in (GAWTHROP; BEVAN,

[19] Evoking the earlier definition of passivity and bridging it with this ideia of ports to account for energy exchanged, a circuit is passive as long as a finite amount of energy only can be withdrawn through its ports.

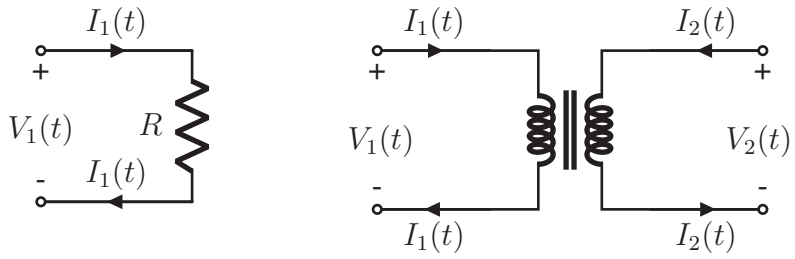

Figure 6 – Trivially defined ports.

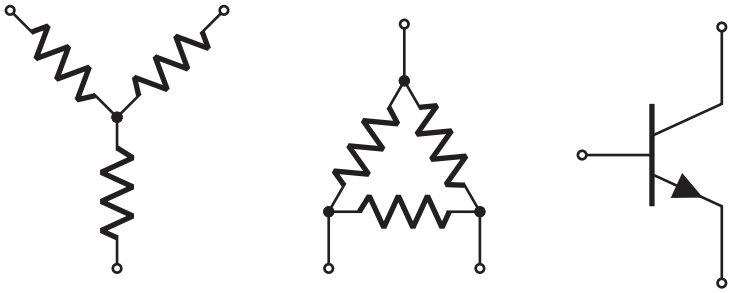

Figure 7 – 3-terminal circuits.

2007): "Power is the universal currency of physical systems". As stated earlier, 2 terminals cannot be chosen at random to form a port but sometimes the choice is self-evident as in some trivial cases like the ones displayed in Figure (6). The choice is nonetheless less obvious even when simple elements as those depicted in Figure (7) are involved.

As is frequently the case, the pairs of terminals may be referenced to some common reference of electric potential thus requiring that as many as half the number of terminals be grounded, *i.e.* n terminals out of a total of $2n$ terminals, one from each pair. When these n terminals are grounded the resulting network then happens to have $n+1$ distinct terminals. But it is important to stress that the 'black box' network still has as many as $2n$ terminals in total, the connection only establishes that each port shares some common potential.

Figure (8) illustrates the idea of interconnection: every time a pair of terminals k and j is connected together they share a voltage and a current[20] according the following formulation: $V_k = V_j$ and $I_k + I_j = 0$. If terminals k and j are grounded, they become one and the same terminal from an electrical standpoint thus reducing the number of terminals by one. One is then allowed to describe the circuit as a 3-terminal, but surely power and energy are still accounted correctly for it still is a 2-port in disguise. Interconnection places local physical constraints on terminal variables whereas ports involve more than one terminal at a time.

[20] Up to a minus sign.

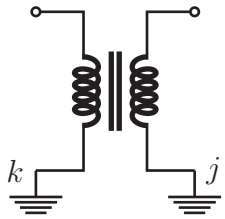

Figure 8 – Interconnection and Grounding.

The bottom line then is that interconnection is materialized via terminals and shall not be confused with energy exchange which is only established via ports: correctly forming ports out the terminals available is fundamental to characterize or model power exchange (load flow) as well as conservation of energy. In particular, it is impossible to express energy flowing into a circuit through a single terminal which is a basic physical constraint. Quoting (WILLEMS, 2010): "Terminals are for interconnection, ports are for energy transfer". One should be judicious in his use of the terminology not to confuse oneself for terminals and ports are usually used interchangeably in the literature, but careful authors do make the distinction. In the end, interconnected systems are accounted on a port basis[21].

As explained earlier, a 2-terminal circuit that satisfies KVL is a 1-port. There is no reason, of course, why a 4-terminal circuit should be a 2-port consisting of two 2-terminal 1-ports.

Assuming a port description of a network which is then characterized by n equations (the port equations). Its n port currents and n port voltages can be related by a $n \times n$ square matrix. The network acts as a linear operator and one can make fruitful use of compact matrix notation for describing a LTI network as a Multi-Input-Multi-Output (MIMO) linear function describing the n-port, in compact, general terms:

$$f(\mathbf{x}) = \mathbf{A}\mathbf{x}, \tag{2.9}$$

such that $\mathbf{A}$ is a $n \times n$ matrix which defines f as a vector-valued linear function, $f : \mathbb{C}^n \to \mathbb{C}^n$, that maps n-vectors to n-vectors. The description of a LTI n-port as a general function $f(\mathbf{x}) = \mathbf{A}\mathbf{x}$, dissociated from physical quantities, has far-reaching benefits, since, as in (BOYD; CHUA, 1982), this general framework may assume many forms that have special names such as impedance, admittance, hybrid, scattering and transmission parameters. Each of these special cases are treated as specific formalisms, representations or parameters associated with n-ports, according to (ALLEN, 2004), (WOHLERS, 1969), (KUO, 1966) and (CHUA; LAM, 1973). Consequently, the form of the system function depends on whether the excitation is a voltage or current source

[21] Passivity is preserved by interconnection.

- or even some linear combination thereof - and whether the response is a specified current or voltage, i.e. it depends on what is assigned as port variables (input-output) and how they are grouped, as pointed out in (KUO, 1966).

Irrespective of the particular form the network port description takes it is an external or exogenous description, based on particular inputs and outputs which is the essence of black-box modelling, *viz.* deriving a model based on experimental data. A decision has therefore to be made as to the measurement setup for data acquisition which assuredly depends on the available instrumentation. As usual, one can either have at his disposal time or frequency domain measurements thus leading to a time or frequency domain modelling approach, this research concentrates exclusively on the latter. The justification for proceeding in this manner is a rather simple one: the data base underpinning this research happens to be in the frequency domain.

The measurements that serve as input to this investigation are indeed frequency response measurements comprising a set of experimental data having the following usual format:

$$\{(\omega_k, |H(\omega_k)|, \phi(\omega_k)) \mid k = 1, \ldots, K\}, \tag{2.10}$$

where ω_k, $|H(\omega_k)|$ and $\phi(\omega_k)$ correspond to angular frequency, magnitude and phase of the frequency response. This initial step leads to a set of tabulated frequency responses of the structure under investigation. Such system description contains all needed information concerning the sinusoidal steady-state response of the system (or network) function for discrete frequency points. Assuming the Laplace Transform is used to describe a given continuous-time linear time-invariant (CT-LTI) system, its network function $\mathbf{H}(s)$ is a rational algebraic function of s (the complex frequency or Laplace variable), relating the Laplace Transform of the input to that of the output with a zero

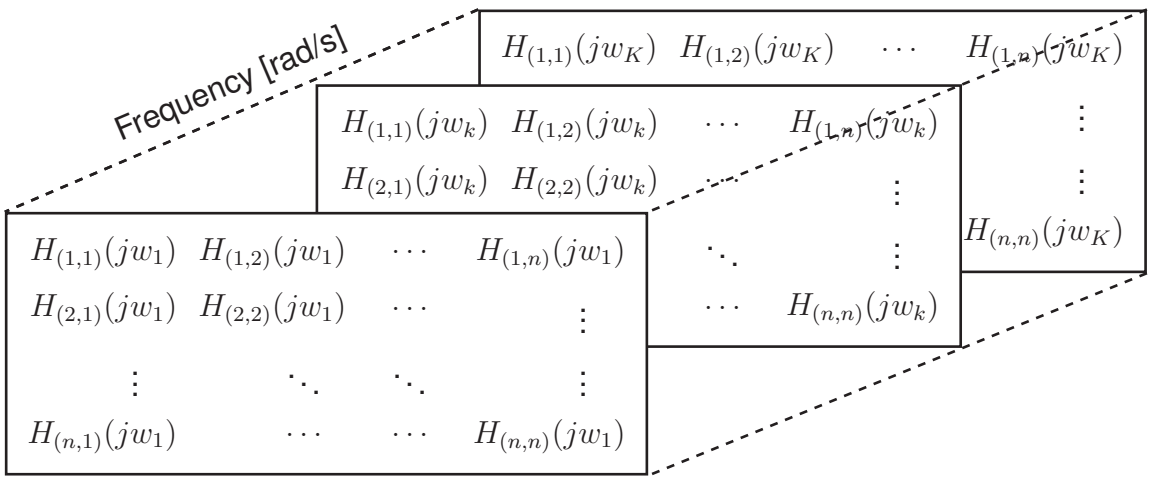

Figure 9 – Data-set for n-port.

initial state (initially inert system). According to (DESOER; KUH, 1969), amplitudes and relative phases of a given sinusoidal input and output are easily measurable quantities and they are related to the network function via the frequency response, since the latter is nothing but the earlier, namely $H(s)$, evaluated at $s = jw_k$.

This is how it is possible to experimentally determine the network function of a system without any knowledge of its topology and its constituent element values, that is to say, a black-box description.

Hence, the entries of the $n \times n \times K$ array given in Figure (9) consist of a set of data just as the one encapsulated by the set (2.10), but generalized to a n-port. In fact, as in (HORN; JOHNSON, 2012), the array is itself a set which allows one to rewrite the (2.10) in set-theoretic notation. Since describing the data in this set formalism is cumbersome (to which one is referred to (BOYD; CHUA, 1982), (WOHLERS, 1969) and (CHUA; LAM, 1973)), and the majority of the literature uses matrix notation, this set-theoretic notation is not herein pursued. The frequency responses for a n-port at every frequency w_k are essentially linear mappings between collections of inputs (independent variables which may be varied at one's discretion) and outputs (dependent variables which are determined by the network once inputs are specified).

The following subsections contain a discussion on specific forms of system functions reflecting the various choices of input-output quantities as well as describing the testing conditions under which they may be obtained, thus assigning different, specific physical meanings to the data set represented in Figure (9), the so-called *network parameters*. Owing to the context, this exposure focuses on the frequency-domain, though all results are equally valid for the time-domain. In general, ports connected to energy sources are denoted driving points of the network or input ports whereas ports connected to loads are called output ports. Ports can be grounded, terminated in open or short circuits and also connected to other ports for interconnection.

2.3.1 Admittance Y-Parameters

When the general system matrix **A** (Equation (2.9)) linearly maps input voltage vectors into output current vectors, it is assigned a specific symbol or notation, namely **Y**, and is called the admittance matrix. In this particular setting, Equation (2.9) can be rewritten in the frequency-domain as:

$$\mathbf{i}(jw) \;=\; \mathbf{Y}(jw)\,\mathbf{v}(jw), \tag{2.11}$$

which is usually referred to in the literature as the admittance representation (or formulation/formalism in a more mathematically inclined discussion, e.g. (ALLEN, 2004), (WOHLERS, 1969) or (CHUA; LAM, 1973)) of a network. Similarly, the entries of the ma-

trix **Y** are known to be the admittance parameters associated with the n-port. Equation (2.11), which is in fact a compact notation for a set of linear equations, can be written out as follows:

$$\begin{bmatrix} I_1(jw) \\ I_2(jw) \\ \vdots \\ I_n(jw) \end{bmatrix} = \begin{bmatrix} Y_{11}(jw) & Y_{12}(jw) & \cdots & Y_{1n}(jw) \\ Y_{21}(jw) & Y_{22}(jw) & \cdots & Y_{2n}(jw) \\ \vdots & \vdots & \ddots & \vdots \\ Y_{n1}(jw) & Y_{n2}(jw) & \dots & Y_{nn}(jw) \end{bmatrix} \times \begin{bmatrix} V_1(jw) \\ V_2(jw) \\ \vdots \\ V_n(jw) \end{bmatrix}, \tag{2.12}$$

such that each $I_i(jw)$ and $V_l(jw)$ correspond to the current and voltage at ports i and l. Every $Y_{il}(jw)$ entry of the admittance matrix is determined by setting the port voltages to zero (by short-circuits), except at the lth port, while measuring the short-circuit current at the ith port; this statement can be framed more pragmatically as:

$$Y_{il}(jw) = \frac{\text{response}}{\text{excitation}} = \frac{I_i(jw)}{V_l(jw)}\Big|_{V_k(jw)=0 \mid k \neq l}. \tag{2.13}$$

Equation (2.13) corresponds to the procedure used in testing and measurement conditions. The diagonal entries $Y_{ii}(jw)$, obtained when both the excitation and response are measured at the same port (or between the same pair of terminals), are referred to as the short-circuit driving-point admittances whereas the otherwise obtained off-diagonal entries $Y_{il}(jw)$, such that $i \neq l$, as short-circuit transfer admittances. The diagonal entries are called the self-admittances whereas the off-diagonal ones the mutual admittances, some authors however prefer the terminology driving-point and transfer admittances for the self and mutual admittances respectively.

Valuable information and further details on the measurement setup for admittance matrices can be found in (GUSTAVSEN, 2004b) and (GUSTAVSEN, 2004a), specially considering the context of power transformers, providing useful schematics as well as touching some numerical issues. A thorough study of the impact of the measurement setup, the measuring cables to be more precise, on the admittance matrix's entries can be found in (GUSTAVSEN, 2012), (SANS; OLIVEIRA; JUNIOR, 2012) and (SANS, 2013).

2.3.2 Impedance Z-Parameters

By interchanging the input and output vectors of equation (2.11), i.e., the system now linearly maps input current vectors into output voltage vectors, the resulting matrix corresponds to the inverse mapping of the previous formulation and is also assigned a

specific symbol, namely **Z**, such that $\mathbf{Z} = \mathbf{Y}^{-1}$. Similarly, matrix **Z** is technically called the impedance matrix and produces the following linear mapping:

$$\mathbf{v}(jw) \;=\; \mathbf{Z}(jw)\,\mathbf{i}(jw), \tag{2.14}$$

whose entries form the impedance parameters associated with the n-port represented by **Z** and is equivalent to:

$$\begin{bmatrix} V_1(jw) \\ V_2(jw) \\ \vdots \\ V_n(jw) \end{bmatrix} = \begin{bmatrix} Z_{11}(jw) & Z_{12}(jw) & \cdots & Z_{1n}(jw) \\ Z_{21}(jw) & Z_{22}(jw) & \cdots & Z_{2n}(jw) \\ \vdots & \vdots & \ddots & \vdots \\ Z_{n1}(jw) & Z_{n2}(jw) & \dots & Z_{nn}(jw) \end{bmatrix} \times \begin{bmatrix} I_1(jw) \\ I_2(jw) \\ \vdots \\ I_n(jw) \end{bmatrix}. \tag{2.15}$$

Each entry $Z_{il}(jw)$ of the impedance matrix is determined by the ratio of the voltage obtained at the ith port due to a current applied to the lth port and the remaining ports open-circuited (currents are zero). Thus,

$$Z_{il}(jw) = \frac{\text{response}}{\text{excitation}} = \frac{V_i(jw)}{I_l(jw)}\Big|_{I_k(jw)=0\,|\,k\neq l}. \tag{2.16}$$

The diagonal entries $Z_{ii}(jw)$ may be referred to as the open-circuit driving-point impedances whereas the off-diagonals as the open-circuit transfer impedances.

2.3.3 Hybrid

According to (HUELSMAN, 2011), for the general system matrix of equation (2.9) to be a set of hybrid parameters, it is simply required that the entries of the output vector $f(\mathbf{x})$ be neither all voltages nor all current variables. Therefore, there is no such thing as the hybrid parameters for a given n-port, but rather various hybrid parameters. In one possible choice of hybrid representation for a n-port, the first $\frac{n}{2}$ coordinates of the n-dimensional input vector can be driving currents whereas the remaining coordinates driving voltages. Conversely, for the n-dimensional output vector, the first $\frac{n}{2}$ coordinates are chosen to be voltages and the remaining ones are currents. Equation (2.9) is a mapping of input current-voltage hybrid vectors into output voltage-current hybrid vectors, thus called a hybrid matrix. For this particular choice the overall structure assumes the following matrix form:

$$\begin{bmatrix} \mathbf{v}_1(jw) \\ \mathbf{i}_2(jw) \end{bmatrix} = \begin{bmatrix} \mathbf{h}_{11}(jw) & \mathbf{h}_{12}(jw) \\ \mathbf{h}_{21}(jw) & \mathbf{h}_{22}(jw) \end{bmatrix} \times \begin{bmatrix} \mathbf{i}_1(jw) \\ \mathbf{v}_2(jw) \end{bmatrix}, \tag{2.17}$$

such that $\mathbf{h}_{11}(jw)$, $\mathbf{h}_{12}(jw)$, $\mathbf{h}_{21}(jw)$ and $\mathbf{h}_{22}(jw)$ are block matrices of dimension $(\frac{n}{2})\times(\frac{n}{2})$ and the input-output vectors are formed by stacking the corresponding vector partitions:

$$\mathbf{v}_1 = \begin{bmatrix} V_1(jw) \\ V_2(jw) \\ \vdots \\ V_{\frac{n}{2}}(jw) \end{bmatrix}; \mathbf{i}_2 = \begin{bmatrix} I_{\frac{n}{2}+1}(jw) \\ I_{\frac{n}{2}+2}(jw) \\ \vdots \\ I_n(jw) \end{bmatrix}; \mathbf{i}_1 = \begin{bmatrix} I_1(jw) \\ I_2(jw) \\ \vdots \\ I_{\frac{n}{2}}(jw) \end{bmatrix}; \mathbf{v}_2 = \begin{bmatrix} V_{\frac{n}{2}+1}(jw) \\ V_{\frac{n}{2}+2}(jw) \\ \vdots \\ V_n(jw) \end{bmatrix}.$$

A closer examination of equation (2.17), reveals that the blocks $\mathbf{h}_{11}(jw)$, $\mathbf{h}_{12}(jw)$, $\mathbf{h}_{21}(jw)$ and $\mathbf{h}_{22}(jw)$ correspond to impedances, voltage-ratio transfer functions, current-ratio transfer functions and admittances. When reduced to a special case of a 2-port, equation (2.17) is usually used in describing simple transistor circuits, applications can be found in (VéLIZ; VARRICCHIO; JR., 2006) and (VARRICCHIO et al., 2018).

As mentioned, equation (2.17) is a particular choice of hybrid parameters. The input-output vectors could also have an alternating pattern, such as:

$$f(x) = \begin{bmatrix} V_1(jw) \\ I_2(jw) \\ \vdots \\ V_{n-1}(jw) \\ I_n(jw) \end{bmatrix}; \qquad x = \begin{bmatrix} I_1(jw) \\ V_2(jw) \\ \vdots \\ I_{n-1}(jw) \\ V_n(jw) \end{bmatrix}.$$

There are many other possibilities, including those with the condition that both variables from at least one of the ports be part of the input-output vectors, but there can be impeding exceptions. In fact, as mentioned in (HUELSMAN, 2011), since a n-port comprises $2n$ variables (to every port is assigned a current and a voltage), there are c possible ways (number of combinations, without considering the permutations) in which these variables once they have been selected, such that:

$$c = \frac{(2n)!}{(n!)^2}, \tag{2.18}$$

where n is the number of ports. Consequently, there are c different sets of parameters for a given n-port. For the simple case of a 2-port, c equals six. These are the usual *z-parameters*, *y-parameters*, *h-parameters*, *g-parameters*, *Transmission-parameters* and *Inverse Transmission-parameters*. For three and four ports the number of sets is even larger: 20 and 70. In fact, it is even possible to form new variables by means of linear combinations of the voltage-current variables. This representation constitutes a formulation in its own right, namely the scattering parameters.

2.3.4 Scattering S-Parameters

In this conceptually different formulation, each coordinate of the input vector is itself a linear combination of the current and voltage associated to a port. Reference (KUO, 1966) stresses that this network characterization is a powerful analytical tool, originally used by transmission engineers. Hence, when Equation (2.9) comprises a linear mapping between linear combinations of the port variables to other linear combinations of the port variables, the matrix is called the scattering matrix **S** and the following notation is used:

$$\mathbf{v}^{-}(jw) \;=\; \mathbf{S}(jw)\,\mathbf{v}^{+}(jw). \tag{2.19}$$

Equation (2.19) is the compact form of:

$$\begin{bmatrix} V_1^-(jw) \\ V_2^-(jw) \\ \vdots \\ V_n^-(jw) \end{bmatrix} = \begin{bmatrix} S_{11}(jw) & S_{12}(jw) & \cdots & S_{1n}(jw) \\ S_{21}(jw) & S_{22}(jw) & \cdots & S_{2n}(jw) \\ \vdots & \vdots & \ddots & \vdots \\ S_{n1}(jw) & S_{n2}(jw) & \ldots & S_{nn}(jw) \end{bmatrix} \times \begin{bmatrix} V_1^+(jw) \\ V_2^+(jw) \\ \vdots \\ V_n^+(jw) \end{bmatrix}, \tag{2.20}$$

where the pluses and minuses, superscripts in the input-output vectors, reflect the original transmission line terminology and allude to incident and reflected voltage waves, or forward- and backward-traveling waves. The input-output column vectors $\mathbf{V}^{-}(jw)$ and $\mathbf{V}^{+}(jw)$ in Equation(2.19), are the following linear combinations of the port variables, as defined in (KUO, 1966) and (HUELSMAN, 2011):

$$\begin{aligned} \mathbf{v}^{+}(jw) &= \tfrac{1}{2}(\mathbf{v}^{n}(jw) + \mathbf{i}^{n}(jw)) \\ \mathbf{v}^{-}(jw) &= \tfrac{1}{2}(\mathbf{v}^{n}(jw) - \mathbf{i}^{n}(jw)) \end{aligned}, \tag{2.21}$$

such that $\mathbf{v}^{n}(jw)$ and $\mathbf{i}^{n}(jw)$ are the normalized (indicated by the superscript n) port voltages and current. Therefore, it is assigned a pair of variables, also called the scattering variables ($V_i^+(jw)$ as input and $V_i^-(jw)$ as output), to each ith port and the variables in the pair are themselves proportional to the sum and difference (linear combinations) of the port's own voltages and currents. By using a constant factor, called the reference impedance, the normalization does not affect the linearity between the port variables and their normalized combination (Equation 2.21). Each port has its own normalization constant r_{oi} and the normalized voltage and current coordinates are

chosen such that:

$$\begin{aligned} V_i^n(jw) &= \frac{V_i(jw)}{(r_{oi})^{\frac{1}{2}}} \\ I_i^n(jw) &= I_i(jw).(r_{oi})^{\frac{1}{2}} \\ Z_i^n(jw) &= \frac{V_i^n(jw)}{I_i^n(jw)} = \frac{Z_i(jw)}{r_{oi}(jw)} \end{aligned} \quad , \tag{2.22}$$

the reference impedance (can be chosen at one's own discretion) is taken to the square root to allow the definition of the normalized impedance as the ratio of the normalized voltages and currents. For clarity, assume a special scalar case of Equation (2.19), i.e., a one-port (Figure 4):

$$V^-(jw) \;=\; S(jw)\, V^+(jw). \tag{2.23}$$

The scattering parameter (unique since it is a scalar simplification) can be defined as:

$$S(jw) = \frac{V^-(jw)}{V^+(jw)} \;=\; \frac{V^n(jw) - I^n(jw)}{V^n(jw) + I^n(jw)} \;=\; \frac{Z^n(jw) - 1}{Z^n(jw) + 1}, \tag{2.24}$$

this interpretation of the scattering parameter (as a ratio containing the normalized impedance) is very useful since it reveals the advantages of the scattering formulation over the other ones. Indeed, if the normalized impedance in equation (2.24) is chosen to equal unity (matched impedances), $S(jw)$ is zero.

The multi-variable analogous of equation (2.23) is, according to (HUELSMAN, 2011):

$$\mathbf{S}(jw) = \; [\mathbf{Z}^n(jw) - \mathbf{I}][\mathbf{Z}^n(jw) + \mathbf{I}]^{-1}, \tag{2.25}$$

where $\mathbf{Z}^n(jw)$ is a diagonal matrix whose entries correspond to the normalized impedances at the various ports and **I** is the $n \times n$ identity matrix. Each entry $S_{il}(jw)$ of the scattering matrix is determined by the ratio of the reflected quantity at the ith port due to the incident quantity at the lth port and the remaining ports with matched impedances. Thus,

$$S_{il}(jw) = \frac{\text{response}}{\text{excitation}} = \frac{V_i^-(jw)}{V_l^+(jw)}\Big|_{Z_k^n(jw)=1 \;|\; k \neq l}. \tag{2.26}$$

Since the entries $S_{il}(jw)$ relate scattered or reflected voltage waves from the network to incident voltage waves upon the network, they have been appropriately named scattering parameters. The diagonal entries $S_{ii}(jw)$ correspond to reflection

coefficients whereas off-diagonal entries $S_{ij}(jw)$ to forward (below the diagonal) or reverse (above the diagonal) transmission coefficients.

Further details on the scattering parameters can be found in the classical references (KUROKAWA, 1965) and (CARLIN, 1956).

2.4 CT-LTI System Identification Basics

The previous sections of this chapter have paved the way for an introductory discussion about one[22] *black-box* modeling technique which is a special subclass within the much larger area of System identification. The basic principle behind the black-box identification machinery is reliance upon exogenous inputs and outputs without prior knowledge such as a first-principle formulation of the system. Specifically, these inputs and outputs are terminal or port variables that come either from direct measurement or simulation and are used to obtain an approximation of the dynamic behavior of those terminals or ports under a few assumptions about the system. As a result, systems equations are thus obtained with coefficients that have no direct physical significance, *i.e.* they are only parameters in a mathematical formula that purportedly represents the terminal or port behavior.

The purpose of this section is then to briefly describe the estimation process which constitutes an assignment of computed numbers to objects in terms of some assumed structural correspondence as well as the algorithm used as the identification engine, *viz.* the Vector Fitting Algorithm, which is largely used and known in the technical community. Since its debut in (GUSTAVSEN; SEMLYEN, 1999), it was rediscovered in (HENDRICKX; DESCHRIJVER; DHAENE, 2006) as a Sanathanan-Koerner-type algorithm based on the pioneering reference (SANATHANN; KOERNER, 1963) and a number of variants with improvements have since arisen: (GUSTAVSEN, 2006; DESCHRIJVER; DHAENE; HAEGEMAN, 2007; BEYGI; DOUNAVIS, 2012; SCHUMACHER; OLIVEIRA, 2017).

2.4.1 The Vector Fitting Algorithm

The Vector Fitting algorithm in its frequency domain formulation is applicable to LTI systems as represented in Definition (15), *i.e.* a linear operator mapping inputs to outputs:

$$\mathbf{y}(s) = \hat{\mathbf{H}}(s)\mathbf{u}(s),$$

[22] Despite being herein avoided altogether, there a number of alternative approaches to the one being pursuited here, not to mention identification using different paradigms like white-box, gray-box and *et cetera*...

whereby $\hat{\mathbf{H}}$ is a Multi-Input-Multi-Output (MIMO) rational transfer matrix function[23]. The hat appearing over the transfer matrix is a usual notation to suggest that $\hat{\mathbf{H}}(\cdot)$ is an approximation of the actual physical system. Instead of representing the model as polynomial ratio, a truncated series expansion can be used:

$$\hat{\mathbf{H}}(s) = \mathbf{R}_0 + \sum_{m=1}^{N} \mathbf{R}_m \Phi_m(s) \tag{2.27}$$

in a way that the input-output mapping reads:

$$\mathbf{y}(s) = \big(\mathbf{R}_0 + \sum_{m=1}^{N} \mathbf{R}_m \Phi_m(s)\big)\mathbf{u}(s)$$

with $\{\mathbf{R}_m\}_{m=0}^{N}$ the set of coefficient matrices, $\{\Phi_m(s)\}_{m=1}^{N}$ is a set of orthogonal basis functions and N is the dynamic order. Note that the same basis functions are used for all entries of $\hat{\mathbf{H}}(s)$, *i.e.* the basis functions are common for all entries. The choice of basis functions is a subject in its own right and it depends on the characteristics of the problem at hand. A discussion on this issue for systems in a unified formulation[24] can be found in (SCHUMACHER; OLIVEIRA, 2018). For the classical Vector Fitting Algorithm, the series expansion (2.27) comprises a pole-residue expansion[25], *i.e.* the basis functions are completely parametrized by the pole set $\{a_m\}_{m=1}^{N}$ as follows:

$$\Phi_m(s) = \frac{1}{s - a_m}$$

when the poles are real or come in complex conjugate pairs

$$\begin{cases} \Phi_m(s) = \dfrac{1}{s - a_m} + \dfrac{1}{s - a_{m+1}} \\ \Phi_{m+1}(s) = \dfrac{j}{s - a_m} - \dfrac{j}{s - a_{m+1}} \end{cases}.$$

Exploring the correspondence between the basis functions and poles more fully, the VF algorithm assigns every entry of the transfer matrix function the same poles thus meaning that all individual transfer functions $H_{ij}(s)$ have a common dynamic behavior. This characteristic is also called common-pole structure in the literature and it leads to simpler realizations when compared with other alternatives such as different poles for each $H_{ij}(s)$ or column-wise common poles, a deeper discussion on this issue can be found in (GRIVET-TALOCIA; GUSTAVSEN, 2016). Assigning a common pole set to a MIMO rational transfer matrix function is equivalent to the assumption that all entries

[23] Noiseless by assumption.
[24] By unified is meant a formulation valid in both the time and frequency domains.
[25] A matrix partial fraction expansion.

have similar resonance peaks, this hypotheses is reasonable for power transformers or even network equivalents. Moreover, because every pole of each individual transfer function is also a pole of the transfer matrix, the more entries have common poles the less they contribute to increasing the overall realization order owing to the lesser order of the least common denominator.

The problem data for the VF algorithm consists of measurements in accordance with Equation (2.10), also depicted in Figure (9). These measurements are allowed to be any of the network representations[26] alluded to earlier in this chapter and notation is easily adapted to reflect so. To ensure notational consistency both measurements and model predictions at a given frequency s_k are denoted $\mathbf{H}(s_k)$ and $\hat{\mathbf{H}}(s_k)$, respectively. As long as acceptable models are concerned, it is readily acknowledged that: $\mathbf{H}(s_k) \approx \hat{\mathbf{H}}(s_k)$ and $\mathbf{H}(s_k) - \hat{\mathbf{H}}(s_k) \approx 0$, *i.e.* model and measurement differ, their difference however must be small in some sense. To search for such a model, the VF algorithm has to solve the following minimization problem:

$$\underset{x}{\text{minimize}} \quad \sum_{i=1}^{P}\sum_{j=1}^{P}\sum_{k=1}^{K} |H_{i,j}(s_k) - \hat{H}_{i,j}(\theta, s_k)|^2, \tag{2.28}$$

whereby all parameters are lumped into the optimization variable θ which is the problem unknown and P, K are the upper limits of summation indices corresponding to the total number of ports and frequency samples respectively. Given the structure assumed for $\hat{\mathbf{H}}(s)$ in Equation (2.27) and substituting it into 2.28 yields:

$$\text{minimize} \quad \sum_{i=1}^{P}\sum_{j=1}^{P}\sum_{k=1}^{K} \left| H_{i,j}(s_k) - \left(R_{i,j,0} + \sum_{m=1}^{N} R_{i,j,m}\Phi_m(s) \right) \right|^2 . \tag{2.29}$$

The minimization problem in Equation (2.29) is readily recognized[27] as an unconstrained nonlinear programm. Consequently, achieving optimality in such circumstances proves to be elusive, for the solution process can sometimes be intractable or even prohibitively time-consuming. A workaround to avoid nonlinear programming techniques is to use the Sanathanan-Koerner iterations in which the problem stated in Equation (2.29) is solved in two stages: (i) a pole relocating mechanism for determining the denominator coefficients and (ii) a batch linear estimation of numerator coefficients. The goal of splitting the solution process into two stages resides in that each stage entails the solution of a *linear in the parameters* problem.

The first stage revolves around the determination of the dynamic modes or system's poles. To that end, a user-prescribed dynamic order must be assigned so that the

[26] Admittance, impedance, scattering *et cetera.*
[27] Some parameters appear in the denominator.

algorithm linearly or logarithmically places a corresponding number of dynamic modes along the frequency axis within the measurement frequency band. These poles are then relocated by means of the SK-iterations, the number of iteration is also user-prescribed. Upon convergence the numerator is fixed and stage two begins. The algorithm also enables the modeler to fully prescribe[28] the poles, *i.e.* the number of poles as well as their location along the frequency axis, thus skipping the SK-iterations. [29]

Once the poles are fixed, the remaining coefficients in Equation (2.29) can be determined by a batch-mode linear least-squares for the matrix containg the basis functions (regressors) is one and the same for all entries $H_{ij}(s)$. A number of tricks and tweaks are applied in each stage in the actual VF implementation out which some are noteworthy:

- The pole relocation mechanism employs a QR factorization which numerically orthonormalizes the pole-residue basis thus reducing the number of arithmetic operations performed and improving the numerical conditiong of the matrices involved given rise to the so called Fast Vector Fitting[30](DESCHRIJVER et al., 2008);
- When Equation (2.29) is evaluated at the set of frequency points the resulting quantities span many orders of magnitude which is particularly detrimental to the numerics involved. To mitigate these effects user-prescribed weighting funtions can be applied.
- The square matrix function $\mathbf{H}(s)$ is assumed to be symmetric thus reducing the number of arithmetic operations by performing computations only for the triangular part.

Despite the fact that the VF algorithm works primarily on a pole-residue basis, *i.e.* all parameters in the estimation process are $\{\mathbf{R}_m\}_{m=0}^{N}$ and $\{a_m\}_{m=1}^{N}$, the latter being equivalent to $\{\Phi_m(s)\}_{m=1}^{N}$, this pole-residue structure is readily converted into a state-space realization. The conversion procedure is best explained with illustrations in (GUSTAVSEN; SEMLYEN, 2004) and (GUSTAVSEN; SEMLYEN, 2009a). An outline of the equivalence is as follows:

[28] This may prove useful for experienced modelers who can spot pole locations simply by plotting the frequency response curve corresponding to measured data. Any dynamic mode lying beyond the measurement band remains elusive, though.

[29] Despite the simple description of this paragraph, pole relocation is the subject of current research in the identification community. However, this brief account should be enough for the purposes of this document and further details are skipped altogether.

[30] This puts the classical Vector Fitting in a common footing with Orthonormal Vector Fitting in which the orthonormalization is performed algebraically. In fact, the numerical orthonormalization is more interesting for the state-space realization thus obtained retains exploitable sparsity structure, which is false for the OVF.

$$\sum_{m=1}^{N} \mathbf{R}_m \Phi_m(s) = [\mathbf{R}_1 \dots \mathbf{R}_N] \begin{bmatrix} \Phi_1(s) & 0 & 0 & 0 & 0 & 0 & 0 \\ 0 & \ddots & 0 & 0 & 0 & 0 & 0 \\ 0 & 0 & \Phi_1(s) & 0 & 0 & 0 & 0 \\ 0 & 0 & 0 & \ddots & 0 & 0 & 0 \\ 0 & 0 & 0 & 0 & \Phi_N(s) & 0 & 0 \\ 0 & 0 & 0 & 0 & 0 & \ddots & 0 \\ 0 & & & 0 & 0 & 0 & \Phi_N(s) \end{bmatrix} \begin{bmatrix} \mathbf{I} \\ \vdots \\ \mathbf{I} \end{bmatrix}$$

$$\sum_{m=1}^{N} \mathbf{R}_m \Phi_m(s) = [\mathbf{R}_1 \dots \mathbf{R}_N] \left(s\mathbf{I} - \mathbf{A}\right)^{-1} \mathbf{B}$$

$$\sum_{m=1}^{N} \mathbf{R}_m \Phi_m(s) = \mathbf{C} \left(s\mathbf{I} - \mathbf{A}\right)^{-1} \mathbf{B}.$$

To complete the equivalence it is easily noticed that simple relabelling yields:

$$\begin{aligned} \mathbf{R}_0 + \sum_{m=1}^{N} \mathbf{R}_m \Phi_m(s) =& \mathbf{R}_0 + \mathbf{C} \left(s\mathbf{I} - \mathbf{A}\right)^{-1} \mathbf{B} \\ =& \mathbf{D} + \mathbf{C} \left(s\mathbf{I} - \mathbf{A}\right)^{-1} \mathbf{B}. \end{aligned}$$

By way of illustration, assuming a three port ($P = 3$) with three dynamic modes ($N = 3$) $\{a_1, a_2, \bar{a}_2\}$[31], the pole-residue series expansion has an associated state-space realization readily obtained as follows:

$$\begin{aligned} \hat{\mathbf{H}}(s) =& \begin{bmatrix} \hat{H}_{11}(s) & \hat{H}_{12}(s) & \hat{H}_{13}(s) \\ \hat{H}_{21}(s) & \hat{H}_{22}(s) & \hat{H}_{23}(s) \\ \hat{H}_{31}(s) & \hat{H}_{32}(s) & \hat{H}_{33}(s) \end{bmatrix} \\ =& \mathbf{R}_0 + \sum_{m=1}^{N} \mathbf{R}_m \Phi_m(s) \\ =& \begin{bmatrix} R_{110} & R_{120} & R_{130} \\ R_{210} & R_{220} & R_{230} \\ R_{310} & R_{320} & R_{330} \end{bmatrix} + \frac{1}{s - a_1} \begin{bmatrix} R_{111} & R_{121} & R_{131} \\ R_{211} & R_{221} & R_{231} \\ R_{311} & R_{321} & R_{331} \end{bmatrix} + \frac{1}{s - a_2} \begin{bmatrix} R_{112} & R_{122} & R_{132} \\ R_{212} & R_{222} & R_{232} \\ R_{312} & R_{322} & R_{332} \end{bmatrix} + \frac{1}{s - \bar{a}_2} \begin{bmatrix} \bar{R}_{112} & \bar{R}_{122} & \bar{R}_{132} \\ \bar{R}_{212} & \bar{R}_{222} & \bar{R}_{232} \\ \bar{R}_{312} & \bar{R}_{322} & \bar{R}_{332} \end{bmatrix} \end{aligned}$$

which is the pole-residue matrix transfer function. After a few rearrangements and presenting it in the time domain it takes on the following form:

[31] The first mode is pure damping whereas the remaining modes are oscillatory in nature and complex conjugates, as indicated by the bar hoovering over the third mode.

$$
[\dot{x}] = \begin{bmatrix}
a_1 & 0 & 0 & 0 & 0 & 0 & 0 & 0 & 0 \\
0 & a_1 & 0 & 0 & 0 & 0 & 0 & 0 & 0 \\
0 & 0 & a_1 & 0 & 0 & 0 & 0 & 0 & 0 \\
0 & 0 & 0 & a_2 & 0 & 0 & 0 & 0 & 0 \\
0 & 0 & 0 & 0 & a_2 & 0 & 0 & 0 & 0 \\
0 & 0 & 0 & 0 & 0 & a_2 & 0 & 0 & 0 \\
0 & 0 & 0 & 0 & 0 & 0 & \bar{a}_2 & 0 & 0 \\
0 & 0 & 0 & 0 & 0 & 0 & 0 & \bar{a}_2 & 0 \\
0 & 0 & 0 & 0 & 0 & 0 & 0 & 0 & \bar{a}_2
\end{bmatrix} [x] + \begin{bmatrix}
1 & 0 & 0 \\
0 & 1 & 0 \\
0 & 0 & 1 \\
1 & 0 & 0 \\
0 & 1 & 0 \\
0 & 0 & 1 \\
1 & 0 & 0 \\
0 & 1 & 0 \\
0 & 0 & 1
\end{bmatrix} [u]
$$

$$
[y] = \begin{bmatrix}
R_{111} & R_{121} & R_{131} & R_{112} & R_{122} & R_{132} & \bar{R}_{112} & \bar{R}_{122} & \bar{R}_{132} \\
R_{211} & R_{221} & R_{231} & R_{212} & R_{222} & R_{232} & \bar{R}_{212} & \bar{R}_{222} & \bar{R}_{232} \\
R_{311} & R_{321} & R_{331} & R_{312} & R_{322} & R_{332} & \bar{R}_{312} & \bar{R}_{322} & \bar{R}_{332}
\end{bmatrix} [x] + \begin{bmatrix}
R_{110} & R_{120} & R_{130} \\
R_{210} & R_{220} & R_{230} \\
R_{310} & R_{320} & R_{330}
\end{bmatrix} [u]
$$

Inspection of this realization reveals that it is a complex-coefficient state-space realization. Despite the immediate equivalence between the pole-residue form and the state-space form, the VF algorithm does a permutation[32] to the columns of matrices $(\mathbf{A}, \mathbf{B}, \mathbf{C})$ so that the poles appear sequentially for each input, *i.e.* a special kind of a column-wise realization whereby the columns have the same poles:

$$
[\dot{x}] = \begin{bmatrix}
a_1 & 0 & 0 & 0 & 0 & 0 & 0 & 0 & 0 \\
0 & a_2 & 0 & 0 & 0 & 0 & 0 & 0 & 0 \\
0 & 0 & \bar{a}_2 & 0 & 0 & 0 & 0 & 0 & 0 \\
0 & 0 & 0 & a_1 & 0 & 0 & 0 & 0 & 0 \\
0 & 0 & 0 & 0 & a_2 & 0 & 0 & 0 & 0 \\
0 & 0 & 0 & 0 & 0 & \bar{a}_2 & 0 & 0 & 0 \\
0 & 0 & 0 & 0 & 0 & 0 & a_1 & 0 & 0 \\
0 & 0 & 0 & 0 & 0 & 0 & 0 & a_2 & 0 \\
0 & 0 & 0 & 0 & 0 & 0 & 0 & 0 & \bar{a}_2
\end{bmatrix} [x] + \begin{bmatrix}
1 & 0 & 0 \\
1 & 0 & 0 \\
1 & 0 & 0 \\
0 & 1 & 0 \\
0 & 1 & 0 \\
0 & 1 & 0 \\
0 & 0 & 1 \\
0 & 0 & 1 \\
0 & 0 & 1
\end{bmatrix} [u]
$$

$$
[y] = \begin{bmatrix}
R_{111} & R_{112} & \bar{R}_{112} & R_{121} & R_{122} & \bar{R}_{122} & R_{131} & R_{132} & \bar{R}_{132} \\
R_{211} & R_{212} & \bar{R}_{212} & R_{221} & R_{222} & \bar{R}_{222} & R_{231} & R_{232} & \bar{R}_{232} \\
R_{311} & R_{312} & \bar{R}_{312} & R_{321} & R_{322} & \bar{R}_{322} & R_{331} & R_{332} & \bar{R}_{332}
\end{bmatrix} [x] + \begin{bmatrix}
R_{110} & R_{120} & R_{130} \\
R_{210} & R_{220} & R_{230} \\
R_{310} & R_{320} & R_{330}
\end{bmatrix} [u]
$$

This latter realization is the one that comes as output of the VF algorithm but the user is also entitled to choose a real-coefficient state-space realization as output since complex poles lack a direct physical significance in time domain, consequently:

[32] To be pedantically accurate, it is a similarity transformation with a permutation matrix.

$$
[\dot{x}] = \begin{bmatrix}
a_1 & 0 & 0 & 0 & 0 & 0 & 0 & 0 & 0 \\
0 & Re(a_2) & Im(a_2) & 0 & 0 & 0 & 0 & 0 & 0 \\
0 & -Im(a_2) & Re(a_2) & 0 & 0 & 0 & 0 & 0 & 0 \\
0 & 0 & 0 & a_1 & 0 & 0 & 0 & 0 & 0 \\
0 & 0 & 0 & 0 & Re(a_2) & Im(a_2) & 0 & 0 & 0 \\
0 & 0 & 0 & 0 & -Im(a_2) & Re(a_2) & 0 & 0 & 0 \\
0 & 0 & 0 & 0 & 0 & 0 & a_1 & 0 & 0 \\
0 & 0 & 0 & 0 & 0 & 0 & 0 & Re(a_2) & Im(a_2) \\
0 & 0 & 0 & 0 & 0 & 0 & 0 & -Im(a_2) & Re(a_2)
\end{bmatrix} [x] + \begin{bmatrix}
1 & 0 & 0 \\ 2 & 0 & 0 \\ 0 & 0 & 0 \\ 0 & 1 & 0 \\ 0 & 2 & 0 \\ 0 & 0 & 0 \\ 0 & 0 & 1 \\ 0 & 0 & 2 \\ 0 & 0 & 0
\end{bmatrix} [u]
$$

$$
[y] = \begin{bmatrix}
R_{111} & \mathrm{Re}(R_{112}) & \mathrm{Im}(R_{112}) & R_{121} & \mathrm{Re}(R_{122}) & \mathrm{Im}(R_{122}) & R_{131} & \mathrm{Re}(R_{132}) & \mathrm{Im}(R_{132}) \\
R_{211} & \mathrm{Re}(R_{212}) & \mathrm{Im}(R_{212}) & R_{221} & \mathrm{Re}(R_{222}) & \mathrm{Im}(R_{222}) & R_{231} & \mathrm{Re}(R_{232}) & \mathrm{Im}(R_{232}) \\
R_{311} & \mathrm{Re}(R_{312}) & \mathrm{Im}(R_{312}) & R_{321} & \mathrm{Re}(R_{322}) & \mathrm{Im}(R_{322}) & R_{331} & \mathrm{Re}(R_{332}) & \mathrm{Im}(R_{332})
\end{bmatrix} [x] + \begin{bmatrix}
R_{110} & R_{120} & R_{130} \\ R_{210} & R_{220} & R_{230} \\ R_{310} & R_{320} & R_{330}
\end{bmatrix} [u]
$$

which is obtained by means of a similarity transformation $\mathbf{x} = \mathbf{T}\tilde{\mathbf{x}}$ as follows[33]:

$$
\tilde{\mathbf{A}} = \mathbf{T}^{-1}\mathbf{A}\mathbf{T}
$$

$$
= \begin{bmatrix}
1 & 0 & 0 & 0 & 0 & 0 & 0 & 0 & 0 \\
0 & 1 & 1 & 0 & 0 & 0 & 0 & 0 & 0 \\
0 & j & -j & 0 & 0 & 0 & 0 & 0 & 0 \\
0 & 0 & 0 & 1 & 0 & 0 & 0 & 0 & 0 \\
0 & 0 & 0 & 0 & 1 & 1 & 0 & 0 & 0 \\
0 & 0 & 0 & 0 & j & -j & 0 & 0 & 0 \\
0 & 0 & 0 & 0 & 0 & 0 & 1 & 0 & 0 \\
0 & 0 & 0 & 0 & 0 & 0 & 0 & 1 & 1 \\
0 & 0 & 0 & 0 & 0 & 0 & 0 & j & -j
\end{bmatrix} \begin{bmatrix}
a_1 & 0 & 0 & 0 & 0 & 0 & 0 & 0 & 0 \\
0 & a_2 & 0 & 0 & 0 & 0 & 0 & 0 & 0 \\
0 & 0 & \bar{a}_2 & 0 & 0 & 0 & 0 & 0 & 0 \\
0 & 0 & 0 & a_1 & 0 & 0 & 0 & 0 & 0 \\
0 & 0 & 0 & 0 & a_2 & 0 & 0 & 0 & 0 \\
0 & 0 & 0 & 0 & 0 & \bar{a}_2 & 0 & 0 & 0 \\
0 & 0 & 0 & 0 & 0 & 0 & a_1 & 0 & 0 \\
0 & 0 & 0 & 0 & 0 & 0 & 0 & a_2 & 0 \\
0 & 0 & 0 & 0 & 0 & 0 & 0 & 0 & \bar{a}_2
\end{bmatrix} \begin{bmatrix}
1 & 0 & 0 & 0 & 0 & 0 & 0 & 0 & 0 \\
0 & \frac{1}{2} & -j\frac{1}{2} & 0 & 0 & 0 & 0 & 0 & 0 \\
0 & \frac{1}{2} & j\frac{1}{2} & 0 & 0 & 0 & 0 & 0 & 0 \\
0 & 0 & 0 & 1 & 0 & 0 & 0 & 0 & 0 \\
0 & 0 & 0 & 0 & \frac{1}{2} & -j\frac{1}{2} & 0 & 0 & 0 \\
0 & 0 & 0 & 0 & \frac{1}{2} & j\frac{1}{2} & 0 & 0 & 0 \\
0 & 0 & 0 & 0 & 0 & 0 & 1 & 0 & 0 \\
0 & 0 & 0 & 0 & 0 & 0 & 0 & \frac{1}{2} & -j\frac{1}{2} \\
0 & 0 & 0 & 0 & 0 & 0 & 0 & \frac{1}{2} & j\frac{1}{2}
\end{bmatrix}
$$

On exit and after successful convergence, the user has two alternative system representations available which can be used in a number of different purposes like time domain simulations by discretization methods, numerical recursive convolution and time-domain trapezoidal integration of state-space differential equations. According to (ANDERSON; VONGPANITLERD, 2006), a state-space realization usually leads to faster and easier computation of time-domain integrations compared with Laplace transforms and their inverses. Furthermore, the state-space approach furnishes a clearer understanding of the internal content of a network description by displaying the model's memory explicitly and is fully amenable to computation underpinned by its matrix structure. The classical Laplace-transform approach places stronger reliance on complex variable analysis instead.

Henceforth the foregoing real-coefficient state-space realization is denoted the VF realization, since it is the output of the VF algorithm. Such realization has system theoretic properties that are important for future developments are therefore highlighted. These properties are best described in (GRIVET-TALOCIA; GUSTAVSEN, 2016)[34]. Therefore, the VF realization is:

[33] Real-coefficient matrices $\tilde{\mathbf{B}}$ and $\tilde{\mathbf{C}}$ can also be readily obtained: $\tilde{\mathbf{B}} = \mathbf{T}^{-1}\mathbf{B}$ and $\tilde{\mathbf{C}} = \mathbf{C}\mathbf{T}$.

[34] This reference also presents a comparison among the multi-SISO, multi-SIMO and minimal MIMO, the latter being the one herein adopted.

- Minimal (controllable and observable);
- Stable;
- Causal;
- Reciprocal (symmetric).

All these properties are granted by construction. A further discussion on reciprocal (symmetric) realizations e their implications is available in (IHLENFELD; OLIVEIRA, 2019). In this list of realization properties, there is a noticeable absence, namely dissipativity or passivity: the vector fitting algorithm is not capable of ensuring that the realization possesses this essential property[35]. As a last parting thought on the VF realization, its numerical properties are also worth mentioning, in particular its sparsity pattern which is used in subsequent chapters to tackle the challenging problem of passivity enforcement.

2.5 Error Metrics

We use this section to summarize two conventional error metrics used to measure algorithmic prediction performance, namely the Root Mean Squared Error (RMSE) and the total sum absolute value quadratic error. Recalling that measured data and model predictions at a given frequency s_k are respectively denoted $\mathbf{H}(s_k)$ and $\hat{\mathbf{H}}(s_k)$, these two error metrics can be used to characterize the "distance" between model prediction and actual measured data, *i.e.* how much their frequency responses differ or how well $\hat{\mathbf{H}}(s_k)$ approximates $\mathbf{H}(s_k)$.

The RMSE index represents the sample standard deviation of the differences between predicted values and observed values, usually called residuals. Mathematically, it is calculated using this formula[36]:

$$\text{RMSE} = \sqrt{\frac{1}{P^2K}\sum_{i=1}^{P}\sum_{j=1}^{P}\sum_{k=1}^{K}\left(\left|\hat{H}_{ij}(jw_k) - H_{ij}(jw_k)\right|\right)^2}. \tag{2.30}$$

The total sum absolute value quadratic error is actual cost function minimized by the approximation algorithms so that we adopt the shorthand Cost Function for it and calculated it as:

$$\text{Cost Function} = \sum_{i=1}^{P}\sum_{j=1}^{P}\sum_{k=1}^{K}\left|\hat{H}_{ij}(jw_k) - H_{ij}(jw_k)\right|^2. \tag{2.31}$$

[35] Sometimes the VF realization is passive, but this is quite by accident as the algorithm has no means to guarantee so.

[36] Note this formula is tailored to the data structure used for MIMO frequency-response measurements.

2.6 A few closing remarks

This chapter contains some fundamental and background concepts that serve the purpose of elucidating the particular kind of systems being modeled as well as some characteristics of the data to be used in the main identification process. The first section is essentially a recapitulation of linear systems and what is meant by a linear dynamical system throughout this document. The subsequent section narrows the sort of systems under considerations further still, *viz.* passive linear systems, a particular class within linear systems. The idea of dissipativity and its particular case denoted passivity are presented for either system representation adopted in the document, and they are equivalent[37]:

$$\mathbf{H}(s) \succeq 0 \iff \begin{bmatrix} -\mathbf{A}^T\mathbf{P} - \mathbf{P}\mathbf{A} & -\mathbf{P}\mathbf{B} + \mathbf{C}^T \\ -\mathbf{B}^T\mathbf{P} + \mathbf{C} & \mathbf{D} + \mathbf{D}^T \end{bmatrix} \succeq 0, \mathbf{P} \succeq 0.$$

By equivalence is meant a time-domain passive system is also a frequency domain passive system, and *vice versa*. Passivity is also shown to be a stronger and more general system property when compared with stability.

Subsequently, an illustration of some basic applications of matrices (Linear Algebra) to circuit theory is made when the customary sets of network parameters and their basic properties are discussed. The difference from one parameter set to another lies in the choice of the independent and dependent variables. Nonetheless, there are some practical issues dictating the parameter choice which is best suited to the application at hand. According to (GUSTAVSEN; SILVA, 2013) and (ZHONGYUAN; FANGCHENG; GUISHU, 2013), there arise a number of difficulties when measuring admittances and impedances at frequencies above 1 MHz. Equations (2.13) and (2.16) require short- and open-circuit conditions for determining the admittance, impedance and hybrid parameters which can be exceedingly difficult to be accurately achieved over a broad band of frequencies since short-circuits behave like “inductors” while open-circuits present leakage and “stray capacitances”. Such difficulties can be circumvented by employing the scattering parameters, since these do not depend on open or short circuit conditions to characterize a network; instead, matched loads are used, as in equation (2.26). These terminations provide numerous practical advantages over the open-circuit and short-circuit terminations when higher frequencies are used. Moreover, from a theoretical standpoint, at higher frequencies the lumped-parameter assumption for a linear network does not exactly hold. Therefore, the scattering parameters of a network characterization are necessary so that the characterization be accurate also at higher frequencies. In (CARLIN, 1956), the author emphasizes that all passive networks possess scattering parameters and, at higher frequencies, incident and reflected

[37] Idem for the scattering case.

parameters play dominant roles while the usual voltage-current description is of lesser importance.

Despite practical considerations that must taken into account, there exist conversion relations for the different network parameters (YZHS) which can be found in (GUSTAVSEN; SILVA, 2013) and (MAVADDAT, 1996). As far as pure algebra is concerned, parameter conversion poses no problem but for the obvious assumptions of matrix invertibility and so on. However, in the realm of numerical matrix analysis and estimation, this can be problematic. In reference (GUSTAVSEN; SILVA, 2013), the author stresses that, in addition to the initial parameter estimation error, a parameter conversion can contribute to even larger errors. This conversion issue can be as subtle as eigenvalue deterioration, e.g., in (GUSTAVSEN, 2014), there is discussion on reducing the error magnification due to inaccurately measured small eigenvalues. Should the operation $\mathbf{Z} = \mathbf{Y}^{-1}$ be necessarily carried out, small eigenvalues of $\mathbf{Y}$ become large eigenvalues of $\mathbf{Z}$ thus enlarging the overall error as well. In (IHLENFELD et al., 2019), there is a discussion concerning measurement issues such as terminations, symmetry and number of ports/terminals in an applied context. In particular, it is shown that measured admittance matrices are not necessarily symmetric due to difficulties associated with the measurement setup. In (OLIVEIRA; IHLENFELD; RODRIGUES, 2019) there is a another discussion concerning the use different network characterizations which are in theory convergent, namely admittance and scattering parameters, but in practice the measurements do not yield the same result. Furthermore, this latter conference paper makes the case in favour of considering scattering parameters for they extend enormously the scope of passivity analysis and enforcement methods to embrace systems that do not have measurable admittance and impedance variables. Except for these scarse remarks and references to the literature, the problem of how measurements are actually done (data acquisition) is sidestepped completely in subsequent chapters.

In the context of power transformers, it is customary to adopt the admittance representation, the reason why favouring admittance matrices in this discussion. Seen as an n-port, the data-acquisition process for a transformer comprises experimentally determining the frequency-responses for all n^2 entries of the admittance matrix at every frequency in the sequence $\{w_k\}_{k=1}^{K}$ of all measured frequencies. Specially favourable to the acquisition process, the experimenter need not determine n^2K admittances, since power transformers are in theory special cases of reciprocal networks. In matrix language, this translates as the admittance matrix $\mathbf{Y}$ of a power transformer being a symmetric one.

According to (HUELSMAN, 2011), reciprocal networks allow the interchange of input (excitation) and output (response) while their ratio remains unchanged. Hence, reciprocity implies $Y_{il}(jw) = Y_{li}(jw)$, i.e., if the excitation is applied at the ith port and

the corresponding response measured at the l-port, or alternatively in reversed order, the same resulting ratio (admittance) is obtained. Therefore, the experiment is only performed for the triangular portion, substantially reducing the number of measurements[38].

The vector fitting algorithm and its associated realization are briefly discussed. It is not the purpose of this research to dissect the inner workings of the VF algorithm in greater detail for it is well documented in the literature, specially in the references listed earlier, hence in the outline herein offered emphasis is placed on what properties the realization thus obtained does and does not possess.

As a last parting thought, one should bear in mind that passivity must be reflected either for the data or the model irrespective of the system's representation being adopted since they are essentially different facets of the same object. Since these alternative representations can be converted into one another, passivity must remain a common existing thread between them.

[38] As stated a few paragraphs earlier, reciprocity or symmetry need not hold in practice due to measurement issues, but can be taken as a working assumption.

3 CONVEX OPTIMIZATION AND GRAPH THEORY

This chapter is devoted to succintly expose a collection of essential theoretical results from both Convex Optimization and Graph Theories that should be instrumental to further developments and are used to underpin the proposed methodologies of subsequent chapters. Therefore, no attempt is made so as to give the most general form of the results as well as furnish all the details, but rather only subsidize some methods proposed in future chapters in a coherent manner.

3.1 Convex Optimization

Convex Optimization or Convex Programming comprises a special class of mathematical optimization problems encompassing least-squares (LS), linear programming (LP), convex quadratic programming (QP), second-order cone programming (SOCP) and semidefinite programming (SDP). In constrast, despite being a larger class of problems subsuming all of the aforementioned predecessors, it is a special subclass of nonlinear programming (NLP). While general nonlinear programs are difficult to solve, convex programms can be efficiently and reliably solved. Of particular interest is the fact that once convexity be established for a given problem, local optima are guaranteed to be global optima, no similar statement can be made for general nonconvex NLPs. As convex methods will be applied throughout this work, an introductory discussion of this rich body of theory is needed. The results we present have been collected from a few selected sources: (BOYD; VANDENBERGHE, 2004) and (BERTSEKAS, 2009) for the basic results; (NESTEROV; NEMEROVSKI, 1994), (BEN-TAL; NEMIROVSKI, 2001) and (CALAFIORE; GHAOUI, 2014) for conic problems and equivalences.

A mathematical optimization problem is herein assumed to have the general canonical form:

$$\begin{aligned} \text{minimize} \quad & f_0(\mathbf{x}) \\ \text{subject to} \quad & f_i(\mathbf{x}) \leq b_i, \quad i = 1, \ldots, m. \\ & h_j(\mathbf{x}) = b_j, \quad j = 1, \ldots, p. \\ & \mathbf{x} \in \mathcal{D} \end{aligned} \tag{3.1}$$

In Equation (3.1), $\mathbf{x} \in \mathcal{D}$ is the *optimization variable* with $\mathcal{D}$ representing some domain of interest, *viz.* $\mathcal{D} \subset \mathbb{R}^n$. The standard form optimization problem has an implicit constraint:

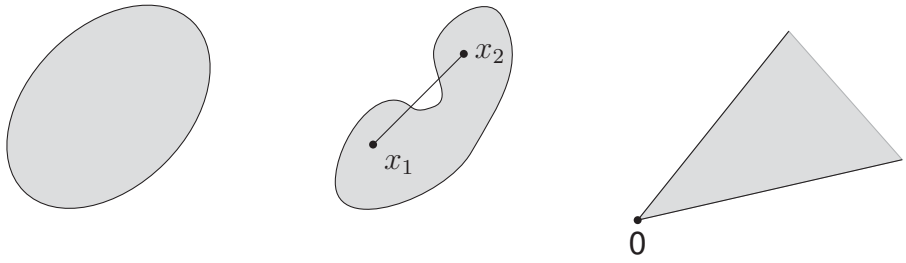

Figure 10 – Left: A convex set ellipse. Middle: A non-convex set. Right: A convex cone.

$$\mathbf{x} \in \mathcal{D} = \left(\bigcap_{i=0}^{m} \mathbf{dom} f_i\right) \cap \left(\bigcap_{i=1}^{p} \mathbf{dom} h_i\right)$$

The function $f_0 : \mathbb{R}^n \mapsto \mathbb{R}$ denotes the *objective function*, each $f_i : \mathbb{R}^n \mapsto \mathbb{R}$ and $h_j : \mathbb{R}^n \mapsto \mathbb{R}$ correspond to respectively an *inequality and equality constraint function* with its associated *bound* or limit b_i and b_j.

Problem (3.1) is a convex optimization problem when the equality constraints functions h_j be affine and the objective f_0 as well as the inequality constraint functions g_i be all convex functions. Establishing convexity of a given function requires convexity of its domain. As Figure (10) shows, a set C is convex if and only if all points along the line segment between any two points in it (a *convex combination*) also belong to it. Along this dissertation, sets of particular topologies will be of interest, hence suppose $C \subseteq \mathbb{R}^n$ is a given set and points $x_1, \ldots, x_k \in C$, then the set C qualifies as:

- *an affine set* provided it contains every affine combination of its points: $\theta_1 x_1 + \cdots + \theta_k x_k$ with $\theta_1 + \cdots + \theta_k = 1$;
- *a convex set* provided it contains every convex combination of its points: $\theta_1 x_1 + \cdots + \theta_k x_k$ with $\theta_1 + \cdots + \theta_k = 1$ and $\theta_i \geq 0, i = 1, \ldots, k$;
- *a conic set, nonnegative homogeneous or simply a cone* provided it contains every conic combination (or nonnegative linear combination) of its points: $\theta_1 x_1 + \cdots + \theta_k x_k$ with $\theta_i \geq 0, i = 1, \ldots, k$;

Convex sets also arise as the result of operations over other convex sets, *i.e.* a convex calculus. Some important operations to build convex domains for convex optimization problems are: intersection[1], affine compositions of convex sets (*e.g.* scaling, translation[2]), projection[3] and Cartesian products of convex sets.

[1] The solution to a convex optimization problem lies in an intersection of many convex sets.
[2] As strict positive definiteness is numerically challenging, this property can be used to shift the exact zero to some small positive constant.
[3] A sparse positive-semidefinite matrix is nothing but a projection of the full matrix onto its non-zero coordinates.

A given function $f(\cdot)$ is convex provided its domain is a convex set and additionally it satisfies the following inequality[4]:

$$f(\alpha x_1 + \beta x_2) \leq \alpha f(x_1) + \beta f(x_2) \tag{3.2}$$

for any two distinct points $x_1, x_2 \in \mathbb{R}^n$ and all $\alpha, \beta \in \mathbb{R}$ such that $\alpha + \beta = 1,\ \alpha \geq 0,\ \beta \geq 0$. This basic inequality can also be alternatively written as[5]

$$f(\theta x_1 + (1-\theta)x_2) \leq \theta f(x_1) + (1-\theta) f(x_2) \tag{3.3}$$

which must hold for $0 \leq \theta \leq 1$, thus $f(\cdot)$ is a convex function. Constraining the parameter θ to that interval corresponds to taking as argument only the points along the closed line segment between x_1 and x_2 which lies above the graph of $f(\cdot)$, as depicted in Figure (11). There are numerous and imediate extentions of the inequalities above, *e.g.* there could be more than just two points forming the argument. In general, the inequality above should be satisfied for an argument of the form $\theta_1 x_1 + \cdots + \theta_k x_k$, provided $\theta_1 + \cdots + \theta_k = 1$ and $\theta_i \geq 0, i = 1, \ldots, k$, *i.e.* a *convex combination* of the points $x_1, \ldots, x_k$. This inequality has a simple interpretation: the image under $f(\cdot)$ of a convex combination of any points in its convex domain is either less than or equal the same convex combination of the image of each the points under $f(\cdot)$. One can think of the convex combination as some kind of weighted average. In this latter sense, what Jansen's inequality states is that the image under $f(\cdot)$ of the weighted average is less than the weighted average of $f(\cdot)$. Such combinations of points can be used to establish convexity or some other topological property of a given set.

Given a function $f(\cdot)$ whose convexity is to be established, there exist five canonical ways of proving it to be a convex function: Jensen's Inequality, first- and second-order conditions (provided $f(\cdot)$ is differentiable), restriction to a line, convexity of its sublevel sets and expressing $f(\cdot)$ either in its epigraph form or as the pointwise supremum of a family of affine functions. All these methods can be found in (BOYD; VANDENBERGHE, 2004) and (BERTSEKAS, 2009), they are useful because what is central in convex optimization is to recognize that the problem can be formulated as a convex problem, a task which reduces to recognizing when a function is convex, which is the essential skill needed. As an example, a norm $f(\cdot) = \|\cdot\|$ can be easily proven to be a convex function by means of Jansen's Inequality (Equation (3.3)):

$$\|\theta x_1 + (1-\theta)x_2\| \leq \|\theta x_1\| + \|(1-\theta)x_2\| = \theta\|x_1\| + (1-\theta)\|x_2\|,$$

[4] This inequality is also called Jansen's Inequality.
[5] Idem.

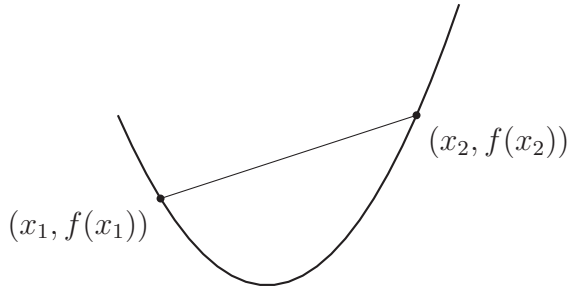

Figure 11 – A convex function and a geometric view of a chord corresponding to points satisfying the inequality 3.2.

whereby $f : \mathbb{R}^n \mapsto \mathbb{R}$ is any norm, $0 \leq \theta \leq 1$ and both the inequality and equality follow from basic norm properties, namely the triangle inequality and homogeneity properties. Convex functions can be thought of as convex atoms that can be combined into more complex convex functions by means of operations that preserve convexity, such operations range from simple addition, scaling, non-negative weighted sums, pointwise maximum or supremum to composition with affine functions.

Turning the attention back to some convex sets and their topologies, some notable convex sets of interest are the *second-order cone*[6] and the *positive-semidefinite cone*.

Definition 22 *The second-order cone is defined as the norm cone for the Euclidean norm:*

$$
\begin{aligned}
C &= \{(x,t) \in \mathbb{R}^{n+1} \mid \|x\|_2 \leq t\} \\
&= \left\{ \begin{bmatrix} x \\ t \end{bmatrix} \;\middle|\; \begin{bmatrix} x \\ t \end{bmatrix}^T \begin{bmatrix} \boldsymbol{I} & 0 \\ 0 & -1 \end{bmatrix} \begin{bmatrix} x \\ t \end{bmatrix} \right\}
\end{aligned}
$$

An example of a second-order cone for $n = 2$ is depicted in Figure (12).

[6] Also called the quadratic cone, Lorentz cone or ice-cream cone.

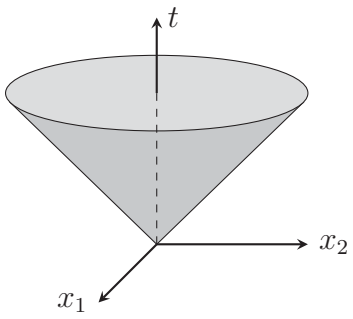

Figure 12 – The second-order cone in $\mathbb{R}^3$.

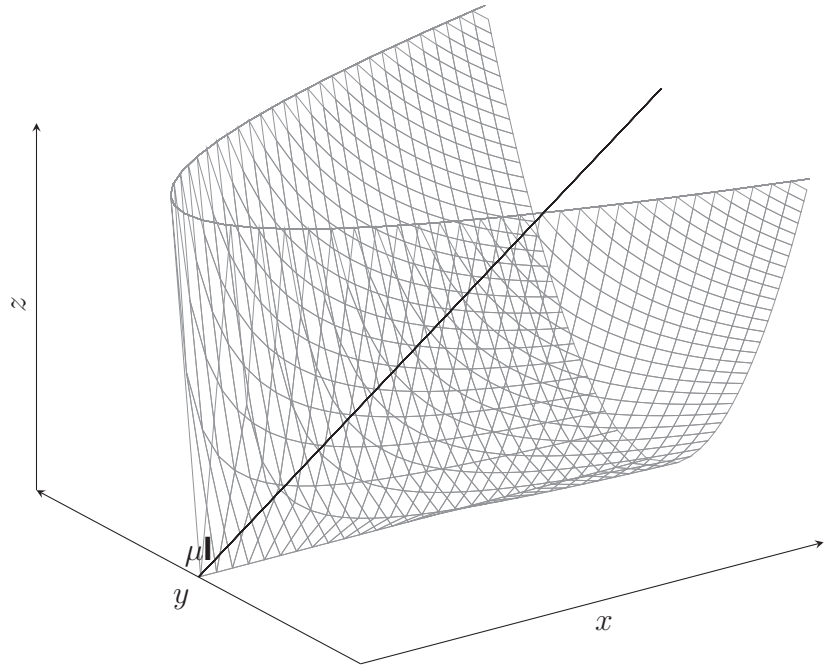

Figure 13 – Boundary of the PSD cone in $\mathbb{S}^2$

Definition 23 *The Positive-semidefinite cone is defined by:*

$$\mathbb{S}_+^n = \{\boldsymbol{X} \in \mathbb{R}^{n \times n} \mid \boldsymbol{X} \succeq 0\}$$

The boundary of the positive-semidefinite cone for $n = 2$ is displayed in Figure (13).

A cone $\mathcal{K}$ is denoted a *proper cone* if it satisfies the following properties:

- $\mathcal{K}$ is convex;
- $\mathcal{K}$ is closed;
- $\mathcal{K}$ has non-empty interior;
- $\mathcal{K}$ is ponted ($x \in \mathcal{K}, -x \in \mathcal{K} \implies x = 0$).

Proper cones play a major role in constructing generalized inequalities to more general sets other than plain $\mathbb{R}$ owing to their assymetric topology, *i.e.* they allow values to be taken in one direction[7] but not the other. Such *generalized inequalities* are partial orderings as opposed to the total or linear scalar orderings in $\mathbb{R}$, *i.e.* not all properties transcend to higher dimensions. Emphasis is herein placed on partial orderings of this

[7] Also called a recession direction or recession cone.

kind: $\mathbf{A} \preceq_{\mathcal{K}} \mathbf{B} \iff \mathbf{B} - \mathbf{A} \in \mathcal{K}$ with $\mathcal{K} = \mathbb{S}_+^n$[8]. As this ordering appears throughout, the subscript $\preceq_{\mathcal{K}}$ is dropped. Generalized inequalities are used to build generalized inequality constraints in optimization problems, *e.g.* semidefinite constraints using functions of a matrix variable like $g_i(\mathbf{X}) \succeq_{\mathcal{K}} 0$ with $\mathcal{K} = \mathbb{S}_+^n$.

A notion that will be important to some arguments in later chapters is that of monotonicity for generalized inequalities, in particular *Matrix Monotone Functions*. Using the notion of a generalized inequality, one can easily extend monotonicity of functions in $\mathbb{R}$ to more a general setting, say $\mathbb{R}^n$ or $\mathbb{S}_+^n$. A function $f : \mathbb{R}^n \mapsto \mathbb{R}$ is denoted $\mathcal{K} - \textit{nondecreasing}$[9] provided:

$$\mathbf{x} \preceq_{\mathcal{K}} \mathbf{y} \implies f(\mathbf{x}) \leq f(\mathbf{y}),$$

with $\mathcal{K}$ a cone of interest, *e.g.* $\mathcal{K} = \mathbb{S}_+^n$[10]. By way of example, two matrices satisfying the partial ordering $\mathbf{X} \preceq_{\mathcal{K}} \mathbf{Y}$ imply some scalar monotone function on this matrix space satisfy the usual total ordering $f(\mathbf{X}) \leq f(\mathbf{Y})$, a norm being a canonical instance.

3.2 Problem Families

To facilitate the recognition and association of convex problems with some concrete context as opposed to general mathematical definitions it is useful to think in terms of **problem families**. The most common problem families are listed in the sequence.

3.2.1 Linear Programming

Whenever all functions involved in a general optimization problem of the form defined by Equation (3.1) are affine, the problem is called a *Linear Programm*, LP for short. It is a particular class of a convex programm and takes on the form:

$$\begin{aligned} \text{minimize} \quad & \mathbf{c}^T\mathbf{x} + d \\ \text{subject to} \quad & \mathbf{G}\mathbf{x} \preceq \mathbf{h} \\ & \mathbf{A}\mathbf{x} = \mathbf{b} \end{aligned} \tag{3.4}$$

whereby the feasible set is a polyhedron and the solution is one of its vertices. The problem data consists of vectors $\mathbf{c} \in \mathbb{R}^n$, $\mathbf{h} \in \mathbb{R}^m$ and $\mathbf{b} \in \mathbb{R}^p$ as well as the matrices $\mathbf{G} \in \mathbb{R}^{m \times n}$ and $\mathbf{A} \in \mathbb{R}^{p \times n}$. Assuming $m \geq n$, the rough approximate number of arith-

[8] Such matrix inequalities do have strict versions as well, but numerical solvers have a working condition assuming only the non-strict version. Therefore, this presentation concentrates on the latter.

[9] *Mutatis mutandis*, similar remarks apply to nonincreasing and their respective strict cases.

[10] Note that the matrix cone $\mathcal{K} = S_+^n$ is a vector cone in $\mathbb{R}^{n(n+1)/2}$.

metic operations required to solve a linear program using an interior-point method is proportional to n^2m.

3.2.2 Quadratic Programming

A natural next level of generalization with respect to linear programms are quadratic programms, as shorthand QP. Not all QPs are convex optimization problems, hence whenever QP's are alluded to in this document, it is a convex QP what is actually meant:

$$\begin{aligned} \text{minimize} \quad & \frac{1}{2}\mathbf{x}^T\mathbf{P}\mathbf{x} + \mathbf{q}^T\mathbf{x} + r \\ \text{subject to} \quad & \mathbf{G}\mathbf{x} \preceq \mathbf{h} \\ & \mathbf{A}\mathbf{x} = \mathbf{b} \end{aligned} \tag{3.5}$$

which is convex quadratic provided $\mathbf{P} \in \mathbb{S}^n_+$, *i.e.* minimize a convex quadratic function over a polyhedron[11]. Note that by making $\mathbf{P} = 0$ one recovers an LP. Contrary to LP, the solutions need not be at a vertex of the polyhedron any more. In fact, the inequality constraints functions could also be convex quadratic as well in which case the problem is usually referred to as *quadratically constrained quadratic programm*, or QCQP for short.

Least-squares is a particular kind of QP, in fact an unconstrained QP, which possesses an analytical solution[12].

$$\text{minimize} \qquad f_0(\mathbf{x}) = \|\mathbf{A}\mathbf{x} - \mathbf{b}\|_2^2 = \sum_{i=1}^{m} (\mathbf{a}_i^T\mathbf{x} - b_i)^2 \tag{3.6}$$

with $\mathbf{A} \in \mathbb{R}^{m\times n}$ $(m \geq n)$, $\mathbf{a}_i^T$ are the rows of $\mathbf{A}$ and $\mathbf{x} \in \mathbb{R}^n$ is the optimization variable. As a standard QP, the objective can be written as $f_0(\mathbf{x}) = \mathbf{x}^T\mathbf{A}^T\mathbf{A}\mathbf{x} + 2\mathbf{b}^T\mathbf{A}\mathbf{x} + \mathbf{b}^T\mathbf{b}$, whose unconstrained verson has the well-known analytical solution via the pseudo-inverse.

The least-squares problem can be solved in a time approximately proportional to n^2m. The *weighted least-squares* cost:

$$\sum_{i=1}^{m} w_i(\mathbf{a}_i^T\mathbf{x} - b_i)^2$$

where $w_1, \ldots, w_m$ are positive. In applications like fitting admittance matrices these weights can be used to reflect different levels of magnitude across matrix elements.

[11] Polytope is another terminology, but some authors interchange the use between polyhedron and polytope. What matters is that the set be bounded.

[12] Should simple constraints like nonnegative solutions be added to the problem description, no analytical solutions exists anymore.

3.2.3 Second-Order Cone Programming

Another class of interest to problems that will be herein formulated are SOCPs of the form:

$$\begin{aligned} \text{minimize} \quad & \mathbf{f}^T\mathbf{x} \\ \text{subject to} \quad & \|\mathbf{A}_i\mathbf{x}+\mathbf{b}_i\|_2 \leq \mathbf{c}_i^T\mathbf{x}+d_i \quad i=1,\ldots,m. \\ & \mathbf{F}x = g \end{aligned} \tag{3.7}$$

with $\mathbf{x}, \mathbf{f}$ and $\mathbf{c}_i \in \mathbb{R}^n$, $\mathbf{A}_i \in \mathbb{R}^{n_i \times n}$, $\mathbf{F} \in \mathbb{R}^{p\times n}$, $\mathbf{b}_i \in \mathbb{R}_i^n$, $\mathbf{g} \in \mathbb{R}^p$ and $d_i \in \mathbb{R}$. Such inequalities are called second-order cone constraints since they are equivalent to constraining each pair $(\mathbf{A}_i\mathbf{x}+\mathbf{b}_i, \mathbf{c}_i^T\mathbf{x}+d_i)$ to lie in the corresponding second-order cone, as defined earlier. Note that if $n_i = 0$, the problem reduces to a simple LP. It is possible to write this problem in standard form by realizing that the second-order cone constraints can be rewritten as $g_i \leq 0$, with $g_i(\mathbf{x}) = \|\mathbf{A}_i\mathbf{x}+\mathbf{b}_i\|_2 - \mathbf{c}_i^T\mathbf{x} - d_i$. Note that SOCPs are yet another level of generalization for it is equivalent to a QP whenever all $\mathbf{c}_i = 0$ and to an LP whenever all $\mathbf{A}_i = 0$.

This second-order cone constraint can be readily written in explicit conic form by noting the equivalence between the constraints $\|\mathbf{A}_i\mathbf{x}+\mathbf{b}_i\|_2 \leq \mathbf{c}_i^T\mathbf{x}+d_i$ and $-(\mathbf{A}_i\mathbf{x}+\mathbf{b}_i, \mathbf{c}_i^T\mathbf{x}+d_i) \preceq_{\mathcal{K}_i} 0$, with $\mathcal{K}_i = \{(\mathbf{x},t) \in \mathbb{R}^{n+1} \mid \|\mathbf{x}\|_2 \leq t\}$.

3.2.4 Semidefinite Programming

A classical example of a conic problem is denoted a semidefinite programm, or SDP. In this particular instance, the problem inequalities are established with respect to the positive semidefinite cone $\mathcal{K} = \mathbb{S}_+^n$ and acquires the following form:

$$\begin{aligned} \text{minimize} \quad & \mathbf{c}^T\mathbf{x} \\ \text{subject to} \quad & \sum_{i=1}^{n} \mathbf{F}_i x_i + \mathbf{G} \preceq_{\mathcal{K}} 0 \\ & \mathbf{A}\mathbf{x} = \mathbf{b} \end{aligned} \tag{3.8}$$

which is a matrix inequality or a matrix ordering, thus the usual terminology **Linear Matrix Inequality**[13] or LMI for short.

Semidefinite Programming is the most general problem form addressed so far in this dissertation. It is also worthwhile to mention that all the predecessors can be converted to an SDP, this process is called *SDP embedding*. By way of example, two SDP embeddings are shown:

[13] The terminology LMI was coined by Jan C. Willems, see (WILLEMS, 1972a). Rigorously, this is an Affine Matrix Inequality.

LP

minimize $\mathbf{c}^T\mathbf{c}$

subject to $\mathbf{Ax} \preceq \mathbf{b}$

Equivalent SDP

minimize $\mathbf{c}^T\mathbf{x}$

subject to $\text{diag}(\mathbf{Ax} - \mathbf{b}) \preceq 0$

SOCP

minimize $\mathbf{f}^T\mathbf{x}$

subject to $\|\mathbf{Ax} + \mathbf{b}\|_2 \leq \mathbf{c}^T\mathbf{x} + \text{d}$

Equivalent SDP

minimize $\mathbf{c}^T\mathbf{x}$

subject to $\begin{bmatrix} (\mathbf{c}^T\mathbf{x} + \text{d})\mathbf{I} & \mathbf{Ax} + \mathbf{b} \\ (\mathbf{Ax} + \mathbf{b})^T & \mathbf{c}^T\mathbf{x} + \text{d} \end{bmatrix} \succeq 0$

3.2.5 Conic Programming

A **Cone Programm** or *Conic Form Problem* is a special problem form capable of encompassing all preceeding classes into a single one, whereby all functions (objective and constraints) in the problem formulation are affine, it is not a simple LP though. As conic form problems extensively use generalized inequalities, they should be understood as a natural generalization of LPs, or alternatively think of LPs as special cases of Cone Problems. A general LP uses the default inequality, *i.e.* the inequality between vectors or component-wise inequality. As in (BERTSEKAS, 2009), the generalization also has interesting geometric interpretations since they correspond to more general problem domains with curvature. In LPs the domains associated with the vector inequalities are called polyhedral conic constraints because the faces connecting vertices have no curvature. A matrix inequality however allows curved domains (as in Figure (13)) and are called nonpolyhedral constraints. A convex Problem is in **conic form** whenever it has the following structure:

$$\begin{aligned} \text{minimize} \quad & \mathbf{c}^T\mathbf{x} \\ \text{subject to} \quad & \mathbf{Fx} + \mathbf{g} \preceq_{\mathcal{K}} 0. \\ & \mathbf{Ax} = \mathbf{b} \end{aligned} \tag{3.9}$$

Conic form problems have gained prominence in both theoretic and applied Convex Optimization as a consequence of the extension of interior-point methods originally used in linear programming to nonlinear convex optimization, in (NESTEROV; NEMEROVSKI, 1994). Furthermore, solvers for convex optimization problems are conic solvers. Conic problems can be readily solved whenever the cone $\mathcal{K}$ is formed as a composition of lower-dimensional cones. In practice, three basic conic forms are ubiquitously used and implemented in state-of-the-art solvers, *viz.* the nonnegative orthant, the second-order cone and the semidefinite cone. These cones can be thought of as building blocks for a higher-dimensional cone:

$$\mathcal{K} = \underbrace{(\quad \mathcal{K}_0 \quad)}_{LPs} \times \underbrace{(\mathcal{K}_1 \times \cdots \times \mathcal{K}_M)}_{SOCPs} \times \underbrace{(\mathcal{K}_{M+1} \times \cdots \times \mathcal{K}_{M+N})}_{SDPs}.$$

The cone $\mathcal{K}$ is formed as the Cartesian product of nonnegative orthant cones, second-order cone and positive semidefinite cones:

$$\begin{aligned}
\mathcal{K}_0 &= \{u \in \mathbb{R}^l \mid u_k \geq 0\}, && k = 1, \ldots, l \\
\mathcal{K}_{k+1} &= \{(u_0, u_1) \in \mathbb{R} \times \mathbb{R}^{r_{k-1}} \mid u_0 \geq \|u_1\|_2\}, && k = 0, \ldots, M-1 \\
\mathcal{K}_{k+M+1} &= \{\mathbf{vec}(u) \mid u \in \mathbb{S}_+^{t_k}\}, && k = 0, \ldots, N-1.
\end{aligned}$$

The dimensions of the constituent cones are $l, r_0, \ldots, r_{M-1}, t_o, \ldots, t_{N-1}$. The optimization variable x lies in the following real vector space:

$$\mathbb{R}^l \times \mathbb{R}^{r_0} \times \cdots \times \mathbb{R}^{M-1} \times \mathbb{R}^{t_o^2} \times \cdots \times \mathbb{R}^{t_{N-1}^2},$$

and the problem has a total of $l + \sum_{k=0}^{M-1} r_k + \sum_{k=0}^{N-1} t_k^2$ inequality constraints. Lumping together each cone constraint $\mathcal{K}_i$ into a single cone constraint $\mathcal{K}$ is the essence of conic form problems. The nonnegative orthant ($\mathbb{R}^+ L^l$) is a polyhedral cone but the second-order ($\{(u_0, u_1) \in \mathbb{R} \times \mathbb{R}^{r_{k-1}}\}$) and semidefinite ($\{\mathbf{vec}(u) \mid u \in \mathbb{S}_+^{t_k}\}$) cones are not polyhedral . By focusing on these symmetric and self-scaled cones[14] (and direct products thereof) one is able to extend and formulate interior-point methods which are completely symmetric primal–dual, *i.e.* methods yielding the same iterates whether one solves the primal or dual problem. This feature is largely exploited both in modeling packages[15] (*e.g.* SDPSOL, MATLAB's LMI Control Toolbox, CVX, YALMIP and CVXPY.) and solvers (*e.g.* SeDuMi, CDSP, SDPA, SDPT3 and DSDP, CVXOPT, CVXPY,MOSEK).

The conversion of a general inequality form optimization problem into a conic inequality is straightfoward as illustrated below by a simple example problem consisting of three standard cones (non-negative orthant, second-order and semidefinite cones) with three decision variables ($x \in \mathbb{R}^3$):

$$\begin{aligned}
&\text{minimize} && t \\
&\text{subject to} && \mathbf{c}^T x + d \leq 0 \\
& && \|\mathbf{A}x + \mathbf{b}\|_2 \leq t \\
& && \sum_{i=1}^{3} \mathbf{F}_i x_i + \mathbf{G} \preceq 0
\end{aligned}$$

$$\begin{aligned}
&\text{minimize} && t \\
&\text{subject to} && \mathbf{P}\tilde{x} \leq \mathbf{q}
\end{aligned}$$

[14] Most research in the literature is indeed on these three symmetric cones, but other nonsymmetric cones do exist and have begun to receive some attention, *e.g.* the exponential cone, the power cone with irrational powers, and p-norm cones with irrational p.

[15] These can be seen as tool boxes to simplify both the specification and solution of SDPs or LMIs.

in which the right-panel formulation is the conic form problem with $\tilde{x} = (x, t)$ and the problem data as follows:

$$\mathbf{P} = \begin{bmatrix} c_1 & c_2 & c_3 & 0 \\ 0 & 0 & 0 & -1 \\ -A_{11} & -A_{12} & -A_{13} & 0 \\ -A_{21} & -A_{22} & -A_{23} & 0 \\ -A_{31} & -A_{32} & -A_{33} & 0 \\ \text{vec}(\mathbf{F}_1) & \text{vec}(\mathbf{F}_2) & \text{vec}(\mathbf{F}_3) & 0 \end{bmatrix} \qquad \mathbf{q} = \begin{bmatrix} d \\ 0 \\ -b_1 \\ -b_2 \\ -b_3 \\ \text{vec}(\mathbf{G}) \end{bmatrix}$$

3.3 Graph Theory

In this section, we set forth the notation concerning some graph-theoretic results as well as laying out the basic terminology from Graph Theory which is used to underpin major results of this dissertation. The terms and definitions were largely drawn from three references: (TRUDEAU, 1993) (DEO, 2016) and (VANDENBERGHE; ANDERSEN, 2015). Graph Theory literally has endless applications but the focus is herein placed on chordal graphs to model sparsity patterns.

Definition 24 *An undirected graph is an ordered pair $\mathcal{G} = (\mathcal{V}, \mathcal{E})$, where $\mathcal{V}$ is a finite set whose elements are called vertices and $\mathcal{E}$ denotes the edge set formed by unordered pairs of distinct elements from the vertex set $\{\{v, w\} \mid \in \mathcal{V}\}$*[16].

Given that graphs are sets with some structure they may well be represented using *extensional* set notation whereby its elements are written out extensively, *e.g.* $\mathcal{V} = \{v_1, v_2, \ldots, v_n\}$ and $\mathcal{E} = \{e_1, e_2, \ldots, e_n\}$, such that to each edge $e_k \in \mathcal{E}$ there corresponds an unordered pair $\{v_i, v_j\}$ of vertices, called the *end vertices* of the associated edge, the so-called incidence relation between edges and vertices, thus edge e_k is said to be *incident with/on/to* vertices v_i and v_j. The nomenclature involved in graph theory is somewhat standard but a number of variations exist, *e.g.* vertices are also frequently called nodes, junctions, points and 0-cells whereas edges are also referred to as branches, lines, elements, arcs and 1-cell. Any vertices v and w are said to be adjacent if $\{v, w\} \in \mathcal{E}$, *i.e.* the same edge is incident on them.

[16] If edges are unordered pairs, no distinction is made between the pair $\{v, w\}$ and $\{w, v\}$

Basic set operations are also defined for graphs, of interest are[17]:

- *Union of Graphs*: it is a binary operation between two graphs $\mathcal{G}_1 = (\mathcal{V}_1, \mathcal{E}_1)$ and $\mathcal{G}_2 = (\mathcal{V}_2, \mathcal{E}_2)$ resulting in a third graph namely $\mathcal{G}_3$ such that $\mathcal{G}_3 = \mathcal{G}_1 \cup \mathcal{G}_2$ with $\mathcal{V}_3 = \mathcal{V}_1 \cup \mathcal{V}_2$ and $\mathcal{E}_3 = \mathcal{E}_1 \cup \mathcal{E}_2$;
- *Intersection of Graphs*: it is a binary operation between two graphs $\mathcal{G}_1 = (\mathcal{V}_1, \mathcal{E}_1)$ and $\mathcal{G}_2 = (\mathcal{V}_2, \mathcal{E}_2)$ resulting in a third graph namely $\mathcal{G}_3$ such that $\mathcal{G}_3 = \mathcal{G}_1 \cap \mathcal{G}_2$ with $\mathcal{V}_3 = \mathcal{V}_1 \cap \mathcal{V}_2$ and $\mathcal{E}_3 = \mathcal{E}_1 \cap \mathcal{E}_2$.

Graphs are commonly represented as *diagrams* whereby vertices are represented as points, circles or rectangles whereas edges are depicted as line segments joining vertices according to the incidence relation. Figure (14) shows an example of an unordered graph along with its vertex and edge sets.

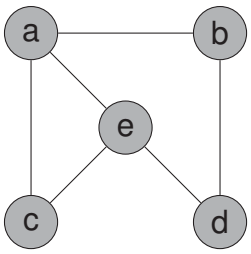

- $\mathcal{V} = \{a, b, c, d, e\}$;
- $\mathcal{E} = \{\{a, b\}, \{a, c\}, \ldots, \{d, e\}\}$;

Figure 14 – Unordered Graph Representation

According to Definition (24), the kind of graphs herein considered are *unordered simple graphs*, *i.e.* graphs in which there is no occurrence of neither *self-loops* nor *parallel edges*. Self-loops occur whenever an edge is associated with a pair $\{v_i, v_i\}$ of repeated vertices, *i.e.* both end vertices coincide, and Parallel edges are those (at least two) whose end vertices (v_i, v_j) are the same, *i.e.* there is more than one edge to the same end vertices.

Definition 25 *A subgraph of $\mathcal{G}$ induced by a subset $W \subseteq \mathcal{V}$ is the undirected graph $\mathcal{G}(W) = (W, \mathcal{E}(W))$ with edge set $\mathcal{E}(W) = \{\{v, w\} \in \mathcal{E} \mid v, w \in W\}$, namely a subset of the vertex set and all edges joining only these vertices.*[18]

Definition 26 *The neighborhood or adjacency set of a given vertex v of a graph $\mathcal{G}$ is the set $adj(v)$ of all vertices adjacent to v:*

$$adj(v) = w \mid \{v, w\} \in \mathcal{E}.$$

[17] Many other operations defined over graphs exist, though.

[18] It is standard in the literature to simply refer to the subgraph W, such that it is implied that what is meant is the subgraph induced by W or the subgraph $\mathcal{G}(W)$.

Definition (26) does not include the vertex v whose neighbourhood is collected as a set. Should the vertex v also be included then the set $\{v\} \cup adj(v)$ is called a *closed neighborhood*.

Definition 27 *The degree of a vertex v is the cardinality of its adjacency set:*

$$deg(v) = |adj(v)|.$$

As defined in (27), the *degree* $deg(v)$ of vertex v is the number of edges incident on a given vertex v [19].

Degrees of vertices are used to infer many important properties of graphs. For instance:

- *Regular Graphs* are those in which all vertices possess the same degree;
- *Isolated Vertex* is a vertex having no incident edge, or a vertex whose degree is zero;
- *Edges in Series* are those with a common vertex of degree two;
- *Odd vertices* have odd degree;
- *Even vertices* even degree.

Definition 28 *A path of length k between any two vertices v and w with $v \neq w$ consists of a sequence of $k+1$ distinct vertices $(v_o = v, v_1, \ldots, v_{k-1}, v_k = w)$ of $\mathcal{V}$ such that the edges are pair-wise adjacent,* i.e. $\{v_i, v_{i+1}\} \in \mathcal{E}$ *for* $i = 0, 1, \ldots, k-1$.

Intuitively, it is a finite alternating sequence of vertices and edges, beginning and ending with vertices, such that each edge is incident with the vertices preceding and following it with no edge and vertex in the sequence is covered or traversed twice[20]. The first and last vertices of the sequence v_o and v_k are called *terminal/end* vertices whereas the remaining vertices $v_1, \ldots, v_{k-1}$ are called interior vertices.

Definition 29 *A cycle*[21] *is path of length k with coincident terminal vertices,* viz. *a sequence of distinct internal vertices $(v_o = v, v_1, \ldots, v_{k-1}, v_k = v)$ of $\mathcal{V}$.*

[19] Degree is also denoted valency in the literature.
[20] Whenever edges are allowed to be traversed more than once the terminology Walk is used.
[21] Cycles are also called circuits, but this terminology is avoided altogether to avoid confusion with electrical circuits.

Note that both paths and cycles can exist as subgraphs of a graph. Paths are useful as a criterium for *connectedness* of a graph. Any two vertices of a given $\mathcal{G}$ are said to be connected whenever at least one path between them can be established with the two vertices as terminal vertices. A graph $\mathcal{G}$ is connected provided every pair of vertices be connected.

Definition 30 *A graph $\mathcal{G}$ is* complete *whenever each pair of distinct vertices is adjacent* $\mathcal{G} = \{\{v, w\} \mid v, w \in \mathcal{V}\}$, viz. *any two vertices are connected by a unique edge*[22].

Definition 31 *A clique W of a graph is a subset of vertices $W \subseteq \mathcal{V}$ that induces a maximal*[23] *complete subgraph,* i.e. $\mathcal{G}(W) = \{\{v, w\} \mid v, w \in W\}$ *is complete.*

Figure (15) displays a graph whose largest clique has cardinality three: $W = \{a, c, e\}$. Note that both $\{a, b\}$ and $\{b, d\}$ are also cliques, with cardinality two instead. Nevertheless, $\{a, c\}$, $\{a, e\}$ and $\{c, e\}$ are not cliques, they are complete subgraphs though. They are not cliques since they are part of larger subset which is complete, a maximal complete subgraph: $\mathcal{G}(W) = (W, \mathcal{E}(W))$, with $\mathcal{G}(W) = \{\{a, c, e\}, \{\{a, c\}, \{a, e\}, \{c, e\}\}\}$. The number of vertices in the largest clique of a graph $\mathcal{G}$ is denoted the clique number of the graph. Therefore the graph depicted in Figure (15) has clique number three.

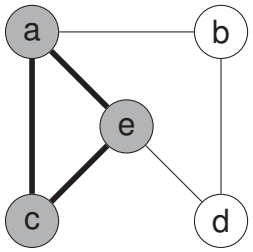

Figure 15 – A Graph and its largest clique

A chord is an edge in a path or cycle that connects two non-consecutive vertices of the path or cycle, as shown in Figure (16). Intuitively, it is a one-edge short-cut.

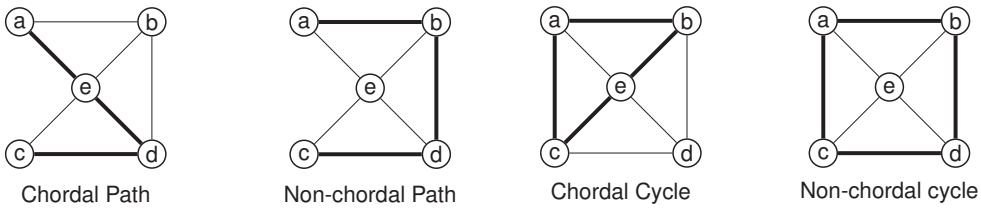

Figure 16 – Chordal versus non-chordal.

[22] Subsequently, complete graphs will be associated with dense matrices.
[23] Some authors use a relaxed definition whereby the induced subgraph is not maximal, complete subgraph is herein used instead.

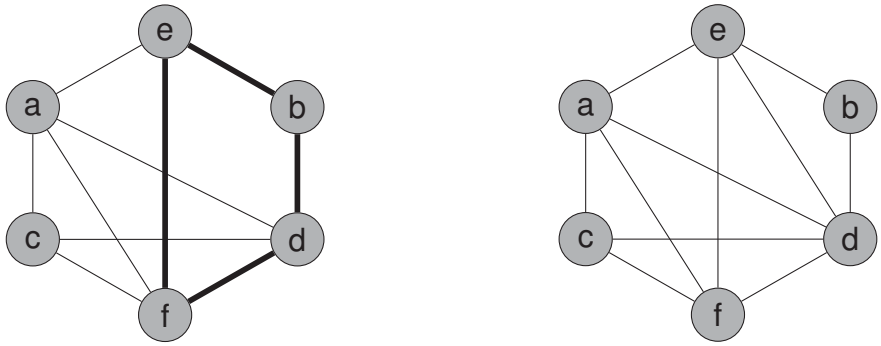

Non-chordal Chordal

Figure 17 – Non-chordal and Chordal Graphs

Definition 32 *An undirected graph $\mathcal{G}$ is chordal*[24] *if every cycle of length greater than three has a chord*[25]*.*

There exists alternative terminology in the literature to designate Chordal Graphs, such as rigid-circuit graphs, triangulated graphs, perfect elimination graphs, decomposable graphs, and acyclic graphs. Figure (17) exemplifies the chordality of a graph (right) which can be seen as a composition of triangles in comparision with a similar non-chordal one (left). The latter is clearly non-chordal for there exists an induced cycle of length four without a chord. The non-chordal graph can be made chordal by inclusion of edge $\{d, e\}$, a process called a chordal embedding of the nonchordal graph.

Chordal graphs possess an important property, namely that is subgraphs $\mathcal{G}(W) = (W, \mathcal{E}(W))$ are also chordal.

Definition 33 *An ordered undirected graph is a triplet $\mathcal{G}_\rho = (\mathcal{V}, \mathcal{E}, \rho)$ whose first two elements are defined just as for undirected graphs and $\rho : \{1, 2, \ldots, |\mathcal{V}|\} \mapsto \mathcal{V}$ is a bijection called an ordering of the vertices.*

The ordering function ρ is an ordered sequence of vertices $\rho = (\rho(1), \rho(2), \ldots, \rho(n))$ with each vertex $v \in \mathcal{V}$ indexed by $\rho^{-1}(v)$. This ordering allows the use of a generalized inequality for the vertices of an ordered undirected graph $v \prec_\rho w$ which inherently implies the usual ordering $\rho^{-1}(v) < \rho^{-1}(w)$.

Ordered undirected graphs can be readily represented in the usual diagramatic form as in Figure (18). Another convenient way to represent ordered graphs is displayed in Figure (19), namely as triangular arrays whereby the vertices' labels sit along the

[24] Chordal graphs are also known as triangulated graphs for chords acting as shortcuts in every cycle of length greater than three be reduced to a cycle of length three which can be represented as a triangle in graph diagrams.

[25] Chordal graphs may be viewed as those for which induced simple cycles of length 4 or more are forbidden.

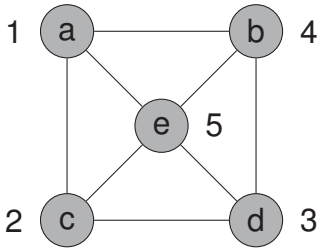

Figure 18 – An ordered undirected graph

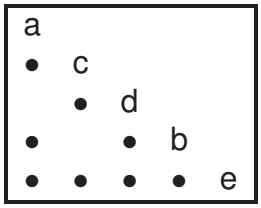

$$\begin{aligned} \text{adj}^+(c) &= \{d, e\} & \text{adj}^-(c) &= \{a\} \\ \deg^+(c) &= \{2\} & \deg^-(c) &= \{1\} \\ \text{col}(c) &= \{c, d, e\} & \text{row}(c) &= \{c, a\} \end{aligned}$$

Figure 19 – Triangular Representation

diagonal and dot marks in the ith row and jth column indicate adjacent vertices $\rho(i)$ and $\rho(j)$ satisfying the inequality $i > j$.

Orderings also permit a distinction to be made concerning the neighborhood of a vertex, *viz.* to separate the idea of neighborhood of a vertex $v \in \mathcal{G}_\rho$ into *higher neighborhood* and *lower neighborhood*:

$$\begin{aligned} \text{adj}^+(v) &= \text{adj}(v) \cap \{w \mid w \succ v\} \\ \text{adj}^-(v) &= \text{adj}(v) \cap \{w \mid w \prec v\} \end{aligned}$$

Similarly, the *higher* and *lower degress* of $v \in \mathcal{G}_\rho$ are:

$$\begin{aligned} \deg^+(v) &= |\text{adj}^+(v)| \\ \deg^-(v) &= |\text{adj}^-(v)|. \end{aligned}$$

By inspection of the triangular array representation in Figure (19), it can be easily seen that the dot marks along a row with index $\rho(v)^{-1}$ indicate the vertices belonging to $\text{adj}^-(v)$ whereas the dot marks down a column with the same index $\rho(v)^{-1}$ indicate the vertices belonging to $\text{adj}^+(v)$. Should the vertex $\rho(v)^{-1}$ also be included, then the higher and lower neighborhoods become closed monotone neighborhoods:

$$\begin{aligned} \text{col}(v) &= \{v\} \cup \text{adj}^+(v) \\ \text{row}(v) &= \{v\} \cup \text{adj}^-(v) \end{aligned}$$

whereby the notation $\text{row}(\cdot)$ and $\text{col}(\cdot)$ for *closed lower neighborhood* and *closed higher neighborhood* respectively is meant to suggest row and column of the associated triangular representation.

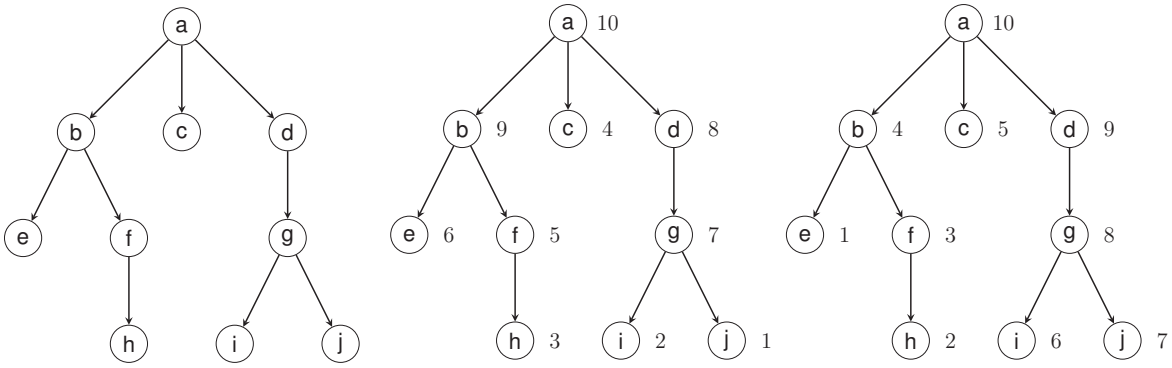

Unordered rooted tree. A topological ordering. A Postordering.

Figure 20 – Rooted trees.

Definition 34 *A tree $\mathcal{T} = (\mathcal{V}, \mathcal{E})$ is a connected undirected graph without any cycles,* i.e. *a connected* acyclic *graph.*

Trees also exist as subgraphs of non-tree graphs. A *Leaf or Pendant Vertex* is a vertex within a tree whose degree is one[26]. Since trees are connected graphs there exist a path between any two of its vertices, but the path has to be unique for any two distinct paths starting and ending at the same two vertices can be concatened and thus form a cycle, which is prohibited by the definition. Owing to this uniqueness of path between every pair of vertices, trees are also known as *minimally connected graphs* for a removal of any single edge from it disconnects the graph. A tree $\mathcal{T}$ with $n = |\mathcal{V}|$ vertices has $n - 1 = |\mathcal{E}|$ edges, which is the minimum number of edges required to fully connect a graph.

Definition 35 *A* rooted tree *$\mathcal{T}$ is defined as a tree in which there is a special vertex called the root of the tree.*

Given two distinct non-root vertices $v, w \in \mathcal{T}$ such that w is the next vertex following v on the unique path starting at v and headed to the root, w is denoted the *parent* of v, $w = p(v)$, and v is a *child* of w. It is possible to establish a parent function: $P : \mathcal{V} \mapsto \mathcal{V}$ to account for ancestry and descendancy among vertices. If k is some nonnegative integer, then a parent of degree k associated with a given vertex $v \in \mathcal{T}$ is defined through a recursion:

$$p^0(v) = v, \quad p^{k+1} = p(p^k(v)).$$

The rooted tree in Figure (20) presents the vertices labelled with words of the alphabet and the parent function for vertex h yields: $p(h) = f, p^2(h) = b, p^3(h) = a$.

[26] An edge incident on a pendant vertex is called a *pendant edge*.

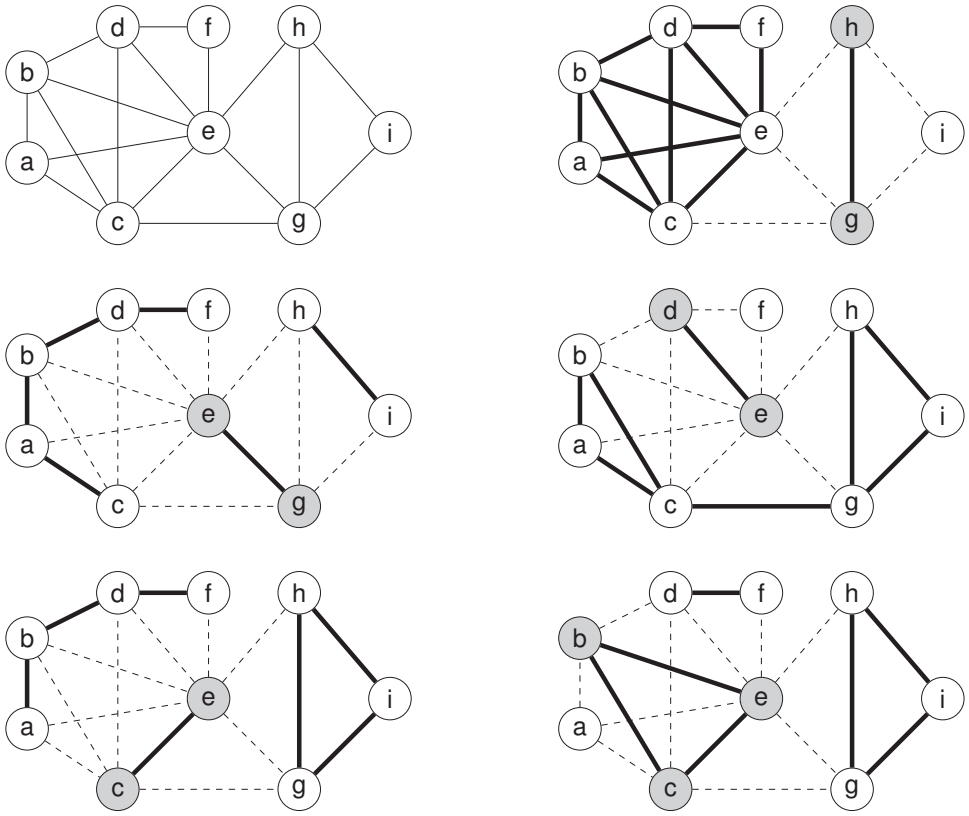

Figure 21 – The five separators of the graph $\mathcal{G}$

Whenever two vertices are related by $w = p^k(v)$ with $k \leq 0$, w is said to be an ancestor of v whereas v is a descendant of w. Vertices can have more than one immediate descendant and such a set is denote $ch(v)$, the children set associated with v. The root-vertex is a parentless vertex while leaves are childless vertices. Trees can be assigned orderings, a rooted tree has a *topological ordering* if $v \geq p(v)$ for every non-root vertex, *i.e.* a parents vertex has a higher index than its children, and the root has the highest index $|\mathcal{V}|$. A more special ordering is the *postordering* whereby descendants of a given vertex v are assigned consecutive numbers. Hence, assuming vertex v has index j, $\rho^{-1}(v) = j$, and k proper descendants, then the proper descendats are numbered $j-k, j-k+1, \ldots, j-1$. Examples of both topological and post orderings are given in Figure (20).

Definition 36 *A set S such that $S \subset \mathcal{V}$ is denoted a* vertex separator *for two vertices v and w of an undirected graph $\mathcal{G} = (\mathcal{V}, \mathcal{E})$, or a vw-separator, if both v and w reside in different connected components of the subgraph $\mathcal{G}(\mathcal{V} \backslash S)$* [27]*. The vertex separator qualifies as a* minimal vertex separator *whenever it has no proper subset which is also a vw-separator.*

[27] Note that $\mathcal{V} \backslash S$ denotes the set subtraction operation, therefore $\mathcal{G}(\mathcal{V} \backslash S)$ is the subgraph of $\mathcal{V}$ with the vertices in S removed.

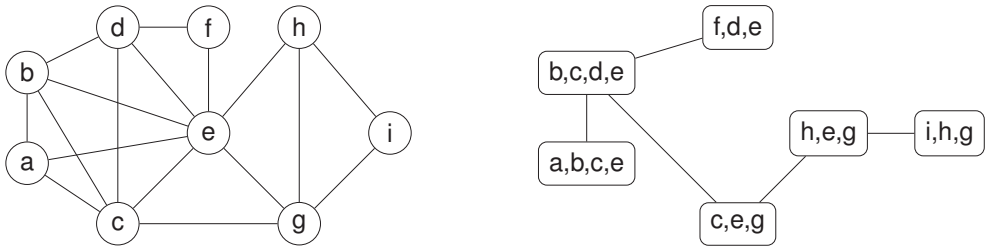

Figure 22 – A $\mathcal{G}$ and one of its clique trees

By way of illustration, Figure (21) depicts a graph $\mathcal{G}$ (upper left) and five distinct separators (vertices represented as circles with grey fill). Removed edges are dashed and thick edges indicate the connected components (subgraphs) after removal of the separator vertices along with edges incident on them. In this context, one can say that $\{c, e\}$ is a minimal ag-separator (bottom left) and $\{b, c, e\}$ is a minimal ad-separator (bottom right). Closer inspection of Figure (21) reveals that vertices a, f, i never appeared in any of the separators, they are called *simplicial vertices*. For chordal graphs, the vertex set can be partitioned into simplicial vertices which belong to exactly one clique and the vertices which are elements of minimal vertex separators, which in turn belong to at least two different cliques.

Even though it is not clear as it now stands, vertex separators will be associated with overlapping entries between submatrices within a larger matrix. Simplicial vertices will be interpreted as entries of a matrix that belong to exactly one submatrix whereas vertices part of separators are to corrrespond to entries belonging to more than one submatrix[28].

Definition 37 *A* Clique Tree $\mathcal{T}$ *of a graph* $\mathcal{G} = (\mathcal{V}, \mathcal{E})$ *is a special tree with cliques of* $\mathcal{G}$ *as its vertices.*

If a graph $\mathcal{G}$ is chordal, then it can be represented as a clique tree, *i.e.* chordality implies the existence of a clique tree. Figure (22) displays a graph and a clique tree for it. Much can be inferred from a clique tree, for instance a complete list of the minimal vertex separators (overlapping entries between distinct submatrices) is immediately given by the edges in the clique tree, *i.e.* adjacent cliques share vertices (each clique corresponding to a full submatrix).

Without any loss of generality and to facilitate the exposure, any clique of a clique tree can be chosen as a root clique to form a rooted clique tree. This allows the use of the parent function for the clique tree $p_c(W)$, with $p_c(\cdot)$ denoting the parent function and

[28] Vertex separators and simplicial vertices have many applications and related theorems in pure graph theory, for the purposes of this research though this simple interpretation in terms of submatrices is enough.

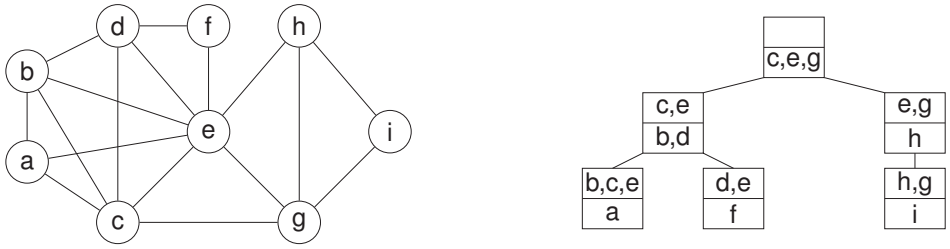

Figure 23 – A $\mathcal{G}$ and one of its rooted clique trees

W its argument which is no longer a single vertex v, rather a set of vertices, a clique W of $\mathcal{G}$. Therefore, each non-root clique W can be partitioned as follows:

$$\text{sep}(W) = W \cap p_c(W) \qquad \text{and} \qquad \text{res}(W) = W \backslash \text{sep}(W)$$

in which the clique partitions sep(W) and res(W) are called *clique separators* and *clique residuals*, respectively. This partitioning is illustrated in Figure (23) which is a rooted version of the one previously presented in Figure (22). Note in Figure (23) that each clique is represented as a square box partitioned into two rows, the top row corresponds to clique separator sep(W) and the bottom row to clique residual res(W), hence $W = \{b, c, d, e\}$ is a clique with res(W) $= \{b, d\}$ and sep(W) $= \{c, e\}$. The root clique, namely $W = \{c, e, g\}$, has sep(W)$= \emptyset$ and res(W)$= \{c, e, g\}$. A chordal graph has at most $n = |\mathcal{V}|$ cliques and $n - 1$ minimal vertex separators.

Definition 38 *An ordered graph $\mathcal{G}_\rho = (\mathcal{V}, \mathcal{E}, \rho)$[29] is* monotone transitive[30] *provided each higher neighborhood $adj^+(v)$ of every vertex $v \in \mathcal{V}$ induces a complete subgraph,* i.e. *:*

$$w, z \in adj^+(v) \implies \{w, z\} \in \mathcal{E}.$$

Stated in other terms, Definition (38) establishes that for a given ordering ρ of a graph, the latter is monotone transitive whenever any two vertices in the higher neighborhood ($w = \rho(j), z = \rho(k) \in adj^+(v)$) of a third vertex ($v = \rho(i)$, with $i < j < k$) are connected, or equivalently:

$$\{\rho(i), \rho(j)\}, \{\rho(i), \rho(k)\} \implies \{\rho(j), \rho(k)\}.$$

Figure (24) illustrates the idea of monotone transitivity. For instance, scanning down the second column it is immediate that $\{d, c, e\} \in adj^+(b)$ and $\{d, c\}, \{d, e\}, \{c, e\} \in \mathcal{E}$. Monotone transitivity has chordality of $\mathcal{G}$ as an immediate consequence for any vertex v in a cycle having the least index $\rho^{-1}(v)$ with w, z as its adjacent neighbors within the

[29] See Definition 33.
[30] Also called Filled Graph.

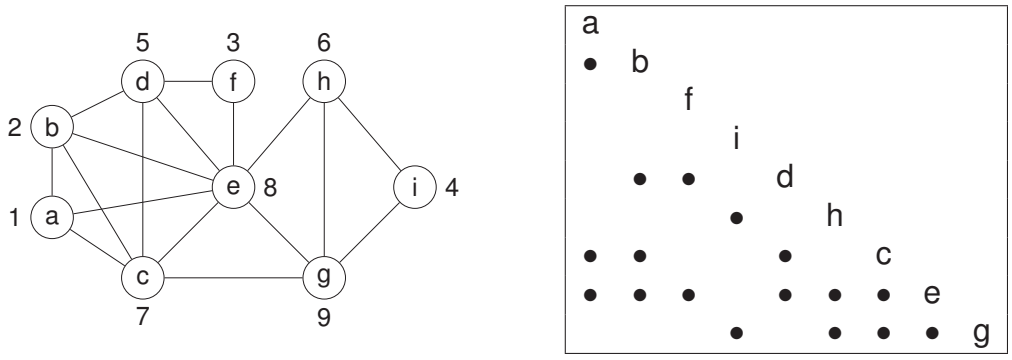

Figure 24 – A monotone transitive graph $\mathcal{G}$

cycle, then vertices w and z belong to $adj^{+}(v)$ and must be adjacent considering that the graph is monotone transitive. The edge $\{w, z\}$ is a chord in the cycle. The converse is also true, *viz.* a chordal graph $\mathcal{G}$ always admits an ordering ρ for which $\mathcal{G}_{\rho}$ is a monotone transitive.

Definition 39 *An ordering ρ of an undirected graph $\mathcal{G} = (\mathcal{V}, \mathcal{E})$ is a* Perfect Elimination Ordering *(PEO) of $\mathcal{G}$ if the ordered graph $\mathcal{G}_{\rho} = (\mathcal{V}, \mathcal{E}, \rho)$ is monotone transitive.*

Perfect Elimination Orderings can be used as a test for chordality and such orderings can be found by a few algorithms, the best of which is the Maximum Cardinality Search (MCS) algorithm, originally proposed in (TARJAN; YANNAKAKIS, 1963; YANNAKAKIS, 1981) . Testing chordality by the MCS algorithm is the easiest method since the algorithm is guaranteed to find a perfect elimination ordering provided the graph be chordal. Should the MCS algorithm fail to find a perfect elimination ordering, then the input graph is not chordal. According to (TARJAN; YANNAKAKIS, 1963; YANNAKAKIS, 1981), the MCS algorithm can be used as a test for chordality based on the following result:

Theorem 1 *A graph is chordal if and only if it admits a perfect ordering.*

The MCS algorithm only requires as input the adjancency matrix associated with sparsity graph. For completeness, the adjacency matrix is defined in Definition (40).

Definition 40 *The Adjacency Matrix or Connection Matrix of a graph $\mathcal{G}$ is a $n \times n$ symmetric matrix $\boldsymbol{A}(\mathcal{G})$ such that $A_{ij} = 1$ whenever exists an edge between the i-th and j-th vertices, $A_{ij} = 0$ otherwise.*

- As the graph $\mathcal{G}$ has no self-loops, all entries along the principal diagonal are zero, *i.e.* $A_{ii} = 0$;

- The degree of each vertex $\deg(v)$ equals the numbers of ones in the corresponding row or column of the adjacency matrix, *i.e.* :

$$\sum_{j=1}^{n} A_{ij} = \deg(v_i), \text{ or alternatively } \sum_{i=1}^{n} A_{ij} = \deg(v_j).$$

Figure (25) illustrates an ordered graph and its corresponding adjacency matrix.

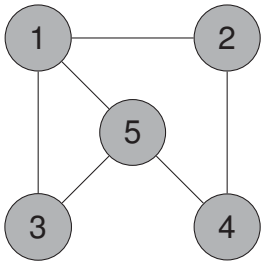

$$\mathbf{A}(\mathcal{G}) = \begin{bmatrix} 0 & 1 & 1 & 0 & 1 \\ 1 & 0 & 0 & 1 & 0 \\ 1 & 0 & 0 & 0 & 1 \\ 0 & 1 & 0 & 0 & 1 \\ 1 & 0 & 1 & 1 & 0 \end{bmatrix}$$

Figure 25 – Unordered Graph and its associated adjacency matrix

3.4 Graphs and Matrices

Chordal Graphs have gained prominence as a tool in sparse matrix analysis, in particular they can be used to model the sparsity pattern of symmetric matrices, the so-called sparsity graph.

Definition 41 *The sparsity graph associated with an $n \times n$ matrix **X** is an unordered graph with $\mathcal{V} = \{1, 2, \ldots, n\}$ such that each edge $\{i, j\} \in \mathcal{E}$ and $i \neq j$, implies $X_{ij} = X_{ji} \neq 0$; and the matrix **X** is said to have sparsity pattern $\mathcal{E}$.*

Therefore, a $n \times n$ symmetric sparsity pattern can be naturally described by a graph $\mathcal{G} = (\mathcal{V}, \mathcal{E})$ and one is allowed to say that the symmetric matrix **X** of order n has the sparsity pattern $\mathcal{E}$ if $i \neq j, \{i, j\} \notin \mathcal{E} \implies X_{ij} = X_{ji} = 0$, *i.e.* for off-diagonal entries whose corresponding vertices are not adjacent, they have zero value. Note that entries X_{ij} with $(i, j) \in \mathcal{E}$ can be zero as well[31], called *numerical zeros*, whereas those X_{ij} with $(i, j) \notin \mathcal{E}$ are zero, the latter are referred to as *structural zeros or syntactic zeros*. In definition (41), all diagonal entries are assumed to be non-zero[32]. A symmetric matrix **X** possessing a sparsity pattern given by $\mathcal{E}$ is denoted $\mathbf{X} \in \mathbb{S}^n_{\mathcal{E}}$. Figure (26) show a symmetric sparse matrix and its sparsity graph.

Just as graphs contain special subgraphs, matrices contain submatrices. Whenever reference is made to submatrices of a matrix, it should be understood as dense

[31] In which case this 'accidental' sparser pattern is embedded in the larger prescribed one.
[32] This non-zero assumption will be latter discussed when this fact becomes more relevant for the discussion.

$$\mathbf{X} = \begin{bmatrix} X_{11} & X_{12} & X_{13} & 0 & X_{15} \\ X_{21} & X_{22} & 0 & X_{24} & 0 \\ X_{31} & 0 & X_{33} & 0 & X_{35} \\ 0 & X_{42} & 0 & X_{44} & X_{45} \\ X_{51} & 0 & X_{53} & X_{54} & X_{55} \end{bmatrix}$$

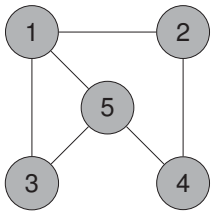

Figure 26 – Sparse Matrix and its Sparsity Graph

submatrices, *i.e.* having nonzero entries, and it implies the existence of matrices in $\mathbb{S}^n_{\mathcal{E}}$ with nonzeros in the corresponding positions.

In this context, it is useful to operate over the indices corresponding to submatrices. Submatrices can be extracted by appropriate indexing which consists of an ordered sequence of distinct integers taken from the set $\mathcal{V} = \{1, 2, \ldots, n\}$ whereby n is the order of the symmetric matrix. Any such sequence of size $r \leq n$ is called an *index set* which can be used to extract the associated submatrix via its selection matrix.

The selection matrix associated with an index set $\beta = (\beta(1), \beta(2), \ldots, \beta(r))$ is an $r \times n$ matrix denoted $\mathbf{P}_\beta$ defined as:

$$(P_\beta)_{ij} = \begin{cases} 1 & j = \beta(i) \\ 0 & \text{otherwise} \end{cases}$$

By multiplying an $n \times n$ matrix $\mathbf{X}$ with $\mathbf{P}_\beta$ on the left and $\mathbf{P}_\beta^T$ on the right, the corresponding $r \times r$ principal submatrix whise rows and columns are indexed by the index set β

is extracted:

$$\mathbf{P}_\beta \mathbf{X} \mathbf{P}_\beta^T = \mathbf{X}_{\beta\beta} = \begin{bmatrix} X_{\beta(1)\beta(1)} & X_{\beta(1)\beta(2)} & \cdots & X_{\beta(1)\beta(r)} \\ X_{\beta(2)\beta(1)} & X_{\beta(2)\beta(2)} & \cdots & X_{\beta(2)\beta(r)} \\ \vdots & \vdots & & \vdots \\ X_{\beta(r)\beta(1)} & X_{\beta(r)\beta(2)} & \cdots & X_{\beta(r)\beta(r)} \end{bmatrix}$$

Careful examination of Figure (26) shows that the set of vertices $W = \{1, 3, 5\}$ is a clique, a maximal complete subgraph of $\mathcal{G}$. Consequently, the principal submatrix whose rows and columns are indexed by W corresponds to a dense principal submatrix within the sparsity pattern defined by the sparsity graph, and it can be extracted as follows:

$$\mathbf{P}_\beta \mathbf{X} \mathbf{P}_\beta^T = X_{\beta\beta} = \begin{bmatrix} X_{11} & X_{13} & X_{15} \\ X_{31} & X_{33} & X_{35} \\ X_{51} & X_{53} & X_{55} \end{bmatrix},$$

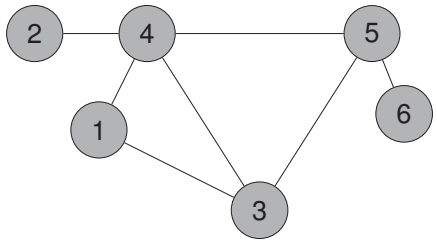

$$X = \begin{bmatrix} X_{11} & 0 & X_{13} & X_{14} & 0 & 0 \\ 0 & X_{22} & 0 & X_{24} & 0 & 0 \\ X_{31} & 0 & X_{33} & X_{34} & X_{35} & 0 \\ X_{41} & X_{42} & X_{43} & X_{44} & X_{45} & 0 \\ 0 & 0 & X_{53} & X_{54} & X_{55} & X_{56} \\ 0 & 0 & 0 & 0 & X_{65} & X_{66} \end{bmatrix}$$

Figure 27 – A sparsity graph for a sparse symmetric matrix

with the selection matrix given by:

$$P_\beta = \begin{bmatrix} 1 & 0 & 0 & 0 & 0 \\ 0 & 0 & 1 & 0 & 0 \\ 0 & 0 & 0 & 0 & 1 \end{bmatrix}.$$

The adjoint operator gives a full matrix with zeros except for the clique entries:

$$\mathbf{P}_\beta^T X_{\beta\beta} \mathbf{P}_\beta = \begin{bmatrix} X_{11} & 0 & X_{13} & 0 & X_{15} \\ 0 & 0 & 0 & 0 & 0 \\ X_{31} & 0 & X_{33} & 0 & X_{35} \\ 0 & 0 & 0 & 0 & 0 \\ X_{51} & 0 & X_{53} & 0 & X_{55} \end{bmatrix}.$$

Definition 42 *A sparsity pattern $\mathcal{E}$ is a chordal sparsity pattern if the corresponding sparsity graph is chordal.*

By way of illustration, Figure (27) contains a generic matrix and its associated sparsity graph. This matrix could well be a terminal description for a network whose labels identify specific terminals at some frequency with the sparsity pattern as defined and fixed for all frequencies.

After considering the ordered graph, it is possible to visualize graph structure such as vertex separators, clique residuals and clique tree as in Figure (28). As graph structure is intimately related with matrix structure, a analysis of Figure (28) reveals a set of submatrices interspersed with zero entries. These submatrices can be seen separately in Figure(29), with each γ_i being an index set for the elements of the cliques (submatrices) using a numerical ordering.

The bottom line then is:

- Cliques correspond to dense principal submatrices;
- Cliques model a partition for the full matrix;

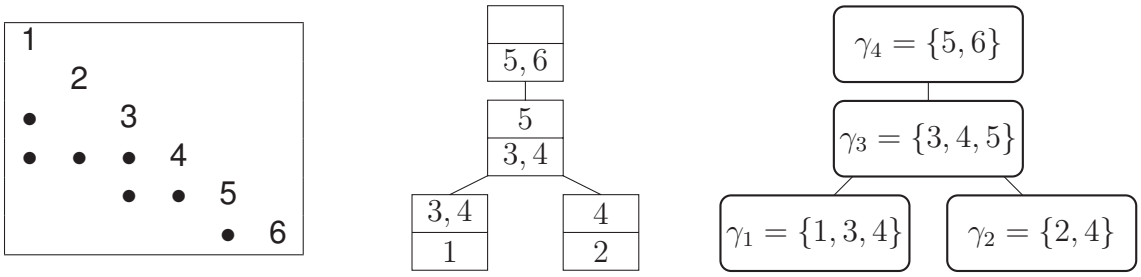

Figure 28 – Triangular representation, clique tree and ordered clique tree.

$$X_{\gamma_1\gamma_1} = \begin{bmatrix} X_{11} & X_{13} & X_{14} \\ X_{31} & X_{33} & X_{34} \\ X_{41} & X_{43} & X_{44} \end{bmatrix} \qquad X_{\gamma_2\gamma_2} = \begin{bmatrix} X_{22} & X_{24} \\ X_{42} & X_{44} \end{bmatrix}$$

$$X_{\gamma_3\gamma_3} = \begin{bmatrix} X_{33} & X_{34} & X_{35} \\ X_{43} & X_{44} & X_{45} \\ X_{53} & X_{54} & X_{55} \end{bmatrix} \qquad X_{\gamma_4\gamma_4} = \begin{bmatrix} X_{55} & X_{56} \\ X_{65} & X_{66} \end{bmatrix}$$

Figure 29 – Dense Principal submatrices.

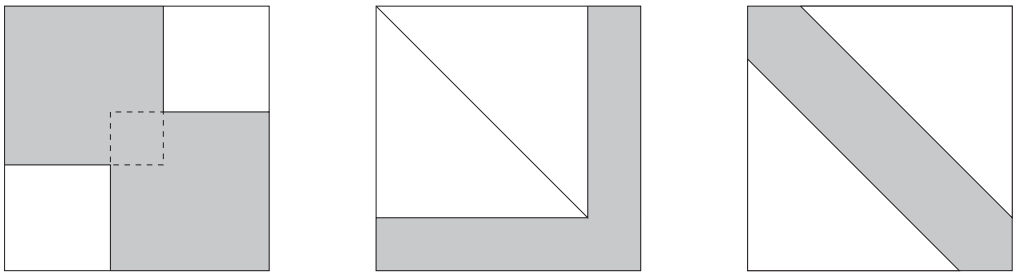

Figure 30 – Overlapping Diagonal Blocks, Arrow and Banded patterns.

- Clique trees reveal the overlapping between submatrices;
- The overlap between adjacent cliques correspond to the cardinality of the clique separators.

Out of general chordal sparsity patterns, there are a few common basic patterns of interest, namely the overlapping diagonal-blocks pattern, the arrow pattern and the band pattern, as shown in Figure (30). Sparsity patterns illustrated in Figure (30) are simple canonical chordal patterns, other combinations formed from them also result in chordal more complex chordal patterns, for instance: there can be more than just two overlapping blocks and both the arrow and banded patterns can combine into banded-arrow pattern. These patterns are so common in applications that their cliques have a standard general form.

Figures (31),(32) and (33) present the general outlook of the cliques trees for their respective sparsity patterns. The overlapping square blocks have dimensions p

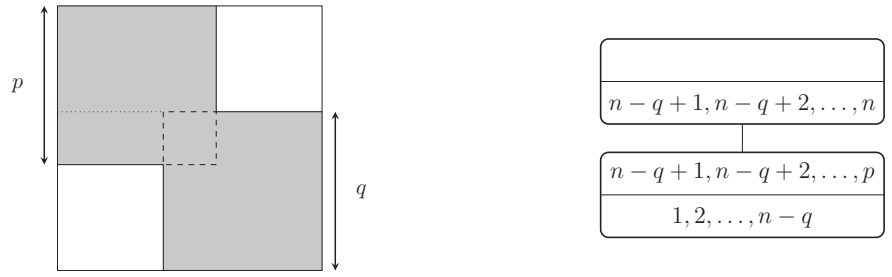

Figure 31 – Block diagonal pattern and its clique tree.

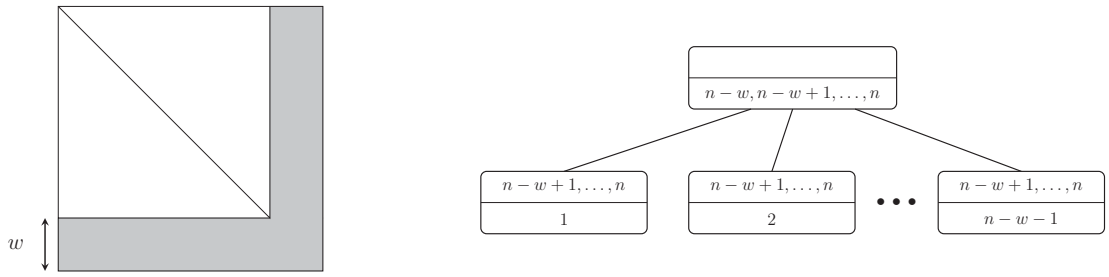

Figure 32 – Arrow pattern and its clique tree.

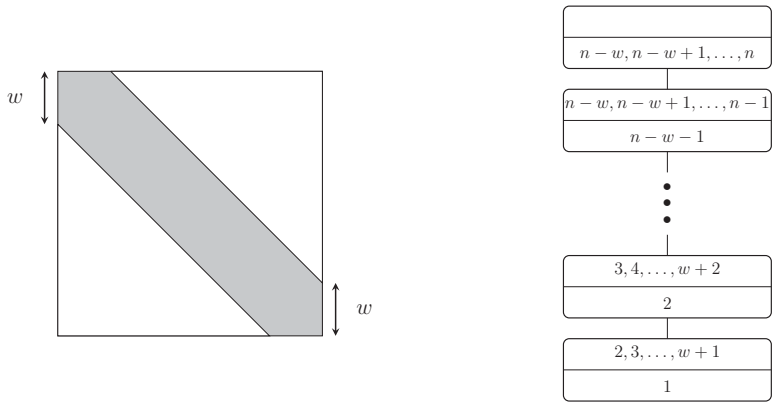

Figure 33 – Banded pattern and its clique tree.

and q, the block arrow pattern has block width w and the banded pattern has bandwidth $2w + 1$.

3.5 A few closing remarks

Contrary to the most usual optimization problems encountered in practice, namely LS, LP, and QP, convex programming inescapably requires a much higher level of expertise and mathematical maturity on the user, in particular for the many transformations required to frame a given problem formulation into its solvable convex equivalent and pass it to the underlying solver, which is designed to handle certain prototypical family of problems known as standard forms having specific structures and adhere to certain conventions. Otherwise, developing a custom method and solver is the only remaining option. Nowadays however many solvers, both commercial and freely distributed, are

readily available and beating their performance is difficult for they trade generality for ease of use and performance. Despite the use herein made of convex programming in system theory, it finds many applications in research areas ranging from machine learning and statistics to finance. As in (BOYD; VANDENBERGHE, 2004): 'The challenge, and art, in using convex optimization is in recognizing and formulating the problem'. The full benefits of convex optimization, in contrast, only come when the problem is known ahead of time to be convex.

Not only recognizing a problem to be convex or even a transformation to an equivalent convex formulation can be challenging but also the full exploitation problem structure such as sparsity. For more general convex cones, like those in SOCPs and SDPs, sparsity can be more fully exploited using graph theory methods for chordal graphs, and much research is now concentrated in providing solver with capabilities to recongnize chordal sparsity patterns. Graphs and matrices have been shown to be intimately related and have many exploitable equivalences, three such equivalences are noteworthy: (i) undirected graphs and sparse matrices, (ii) cliques and positive maximal dense principal submatrices and (iii) clique minimal vertex separators and overlapping entries of submatrices. In a sense graphs and matrices can be understood as mere different representations of the same mathematical object, namely a mathematically structured set. As one of the leading purposes of mathematics is to make inferences about its congnitive constructs, some properties are more easily noticed in one representation than in the other. Starting with an abstract object, the set, the diagram[33], the triangular array and matrices representations for graphs all have their associated operations and factorizations so that they all impart different, complementary insight into a problem.

[33] Also called Geometric/Pictorial representation.

4 PASSIVITY ASSESSMENT AND ENFORCEMENT

The first part of the chapter is devoted to passivity assessment methods which are essentially mathematical criteria translated into algorithms that permit distinguishing passive systems from non-passive ones. The exposure on assessment is a consolidation of the techniques currently in vogue in the technical literature.

Subsequently, the chapter is concerned with Passivity Enforcement a modeling step intended for ensuring that the model's dynamic behavior be strictly passive under any circumstances; it basically hinges on either deriving a passive model from a non-passive one or directly devising a passive model from data and these two approaches better be distinguished. Therefore, the first part of the chapter is committed to perturbative model passivity enforcement (estimate parameters and then enforce passivity) whereas the second part focuses on non-perturbative passive approximation (enforce passivity as parameters are estimated).

This discussion is independent of any previous attempts at taming passivity during the pre-processing stage, whether they have proved fruitful or not, and even the general case for which no pre-processing is used.

4.1 Assessment Techniques

Passivity assessment constitutes a system analysis problem intended for determining the inability of a given system to generate energy: the distinguishing feature of passive systems. This analysis can be made rather rigorous with precise mathematical definitions, which in turn depend on the description adopted for the n-port network. According to (WILLEMS, 1972a), dissipative systems are of particular interest in engineering and physics. The dissipation hypothesis, which distinguishes such systems from general dynamic systems, results in a fundamental constraint on their dynamical behavior. The terminology dissipative is more formal and can be used as a generalization of the concept of passivity. As early as 1931, besides coining the term positive-real function, Otto Brune ((BRUNE, 1931)) first established the association between passivity and positive-real functions. In fact, Brune proved that a rational positive-real function could be realized as a immittance (impedance or admittance) representation of a network consisting of resistors, capacitors, inductors and transformers, i.e., admittance and impedance parameter matrices of passive electrical networks are positive real matrix rational functions.

In 1954 a proof that extends this association to the multi-variable case was provided in (RAISBECK, 1954). From the late 1950's through the 1960's, electrical

engineers had a running debate on the axioms of network theory. As in reference (ALLEN, 2004), the referred debate centered on listing the minimal properties of an n-port to obtain the standard formalisms of traditional circuit theory. More formal proofs appeared such as the classical proof (YOULA; CARLIN, 1959) and others based on distribution theory (as in (WOHLERS, 1969) and (ZEMANIAN, 1963)). Such advanced mathematical background prompted a search for alternative means to prove and assess the passivity property. While positive-realness is a necessary condition, it is not sufficient to establish passivity. In reference (BOYD; CHUA, 1982) a formal proof using general coordinates (which can be derived for any of the representations of the last section) of the passivity criteria is provided, employing Measure Theory but no Distributions. Some methods for assessing passivity of LTI n-ports have been perfected while others have arisen. What follows is a compilation of existing passivity assessment criteria currently being employed to LTI n-ports, starting with classical transfer function/matrix criteria and later evolving to modern methods.

4.1.1 Frequency Sweeping test

Considering a LTI n-port defined in Definition (15), such that the transfer matrix $\mathbf{H}(s)$ assumes any of the specific representations (as earlier defined: admittance, impedance and etc.) and the following definition:

$$\mathbf{\Psi}(s) = \begin{cases} \mathbf{H}(s) + \mathbf{H}^H(s) & (\text{hybrid representations}) \\ \mathbf{I} - \mathbf{H}^H(s)\mathbf{H}(s) & (\text{scattering representations}) \end{cases}, \tag{4.1}$$

where the superscript ^{H} denotes Hermitian transpose, the LTI n-port thus characterized by $\mathbf{H}(s)$ is positive-real matrix of the complex variable s, as stated in reference (TRIVERIO et al., 2007), if the following conditions are satisfied in the open right-half s-plane (i.e., for $\mathrm{Re}(s) > 0$):

1) each $H_{il}(s)$ in $\mathbf{H}(s)$ is defined and analytic;

2) $\mathbf{\Psi}(s) \succeq 0$;

3) $\mathbf{H}(s^*) = \mathbf{H}^*(s)$;

such that the superscript * denotes complex conjugate. The matrix transfer function of a linear time-invariant system that is positive real satisfies analyticity, conjugacy and positive-definiteness. When $\mathbf{H}(s)$ comprises a scattering representation, and since the second condition poses a unitary bound for $\mathbf{\Psi}(s)$, these three conditions are equivalent to requiring bounded-realness, a terminology that appropriately generalizes the fact that each port has reflection coefficient smaller than one, meaning the reflected or

transmitted waves can only be a fraction of the incident wave (when considering the incident and reflected waves interpretation for the scattering parameters).

As noted in (TRIVERIO et al., 2007), the fact that each $H_{il}(s)$ is analytic also implies BIBO (Bounded-Input-Bounded-Output) stability, while the second one is a multi-variable generalization for the fact that any passive one-port impedance/admittance has a positive real part. The third condition also ensures that the system impulse response be real. Despite being a side issue that will be later addressed, it is noteworthy that conditions one and three can be even satisfied by default as a direct consequence of the adopted model structure. Satisfying the second condition can be numerically critical, though. Conditions one through three have to be satisfied for all s in the right-half plane ($\mathrm{Re}(s) > 0$) however, according to (WOHLERS, 1969) and (TRIVERIO et al., 2007), the lumped-parameter assumption which implies a rational transfer matrix permits testing only along the imaginary axis (i.e., $s = j\omega$).

Consequently, a simple passivity assessment test broadly used in the literature is:

$$\mathbf{\Psi}(j\omega) \succeq 0 \qquad \forall\, \omega, \tag{4.2}$$

namely checking positive realness for hybrid representations or bounded realness for scattering ones. In the context of measured port data, Equation (4.2) is evaluated only at each frequency in the finite sequence $\{w_k\}_{k=1}^{K}$ of all measured frequencies (as opposed to all the infinite imaginary axis), thus the terminology frequency-sweeping assessment.

Under the working assumption of a symmetric system, this frequency-sweeping assessment test can be further tailored to simpler forms. Then, let the LTI n-port measured data to be represented in terms of its admittance matrix, thus $\mathbf{H}(j\omega) = \mathbf{Y}(j\omega)$. Therefore, the positive-realness condition as given by Equation (4.2) for all measured frequencies yields:

$$\mathbf{Y}^H(jw_k) + \mathbf{Y}(j\omega_k) \succeq 0 \qquad \Longleftrightarrow \qquad \mathbf{G}(j\omega_k) \succeq 0. \tag{4.3}$$

In such circumstances, passivity requires that the conductance matrix ($\mathbf{G}(j\omega_k) = \mathrm{Re}[\mathbf{Y}(j\omega_k)]$) be positive real. Should the inequality in Equation (4.3) hold, then the following inequality also holds:

$$\mathbf{P}_{pot}(j\omega_k) = \mathrm{Re}\{\mathbf{v}^H(jw_k)\mathbf{Y}(j\omega_k)\mathbf{v}(j\omega_k)\} = \mathrm{Re}\{\mathbf{v}^H(j\omega_k)\mathbf{G}(j\omega_k)\mathbf{v}(j\omega_k)\} > 0. \tag{4.4}$$

In the quadratic form of Equation (4.4) whose associated physical interpretation is that of absorbed active power, $\mathbf{v}(j\omega_k)$ is a voltage vector. It is a well-established fact

from linear algebra that the eigenvalues of a positive real quadratic form such as the one in Equation (4.4) are all strictly positive; references such as (GOLUB; LOAN, 2012) and (HORN; JOHNSON, 2012) discuss this matter at greath length. If all eigenvalues of $\mathbf{G}(j\omega_k)$ are strictly positive, so is the smallest one. Thus, the passivity assessment condition can take the even simpler form:

$$\lambda_{min}(\mathbf{G}(j\omega_k)) > 0, \tag{4.5}$$

where $\lambda_{min}(\,\cdot\,)$ denotes the smallest eigenvalue of a matrix. Stated in other terms, if the smallest eigenvalue of $\mathbf{G}(j\omega_k)$ is negative, the passivity condition is said to be locally violated. The violation is local in the sense that once a violation is confirmed at frequency ω_k there is no implication so as to violations at frequencies ω_{k-1} nor ω_{k+1}, i.e., passivity has to be verified in the frequency sweeping manner. As a matter of fact, Equations (4.3) through (4.5) are equivalent. According to (TRIVERIO et al., 2007), if $\mathbf{H}(j\omega) = \mathbf{S}(j\omega)$, the LTI n-port is a scattering representation and similar assessment criteria can be derived. In this case, the positive-realness condition for $\mathbf{\Psi}(j\omega_k)$ produces:

$$\mathbf{I} - \mathbf{S}^H(j\omega_k)\mathbf{S}(j\omega_k) \succeq 0. \tag{4.6}$$

If $\mathbf{\Psi}(j\omega_k)$ is a positive-real matrix, then $\mathbf{S}(j\omega_k)$ is bounded-real or unitary bounded, following the usual literature terminology. From Equation (4.6), the requirement for passivity is that the eigenvalues of the Gram matrix $\mathbf{S}^H(j\omega_k)\mathbf{S}(jw_k)$ be smaller than or equal those of the identity, and therefore smaller than or equal one. Since the square roots of the non-zero eigenvalues of the associated Gram matrix are the singular values of the original matrix $\mathbf{S}(j\omega_k)$, it has become standard procedure in the literature to establish the passivity criterion in terms of the singular values of $\mathbf{S}(j\omega_k)$ rather than the eigenvalues of the associated Gram matrix. Thus,

$$\sigma_{max}(\mathbf{S}(j\omega_k)) \leq 1, \tag{4.7}$$

where $\sigma_{max}(\,.\,)$ denotes largest singular value of a matrix. Equations (4.6) and (4.7) are the analogues, for the scattering representation, of Equations (4.3) and (4.5), respectively. Hence, if the largest singular value of $\mathbf{S}(j\omega_k)$ is larger than one, the nonexpansivity (scattering analogous of passivity) condition is also said to be locally violated.

Table (4.1.1) summarizes all the discussion on frequency-sweeping assessment techniques for LTI n-ports.

Table 1 – Physicality Constraints

Representation	Y (Z or hybrid)	S	H
Symmetry	$\mathbf{Y} = \mathbf{Y}^T$	$\mathbf{S} = \mathbf{S}^T$	-
Realness	$\mathbf{Y}(s) = \mathbf{Y}^*(-s)$	$\mathbf{S}(s) = \mathbf{S}^*(-s)$	$\mathbf{H}(s) = \mathbf{H}^*(-s)$
Passivity	$\lambda_{min} > 0$	$\sigma_{max} < 1$	-
Matrix Dimension	$n \times n$	$n \times n$	$n_{output} \times n_{input}$

4.1.2 Frequency Sweeping test revisited: positive-real submatrices

The preceeding section has brought a general discussion on passivity assessment at discrete frequencies considering the system matrix in its entirety, *i.e.* all ports evaluated at once. The root cause for passivity violations to arise may sometimes remains concealed in the inner parts of the system matrix, *viz.* in one or more of its constituent subsystems. There exist necessary conditions on the subsystems that could be used along with the necessary and sufficient condition presented in the previous section. These conditions are essential results from Linear Algebra available in references such as (GOLUB; LOAN, 2012; MEYER, 2000; HORN; JOHNSON, 2012) and herein enumerated for hybrid representations. Let $n \times n$ transfer matrix $\mathbf{H}(s)$ be positive-real, then the following necessary conditions should also hold in the open right-half s-plane (i.e., for $\mathrm{Re}(s) > 0$):

(i) Each diagonal subsystem is positive-definite, *i.e.* $H_{ii}(s) > 0$ for $1 \leq i \leq n$;

(ii) $\big(\mathrm{Re}(H_{ij})\big)^2 < \big(\mathrm{Re}(H_{ii})\big)\big(\mathrm{Re}(H_{jj})\big)$ for all $i \neq j$[1];

(iii) $\max_{i,j} \|H_{ij}(s)\|$ lies along the diagonal $\forall s$.

Condition (i) is equivalent to stating that negative conductances/resistances are not tolerated along the diagonal, which is not particularly surprising. However, since measurements usually comprise magnitude and phase angles, a negative conductance/resistance could easily pass unnoticed until the entire matrix is assembled and processed. Being able to spot passivity violations at an earlier stage during the data acquistion could even subsidize the detection of measurement mistakes.

These conditions are not meant to assert that a system is passive whenever they are satisfied but rather they can be used to assert that violations exist should they fail to be satisfied. These conditions are used in the novel passivity assessment algorithm to be proposed in the sequel.

[1] This condition is equivalent to row and column dominance of the diagonal elements, it could also have been stated as $2\big(\mathrm{Re}(H_{ij})\big) < \big(\mathrm{Re}(H_{ii})\big) + \big(\mathrm{Re}(H_{jj})\big)$

4.1.3 LMI-based test

This assessment method relies upon a connection between the feasibility of linear matrix inequalities associated with a state-space description and the positive-realness (bounded-realness) condition of the transfer matrix. The LTI system transfer matrix system is positive real if its state space realization satisfies the Positive Real Lemma (PRL). These concepts originate in Control Theory and are associated with the solution to the Lur'e equation. In reference (KALMAN, 1964) this connection is first established for Single-Input-Single-Output (SISO) systems, the extension of this result to the multi-variable case (MIMO) appeared later in (ANDERSON, 1967b). Considering a LTI n-port as characterized by Equation (2.4) and is repeated below for reference, a system thus characterized is passive only if the following LMI, whose variable $\mathbf{P}$ is a $n \times n$ matrix, is feasible:

$$\begin{bmatrix} -\mathbf{A}^T\mathbf{P} - \mathbf{P}\mathbf{A} & -\mathbf{P}\mathbf{B} + \mathbf{C}^T \\ -\mathbf{B}^T\mathbf{P} + \mathbf{C} & \mathbf{D} + \mathbf{D}^T \end{bmatrix} \succeq 0$$

with feasibility meaning that the solution set to Equation (2.4) is nonempty, i.e., there exists at least one matrix $\mathbf{P}$ such that it is symmetric and positive-semidefinite ($\mathbf{P} = \mathbf{P}^T \succeq 0$). Otherwise, the system is said to be non-passive. Feasibility of the LMI is a sufficient condition to establish system passivity, since it implies that $\mathbf{H}^H(s) + \mathbf{H}(s) \succeq 0$ for all $\mathrm{Re}(s) > 0$, i.e., the system is globally passive. Thus, in this sense, feasibility and passivity are equivalent statements. According to (CURTAIN, 1999) and (BOYD et al., 1994), the result in Equation (2.4), the positive-real lemma (PRL), is also usually called the Yakubovich-Kalman-Popov-Anderson or Kalman-Yakubovich lemma to reflect its authorship. The nonexpansivity condition for the scattering representation in terms of a LMI test, derived in (ANDERSON, 1967a), is called the bounded-real lemma (BRL) in the variable $\mathbf{P}$ and its associated matrix inequality is Equation (2.6):

$$\begin{bmatrix} \mathbf{A}^T\mathbf{P} + \mathbf{P}\mathbf{A} & \mathbf{P}\mathbf{B} & \mathbf{C}^T \\ \mathbf{B}^T\mathbf{P} & -\mathbf{I} & \mathbf{D}^T \\ \mathbf{C} & \mathbf{D} & -\mathbf{I} \end{bmatrix} \preceq 0,$$

such that $\mathbf{P} = \mathbf{P}^T \succeq 0$. If the BRL is satisfied, then $\mathbf{S}(s)$ is a bounded-real matrix: $\mathbf{S}^H(s)\mathbf{S}(s) \preceq \mathbf{I}$ for all $\mathrm{Re}(s) > 0$ and the system is globally nonexpansive. As noted in (BOYD et al., 1994), this fact can also be expressed as $\|\mathbf{S}\|_\infty \leq 1$. In reference (CURTAIN, 1999), one can find some extensions of these results to the infinite-dimensional case as well as further perspectives.

4.1.4 Hamiltonian test

The spectral properties of certain Hamiltonian matrices provide yet another connection to the positive/bounded-realness of the transfer matrix. A proof of this connection is established in reference (BOYD; BALAKRISHNAN; KABAMBA, 1989), whence the following definition of a Hamiltonian matrix **M** is a simple restatement of:

$$\mathbf{J}^{-1}\mathbf{M}\,\mathbf{J} = -\mathbf{M}^T \qquad \text{where} \qquad \mathbf{J} = \begin{bmatrix} \mathbf{0} & \mathbf{I} \\ -\mathbf{I} & \mathbf{0} \end{bmatrix}, \tag{4.8}$$

i.e., a matrix **M** satisfying Equation (4.8), with $\mathbf{J}^{-1} = \mathbf{J}^T = -\mathbf{J}$, is a Hamiltonian Matrix. Besides, as emphasized in (GRIVET-TALOCIA, 2004), its spectrum is symmetric with respect to both the real and imaginary axis and its characteristic polynomial is real and even-ordered. Therefore, if λ_i is an eigenvalue of **M** ($\lambda_i \in \{\lambda(\mathbf{M})\}$) then, due to the spectral symmetry, $-\lambda_i$ is also an eigenvalue of **M**: $-\lambda_i \in \{\lambda(\mathbf{M})\}$.

Assuming a LTI n-port characterized as in Equation (2.1), the system associated Hamiltonian matrices are formed as follows:

$$\mathbf{M}_\delta = \begin{bmatrix} \mathbf{A} + \mathbf{B}\big(2\delta\,\mathbf{I} - \mathbf{D} - \mathbf{D}^T\big)^{-1}\mathbf{C} & \mathbf{B}\big(2\delta\,\mathbf{I} - \mathbf{D} - \mathbf{D}^T\big)^{-1}\mathbf{B}^T \\ -\mathbf{C}^T\big(2\delta\,\mathbf{I} - \mathbf{D} - \mathbf{D}^T\big)^{-1}\mathbf{C} & -\mathbf{A}^T - \mathbf{C}^T\big(2\delta\,\mathbf{I} - \mathbf{D} - \mathbf{D}^T\big)^{-1}\mathbf{B}^T \end{bmatrix}, \tag{4.9}$$

for hybrid representations and

$$\mathbf{M}_\gamma = \begin{bmatrix} \mathbf{A} - \mathbf{B}\big(\mathbf{D}^T\mathbf{D} - \gamma^2\,\mathbf{I}\big)^{-1}\mathbf{D}^T\mathbf{C} & -\gamma\mathbf{B}\big(\mathbf{D}^T\mathbf{D} - \gamma^2\,\mathbf{I}\big)^{-1}\mathbf{B}^T \\ \gamma\mathbf{C}^T\big(\mathbf{D}\mathbf{D}^T - \gamma^2\,\mathbf{I}\big)^{-1}\mathbf{C} & -\mathbf{A}^T + \mathbf{C}^T\mathbf{D}\big(\mathbf{D}^T\mathbf{D} - \gamma^2\,\mathbf{I}\big)^{-1}\mathbf{B}^T \end{bmatrix}, \tag{4.10}$$

for the scattering representation whose respective parameters (δ and γ) are both strictly positive and δ is not an eigenvalue of $(\mathbf{D} + \mathbf{D}^T)/2$ whereas γ is not a singular value of **D**. Thus, the following connection can be established:

$$\begin{cases} \delta \in \{\lambda(\mathbf{H}(jw_k))\} \;\longleftrightarrow\; jw_k \in \{\lambda(\mathbf{M}_\delta)\} & \text{(for hybrid representations)} \\ \gamma \in \{\sigma(\mathbf{H}(jw_k))\} \;\longleftrightarrow\; jw_k \in \{\lambda(\mathbf{M}_\gamma)\} & \text{(for scattering representations)} \end{cases}, \tag{4.11}$$

such that the parameters δ and γ are respectively eigenvalues and singular values of the corresponding transfer matrix if and only if the associated hamiltonian matrix has purely imaginary eigenvalues, as proved in (BOYD; BALAKRISHNAN; KABAMBA, 1989). According to (GRIVET-TALOCIA, 2004), this result permits one to determine the exact frequencies at which the eigenvalues and singular values cross or are set in the neighbourhood of a given threshold which correspond to the values assigned to

parameters δ and γ. If the hamiltonian matrix has no purely imaginary eigenvalue, the assigned threshold is not crossed nor "touched". The threshold of interest is zero ($\delta = 0$) for hybrid representations and one ($\gamma = 1$) for the scattering case. In this particular setting, purely imaginary eigenvalues of the corresponding hamiltonian matrix (if any) should provide evidence as to the violation of the positive-realness condition posed by Equation (4.2). Therefore, a LTI n-port given in terms of Equation (2.1) is passive, or nonexpansive, under this Hamiltonian criterion, if and only if:

$$\mathbf{M}_{(\delta=0)} = \begin{bmatrix} \mathbf{A} - \mathbf{B}\big(\mathbf{D} + \mathbf{D}^T\big)^{-1}\mathbf{C} & \mathbf{B}\big(\mathbf{D} + \mathbf{D}^T\big)^{-1}\mathbf{B}^T \\ -\mathbf{C}^T\big(\mathbf{D} + \mathbf{D}^T\big)^{-1}\mathbf{C} & -\mathbf{A}^T + \mathbf{C}^T\big(\mathbf{D} + \mathbf{D}^T\big)^{-1}\mathbf{B}^T \end{bmatrix}, \tag{4.12}$$

for hybrid representations and

$$\mathbf{M}_{(\gamma=1)} = \begin{bmatrix} \mathbf{A} + \mathbf{B}\big(\mathbf{I} - \mathbf{D}^T\mathbf{D}\big)^{-1}\mathbf{D}^T\mathbf{C} & \mathbf{B}\big(\mathbf{I} - \mathbf{D}^T\mathbf{D}\big)^{-1}\mathbf{B}^T \\ -\mathbf{C}^T\big(\mathbf{I} - \mathbf{D}^T\mathbf{D}\big)^{-1}\mathbf{C} & -\mathbf{A}^T - \mathbf{C}^T\mathbf{D}\big(\mathbf{I} - \mathbf{D}^T\mathbf{D}\big)^{-1}\mathbf{B}^T \end{bmatrix} \tag{4.13}$$

for the scattering representation have no purely imaginary eigenvalues. By construction, $\mathbf{M}$ is a matrix of size $2n \times 2n$, twice the size of the state dynamics matrix and, as stressed in references (GRIVET-TALOCIA; UBOLLI, 2008) and (GRIVET-TALOCIA, 2004), this passivity assessment is frequency-independent with the resultant Hamiltonian matrices also being constant since its parameters are the matrices $\{\mathbf{A}, \mathbf{B}, \mathbf{C}, \mathbf{D}\}$ associated to the LTI system. Hence, it is possible to conclude that the absence of purely imaginary eigenvalues in the referred set implies feasibility of the LMI's, Equations (2.4) and (2.6), as well as positive realness of Equation (4.1). On the other hand, if there exists at least one purely imaginary eigenvalue, the system is non-passive.

The mere existence of purely imaginary eigenvalues of the Hamiltonian matrix is sufficient for distinguishing passive from non-passive behavior. However, further information can be obtained. By way of illustration, assume a Hamiltonian matrix (associated to a system as described by Equation (2.1) whose k positive imaginary eigenvalues form the following set:

$$\Omega \ = \{\lambda_1 = j\omega_1, \lambda_2 = j\omega_2, \ldots, \lambda_k = j\omega_k\}. \tag{4.14}$$

such that the eigenvalues are sorted in ascending order and $k \leq \frac{n}{2}$. Each of these eigenvalues correspond to the frequencies at which the positive-realness threshold of Equation (4.2) is reached, *i.e.* , if:

$$\mathbf{\Psi}(j\omega_i) \not\succeq 0 \qquad \forall\ \lambda_i = j\omega_i \ \in \ \Omega. \tag{4.15}$$

Nonetheless, since the eigenvalues or singular values are a continuous function of frequency, it is possible to characterize how the boundary is reached, that is to say, whether non-passive (or passive) behavior is found at frequencies higher than some jw_i or otherwise.

Using a first-order approximation based on Perturbation Theory, the author in (GRIVET-TALOCIA, 2004) derives a continuous function of frequency for the eigenvalues or singular values whose slope at the threshold can be evaluated, e.g., the frequencies at which the eigenvalues of $\mathbf{G}(jw)$ change sign. Hence, the elements in the set Ω define breakpoints between passive and non-passive behavior depending on the slope at each jw_i thus eliminating the need for sweeping along the frequency axis. As a result, passivity can be characterized in terms of bands of violation. With the set Ω and knowledge of the slopes at each of its k breakpoints, or crossover frequencies, the whole spectrum of frequencies can be divided into intervals, e.g., $(0, \omega_1), (\omega_2, \omega_3), ..., (\omega_k, \infty)$, such that the behavior within each (ω_{i-1}, ω_i) can be specified. It is even possible to quantify the maximum violation in each band (ω_{i-1}, ω_i) using the bisection algorithm, as proposed in (BOYD; BALAKRISHNAN; KABAMBA, 1989). Alternatively, bands of violation can also be identified more pragmatically by evaluating the positive-realness criterium, Equation (4.2), at the midpoint frequency between each successive element in the set Ω, e.g., $(\omega_{i-1} + \omega_i)/2$. Hence, if the positive-realness criterium fails to hold at the midpoint frequency $(\omega_{i-1} + \omega_i)/2$, then (ω_{i-1}, ω_i) defines a violation band. Furthermore, evaluate the same criterium at $w_1/2$ (from DC to w_1) and $2w_n$ (from w_n to ∞, asymptotic behavior).

Finer details, generalizations and further technical assumptions can be found in (GRIVET-TALOCIA, 2004), (BOYD; BALAKRISHNAN; KABAMBA, 1989), (GOLUB; LOAN, 2012) and references therein. Some technical difficulties arise when computing the purely imaginary eigenvalues of a Hamiltonian matrix that define frequency boundaries for passivity violations: (i) the eigenvalues are not purely imaginary but have a small real component due to numerical noise and (ii) the Hamiltonian matrix is twice as large as the associated state-dynamics matrix, thus leading to a time-consuming eigenvalue computation for large models. Considering its symmetrical spectrum, the Hamiltonian eigenvalues appear in pairs and quadruples. Therefore, there is redundancy in computing the same information twice. Under some special conditions, the subsequent test can be used in place of the traditional Hamiltonian matrix.

4.1.5 Half-size Test Matrix

The Half-size test comprises yet another algebraic passivity assessment method applicable to both passive and contractive systems, *i.e.* determining whether the positive-real condition as in Definition (19) and/or bounded-real condition as in Definition

(20) are satisfied. Furthermore, the test also enables the characterization of existing violations into frequency bands based on the parameters of the system's state-space realization. The test encompasses an upside and a downside relative to its predecessor Hamiltonian test: its associated test matrix is half[2] the size of the Hamiltonian but it is only applicable to externally symmetric[3] systems[4]. Despite being applicable symmetric systems only, large computational savings can be obtained so as to establish the crossover frequencies and the passivity violating intervals with matrices whose size are half that of the Hamiltonian matrix, thus its appeal.

These test matrices haven been proposed in references (GUSTAVSEN; SEMLYEN, 2009a) and (GUSTAVSEN; SEMLYEN, 2008; DESCHRIJVER; DHAENE, 2009) for admittance (impedance) and scattering representations respectively. Owing to some incorrect statements in (GUSTAVSEN; SEMLYEN, 2009a), the authors made a revision to their own claims in (GUSTAVSEN; SEMLYEN, 2009b), but a read of a further discussion on this issue as presented in (WONG; ZHANG, 2010) and (GRIVET-TALOCIA, 2010) is also recommended. A reduction in the size of the test matrix by a factor of two corresponds to the computational complexity to fall off by a factor of nearly eight (due to the cubic complexity relation), thus making the eigenvalue computation less of an issue. The numerical noise problem in the eigenvalues is also compensated since the eigenvalues of the half-size matrix are noiseless purely real and whose square roots correspond to the crossover frequencies that determine the breakpoints between passive and non-passive behavior hence also corresponding to the eigenvalues of the Hamiltonian matrix, with no redundancy.

Assuming a symmetric LTI n-port expressed as in Equation (2.1), the frequency-domain positive-realness condition is as follows:

$$\begin{aligned}
&\mathbf{H}(j\omega) + \mathbf{H}^H(j\omega) \succeq 0 \\
&\mathbf{H}(j\omega) + \mathbf{H}^T(-j\omega) \succeq 0 \\
&Re\{\mathbf{H}(j\omega)\} \succeq 0.
\end{aligned}$$

Passivity violations correspond to zero-crossings, *i.e.* whenever $Re\{\mathbf{H}(j\omega)\} = 0$. Therefore, the problem consists of finding the frequencies for which the homogeneous equation $Re\{\mathbf{H}(j\omega)\}$ holds, *viz.* its zeroes or singularities. Recalling that the system is represented as $\mathbf{H}(j\omega) = \mathbf{C}(j\omega\mathbf{I} - \mathbf{A})^{-1}\mathbf{B} + \mathbf{D}$ and considering the following equality

$$\big(j\omega\mathbf{I} - \mathbf{A}\big)^{-1} = -\mathbf{A}\big(\omega^2\mathbf{I} + \mathbf{A}^2\big)^{-1} - j\omega\big(\omega^2\mathbf{I} + \mathbf{A}^2\big)^{-1},$$

[2] thus its name: Half-size test matrices.
[3] Also called reciprocal. The VF realization satisfies this reciprocity condition.
[4] The Hamiltonian is twice as large but requires no symmetry assumptions

the system can be represented in the equivalent form:

$$\mathbf{H}(j\omega) = -\mathbf{CA}\left(\omega^2\mathbf{I} + \mathbf{A}^2\right)^{-1}\mathbf{B} - j\omega\mathbf{C}\left(\omega^2\mathbf{I} + \mathbf{A}^2\right)^{-1}\mathbf{B} + \mathbf{D}.$$

The real part thereof can now be extracted by inspection:

$$Re\{\mathbf{H}(j\omega)\} = -\mathbf{CA}\left(\omega^2\mathbf{I} + \mathbf{A}^2\right)^{-1}\mathbf{B} + \mathbf{D},$$

whose zeros are to be determined. The zeros of $Re\{\mathbf{H}(j\omega)\}$ can be determined as the poles of $\left(Re\{\mathbf{H}(j\omega)\}\right)^{-1} = \mathbf{D}^{-1}\mathbf{CA}\left(\omega^2\mathbf{I} + \mathbf{A}^2 - \mathbf{BD}^{-1}\mathbf{CA}\right)^{-1}\mathbf{BD}^{-1} + \mathbf{D}^{-1}$, therefore a simple eigenvalue problem[5]:

$$\text{eig}\left((\mathbf{BD}^{-1}\mathbf{C} - \mathbf{A})\mathbf{A}\right) = \text{eig}\left(\mathbf{T}_{\text{hybrid}}\right), \tag{4.16}$$

whereby $\mathbf{T}_{\text{hybrid}}$ is denoted the singularity test or Half-size test and within its set of eigenvalues the subset containing only positive-real eigenvalues ω^2 gives the frequencies ω for which the real part of the admittance representation changes sign, *i.e.* where the eigenvalues of the conductance matrix transition from a positive trajectory to a negative one. A similar test matrix can be obtained *mutatis mutandis* to the bounded-real case[6]:

$$\mathbf{T}_{\text{scatter}} = \left(\mathbf{A} - \mathbf{B}(\mathbf{D} - \mathbf{I})^{-1}\mathbf{C}\right)\left(\mathbf{A} - \mathbf{B}(\mathbf{D} + \mathbf{I})^{-1}\mathbf{C}\right) \tag{4.17}$$

whereby the negative-real eigenvalues of $\mathbf{T}_{\text{scatter}}$ delimit frequency points where unity is crossed. In a procedure similar to that of the Hamiltonian matrix, the crossover frequencies can be identified as the square root of the positive-real and negative-real eigenvalues of $\mathbf{T}$, for the admittance and scattering representations respectively. Therefore, the admittance Half-size test equivalent of the set given in Equation (4.14) yields:

$$\Omega \ = \{\lambda_1 = \omega_1^2, \lambda_2 = \omega_2^2, \ldots, \lambda_k = \omega_k^2\}. \tag{4.18}$$

The rest of the procedure to determine the violating frequency bands follows the same steps as explained for the Hamiltonian matrix. A performance comparison between the half-size test and hamiltonian test matrices is made in (GUSTAVSEN; SEMLYEN, 2009a).

[5] Should matrix **D** be singular, then one must resort to the Hamiltonian test.
[6] Idem.

4.1.6 Discussion on Assessment

These assessment techniques or passivity criteria have been ordered as they have historically appeared in the literature and permit passivity characterization at different levels of detail. Deciding upon which one to use is not at one's full discretion. For instance, assessing passivity before a model is synthesized rules out any choice of assessment technique based on model parameters. Hence, passivity assessment on raw data can only be accomplished with a search over measured frequencies, i.e., the sweeping technique. As for the parameter-based techniques, they assume a state-space realization to assemble the test matrices, which is by no means the only model structure usually deployed. Rational models constitute yet another commonly used structure in the context of frequency-dependent behaviour, specially the ubiquitous *pole-residue* rational form. Even though the majority of passivity criteria is formulated in terms of $\{\mathbf{A}, \mathbf{B}, \mathbf{C}, \mathbf{D}\}$ parameter set, a model initially synthesized in rational form can be converted into a state-space realization so that the test matrices be correctly assembled, an example of the conversion procedure can be found in (GUSTAVSEN; SEMLYEN, 2004). Each assessment technique has its own pros and cons and the right choice of assessment must also best reflect one's interest in assessing passivity, e.g., a simple passivity certificate or a more detailed and refined passivity characterization so as to identify some localized equipment pathology.

Applicable to both raw data and model, the frequency-sweeping tests constitute the simplest form of assessing passivity, at least conceptually. They are frequency-dependent in the sense that the test must be performed at every single frequency point: theoretically in the whole continuum of the right-half s-plane, $\mathrm{Re}(s) > 0$, and experimentally for the finite set $\{w_k\}_{k=1}^{K}$ of measured frequencies. Searching for positive-real matrices over a discrete set of measured frequencies imposes major limits on what conclusions can be reached due to inexorable experimental obstacles such as upper and lower bounds of the acquisition process and coarse sampling intervals. Owing to these two illustrative difficulties, one remains ignorant of what the system behavior can be between successive frequency samples as well as beyond the upper and lower bounds. As a result, if no negative eigenvalue is found at any frequency, test is inconclusive for positive-realness is only a necessary condition for passivity (not sufficient). Nonetheless, if this same procedure returns a single negative eigenvalue at a single frequency point, the system is assuredly non-passive since the necessary condition is not fulfilled. Therefore, this test is remarkably effective in furnishing a non-passivity certificate, but ineffective otherwise.

The LMI-based tests are very efficient in furnishing a global passivity certificate, in fact this test provides a single bit of information: the system is either passive or otherwise, no further information can be retrieved. It is a frequency-independent test

for there is no search over frequencies and only applicable once a model has been synthesized, since it is parameter-dependent. The passivity certificate is issued as soon as a single matrix **P** is found, this constitutes a feasibility problem that can be formulated as in (BOYD; VANDENBERGHE, 2004). If there is no such **P**, i.e., the solution set to the LMI is empty, the problem is infeasible and the system is non-passive but there are no means so as to specify where along the frequency axis the violations occur.

The Hamiltonian test is the most detailed among all the assessment tests. It involves no search over frequencies, thus frequency-independent, but it does require models parameters, hence a parameter-dependent test. Its appealing feature lies precisely in the possibility of specifying where along the frequency axis violations occur, if they ever do. Recalling that the purely imaginary eigenvalues of the Hamiltonian matrix are sorted in ascending order and the continuous bands of frequencies arranged in ascending order from $\omega = 0$ up to $\omega \to \infty$, i.e., $(0, \omega_1), (\omega_2, \omega_3), ..., (\omega_n, \infty)$; the first $(0, \omega_1)$ and last (ω_n, ∞) bands allow passivity assessment in d.c. and asymptotic terms, therefore a global continuous assessment (as opposed to finite discrete frequencies). Furthermore, as in reference (GRIVET-TALOCIA, 2004), these results are not compromised in case of inaccurate sampling.

In many aspects the Half-size test is similar to the Hamiltonian test. As a matter of fact, according to (GUSTAVSEN; SEMLYEN, 2008) and (GUSTAVSEN; SEMLYEN, 2009a), the motivations for deriving it were specially the Hamiltonian matrix's long eigenvalue computation time that can be very time-consuming for large models and also their sensitivity to noise resulting in small real components as opposed to the purely imaginary form. The eigenvalue computation can actually dominate the total computation time of further modeling steps, e.g., parameter estimation or passivity enforcement. Half-size tests are frequency-independent and parameter-dependent as well, they can reduce the eigenvalue computation time by a factor of nearly eight but have a major restriction: they are only applicable to symmetric models.

The frequency-independent methods are more reliable, namely the LMI-based, Hamiltonian and Half-size tests, since the usual problems associated with the sweeping method such as determining how fine a search over the frequencies should be do not arise. However, the only choice for assessing passivity before parameter estimation is the sweeping assessment which can effectively provide a passivity violation certificate if there is at least a single negative eigenvalue (or a singular value larger than one) for at least one frequency point. Otherwise, knowledge of passivity violations remains inconclusive.

Even though most of the literature on passivity assessment concentrates on symmetrical models on the grounds that physical systems result in symmetrical port matrices there is something of note regarding any model symmetry assumption. For

instance, the simplifying correspondence established in Equation (4.3) and the arguments of Equations (4.4) and (4.5) are strictly valid provided the system is symmetric, as noted in (GUSTAVSEN; SEMLYEN, 2009a) and (WONG; ZHANG, 2010). However, the positive-realness condition for the general form of Equation (4.2) must hold for a passive system, irrespective of any symmetry assumptions. The Half-size tests are valid exclusively for symmetric systems whereas the LMI-based and Hamiltonian tests apply even when the system is devoid of symmetry. In the case of power transformers, symmetry is generally not an issue but care must be taken when synthesizing a model for some strategies aimed at reducing the computational time of parameter estimation can break the symmetry of the original data. A practical illustration of this difficulty comprises the use of *pole-residue* modeling obtained via the algorithm known as Vector Fitting (VF), as in (GUSTAVSEN; SEMLYEN, 1999), employing its column-wise fitting procedure aiming at computational savings thus resulting in slightly unsymmetrical models. Furthermore, conversion from the rational to the state-space forms requires a specific procedure so that symmetry is not broken, as demonstrated in (GUSTAVSEN; SEMLYEN, 2004) and (GUSTAVSEN; SEMLYEN, 2008).

It is of paramount importance to interpret the common occurrence of inconsistent time-domain simulations of intrinsically passive systems. Examples of such difficulties abound in the literature and their root causes are usually associated with unmodeled characteristic features such as stability, causality, and chiefly passivity, both in the data used in model derivation or the model itself. Obviously, these arguments favouring passivity as a desired or characteristic feature exclude the cases concerning data and models of explicit sources such as generators. These passivity assessment techniques are essentially passivity conditions expressed as mathematical criteria that through various equivalent algebraic conditions provide means to distinguish passive systems from non-passive ones within the broader general set of all linear systems. Even though this research dwells on the linearity assumption, most of the results can be extended, *mutatis mutandis*, to time-varying and infinite dimensional systems as well.

4.2 Perturbative Passivity Enforcement

Passivity enforcement is a procedure whose sole purpose is to ascertain that the passivity criteria be fulfilled by computing a correction or perturbation to an existing model of a given frequency response. In the search for a passive model to a passive system, it is precisely passivity violation as identified by some assessment method what prompts the enforcement task to be performed. As passivity has remained an unmodeled effect during parameter estimation, the estimated parameters do not reflect the exact system dynamics and must therefore be changed insofar as passive behavior be recovered. Model parameters are usually evaluated by means of some

minimizing criteria so as to yield an optimal approximation to data, hence any parameter perturbation must be minimal as well. Typically, not all but only some parameters are actually perturbed to compensate passivity violations specially those permitting some further structure simplification to be favourably exploited, e.g., linearity. In general terms, a parameter perturbation comprises computing a $\boldsymbol{\Delta}$ to be incorporated into a set of parameters $\widehat{\Theta}$, i.e.,

$$\widehat{\boldsymbol{\Theta}}' = \widehat{\boldsymbol{\Theta}} + \boldsymbol{\Delta}, \tag{4.19}$$

such that the computed perturbation simultaneously renders the model passive and has a least impact on the original model:

$$\min \|\boldsymbol{\Delta}\|. \tag{4.20}$$

As a result, any compensation made to the original parameters is minimal in terms of the resulting model approximation error.

4.2.1 Discrete-frequency Passivity Enforcement

This particular enforcement strategy presupposes an existing accurate model in some functional form whose parameters serve as the starting point for further developments. As the discrete-frequency qualifier indicates, this procedure entails formulating a problem constraint that ensures the direct enforcement of the passivity condition for all or some judiciously selected frequency samples at which passivity is violated so as to recover a global passive behavior. Since the method relies on discrete enforcement, it is therefore unable to guarantee that a globally passive behavior be attained. Nevertheless, to overcome this difficulty, the enforcement algorithm can be embedded into an iterative procedure associated with the right assessment methods so that strategic frequencies be chosen and a global solution is thus obtained. As a consequence, the difference between existing formulations in the literature lies in the choice of the adaptive frequency sampling employed and the optimization strategy used to formulate an objective function as well its constraints. Common implementations include Linear Programming (LP) in (SARASWAT; ACHAR; NAKHLA, 2004), Quadratic Programming (QP) in (GUSTAVSEN; SEMLYEN, 2001) and Second-order Cone Programming (SOCP) in (GRIVET-TALOCIA; UBOLLI, 2008). The problem constraints must establish a functional correspondence between parameter and eigenvalue perturbation, such correspondence is usually a non-linear one thus leading to another iterative procedure in order to attain a satisfactory result. In terms of problem formulation, parameter perturbations resulting in a minimal change to the initial approximation can be computed by some optimization-based algorithm.

First developed in (GUSTAVSEN; SEMLYEN, 2001), the passivity enforcement method accompanying the Vector Fitting (VF) algorithm (GUSTAVSEN; SEMLYEN, 1999) is based on Quadratic Programming and called Residue Perturbation Driver (RPD). The overall package structure, i.e., estimation and enforcement was packed into a single routine in (GUSTAVSEN, 2002) and (GUSTAVSEN, 2007). In this particular setting, the existing initial approximation is structured as a *pole-residue* model, as parameterized by the VF algorithm:

$$\mathbf{H}(s) \;\cong\; \hat{\mathbf{H}}(s) = \sum_{m=1}^{N} \frac{\mathbf{R}_m}{jw - a_m} + \mathbf{D} + s\mathbf{E}, \tag{4.21}$$

whose parameters $\mathbf{R}_m$, a_m, **D** and **E** can be modified so that the passivity criterion be fully satisfied; see (GUSTAVSEN, 2007). By keeping the parameters in the denominator unchanged (*i.e.* holding the system's poles a_m fixed), the initial unconstrained model as determined by Vector Fitting algorithm is linearly dependent on the remaining parameters; consequently, any incremental changes made to them are also linearly related to incremental changes to the model. Since admittance characterizations comprise a core application, it is assumed that $\hat{\mathbf{H}}(s) = \hat{\mathbf{Y}}(s)$, some linear network is approximated with a *pole-residue* model. The admittance matrix is symmetric by construction during the identification process owing to the common-pole construction embedded in the VF algorithm, thus all parameter matrices $\mathbf{R}_m$, **D** and **E** are symmetric.

The following formulation for passivity enforcement was initially devised in (GUSTAVSEN; SEMLYEN, 2001) and later refined in (GUSTAVSEN, 2007), the strategy revolves around residue perturbation. Hence, the objective is to perturb model parameters so that the approximation remains as accurate as possible and the passivity criterion be fully satisfied, thus:

$$\begin{aligned} &\text{minimize} && \|\Delta\hat{\mathbf{Y}}(\theta, s)\|_2 \\ &\text{subject to} && \big(\hat{\mathbf{Y}}(s) + \Delta\hat{\mathbf{Y}}(\theta, s)\big) + \big(\hat{\mathbf{Y}}(s) + \Delta\hat{\mathbf{Y}}(\theta, s)\big)^H \succeq 0 \end{aligned} \tag{4.22}$$

whereby θ is a vector lumping all free parameters, $s = j\omega$ and the superscript ^{H} denotes Hemitian conjugate. The optimization variable θ is formed by stacking the parameters ($\Delta\mathbf{R}_m, \Delta\mathbf{D}$), *i.e.* the perturbations for the model parameters. For a general case comprising an admittance matrix of size $P \times P$ and an approximation order of N, the vector θ containing the $\big(P(P+1)(N+1)\big)/2$[7] stacked parameter perturbations can be formed as follows:

$$\theta^T = [\Delta R_{11,1} \ldots \Delta R_{11,N}\ \Delta D_{11}\ R_{21,1} \ldots \Delta R_{21,N}\ \Delta D_{21} \ldots \Delta R_{PP,1} \ldots \Delta R_{PP,N}\ \Delta D_{PP}]^T .$$

[7] Assuming a symmetric model thus reducing the number of variables to the triangular part of the system.

Since the model is symmetric, the objective can be rewritten as:

$$\begin{aligned} &\text{minimize} && \|\Delta\hat{\mathbf{Y}}(\theta,s)\|_2 \\ &\text{subject to} && \hat{\mathbf{G}}(s)+\Delta\hat{\mathbf{G}}(\theta,s)\succeq 0 \end{aligned}$$

where $\hat{\mathbf{G}}(s)+\Delta\hat{\mathbf{G}}(\theta,s)=\text{Re}\big(\hat{\mathbf{Y}}(s)+\Delta\hat{\mathbf{Y}}(\theta,s)\big)$, *i.e.* a perturbation to the conductance matrix. This problem is equivalent to:

$$\begin{aligned} &\text{minimize} && \|\Delta\hat{\mathbf{Y}}(\theta,s)\|_2 \\ &\text{subject to} && \lambda\big(\hat{\mathbf{G}}(s)+\Delta\hat{\mathbf{G}}(\theta,s)\big)\geq 0 \end{aligned}$$

with $\lambda(\cdot)$ denoting an operator extracting the eigenvalues of the matrix passed as argument and $\geq$ is a component-wise inequality on each eigenvalue. Then, this problem can be further simplied to:

$$\begin{aligned} &\text{minimize} && \|\Delta\hat{\mathbf{Y}}(\theta,s)\|_2 \\ &\text{subject to} && \lambda_{min}\big(\hat{\mathbf{G}}(s)+\Delta\hat{\mathbf{G}}(\theta,s)\big)\geq 0 \end{aligned}$$

where $\lambda_{min}(\,\cdot\,)$ denotes the smallest eigenvalue of the perturbed conductance matrix. Solving this problem is no simple task for two major reasons: (i) the inequality has to be enforced along the continuum of the frequency spectrum and (ii) the function $\lambda_{min}(\theta,s)$ is highly nonlinear in its parameters. On the assumption that passivity violations be small[8,9], the functional dependence of the passivity criterion upon the model parameters can be linearized as follows:

$$\begin{aligned} \big(\hat{\mathbf{G}}+\Delta\hat{\mathbf{G}}-(\lambda+\Delta\lambda)\mathbf{I}\big)\big(\mathbf{u}+\Delta\mathbf{u}\big) &= 0 \\ \big(\hat{\mathbf{G}}+\Delta\hat{\mathbf{G}}\big)\big(\mathbf{u}+\Delta\mathbf{u}\big)-\big((\lambda+\Delta\lambda)\mathbf{I}\big)\big(\mathbf{u}+\Delta\mathbf{u}\big) &= 0 \\ \hat{\mathbf{G}}\mathbf{u}+\Delta\hat{\mathbf{G}}\mathbf{u}+\hat{\mathbf{G}}\Delta\mathbf{u}+\Delta\hat{\mathbf{G}}\Delta\mathbf{u}-(\lambda+\Delta\lambda)\mathbf{u}-(\lambda+\Delta\lambda)\Delta\mathbf{u} &= 0 \\ \hat{\mathbf{G}}\mathbf{u}+\Delta\hat{\mathbf{G}}\mathbf{u}+\hat{\mathbf{G}}\Delta\mathbf{u}-(\lambda+\Delta\lambda)\mathbf{u}-\lambda\Delta\mathbf{u} &= 0 \\ \big(\Delta\hat{\mathbf{G}}-\Delta\lambda\big)\mathbf{u} &= 0 \\ \mathbf{u}^T\big(\Delta\hat{\mathbf{G}}-\Delta\lambda\big)\mathbf{u} &= 0 \\ \Delta\lambda &= \mathbf{u}^T\text{Re}\{\Delta\hat{\mathbf{Y}}\}\mathbf{u} \end{aligned}$$

where $\mathbf{u}$ stands for a normalized eigenvector of the matrix $\hat{\mathbf{G}}$[10] and to avoid clutter we have omitted the arguments of each term, namely either (s)[11] or (θ,s)[12]. All these steps

[8] Small is the common terminology employed in the literature but there does not seem to exist a consensus as to how small a negative eigenvalue should be to qualify as small.
[9] This assumption is commonly true, though need not be so in general.
[10] This means $\mathbf{u}$ is problem data since it only depends on the frequency.
[11] For the original unconstrained model.
[12] For model perturbation.

beginning with an eigenvalue problem for the perturbed system ultimately resulted in a linear correspondence between the parameter perturbation and the eigenvalue shift ($\Delta\lambda(s)$) for the real part of the perturbed model $\hat{\mathbf{G}} + \Delta\hat{\mathbf{G}}$. More precisely, we have:

$$\Delta\lambda(s) = \mathbf{u}^T(s)\text{Re}\{\Delta\hat{\mathbf{Y}}(\theta, s)\}\mathbf{u}(s).$$

The eigenvalue shift is only needed at those frequencies at which passivity violations occur, therefore it should be an upshift to cancel the negative eigenvalues characterizing passivity violations. These frequencies can be found with passivity assesment methods such as the ones discussed in the previous Section (4.1), specifically those in Subsections (4.1.4) and (4.1.5), the latter is the fastest but only applicable to symmetric systems which happens to be case whenever a common-pole VF realization is used. Even though these passivity assessment methods determine intervals containing passivity violations, each of these intervals have an infinite number of frequency points. In practice, the upshift is applied at the minimum eigenvalues within each violation interval and, of course, the upshifts must equal in magnitude these minimum eigenvalues, *i.e.* for each minimum eigenvalue of each interval we set:

$$\Delta\lambda(s) = -\lambda(\hat{\mathbf{G}}(s)).$$

Setting the eigenvalue shift to be equal the largest violations but with opposite sign has the effect of bringing negative eigenvalues to the zero threshold, thus annihilating them. Therefore, the passivity enforcement problem can be stated as follows:

$$\begin{aligned} &\text{minimize} && \|\Delta\hat{\mathbf{Y}}(\theta, s)\|_2 \\ &\text{subject to} && \mathbf{u}^T(s)\text{Re}\{\Delta\hat{\mathbf{Y}}(\theta, s)\}\mathbf{u}(s) \geq -\lambda(\text{Re}\{\hat{\mathbf{G}}(s)\}) \end{aligned} \tag{4.23}$$

In practice, this problem is solved iteratively. The objective is quadratic (a norma minimization) and the inequality constraint is a linear inequality. The objective is minimized over a finite discrete set of measured frequencies $\{\omega_k\}_{k=1}^K$ whereas the constraints are enforced at the set of frequencies corresponding to largest violations found for each violation interval $\{\omega_l\}_{l=1}^L$.

Therefore, bringing Equation (4.23) to a standard QP (Quadratic Programming) form, we get:

$$\begin{aligned} &\text{minimize} && (1/2)\theta^T(\mathbf{K}^T\mathbf{K})\theta \\ &\text{subject to} && \mathbf{F}\theta < \mathbf{c} \end{aligned} \tag{4.24}$$

K is a matrix built upon a linear relation between parameter and admittance perturbation whereas **F** comprises the passivity constraint matrix based on the approximate linear

relation between parameter perturbation and eigenvalue shift. Equation (4.24) defines a constrained least squares fitting whose constraints are directly related to the passivity requirement. Consequently, any correction made to the initial approximation is minimal in terms of the resulting fitting error, since it ensures passivity with a smallest possible increase in a least-squares sense, which can also be manipulated by some weighting scheme. As already stressed, this problem is solved iteratively owing to the actual nonlinear relation existing between parameter pertrubation and violating eigenvalues, but was linearized for that formulation.

Matrix **K** in Equation (4.24) is formed by stacking all row blocks $\mathbf{K}_k(j\omega_k)$ corresponding to each every individual frequency sample ω_k from the set $\{\omega_k\}_{k=1}^{K}$. The matrix $\mathbf{K}_k(j\omega_k)$ that establishes the linear relation is based on the assumptions that the set of poles $\{a_m\}$ initially estimated are held fixed while the other parameters are readjusted. Therefore, $\mathbf{K}_k(j\omega_k)$ equals:

$$\mathbf{K}_k(j\omega_k) = \begin{bmatrix} \frac{1}{s-a_1} & \dots & \frac{1}{s-a_N} & 1 & 0 & \dots & 0 & 0 & \dots & 0 & \dots & 0 & 0 \\ 0 & \dots & 0 & 0 & \frac{1}{s-a_1} & \dots & \frac{1}{s-a_N} & 1 & 0 & \dots & \dots & 0 & 0 \\ \vdots & \dots & \vdots & \vdots & 0 & \dots & 0 & 0 & \ddots & 0 & \ddots & \vdots & \vdots \\ \vdots & \ddots & \vdots & \vdots & \vdots & \ddots & \vdots & \vdots & \ddots & 0 & \dots & 0 & 0 \\ 0 & \dots & 0 & 0 & 0 & \dots & 0 & 0 & 0 & \frac{1}{s-a_1} & \dots & \frac{1}{s-a_N} & 1 \end{bmatrix}.$$

As for the matrix **F** in Equation (4.24), it defines the linearization between the parameter perturbation vector θ and the vector **c** containing all violating eigenvalues at frequencies $\{\omega_l\}_{l=1}^{L}$, such that $\mathbf{F} = \mathbf{QK}$. Matrix **Q** consists of the stacked $\mathbf{Q}_k(j\omega_k)$ block matrices for each violating frequency containing the following arrangements of the normalized eigenvectors of the inital model:

$$\mathbf{Q}_k(jw_k) = \begin{bmatrix} u_1^T & 0 & \dots & 0 \\ 0 & u_2^T & \dots & 0 \\ \vdots & 0 & \ddots & 0 \\ 0 & 0 & \dots & u_n^T \end{bmatrix} \begin{bmatrix} u_1^T & \dots & 0 \\ \vdots & \ddots & 0 \\ 0 & \dots & u_1^T \\ u_2^T & \dots & 0 \\ \vdots & \ddots & \vdots \\ \vdots & \ddots & \vdots \\ 0 & \dots & u_{n-1}^T \\ u_n^T & \dots & 0 \\ \vdots & \ddots & 0 \\ 0 & \dots & u_n^T \end{bmatrix}.$$

such that $u_1, \dots, u_n$ are the normalized eigenvectors of the associated diagonalization of the measured admittance matrix, *i.e.* , the columns of the matrix of eigenvector

U in $\mathbf{Y}(j\omega_k) = \mathbf{U}(j\omega_k)\mathbf{\Lambda}(j\omega_k)\mathbf{U}^{-1}(j\omega_k)$. Matrices **K** and **F** in Equation (4.24) owe their sizes to the number of measured frequencies and the number of violating frequencies respectively, the higher the number of frequencies the larger the matrices, hence implying a longer computation time. In its earliest formulation in reference (GUSTAVSEN; SEMLYEN, 2001), all frequency samples found to violate the passivity criteria are involved in the process of adjusting the residues, with an impact on the size of matrix **F** in Equation (4.24). This process was later refined in (GUSTAVSEN, 2007) for which the authors use the Hamiltonian matrix to define strategic frequencies within every violation band instead of sweeping the whole measured spectrum and including all violating frequencies in the constraint equations. With the Hamiltonian assessment method, the constraint equations are significantly reduced in size by only including the frequencies for which the passivity violation is the largest within every band instead of the entire violating band. Nonetheless, assessing passivity with the Hamiltonian matrix requires that the model be converted from the pole-residue form to the state-space form, conversion details can be found in (GUSTAVSEN; SEMLYEN, 2004) and (GUSTAVSEN; SEMLYEN, 2009a).

The main drawback of being selective in choosing the frequencies to constitute the problem constraint is that unpredicted violations can be created at frequencies other than those initially assessed, which is why the robust iterative procedure proposed in the paper (GUSTAVSEN, 2007) is used. Its basic strategy is to include in the constraint matrix **F** additional samples chiefly outside the fitting band which are assigned a small weight so that the enforcement scheme does not concentrate within the bounds of the fitting range.

However, the problem reduction via the Hamiltonian assessment greatly improves computation times since matrix **F** is full but only contains as many rows as ones chooses for the enforcement. On the other hand, matrix **K** is sparse thus permitting this feature to be favourably exploited. One last remark about the Hamiltonian assessment method is that it allows to include frequency points beyond the fitting range, not possible with in the earlier formulation using sweeping assessment methods, thus allowing a global passivity enforcement to be attained in an iterative scheme.

It is noted that the vector θ does not include any ΔE_{ij}. As discussed in (CIP-PARRONE; GUSTAVSEN; SEMLYEN, 2001), even if the improper term **E** is non zero, it does not exert influence on the matrix $\mathrm{Re}(\hat{\mathbf{Y}}(j\omega_k))$ whose eigenvalues should be perturbed. Therefore any ΔE_{ij} is not related to the passivity requirement, it can however be enforced to be positive-definite for circuit realization purposes. As a matter of fact, in its earliest formulation published in (GUSTAVSEN; SEMLYEN, 2001), the vector θ contained only the residue terms and passivity was enforced separately to both **D** and **E** with an algebraic procedure based on matrix diagonalization. For this reason, this

particular passivity enforcement scheme is known as Residue Perturbation (RP). Gustavsen has uploaded his Matlab implementation for this code on the internet, reference to this code is henceforth denoted RPD, which stands for Residue Perturbation Driver.

The RP scheme enforces passivity while minimizing the approximation change to the measurements in an element-wise fashion. There is however a sensitivity problem concerning n-port systems (e.g., power transformers) with a large spread in the admittance matrix eigenvalues, i.e., a significant disparity in the magnitudes of the eigenvalues. This poses a difficulty in cases requiring matrix inversion due to testing a model with terminal conditions other than those assumed for parameter estimation. A common example is the inversion of an estimated admittance matrix so that a open-circuit terminal configuration be simulated or even using current sources as input to the model instead voltage sources. Care must be taken in matrix inversion processes, specially where the maximum-to-minimum eigenvalue ratio is large. As consequence of linear algebra, small eigenvalues of $\hat{\mathbf{Y}}(j\omega)$ become large eigenvalues of $\hat{\mathbf{Z}}(j\omega) = \hat{\mathbf{Y}}^{-1}(j\omega)$ giving rise to numerical issues. Therefore, parameter perturbations should take into account this relative impact on each system mode.

As a result, a Modal Perturbation (MP) was proposed in (GUSTAVSEN, 2008b). Basically, this MP approach comprises a reformulation of Equation (4.24) so that the perturbation size of the admittance eigenvalues is inversely proportional to the eigenvalue size. The reformulated objective writes as follows:

$$\begin{gathered}\left(\sum_{m=1}^{N}\frac{\Delta\mathbf{R}_m}{j\omega - a_m} + \Delta\mathbf{D}\right)\left(\frac{\mathbf{t}_i(jw)}{|\lambda_i(j\omega)|}\right) \approx 0 \\ \widehat{\mathbf{G}}(j\omega) + \Delta\mathbf{G}(j\omega) \succ 0\end{gathered} \tag{4.25}$$

where $\mathbf{u}_i(j\omega)$ and $|\lambda_i(j\omega)|$ are the eigenvectors and eigenvalues associated with $\mathbf{Y}(j\omega) = \mathbf{U}(j\omega)\mathbf{\Lambda}(j\omega)\mathbf{U}^{-1}(j\omega)$. This reformulation basically includes a weighting scheme for which the sizes of the perturbations are inversely proportional to that of the corresponding eigenvalue magnitudes, thereby avoiding uneven perturbational effects over small modes (eigenvalues) such that they are perturbed relatively to their size, thus preserving the overall model behavior when using hybrid terminations. The relative weighting scheme comes at the cost of a relative higher computation time for enforcement, thus its main drawback as compared with the preceding RP and thereby limiting the MP approach to small and medium-scale problems associated with the need of parameter conversion and arbitrary terminal configurations. This modal perturbation resulted in a reformulation of the vector fitting main algorithm (VF) for special uses addressing arbitrary terminal conditions, as in reference (GUSTAVSEN; HEITZ, 2008).

Even though both the RP and MP approaches have a small perturbational effect over the initial parameter, they are relatively demanding in terms of computation time.

In (GUSTAVSEN, 2008a), the author proposes another refinement to RP and MP enforcement methods which significantly reduces the computation time at the expense of a slightly poorer approximation, i.e, a larger modelling error. The idea is to reduce the number of variables in the vector θ of the QP formulation in Equation (4.24). The reduction is attained by perturbing only the eigenvalues of each matrix $\Delta\mathbf{R}_m$ and $\Delta\mathbf{D}$ (also $\Delta\mathbf{E}$, if applicable) as opposed to the earlier strategies that perturb each individual entry of these matrices. This procedure leads to the Fast Residue Perturbation (FRP) and the Fast Modal Perturbation (FMP) methods, both described in (GUSTAVSEN, 2008a).

Therefore, the discrete-enforcement scheme as formulated by Equation (4.22) comes in four variations, namely the Residue Perturbation (RP), Modal Perturbation (MP), Fast Residue Perturbation (FRP) and Fast Modal Perturbation (FMP). A performance comparison can be found in reference (GUSTAVSEN, 2008a).

4.2.2 Hamiltonian Perturbation Methods

This passivity enforcement scheme is a natural continuation of the Hamiltonian assessment method for which the initial approximation is structured as a *state-space* model. Its applicability encompasses all the LTI n-port representations earlier discussed, i.e., any state-space realization whose input-output transfer matrix is in admittance, impedance, hybrid, or scattering form. Basically, the process entails the determination of a compensation to the state-space matrices $\{\mathbf{A}, \mathbf{B}, \mathbf{C}, \mathbf{D}\}$ such that the perturbed system is rendered passive at the cost of a minimal change to system's input-output characteristic response. Under the Hamiltonian perspective, a given system is passive if its associated Hamiltonian matrix has no purely imaginary eigenvalues, thus meaning that the compensated state-space realization obtained from this passivity enforcement must have an associated Hamiltonian matrix whose set of eigenvalues does not contain a single purely imaginary eigenvalue. In (GRIVET-TALOCIA, 2004), a perturbation scheme is devised so as to displace these purely imaginary eigenvalues off the imaginary axis (a passivity requirement) and yet cause a least change to the system's input-output characteristic response. This objective is pursued by applying a perturbation to associated matrix **C** only, leaving the remaining matrices unchanged. According to (GUSTAVSEN; SEMLYEN, 2004), the matrix **C** of a *state-space* model corresponds to all residue matrices of a *pole-residue* model and, in this sense, this Hamiltonian perturbation scheme is also referred to in the literature as a residue perturbation.

In order to guarantee that the deviation of the perturbed system's input-output response from those of the original system be minimal, the cost function in the variable $\Delta\mathbf{C}$ used as criteria for a least deviation minimizes the energy associated with the change of each matrix element's impulse responses. The task involves computing a

$\Delta\mathbf{C}$ that perturbs the initially estimated state matrix $\mathbf{C}$, i.e., $\mathbf{C}' = \mathbf{C} + \Delta\mathbf{C}$, such that the perturbed system $\{\mathbf{A}, \mathbf{B}, \mathbf{C}', \mathbf{D}\}$ be passive while minimizing the cumulative energy of the induced perturbation on the system's impulse responses:

$$E = \sum_{i,j=1}^{n} \int_{0}^{\infty} |(\Delta h)_{i,j}(t)|^2 dt = \text{tr}(\Delta\mathbf{C}\,\mathbf{W}\,\Delta\mathbf{C}^T) \tag{4.26}$$

where tr(·) denotes the trace operator that takes as argument a square matrix and $\mathbf{W}$ is the system controllability Gramian (defined in (CHEN, 1999)), computed as the unique, symmetric and positive definite solution of the Lyapunov equation $\mathbf{AW} + \mathbf{WA}^T = -\mathbf{BB}^T$. The right-hand side of Equation (4.26) can be further simplified by means of a suitable coordinate change, namely $\Delta\mathbf{C}_k = \Delta\mathbf{C}\,\mathbf{K}^T$, such that $\mathbf{K}^T$ is derived from the Cholesky factorization of the Gramian ($\mathbf{W} = \mathbf{K}^T\mathbf{K}$), thus yielding:

$$E = \text{tr}(\Delta\mathbf{C}_k\Delta\mathbf{C}_k^T) = ||\Delta\mathbf{C}_k||_F^2 = ||\text{vec}(\Delta\mathbf{C}_k)||_2^2 \tag{4.27}$$

with vec(·) denoting an operator that stacks the columns of a matrix into a single column vector and the subscript $_F$ standing for the Frobenius norm. According to (GRIVET-TALOCIA, 2004), Equation (4.27) establishes a correspondence between the minimization of the system impulse-response perturbations and the perturbation of the state matrix $\mathbf{C}$ which is minimal in this sense, using the appropriate coordinate system.

Again, the relation between the residues (free variables) and the passivity condition is a nonlinear one, thus a first-order perturbation (linearization) will be applied to the system's original Hamiltonian matrix ($\mathbf{M}_{\delta=0}$ in the hybrid case and $\mathbf{M}_{\gamma=1}$ for scattering representations) so as to displace its imaginary eigenvalues, in an iterative scheme, hence forcing them to eventually move off the imaginary axis. The perturbed Hamiltonian matrix whose set of eigenvalues contains no purely imaginary element can be written as:

$$\begin{aligned} \mathbf{M}'_{\delta=0} &\cong \mathbf{M}_{\delta=0} + \Delta\mathbf{M}_{\delta=0} \\ \mathbf{M}'_{\gamma=1} &\cong \mathbf{M}_{\gamma=1} + \Delta\mathbf{M}_{\gamma=1} \end{aligned}$$

for both hybrid and scattering representations, respectively. The first-order terms are themselves Hamiltonian matrices in terms of the free variable $\Delta\mathbf{C}$, assembled as follows:

$$\Delta\mathbf{M}_{\delta=0} = \begin{bmatrix} \mathbf{B}\mathbf{Q}_\delta^{-1}\Delta\mathbf{C} & \mathbf{0} \\ -\mathbf{C}^T\mathbf{Q}_\delta^{-1}\Delta\mathbf{C} - \Delta\mathbf{C}^T\mathbf{Q}_\delta^{-1}\mathbf{C} & -\Delta\mathbf{C}^T\mathbf{Q}_\delta^{-1}\mathbf{B}^T \end{bmatrix}, \tag{4.28}$$

with $\mathbf{Q}_\delta = 2\delta\,\mathbf{I} - \mathbf{D} - \mathbf{D}^T$ for hybrid representations and

$$\Delta\mathbf{M}_{\gamma=1} = \begin{bmatrix} -\mathbf{B}\mathbf{R}_\gamma^{-1}\mathbf{D}^T\Delta\mathbf{C} & \mathbf{0} \\ \mathbf{C}^T\mathbf{S}_\gamma^{-1}\Delta\mathbf{C} + \Delta\mathbf{C}^T\mathbf{S}_\gamma^{-1}\mathbf{C} & \Delta\mathbf{C}^T\mathbf{D}\mathbf{R}_\gamma^{-1}\mathbf{B}^T \end{bmatrix}, \tag{4.29}$$

with $\mathbf{R}_\gamma = \mathbf{D}^T\mathbf{D} - \gamma^2\mathbf{I}$ and $\mathbf{S}_\gamma = \mathbf{D}\mathbf{D}^T - \gamma^2\mathbf{I}$ for scattering representations. By changing the initial parameter matrix $\mathbf{C}$, the first order perturbation induces a displacement of each imaginary eigenvalue jw_i which is given by the following linear expression:

$$j\Delta w_i = \frac{\mathbf{v}_i^H\mathbf{J}\Delta\mathbf{M}\mathbf{v}_i}{\mathbf{v}_i^H\mathbf{J}\mathbf{v}_i} \tag{4.30}$$

where $\mathbf{v}_i$ are the eigenvectors associated to the purely imaginary eigenvalues jw_i of the original unperturbed Hamiltonian matrix and the matrix $\mathbf{J}$ as defined in Equation (4.8). Equation (4.30) contains the prescribed amount by which the eigenvalues can be displaced under the first-order perturbation scheme and its numerator is a linear function of the free variable $\Delta\mathbf{C}$, as in Equations (4.28) and (4.29) depending on the representation adopted. This linear relation is used to derive a linear equality between parameter perturbation and eigenvalue displacement. According to (GRIVET-TALOCIA, 2004), this linear relation can be written as:

$$\mathrm{Re}[\mathbf{v}_{i1}^T \otimes \mathbf{z}_i^H]\mathrm{vec}(\Delta\mathbf{C}_k) = -\,\mathrm{Im}[\mathbf{v}_{i1}^H\mathbf{v}_{i2}](\Delta w_i) \tag{4.31}$$

where the original Hamiltonian matrix eigenvector $\mathbf{v}_i$ has been partitioned as $\mathbf{v}_i = [\mathbf{v}_{i1}^T\ \mathbf{v}_{i2}^T]^T$, $\otimes$ is the Kronecker product (defined in (LOAN, 2000)) and $\mathbf{z}_i = -\mathbf{Q}_\delta^{-1}\mathbf{B}^T\mathbf{v}_{i2} - \mathbf{Q}_\delta^{-1}\mathbf{C}\mathbf{v}_{i1}$ is used for hybrid representations whereas $\mathbf{z}_i = \mathbf{D}\mathbf{R}_\gamma^{-1}\mathbf{B}^T\mathbf{v}_{i2} + \mathbf{S}_\gamma^{-1}\mathbf{C}\mathbf{v}_{i1}$ for the scattering representations. Equation (4.31) establishes a linear constraint to every violating eigenvalue jw_i of the original unperturbed Hamiltonian matrix. Therefore, by minimizing the system energy criterion devised in Equation (4.27) constrained by the equalities given by Equation (4.31), the following optimization problem is formulated:

$$\begin{aligned} &\text{minimize} && ||\mathrm{vec}(\Delta\mathbf{C}_k)||_2 \\ &\text{subject to} && \mathbf{Z}\mathrm{vec}(\Delta\mathbf{C}_k) = \mathbf{y} \end{aligned}, \tag{4.32}$$

such that $\mathbf{Z}$ and $\mathbf{y}$ are formed by the left- and right-hand sides of the constraint Equation (4.31) for every purely imaginary eigenvalue in the set Ω. As observed in (GRIVET-TALOCIA; UBOLLI, 2008), the above formulation is not convex which implies that an iterative application of Equation (4.32) may fail to converge, its solution however can be obtained for every iteration via standard pseudo-inverse methods.

4.3 Non-perturbative Passive Enforcement

This second class of passivity enforcement differs from its predecessor in that no perturbation is applied, instead these methods enable the identification of *a priori* guaranteed passive models by construction, thus meaning that the customary passivity assessment and the consequential enforcement based on parameter-perturbation are no longer required. Both methods herein presented are technically underpinned by convex optimization methods and a prescribed set of system poles, i.e., a fixed-denominator strategy will be used.

4.3.1 Convex Optimization Methods I - PRL/BRL

Originally devised in (COELHO; PHILLIPS; SILVEIRA, 2001) and (COELHO; PHILLIPS; SILVEIRA, 2004), this method assumes *a priori* knowledge of the system poles. In a *state-space* context, this statement corresponds to having as starting point a prescribed state-dynamics matrix **A**. In practice, this initial information is derived from a system-identification procedure attaining satisfactory accuracy such that all parameters are discarded, with exception of the system poles. Since the authors in the aforementioned references claim that any convenient rational approximation algorithm can be used to generate this initially prescribed pole structure, no reference to any specific algorithm is herein made, even though some possible choices have been mentioned earlier in this text. The early assumption made on the matrix **A** of a state-space characterization as given by Equation (2.1) leads to a linear model, for the denominator is fixed. As opposed to the previous methods based on additive compensation of the transfer function, the objective is no longer to seek for a minimal perturbation so that the model be rendered passive but rather compute (re-compute) the remaining parameters from scratch and under passive constraints. Therefore, the problem is twofold: pole estimation and the subsequent estimation of the remaining parameters (chiefly the residues) under the passivity constraints. This latter part is then formulated as a convex programming problem since the passivity constraint as represented by the positive(bounded)-real lemma is a linear matrix inequality (LMI), thus convex.

Therefore, suppose a transformer admittance matrix with a given initial pole set, a guaranteed passive approximation for a LTI n-port in hybrid representation can be

attained by solving the following problem:

$$\begin{aligned} \text{minimize} \quad & \sum_{i=1}^{n}\sum_{l=1}^{n}\sum_{k=1}^{K} |\Xi_{il}(jw_k)| \left| Y_{il}(jw_k) - \hat{Y}_{il}(jw_k) \right|^2 \\ \text{subject to} \quad & \begin{bmatrix} -\mathbf{A}^T\mathbf{P} - \mathbf{P}\mathbf{A} & -\mathbf{P}\mathbf{B} + \mathbf{C}^T \\ -\mathbf{B}^T\mathbf{P} + \mathbf{C} & \mathbf{D}^T + \mathbf{D} \end{bmatrix} \succeq 0 \\ & \mathbf{P} \succeq 0 \end{aligned} \tag{4.33}$$

where $\Xi_{il}(jw_k)$ is a weighting function, $Y_{il}(jw_k)$ correspond to data measurement whereas $\hat{Y}_{il}(jw_k) = \mathbf{D}_{il} + \mathbf{C}_i[jw_k\mathbf{I} - \mathbf{A}]^{-1}\mathbf{B}_l$ is the corresponding model approximation for every matrix entry, the difference between the two which is to be minimized for all entries at all frequency points is the objective function. For simplicity, each weighting function $\Xi_{il}(jw_k)$ could assumed to be $\Xi_{il}(jw_k) = 1$ without any loss of generality. This particular optimization problem is also formulated in (OLIVEIRA; RODIER; IHLENFELD, 2016). Considering the use of a controllable canonical form for the system $\{\mathbf{A}, \mathbf{B}, \mathbf{C}, \mathbf{D}\}$ and the *a priori* knowledge of **A**, the remaining system matrices **C** and **D** as well as the matrix **P** in the LMI (Positive-real Lemma, as in Equation (2.4)) constitute the problem variables. The assumption of a controllable form for the re-estimation of parameters is not a restricting one, since it reflects the fact that only pole preservation is actually relevant for this procedure, irrespective of any specific coordinate system.

Hence, the objective and constraint functions of Equation (4.33) are linear (affine) in the variables. Basically, the matrix numerator **C** and the constant term **D** are re-calculated so that the PRL is satisfied and the error between the measurements and the model approximation is minimized. The formulation for scattering representations is identical, except that the LMI constraint should be replaced by the Bounded-real Lemma (BRL), Equation (2.6). Convexity ensures that the final result is the best passive approximation of the data, given the pole set. As in (COELHO; PHILLIPS; SILVEIRA, 2004), Equation (4.33) can be rewritten in an equivalent form. Let $\mathbf{e}_i$ denote ith column of the identity matrix as well as matrices $\mathbf{F}_{il} \in \mathbb{R}^{2K\times n}$ and $\mathcal{Y}_{il} \in \mathbb{R}^{2K}$ be defined as follows:

$$\begin{aligned} \mathbf{F}_{il}(k,:) &= \begin{cases} \Xi_{il}(jw_k)\,\mathrm{Re}[\mathbf{J}(k)] & k \leq K \\ \Xi_{il}(jw_k)\,\mathrm{Im}[\mathbf{J}(k-K)] & k > K \end{cases} \\ \mathcal{Y}_{il}(k) &= \begin{cases} \Xi_{il}(jw_k)\,\mathrm{Re}[\mathbf{Y}(k)] & k \leq K \\ \Xi_{il}(jw_k)\,\mathrm{Im}[\mathbf{Y}(k-K)] & k > K \end{cases} \end{aligned} \tag{4.34}$$

such that $\mathbf{J}(k) = [\mathbf{B}_l^T[jw_k\mathbf{I} - \mathbf{A}]^{-1}\mathbf{e}_{(l)}^T]$ is a row vector, $\mathcal{Y}_{il}(k)$ contains the real and imaginary parts of each admittance entry measurement (i,l) for all jw_k and each k

comprises the sequence of measured frequencies. Hence, these definitions permit the rewriting of the objective function in Equation (4.33) as:

$$\sum_{i=1}^{n}\sum_{l=1}^{n}\sum_{k=1}^{K}|\Xi_{il}(jw_k)|\|Y_{il}(jw_k)-\hat{Y}_{il}(jw_k)\|^2=\sum_{i=1}^{n}\sum_{l=1}^{n}\|\mathbf{F}_{il}\mathbf{X}_i-\mathcal{Y}_{il}\| \tag{4.35}$$

such that $\mathbf{X}_i$ is the ith column of the matrix $\mathbf{X}$ containing all model parameters to be estimated:

$$\mathbf{X}=\begin{bmatrix}\mathbf{C}^T\\ \mathbf{D}^T\end{bmatrix}.$$

With the standard QR factorization, every $\mathbf{F}_{il}$ becomes $\mathbf{F}_{il}=\mathbf{Q}_{il}\mathbf{R}_{il}$, where $\mathbf{Q}_{il}$ is an orthogonal matrix ($\mathbf{Q}_{il}^T\mathbf{Q}_{il}=\mathbf{I}$) and $\mathbf{R}_{il}$ full rank. Thus,

$$\|\mathbf{F}_{il}\mathbf{X}_i-\mathcal{Y}_{il}\|=[\mathbf{F}_{il}\mathbf{X}_i-\mathcal{Y}_{il}]^T[\mathbf{F}_{il}\mathbf{X}_i-\mathcal{Y}_{il}]=\mathbf{E}_{il}^T\mathbf{E}_{il}+\delta_{il}^2, \tag{4.36}$$

such that $\delta_{il}^2=\mathcal{Y}_{il}^T[\mathbf{I}-\mathbf{Q}_{il}\mathbf{Q}_{il}^T]\mathcal{Y}_{il}$ and $\mathbf{E}_{il}=[\mathbf{R}_{il}\mathbf{X}_i-\mathbf{Q}_{il}^T\mathcal{Y}_{il}]$. It is noteworthy that all these matrices are real by construction (according to Equation (4.34)), thus leading to real parameter matrices as solutions. Therefore, the equivalent formulation of problem (4.33) is:

$$\begin{aligned}
&\text{minimize} && t(\mathbf{C},\mathbf{D},\mathbf{P})\\
&\text{subject to} && \begin{bmatrix}-\mathbf{A}^T\mathbf{P}-\mathbf{P}\mathbf{A} & -\mathbf{P}\mathbf{B}+\mathbf{C}^T\\ -\mathbf{B}^T\mathbf{P}+\mathbf{C} & \mathbf{D}^T+\mathbf{D}\end{bmatrix}\succeq 0\\
&&& \mathbf{P}\succeq 0\\
&&& \left.\begin{array}{l}\mathbf{E}_{il}^T\mathbf{E}_{il}+\delta_{il}^2\le t_{il}\\ t\ge 0\\ t_{il}\le t\end{array}\right|\ 1\le i,l\le n
\end{aligned} \tag{4.37}$$

which is a convex problem in its *epigraph* form. This formulation is due to (COELHO; PHILLIPS; SILVEIRA, 2004) and *epigraph* forms are explained in (BOYD; VANDENBERGHE, 2004). Other optimization goals could have been established to solve this problem, nevertheless. The error constraint, namely $\mathbf{E}_{il}=[\mathbf{R}_{il}\mathbf{X}_i-\mathbf{Q}_{il}^T\mathcal{Y}_{il}]$, can be further rewritten in terms of its semi-definite equivalent formulation via the Schur complement and therefore be replaced in Equation (4.37) by the following LMI:

$$\begin{bmatrix}t_{i,l}-\delta_{i,l}^2 & \mathbf{E}_{il}^T\\ \mathbf{E}_{il} & \mathbf{I}\end{bmatrix}\succeq 0. \tag{4.38}$$

This problem can be solved with CVX, a package for specifying and solving convex programs (RESEARCH, 2012),(GRANT; BOYD, 2008) with core solver SEDUMI (STURM, 1999). *Ad hoc* problem reformulations can be done, specially structure-exploiting ones thus leading to better efficiency. In (COELHO; PHILLIPS; SILVEIRA, 2004), the explicit positive-real lemma LMI constraint and its accompanying matrix variable **P** are removed. Furthermore, the constraint $\mathbf{E}_{il}^T\mathbf{E}_{il} + \delta_{il}^2 \leq t_{i,l}$ is a second-order cone which allows specific SOCP reformulations as well. The formulation herein presented can be employed to any MIMO system with no specific assumption on matrix structure. Many approximation methods fit MIMO systems in parts, i.e., a matrix can have its columns fit independently as if each column consisting of SIMO systems so that the overall MIMO system is eventually obtained by column concatenation. This strategy is well illustrated in (COELHO; PHILLIPS; SILVEIRA, 2001), for the positive-real lemma formulation.

The PRL approach can also be formulated as a perturbative enforcement scheme, an example is provided by (GRIVET-TALOCIA; UBOLLI, 2008). A similar formulation of the PRL constrained problem has been implemented to serve as a test bed for the case studies analyzed in the subsequent chapter. Details can be found in (OLIVEIRA; RODIER; IHLENFELD, 2016), in essence it involves the use of orthonormal basis functions (Takenaka-Malmquist) and the Sanathanan-Koerner iterations for the pole estimation. Basically, the constrained problem of Equation (4.33) is reworked into a semi-definite formulation by transforming quadratic inequalities to linear matrix inequalities (LMI's) via Schur complement.

4.3.2 Convex Optimization Methods II - PFVF

Another non-perturbative enforcement method that estimates parameters ensuring *a priori* passive behavior is the Positive Fraction Vector Fitting (PFVF). It first appeared in (TOMMASI; DESCHRIJVER; DHAENE, 2008) for single-input single-output (SISO) systems and was later extended to multi-input multi-output (MIMO) systems in (TOMMASI et al., 2011). Although this method also relies on convex programming for parameter estimation, passivity is not enforced by requiring that the positive(bounded) real lemma be satisfied which was the case in the previous convex approach. The Vector Fitting algorithm is used to determine an initial set of poles for the system's transfer matrix, therefore a fixed-pole structure is also pursued. Considering the *pole-residue* model structure, the transfer matrix is expanded as a truncated series of residue matrices and the associated poles. Essentially, the method obtains an overall passive transfer matrix by constraining each individual term of the series to be positive-real, i.e., each subsystem is passive. Therefore, the PFVF combines pole identification via the Vector Fitting (VF) algorithm with convex constrained residues identification, once the poles are known the problem constraints are easily written in convex form. The overall strategy

of the PFVF method defines a sufficient condition to guarantee positive-realness for the overall transfer matrix, but not a necessary condition. Considering a *pole-residue* expansion of the transfer matrix with fixed poles as in Equation (4.21), a passive transfer function can be attained by requiring that each model constituent fraction is positive-real, namely:

$$\mathbf{D} \succeq 0 \ , \ \mathbf{E} \succeq 0, \ , \ \mathbf{R}_1 \succeq 0 \ , \ldots , \ \mathbf{R}_N \succeq 0.$$

Since the system poles are known, these constraints comprise LMI constraints, thus convex. In case the set of poles contains complex conjugate pairs $\frac{\mathbf{R}_i}{jw-a_i}$ and $\frac{\mathbf{R}_i^*}{jw-a_i^*}$, they enter the constraint set as two distinct matrices:

$$\begin{aligned} -\big(\operatorname{Re}(a_i)\operatorname{Re}(\mathbf{R}_i) + \operatorname{Im}(a_i)\operatorname{Im}(\mathbf{R}_i)\big) \succeq 0 \\ -\big(\operatorname{Re}(a_i)\operatorname{Re}(\mathbf{R}_i) - \operatorname{Im}(a_i)\operatorname{Im}(\mathbf{R}_i)\big) \succeq 0 \end{aligned}$$

Hence, a guaranteed passive approximation for a LTI n-port in admittance representation can be realized by solving the following convex problem:

$$\begin{aligned} \text{minimize} \quad & \sum_{i=1}^{n}\sum_{l=1}^{n}\sum_{k=1}^{K}\left|Y_{il}(jw_k) - \hat{Y}_{il}(jw_k)\right|_2 \\ & \mathbf{D} \succeq 0 \\ & \mathbf{E} \succeq 0 \\ \text{subject to} \quad & \mathbf{R}_1 \succeq 0 \\ & \vdots \\ & \mathbf{R}_N \succeq 0 \end{aligned} \tag{4.39}$$

where each $Y_{il}(jw_k)$ corresponds to admittance measurement and $\hat{Y}_{il}(jw_k)$ is a linear function of model parameters. As proposed in (TOMMASI et al., 2011), this problem is solved with CVX, a package for specifying and solving convex programs (RESEARCH, 2012),(GRANT; BOYD, 2008).

4.4 Discussion

The essence of all passivity enforcement schemes is to use the passivity conditions defined in Chapter (2) as problem constraints so that passivity be either recovered as in perturbative schemes or secured as in non-perturbative schemes. All enforcement approaches seek the best compromise by being rigorous and offering global guarantees on positive-realness at the cost of a small accuracy loss due to further constraining the modeling process. As passivity enforcement enters the modeling process it seems natural to conjecture that sacrificing model optimality for passive behavior might be

fruitless. Obviously, under passivity enforcement the problem is further constrained and the unconstrained approximation is shifted from the allegedly optimal solution thus prompting a sense of a degraded solution. Nonetheless, model parameter estimation that exclusively relies on accuracy as a guiding criterion can only provide allegedly optimal approximations since it is based on data that is sampled, incomplete, noisy and finite in range thus failing to contain the system's genuine dynamics as also expressed by passive behaviour. Therefore, passivity constraints displace allegedly optimal solutions to genuinely optimal passive solutions.

This chapter has been divided into two sections in order to distinguish the striking features between perturbative and non-perturbative enforcement procedures. A key factor contributing to large deviations between a passive approximation and data is the eigenvalue spread, i.e., how large the negative eigenvalues are. Algorithms employing parameter perturbation are more sensitive to the presence of significant violations since they are based on first-order approximations which are valid under the assumption that correcting the eigenvalues only requires small perturbations. This can become remarkably delusional for anyone evaluating model performance, for approximations are tested within the frequency range of the available measurements while ignorance prevails as to what the system dynamics is beyond the observations. This is a distinguishing feature between the two perturbative methods: discrete-frequency samples and the Hamiltonian perturbation. The earlier places stronger emphasis on observed data to compensate passivity violations thus keeping good in-band accuracy whereas the second compensates passivity even for out-of-band behavior hence requiring a possibly larger parameter perturbation since the model may have large out-of-band passivity violations, perhaps even larger than the in-band ones, reflecting in a poorer in-band fit for the Hamiltonian method.

Therefore, the best local accuracy must be carefully weighed against the averagely global passive behavior. For perturbative methods, an increased number of iterations may be required since it is not guaranteed that for every iteration all violating eigenvalues are suppressed in addition to the fact that parameter perturbation can generate new violations, hence the need for a recursively applied process. These limitations obviously influence the number of iterations required before convergence is attained thus leading to increased accuracy degradation or even divergence for some pathological cases with large violating eigenvalues. Specially critical for perturbative methods, the assumption of small accuracy degradation during passivity enforcement is only valid provided passivity violations are small. This is a consequence of using linearization to establish the passivity constraints. Large violations can inflict lack of convergence or large model degradation. Such large violations can be suppressed in a pre-processing procedure based on data passivity enforcement so that the model be more amenable to passivity enforcement which in turn becomes more effective and

substantial accuracy gains be accomplished.

Instead of applying parameter perturbation, both convex optimization methods are frequency-independent and rely on fixed-pole parameter estimation permitting the identification of *a priori* guaranteed passive models thus eschewing the passivity check and consequential parameter perturbation as required by most of the other available algorithms. The intrinsic limitations of first-order linearization no longer apply, therefore these methods are less sensitive to the eigenvalue spread. The PRL/BRL approach is the most general of the two convex-based approaches, since the positive-real lemma constraints provide necessary and sufficient conditions for system passivity. The major drawback of the PRL/BRL approach lies in the fact that the number of problem variables considerably increases due to the additional LMI matrix variable **P** which suggests its use for problems of moderate complexities.

The PFVF formulation was motivated precisely by the fact that the PRL/BRL approach is relatively involved and requires unacceptable computation time for LTI systems with a large number of ports. Since the PFVF establishes sufficient but not necessary passivity conditions, sub-optimal solutions are usually attained. The number of optimization variables grows linearly with system order for the PFVF, as opposed to the quadratic relation of the PRL/BRL approach (due to the LMI constraint matrix **P**). Therefore, computational efficiency and straightforward criteria come at the price of sub-optimality. Choosing which constraints to be applied is a problem that can affect the effectiveness of the enforcement procedure. Constraints must guarantee that the transfer function be positive-real but be only as restrictive as necessary to allow the algorithm to search all possible models that are passive given the pole set. Over-constraints can result in problem infeasibility, i.e., there are no parameters that guarantee passive behavior within some small approximation tolerance. According to (COELHO; PHILLIPS; SILVEIRA, 2004), constraining each subsystem to be positive-real ensures that the overall system be indeed positive-real, but it could also exceedingly over-constrain the problem instead of admitting all passive models and thus leading to inaccurate models.

It is possible to conclude that there is some trade-off between perturbative and non-perturbative algorithms: the former can lead to accuracy degradation or even fail to converge but the computational cost rises favourably with model order, the latter is insensitive to the eigenvalue spread and *a priori* guaranteed to provide a passive result but can be impractical for large models in terms of computation time. A comparative study providing illustrative examples of each enforcement scheme can be found in (GUSTAVSEN, 2008b) and (CHIARIELLO et al., 2010).

5 POSITIVE (SEMI-)DEFINITE COMPLETION ENFORCEMENT

This chapter commences with an introduction to the Positive (semi-)Definite Completion Problem (PDCP) which involves the specification of a partial positive matrix as an initial preprocessing step followed by the computation of the remaining unespecified entries. The subsequent sections then present novel formulations for both passivity assessment and enforcement of CT-LTI systems via a convex formulation associated with chordal methods, a generalization of the completion problem. The later part of the chapter contains numerical results obtained with the proposed formulation and an analysis as to how the proposed methodology compares with existing methods.

5.1 Positive (semi-)Definite Completion Problem

This preliminary section introduces some basic terminology and collects some results concerning the Positive (semi-)Definite Completion Problem. A chief idea behind completion problems is to analyze some underlying structure of a given matrix of interest by examining its constituent parts, for the overall properties of matrices are intimately related to such parts. What is meant by constituent parts requires the notion of principal submatrices and principal minors. According to (MEYER, 2000) or (HORN; JOHNSON, 2012):

Definition 43 *Let* ***X*** *be a* $P \times P$ *matrix*[1]*. A* $r \times r$ ***principal submatrix*** *of* ***X*** *is formed by deleting* $P - r$ *rows as well as the same* $P - r$ *columns of* ***X****, for some* $1 \leq r \leq P$*. The determinant of a principal submatrix of* ***X*** *is called a* ***principal minor*** *of* ***X****.*

Observe that the Definition (43) does not specify which $P - r$ rows and columns are to be excluded, only that their indices must be the same. An $P \times P$ matrix **X** has as many principal submatrices as $\binom{P}{1} + \binom{P}{2} + \cdots + \binom{P}{P} = 2^P - 1$ where each term $\binom{P}{r}$ accounts for the number of distinct principal submatrices of size r.

Definition 44 *Let* ***X*** *be an* $P \times P$ *matrix*[2]*. The* $r \times r$ ***leading principal submatrix*** *of* ***X*** *is formed by deleting the last* $P - r$ *rows and columns, for some* $1 \leq r \leq P$*. The determinant of a leading principal submatrix of* ***X*** *is called a* ***leading principal minor*** *of* ***X****.*

Definition (44) does specify which $P - r$ rows and columns are to be deleted, namely those resulting in the submatrices taken from the upper-left-hand corner of **X**.

[1] The entries of this matrix could be real or complex numbers.
[2] Idem.

$$\begin{bmatrix} X_{11} & X_{12} & X_{13} & X_{14} \\ X_{21} & X_{22} & X_{23} & X_{24} \\ X_{31} & X_{32} & X_{33} & X_{34} \\ X_{41} & X_{42} & X_{43} & X_{44} \end{bmatrix}$$

$$\begin{bmatrix} X_{11} & X_{12} & X_{13} \\ X_{21} & X_{22} & X_{23} \\ X_{31} & X_{32} & X_{33} \end{bmatrix} \begin{bmatrix} X_{11} & X_{12} & X_{14} \\ X_{21} & X_{22} & X_{24} \\ X_{41} & X_{42} & X_{44} \end{bmatrix}$$

$$\begin{bmatrix} X_{11} & X_{13} & X_{14} \\ X_{31} & X_{33} & X_{34} \\ X_{41} & X_{43} & X_{44} \end{bmatrix} \begin{bmatrix} X_{22} & X_{23} & X_{24} \\ X_{32} & X_{33} & X_{34} \\ X_{42} & X_{43} & X_{44} \end{bmatrix}$$

$$\begin{bmatrix} X_{11} & X_{12} \\ X_{21} & X_{22} \end{bmatrix} \begin{bmatrix} X_{11} & X_{13} \\ X_{31} & X_{33} \end{bmatrix} \begin{bmatrix} X_{11} & X_{14} \\ X_{41} & X_{44} \end{bmatrix}$$

$$\begin{bmatrix} X_{22} & X_{23} \\ X_{32} & X_{33} \end{bmatrix} \begin{bmatrix} X_{22} & X_{24} \\ X_{42} & X_{44} \end{bmatrix} \begin{bmatrix} X_{33} & X_{34} \\ X_{43} & X_{44} \end{bmatrix}$$

$$[X_{11}] \qquad [X_{22}] \qquad [X_{33}] \qquad [X_{44}]$$

Figure 34 – 4×4 matrix and its 15 principal submatrices

An $P \times P$ matrix has a total of P leading principal submatrices of sizes ranging from 1 to P and only a single leading principal submatrix of size r.

For the sake of illustration, the 3×3 matrix **X** below is shown along with all its principal submatrices and leading principal submatrices:

$$\begin{bmatrix} X_{11} & X_{12} & X_{13} \\ X_{21} & X_{22} & X_{23} \\ X_{31} & X_{32} & X_{33} \end{bmatrix}, \begin{bmatrix} X_{11} & X_{12} \\ X_{21} & X_{22} \end{bmatrix}, \begin{bmatrix} X_{11} & X_{13} \\ X_{31} & X_{33} \end{bmatrix}, \begin{bmatrix} X_{22} & X_{23} \\ X_{32} & X_{33} \end{bmatrix}, [X_{11}], [X_{22}], [X_{33}].$$

X has a total of $\binom{3}{1} + \binom{3}{2} + \binom{3}{3} = 2^3 - 1 = 7$ principal submatrices and 3 leading principal submatrices[3].

The number of principal submatrices is then dictated by a simple combinatorial law and as such this number scales very rapidly with matrix order. By increasing the order from 3 to 4, the number of principal submatrices precipitously rises from 7 to 15 principal submatrices as depicted in Figure(34). The number of leading principal submatrices however rises linearly with order.

In perspective, the number of principal submatrices in an $P \times P$ matrix **X** is governed by an exponential law, $2^P - 1$, whereas the total number of entries is dictated

[3] Note that $[X_{11}]$, $\left[\begin{smallmatrix} X_{11} & X_{12} \\ X_{21} & X_{22} \end{smallmatrix}\right]$ and **X** itself are the leading principal submatrices.

by a quadratic law, P^2, consequently the number of principal submatrices exceeds that of total entries for $P \geq 5$.

According to (GRIFFIN; TSATSOMEROS, 2006a), there exist many instances in both pure mathematics and applied contexts where the principal submatrices and their associated minors need to be examined, sometimes even their exact value is needed and other times only qualitative information, such as their signs is required[4]. Most notably, these instances include the detection of $P-$matrices, *i.e.* matrices with positive definite principal submatrices or positive principal minors, which is in essence an assessment problem. A Matlab implementation for this assessment problem can be found in (GRIFFIN; TSATSOMEROS, 2006a).

A related notoriously hard problem is the so-called principal minor assignment problem (PMAP), in which a matrix with specified principal minors (having a fixed user-prescribed determinant value) is sought. This problem has been tackled with the implementation described in (GRIFFIN; TSATSOMEROS, 2006b), as a natural continuation of their preceeding paper. As the authors remark, the PMAP is equivalent to the inverse eigenvalue problem of finding a matrix with prescribed spectra (and thus characteristic polynomials) for all of its principal submatrices[5]. For example in (CRAVO; SILVA, 2003), the authors describe how the eigenvalues, or the associated characteristic polynomials, of submatrices that partition a full matrix each having different orders can be arbitrarily prescribed. However, constraining all principal minors to have prescribed values constitutes an NP-hard problem, as discussed in (COXSON, 1994) and (FONIOK, 2007).

As alluded to in the previous paragraph, such problems bear numerical challenges for a matrix has many more principal minors than entries for order larger than five and these principal minors are dependent on each other. This mutual dependence of matrices and their submatrices can be intuitively formulated as larger principal submatrices being expressed in terms of the smaller principal submatrices within them. In a somewhat inside out procedure, the problem of checking whether a given matrix is positive definite (a P-matrix) or not can be solved in their of positive definiteness of all its principal submatrices since a matrix is positive definite provided all its principal submatrices are positive definite, as shown in (TSATSOMEROS; LI, 2000) for real and in (GRIFFIN; TSATSOMEROS, 2006a) for complex matrices. Other structure can be inferred from submatrices, *e.g.* Hessenberg or Toeplitz type matrices.

In a series of papers (THOMPSON; MCENTEGGERT, 1968), (THOMPSON,

[4] Positivity and negativity for passivity assessment.

[5] This assessment and assignment techniques are very different, both in complexity and the methods employed, than the ones being proposed later on in this dissertation which consider matrix functions whose values are determined by parameters as opposed to a single numerical instance of a data matrix.

1968a), (THOMPSON, 1969a), (THOMPSON, 1968b), (THOMPSON, 1969b), (THOMPSON, 1968c), (THOMPSON, 1972b),(THOMPSON, 1972a), (THOMPSON; MCENTEGGERT, 1968), (THOMPSON, 1972c), the so-called eigenvalue interlacing properties are demonstrated. These properties involve bounding by inequalities and location theorems all the eigenvalues of a Hermitian $P \times P$ matrix $\mathbf{X}$ and the eigenvalues of all its principal $r \times r$ submatrices. Additional inequalities are also obtained for expressions involving $r \times r$ subdeterminants (principal minors) of the full matrix into which they are embedded. Since these interlacing inequalities impart important intuition on future developments and arguments, a few words on them are in order. If the set of sorted eigenvalues for a full $P \times P$ Hermitian matrix is denoted $\{\lambda(\mathbf{X}_{P\times P})\} = \{\lambda_1 \leq \lambda_2 \leq \cdots \leq \lambda_P\}$ and let the set of sorted eigenvalues of each $r \times r$ principal submatrix[6] be denoted $\{\xi(\mathbf{X}_{r\times r})\} = \{\xi_{r1} \leq \xi_{r2} \leq \cdots \leq \xi_{rr}\}$, with $1 \leq r \leq P-1$, then the interlacing inequalities read as follows:

$$\lambda_1 \leq \xi_{r1} \leq \lambda_2 \leq \xi_{r2} \leq \cdots \leq \xi_{r,P-1} \leq \lambda_P,$$

which is equivalent to the statement that eigenvalues of the submatrices are bounded by the eigenvalues of the full matrix, *i.e.* λ_1 and λ_P are the lower and upper bounds respectively for the eigenvalues of all principal submatrices. For each ξ_{rj}[7] one can find an interval interval $[\lambda_j, \lambda_{j+1}]$ for which $\xi_{rj} \in [\lambda_j, \lambda_{j+1}]$. These inequalities hint at the fact that shifting negative eigenvalues of submatrices towards the zero threshold is never worse than shifting the negative eigenvalues of the full matrix[8]. The fact that the interlacing properties are transitive is explored in (QUEIRO; DUARTE, 2009) and (KATSOULEAS; MAROULAS, 2013), where the authors refer to the user-prescribed properties as imbedding relations between matrices and their submatrices and describe conditions on imbeddability[9].

Once the dependence of a full matrix upon its inner structure is understood, the concept of a completion can be presented. Matrix completion problems constitue an important research topic in matrix theory and a number of authors have studied several related questions.The survey papers, (LUNDQUIST; JOHNSON, 1991; BARRETT; JOHNSON; LOEWY, 1996a; BARRETT; JOHNSON; LOEWY, 1996b; CRAVO, 2009; CRAVO, 2012) have been consulted to write the bulk of the remaining material in this section on the positive (semi-)definite completion problem. A general Matrix Completion Problem consists in studying the possibility to 'complete' a matrix having some of its entries prescribed, *i.e.* prescribed entries are known fixed numbers, such that the

6 For all r such that $r \leq P$.

7 This reads: the j-th eigenvalue of some $r \times r$ principal submatrix.

8 This fact is used as an underpinning hypothesis to justify better accuracy attained by the herein proposed methods for systems using submatrices as subsystems.

9 In mathematics jargon prescribing a submatrix or its determinant value is also refered to as embedding or compressing the submatrix in the larger one.

resulting matrix satisfies certain properties[10]. In this particular context 'to complete' means to attribute values to the remaining unespecified entries, the problem variables. The matrix thus obtained is called the completed matrix and it satisfies the required properties. According to (CRAVO, 2009), this type of problem belongs to an important class of problems within Matrix Theory, known as the Matrix Inverse Problems, consisting in the study of existence conditions for matrices or a combination of matrices to satisfy certain properties, say positive definiteness. As pointed out in (BARRETT; JOHNSON; LOEWY, 1996a), Completion problems have proved to be a useful perspective to study fundamental matrix structure and the Positive Definite Completion Problem has received the most attention as compared with other completion problems owing to its pervasiveness as it finds applications in probability, statistics, image enhancement, systems engineering, geophysics, mathematical programming *et cetera*.

Therefore, in a completion problem two matrices are involved: a *partial matrix* and a *completed matrix* or just a completion.

Definition 45 *A partial matrix $\tilde{\boldsymbol{X}}$ of size $P \times P$ defined in some number field ($\mathbb{R}$ or $\mathbb{C}$) consists of a matrix in which some of the entries are specified numbers and the remaining ones are variables to be chosen from some set.* [11]

Definition 46 *A completed matrix $\boldsymbol{X}$ of size $P \times P$ is a fully specified matrix whose entries agree with an associated partial matrix $\tilde{\boldsymbol{X}}$,* i.e. $X_{ij} = \tilde{X}_{ij}$ *whenever $\tilde{X}_{ij}$ is specified, and the remaining entries have been chosen from some specified set so that the fully specified matrix thus otained satisfies some desired properties.*

Completed matrices or completions are commonly required to be positive definite, symmetric, hermitian, sparse or even some combination thereof. Under such circumstances, their associated partial matrices must be specified so as to satisfy these properties, *i.e.* the attributes for the completion must be satisfied by the partial matrices as well for the completed matrix is to inherit these properties. Consequently, partial matrices possessing these properties are appropriately referred to as partial positive, partial symmetric, partial hermitian and so on[12]. For the Positive Definite Completion Problem to have a solution a partial positive definite matrix must therefore be specified in the first place[13]. A partial positive matrix and a completion for it are illustrated in Figure (35), question marks indicate zeros to be replaced by other numerical values taken from some set so that the completion satisfies some specified properties.

[10] Should these desired properties correspond to positive definitiness, then a positive definite completion problem is formulated. Other properties exist though.

[11] For instance, a Positive semi-definite cone.

[12] These conditions are necessary but no sufficient for a completion to exist. As will be dicussed later, for the PDCP chordality guarantees sufficiency.

[13] This is the essence of the novel passivity assessment method proposed in the subsequent section.

Partial Positive Definite	Positive Completion
$\begin{bmatrix} 5 & 2 & ? \\ 2 & 4 & 2 \\ ? & 2 & 3 \end{bmatrix}$	$\begin{bmatrix} 5 & 2 & 1 \\ 2 & 4 & 2 \\ 1 & 2 & 3 \end{bmatrix}$

Figure 35 – A partial positive matrix and a completion.

Concentrating on the positive definite completion problem and leaving other kinds of completions aside, positive (semi-)definiteness of the partially specified matrix is a necessary condition for the positive (semi-)definite completion problem, this is demonstrated in (GRONE et al., 1984). As such, some possibilities arise: (i) solutions need not exist, (ii) a unique solution exists or (iii) infinitely many solutions exist[14]. In order to specify a partial positive matrix $\tilde{\mathbf{X}}$, one can always assume without loss of generality that the diagonal entries of $\tilde{\mathbf{X}}$ are specified. If a diagonal entry, say $\tilde{X}_{ii}$, were not specified, then it could be taken to be infinitely large, *i.e.* $\tilde{X}_{ii} \to +\infty$. Hence the condition that $\tilde{\mathbf{X}} \succeq 0$ reduces to $\tilde{\mathbf{X}}' \succeq 0$, with $\tilde{\mathbf{X}}'$ the matrix $\tilde{\mathbf{X}}$ without the i-th row and column. Repeating this procedure for each unspecified diagonal entry of $\tilde{\mathbf{X}}$, one can just as well consider some submatrix of $\tilde{\mathbf{X}}$ with specified diagonal entries.

As the positions of the specified entries in a partial matrix $\tilde{\mathbf{X}}$ can be naturally described by a graph, graph theory can be used to derive completability conditions for a given partial positive matrix. As proved in (GRONE et al., 1984), a solution to the PDCP exists if and only if[15] the undirected graph $\mathcal{G}$ of the specified entries of $\tilde{\mathbf{X}}$ is chordal. In (GRONE et al., 1984; GLUNT et al., 1999; JOHNSON; WOLKOWICZ, 1998; LEE; SEOL, 2001), nonuniqueness of a completion is demonstrated for partial positive matrices whose associated graph is chordal, this graph is commonly referred to in the literature as the *Pattern Graph* or the *Specification graph*. Extensive discussion on the convex semidefinite formulation for the PDCP can be found in (JOHNSON; WOLKOWICZ, 1998; WOLKOWICZ; ANJOS, 2002; SMITH, 2008), these algorithms are shown to be efficient for large sparse problems with chordal sparsity patterns using the interior-point approach is turned out to be very efficient and robust. Much research has been concentrated in finding algorithms for a solution possessing a maximum determinant, *e.g.* (GRONE et al., 1984; GLUNT et al., 1999; JOHNSON; WOLKOWICZ, 1998). Contrary to that, this research focuses on determining a positive (semi-)definite completion that minimizes some convex cost function.

[14] The latter case being the interesting, relevant one for it leaves the possibility open for employing optimization methods to find a solution which is best in some user-specified sense.

[15] For a partial positive matrix, chordality of the associated sparsity pattern is then both necessary and sufficient.

5.2 PDCP and related Convex Cones

The positive definite completion problem (PDCP) may be viewed as the problem of deciding whether two convex sets intersect, *i.e.* the completed matrix and the open cone of all positive definite matrices. Geometrically, the problem is equivalent to expressing a partial matrix $\tilde{\mathbf{X}} \in \mathbb{S}^n_{\mathcal{E}}$ as the projection $\Pi_{\mathcal{E}}(\mathbf{X})$ of a full positive definite matrix $\mathbf{X}$ on the subspace $S^n_{\mathcal{E}}$ of symmetric matrix space. A partially specified matrix can be represented as a sparse matrix in which the diagonal and off-diagonal entries X_{ij} with $\{i,j\} \in \mathcal{E}$ are fixed. All remaining off-diagonal entries $\{i,j\} \notin \mathcal{E}$ are free to be chosen, *i.e.* the problem variables. The set of Positive semidefinite matrices with sparsity pattern $\mathcal{E}$ can be denoted as:

$$\mathbb{S}^n_+ \cap \mathbb{S}^n_{\mathcal{E}} = \{\tilde{\mathbf{X}} \in \mathbb{S}^n_{\mathcal{E}} \mid \tilde{\mathbf{X}} \succeq 0\}, \tag{5.1}$$

which is a convex cone called the Sparse Positive Semidefinite Matrix Cone. Such a cone has special topological properties: (i) it is closed convex cone formed by the intersection of closed convex cone $\mathbb{S}^n_+$ and subspace; (ii) it possesses a nonempty interior given by the set $\mathbb{S}^n_{++} \cap \mathbb{S}^n_{\mathcal{E}}$, with $\mathbb{S}^n_{++} = \{\tilde{\mathbf{X}} \in \mathbb{S}^n_{\mathcal{E}} \mid \tilde{\mathbf{X}} \succ 0\}$ [16]; (iii) it is pointed: $\tilde{\mathbf{X}} \in \mathbb{S}^n_+ \cap \mathbb{S}^n_{\mathcal{E}}$ and $-\tilde{\mathbf{X}} \in \mathbb{S}^n_+ \cap \mathbb{S}^n_{\mathcal{E}}$ implies $\tilde{\mathbf{X}} = 0$.

Assuming that the sparsity pattern defined by $\mathcal{E}$ is chordal, then the cone $\mathbb{S}^n_+ \cap \mathbb{S}^n_{\mathcal{E}}$ admits a decomposition as a sum of simple lower-dimensional convex cones, this fact is the Decomposition Theorem, as proved in (GRIEWANK; TOINT, 1984) and (KAKIMURA, 2010).

Theorem 2 *A partial matrix $\tilde{\boldsymbol{X}} \in \mathbb{S}^n_+ \cap \mathbb{S}^n_{\mathcal{E}}$, with $\mathcal{E}$ a chordal sparsity pattern, admits the following decomposition:*

$$\tilde{\boldsymbol{X}} = \sum_{\gamma_i \in \mathcal{T}} \boldsymbol{P}^T_{\gamma_i} \boldsymbol{H}_{\gamma_i} \boldsymbol{P}_{\gamma_i} \succeq 0$$

with $\mathcal{T}$ denoting a family of cliques for the sparsity graph, *i.e.* the clique tree, and $\mathbf{P}_{\gamma_i}$ is a selection matrix with index set γ_i.[17] Figure (36) illustrates the decomposition theorem for a simple chordal pattern consisting of three overlapping diagonal blocks.

A partial positive semidefinite matrix $\tilde{\mathbf{X}}$ with a non-chordal sparsity pattern may admit a decomposition such as the one described in Theorem (2), but it is not guaranteed in general. The result expressed in Theorem (2) can be rewritten in terms of its constituents cones more explicitly:

[16] An important consequence of this property is that identity matrix $\mathbf{I}$ is in its interior.
[17] Selection matrices are illustrated in Section (3.4).

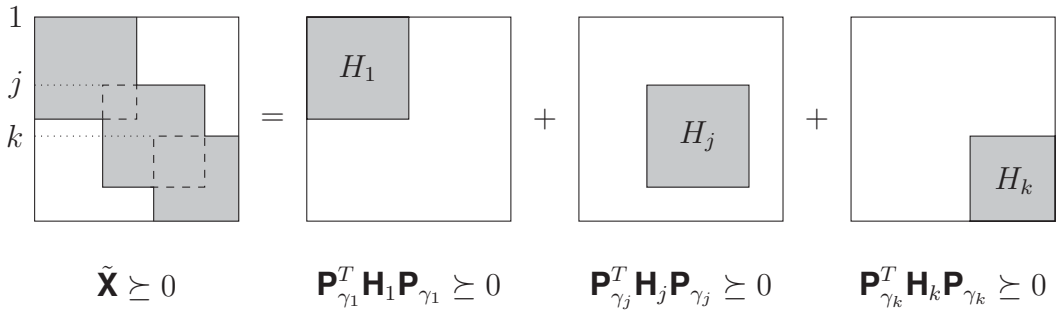

Figure 36 – Decomposition theorem for three overlapping dense blocks.

$$\mathbb{S}_+^n \cap \mathbb{S}_{\mathcal{E}}^n = \sum_{\gamma_i \in \mathcal{T}} \mathcal{K}_{\gamma_i}, \qquad \mathcal{K}_{\gamma_i} = \{\mathbf{P}_{\gamma_i}^T \mathbf{H}_{\gamma_i} \mathbf{P}_{\gamma_i} \mid \mathbf{H}_{\gamma_i} \succeq 0\}.$$

Each cone has nonzero elements in the rows and columns indexed by the associated clique γ_i, the remaining entries are the syntatic zeros. Note that the cones $\mathcal{K}_{\gamma_i}$ are closed, convex, pointed, but improper for they do have empty interiors. Another related convex cone is the set of completable partial positive semidefinite matrices[18], denoted as:

$$\Pi_{\mathcal{E}}(\mathbb{S}_+^n) = \{\Pi_{\mathcal{E}}(\mathbf{X}) \mid \mathbf{X} \succeq 0\}, \tag{5.2}$$

whereby $\Pi_{\mathcal{E}}(\mathbf{X})$ means the projection of the full positive definite matrix $\mathbf{X}$ into the spasity pattern defined by $\mathbb{S}_{\mathcal{E}}^n$. This cone is closed, pointed, has non-empty interior and is the dual of the cone $\mathbb{S}_+^n \cap \mathbb{S}_{\mathcal{E}}^n$. The projection $\tilde{\mathbf{X}}$ of a matrix $\mathbf{X} \in \mathbb{S}^n$ on the subspace $\mathbb{S}_{\mathcal{E}}^n$, denoted by $\tilde{\mathbf{X}} = \Pi_{\mathcal{E}}(\mathbf{X})$, *i.e.* $\tilde{X_{ij}} = X_{ij} = X_{ji}$ if $\{i, j\} \in \mathcal{E}$, otherwise $\tilde{X_{ij}}_{ij} = 0$. The two convex cones are related via duality:

$$\begin{aligned}
\mathcal{K}^* &= (\Pi_{\mathcal{E}}(\mathbb{S}_+^n))^* \\
(\Pi_{\mathcal{E}}(\mathbb{S}_+^n))^* &= \{\mathbf{Y} \in \mathbb{S}_{\mathcal{E}}^n \mid \mathbf{tr}(\tilde{\mathbf{X}}\mathbf{Y}) \geq 0, \forall \tilde{\mathbf{X}} \in \Pi_{\mathcal{E}}(\mathbb{S}_+^n)\} \\
&= \{\mathbf{Y} \in \mathbb{S}_{\mathcal{E}}^n \mid \mathbf{tr}(\Pi_{\mathcal{E}}(\mathbf{X})\mathbf{Y}) \geq 0, \forall \mathbf{X} \succeq 0\} \\
&= \{\mathbf{Y} \in \mathbb{S}_{\mathcal{E}}^n \mid \mathbf{tr}(\mathbf{X}\mathbf{Y}) \geq 0, \forall \mathbf{X} \succeq 0\} \\
&= \mathbb{S}_+^n \cap \mathbb{S}_{\mathcal{E}}^n.
\end{aligned}$$

In summary, there exist relationships between the structure of the graph and the conditions for completability:

- $\mathcal{K} = \Pi_{\mathcal{E}}(\mathbf{X})$,$\mathbf{X} \succeq 0$, is the cone of PSD completable matrices with sparsity pattern $\mathcal{E}$;

[18] Alternetively, the set of matrices admitting a positive semidefinite completion or matrices for which a completion exists.

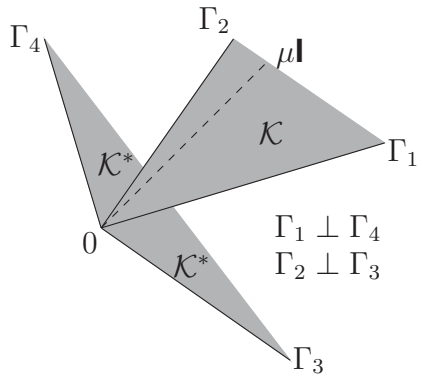

Figure 37 – The topology of the cones $\mathcal{K}$ and $\mathcal{K}^*$.

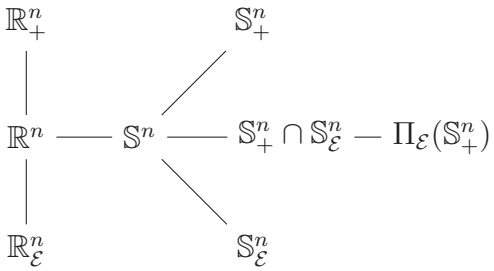

Figure 38 – Set inclusions.

- $\mathcal{K}^* = \mathbb{S}^n_+ \cap \mathbb{S}^n_{\mathcal{E}}$ is the cone of positive semidefinite matrices with sparsity pattern $\mathcal{E}$;
- $\tilde{\mathbf{X}} = \Pi_{\mathcal{E}}(\mathbf{X}), \mathbf{X} \succeq 0 \iff \mathbf{tr}(\tilde{\mathbf{X}}\mathbf{Y}) \geq 0, \forall \mathbf{Y} \in \mathbb{S}^n_+ \cap \mathbb{S}^n_{\mathcal{E}}$;
- $\tilde{\mathbf{X}}$ has a positive (semi-)definite completion if and only if $\tilde{\mathbf{X}}_{\gamma_i\gamma_i} \succeq 0, \ \forall \gamma_i \in \mathcal{T}$;
- Both cones $\mathcal{K}$ and $\mathcal{K}^*$ are closed and convex;
- Both cones $\mathcal{K}$ and $\mathcal{K}^*$ have non-empty interior, meaning: $\mu\mathbf{I} \in \mathcal{K}$ (similarly $\mu\mathbf{I} \in \mathcal{K}^*$) and $\mu\mathbf{I} \in \mathcal{K}^*$ (similarly $\mu\mathbf{I} \in \mathcal{K}$)[19];
- Both cones $\mathcal{K}$ and $\mathcal{K}^*$ are pointed, *i.e.* if $\tilde{\mathbf{X}} \in \mathcal{K}$ (similarly $\tilde{\mathbf{X}} \in \mathcal{K}^*$), then $-\tilde{\mathbf{X}} \in \mathcal{K}$ (similarly $-\tilde{\mathbf{X}} \in \mathcal{K}^*$) $\iff \tilde{\mathbf{X}} = 0$.

For increased and better intuition, Figure (37) shows a simple planar illustration of the topology relating the two cones $\mathcal{K}$ and $\mathcal{K}^*$. Note that $\Gamma_1, \Gamma_2, \Gamma_3,$ and Γ_4 are hyperplanes defining the boundary of their respective cones. Figure (38) gives some sort of hierarchy between sets (not all convex) to put them in some perspective.

[19] This basically says that there exists a known interior-point to each cone, *viz.* $\mathbf{P} = \mathbf{I} \succeq 0$.

5.3 Partial Positive Matrix Passivity Assessment (PPMPA)

In this section we address the problem concerning the specification of a completable partial positive system as the Positive (semi-)Definite Completion Problem presumes the existence of a partial positive matrix with a chordal pattern graph which is to be completed. Furthermore, this partial positive matrix need not be just a matrix, rather it can be a partial positive matrix function, *e.g.* a system parametrized by a state-space realization, a much more general problem. Henceforth, a partial positive matrix function is denoted a partial positive (linear) system and each submatrix function forming the partial system is denoted a positive subsystem. It is also assumed throughout that the full system is square having a number of rows and columns determined by its number of ports P, simply referred to as a full $P \times P$ system. A potential source of non-passive systems embedding partial positive subsystems is the output of the VF Algorithm, presented in Subsection (2.4.1), recalling that the state-space realization thus obtained need not be passive in its entirety for the VF algorithm has no means to guarantee so.

In other words, the goal is to specify a partial positive system (matrix function) which is embedded within a larger non-passive system, a task which essentially constitutes a passivity assessment problem. However, all existing passivity assessment algorithms presented in Section (4.1) apply to systems as a whole, its constituent parts or its subsystems remain unassessed, though. Therefore, a novel assessment technique is here needed with the capabilities to probe deeper into the system's equations and extract precisely those parts which simultaneously satisfy two criteria: (i) positive (semi-)definiteness and (ii) chordal aggregate sparsity pattern. These subsystems comprise a partial positive system for which a completion exists. Otherwise, no completion exists, even when a partially specified positive subsystem is found.

This assessment can be quite challenging for a number of reasons: (i) a full $P \times P$ system has as many as $2^P - 1$ subsystems[20] (ii) among these $2^P - 1$ subsystems there can be at most P cliques[21], formed by some combination of the $2^P - 1$ subsystems and (iii) not all cliques need to be positive cliques, *i.e.* correspond to positive (semi-)definite subsystems[22].

Given the unpredictability of how the positive cliques[23] are distributed within the full system and the existence conditions for completability, the Partial Positive Matrix Passivity Assessment (PPMPA) must be endowed with capabilities beyond simply assessing whether a system is passive or nonpassive. Following the existence

[20] For as low as $P = 5$, subsystems outnumber individual scalar entries, *i.e.* $2^5 - 1 = 31$ subsystems versus $5^2 = 25$ scalar systems.
[21] Recall that cliques correspond to submatrices/subsystems.
[22] In fact, there could well be no positive clique whatsoever.
[23] Assuming at least one exists.

requirements discussed in Section (5.1), for a positive definite completion problem all diagonal entries must be specified, *i.e.* all 1×1 principal subsystems are assumed to be known fixed parameters and satisfy the positivity criterium. Otherwise, these diagonal scalar subsystems can be freely specified. Therefore, a system $\mathbf{H}(s)$ must be first scanned along its diagonal for scalar positive subsystems, alternatively the condition $H_{ii}(s) \geq 0$, with $i \in \{1, 2, \dots P\}$, is satisfied. If $\exists i, i \in \{1, 2, \dots P\},$ and $H_{ii}(s) \ngeq 0$, then a scalar passivity enforcement replaces the violating scalar subsystem with a fully compliant one. Consequently, for a $P \times P$ system, the following can be assumed:

$$\{H_{11}(s) \geq 0, H_{22}(s) \geq 0, \dots, H_{PP}(s) \geq 0\}, \forall i, i \in \{1, 2, \dots P\}.$$

Once a partial positive diagonal system is specified, the search for higher-order positive subsystems that aggregate into a chordal pattern initiates. The assessment cannot *a priori* predict what exact chordal pattern is to be achieved for it depends on the positive clique distribution[24].

A highly desirable clique distribution is the one corresponding to a nearly complete graph (See Definition (30)) for this translates into having almost all entries specified, relaxing as few entries as possible and therefore doing the least computation. This indicates the assessment is by no means neutral or unbiased: the search favours cliques with large clique numbers[25] incorporating other positive submatrices and large overlaps between adjacent cliques[26].

This assessment problem then requires that each of the $2^P - 1$ subsystems be assessed for positive (semi-)definiteness. The offending ones are discarded altogether for only the positive (semi-)definite ones qualify for forming a partial positive system. Out of those satisfying the positivity criterium, only the ones aggregating into a chordal pattern shall remain as specified subsystems. Despite the exponential law governing the number of subsystems that can be embedded in a full $P \times P$ system, any passivity assessment method presented in Section (4.1) depending only on a state-space description can be used. When it comes to computation speed, not all of them perform equally well, though. The fastest method is the Half-size Test (4.1.5) which is adopted throughout. The Half-size Test takes as input a given state-space realization and looks for passivity violations based on spectral information of the following matrices $\mathbf{T}$:

$$\mathbf{T}_{\text{hybrid}} = \mathbf{A}\big(\mathbf{B}\mathbf{D}^{-1}\mathbf{C} - \mathbf{A}\big),$$
$$\mathbf{T}_{\text{scatter}} = \big(\mathbf{A} - \mathbf{B}(\mathbf{D} - \mathbf{I})^{-1}\mathbf{C}\big)\big(\mathbf{A} - \mathbf{B}(\mathbf{D} + \mathbf{I})^{-1}\mathbf{C}\big),$$

[24] The term distribution is used in a similar way to charge and mass distribution in macroscopic objects, *i.e.* the arrangement of these mathematical or physical objects in some context.

[25] This corresponds to the order of the largest dense positive principal submatrix/subsystems embedded within the full system.

[26] This corresponds to vertex separators having large cardinalities.

introduced earlier as Equations (4.16) and (4.17), repeated just for reference. This test is applicable to the full $P \times P$ system as well as any of its $r \times r$ subsystems indexed by an appropriate selection matrix $\mathbf{P}_\beta$, with an index set $\beta = (\beta(1), \beta(2), \ldots, \beta(r))$ with $r \leq P$, as discussed in Section (3.4). Consequently, each of the $2^P - 1$ subsystems can be completely parametrized by the appropriate subset of the full state matrices $\{\mathbf{A}, \mathbf{B}, \mathbf{C}, \mathbf{D}\}$ so that the corresponding subsystem realization is denoted as $\mathbf{H}_{\beta\beta}(s) \iff \{\mathbf{A}_{\beta\beta}, \mathbf{B}_{\beta\beta}, \mathbf{C}_{\beta\beta}, \mathbf{D}_{\beta\beta}\}$, then *mutatis mutandis* its passivity assessment is computed as follows:

$$\mathbf{T}_{\beta\beta} = \mathbf{A}_{\beta\beta}\big(\mathbf{B}_{\beta\beta}\mathbf{D}_{\beta\beta}^{-1}\mathbf{C}_{\beta\beta} - \mathbf{A}_{\beta\beta}\big).$$

All subsystems $\mathbf{H}_{\beta\beta} \not\succeq 0$ are discarded whereas those $\mathbf{H}_{\beta\beta} \succeq 0$ are segregated into candidates to be assembled into a chordal pattern. Among those candidates a search for maximal complete subgraphs is performed, *i.e.* the goal is to find all positive cliques that ultimately correspond to the largest dense submatrices/subsystems within the full system. For a $P \times P$ full system, the existing subsystems have an order range given by $(P-1) \times (P-1), (P-2) \times (P-2), \ldots, (2) \times (2), (1) \times (1)$. Note that there exist many inclusions[27] to be accounted for, *e.g.* a 3-port corresponding to a 3×3 system with $(2) \times (2)$ and $(1) \times (1)$ subsystems :

$$\underset{\not\succeq 0}{\begin{bmatrix} H_{11} & H_{12} & H_{13} \\ H_{21} & H_{22} & H_{23} \\ H_{31} & H_{32} & H_{33} \end{bmatrix}} \supset \left\{ \underset{\succeq 0}{\begin{bmatrix} H_{11} & H_{12} \\ H_{21} & H_{22} \end{bmatrix}}, \underset{\not\succeq 0}{\begin{bmatrix} H_{11} & H_{13} \\ H_{31} & H_{33} \end{bmatrix}}, \underset{\not\succeq 0}{\begin{bmatrix} H_{22} & H_{23} \\ H_{32} & H_{33} \end{bmatrix}}, \begin{matrix} [H_{11}] \succeq 0, \\ [H_{22}] \succeq 0, \\ [H_{33}] \succeq 0 \end{matrix} \right\},$$

with each H_{ij} a function of frequency, $H_{ij}(s)$. By taking only positive subsystems that aggregate into positive cliques, a chordal partial positive system can be specified as:

$$\underset{\succeq 0}{\begin{bmatrix} H_{11} & H_{12} & 0 \\ H_{21} & H_{22} & 0 \\ 0 & 0 & H_{33} \end{bmatrix}} \supset \left\{ \underset{\succeq 0}{\begin{bmatrix} H_{11} & H_{12} \\ H_{21} & H_{22} \end{bmatrix}}, [H_{33}] \succeq 0 \right\}, \tag{5.3}$$

whereby $\mathbf{H}_{\gamma_1\gamma_1} = \left[\begin{smallmatrix} H_{11} & H_{12} \\ H_{21} & H_{22} \end{smallmatrix}\right]$ and $\mathbf{H}_{\gamma_2\gamma_2} = [H_{33}]$[28] are the positive cliques embedded in the system forming a clique tree with index sets $\gamma_1 = [1, 2]$ and $\gamma_2 = [3]$. Note that the number of positive subsystems is larger than the number of positive cliques, because

[27] Despite the somewhat deliberate informal notation employed, these inclusions should be understood in terms of the associated convex cones.

[28] Both $[H_{11}]$ and $[H_{22}]$ are not cliques insofar as they find themselves embedded in a clique, cliques always correspond to maximal dense principal submatrices. Since $[H_{33}]$ is not embedded in any positive clique, it is itself a clique.

positive cliques are maximal dense positive subsystems that include lower-order positive subsytems. Zeros correspond to relaxed subsystems, *i.e.* those to be computed once a completion is found, recalling that a partially positive system with chordal pattern admits a completion. This simple example illustrates a situation which is favorable to completion: the specified subsystems outnumber the unespecified subsystems. The reason is simple: specified subsystems correspond to known fixed parameters in an estimation problem whereas unespecified subsystems correspond to parameters to be estimated, *i.e.* problem variables.

A partial positive system matrix function must be converted into a completable data cone by means of two correspondences: (i) the passivity correspondence and (ii) the chordality correspondence. The first correspondence simply relates the two alternative system representations defined in Chapter (2):

$$\mathbf{H}(s) \succeq 0 \iff \begin{bmatrix} -\mathbf{A}^T\mathbf{P} - \mathbf{P}\mathbf{A} & -\mathbf{P}\mathbf{B} + \mathbf{C}^T \\ -\mathbf{B}^T\mathbf{P} + \mathbf{C} & \mathbf{D} + \mathbf{D}^T \end{bmatrix} \succeq 0, \mathbf{P} \succeq 0,$$

with $\mathbf{P} \succeq 0$ a free parameter. By choosing $\mathbf{P} = \mathbf{I} \succeq 0$, a completable cone $\Pi_{\mathcal{E}}(\mathbb{S}^n_+)$ is obtained as the following data matrix:

$$\mathbf{H}(s) \succeq 0 \iff \begin{bmatrix} -\mathbf{A}^T - \mathbf{A} & -\mathbf{B} + \mathbf{C}^T \\ -\mathbf{B}^T + \mathbf{C} & \mathbf{D} + \mathbf{D}^T \end{bmatrix} \succeq 0.$$

The choice $\mathbf{P} = \mathbf{I} \succeq 0$ is grounded in the fact that the identity lies inside the interior of the convex cone $\Pi_{\mathcal{E}}(\mathbb{S}^n_+)$, *i.e.* an interior-point. This is the key to build a chordality correspondence between a positive (semi-)definite matrix function and a completable cone. For instance, take the 3×3 partial positive system specified in Equation (5.3) with overlapping diagonal blocks[29]:

$$\begin{aligned} \mathbf{H}_{\mathcal{E}}(s) &= \begin{bmatrix} \hat{H}_{11}(s) & \hat{H}_{12}(s) & 0 \\ \hat{H}_{21}(s) & \hat{H}_{22}(s) & 0 \\ 0 & 0 & \hat{H}_{33}(s) \end{bmatrix} \\ &= \begin{bmatrix} R_{110} & R_{120} & 0 \\ R_{210} & R_{220} & 0 \\ 0 & 0 & R_{330} \end{bmatrix} + \frac{1}{s-a_1}\begin{bmatrix} R_{111} & R_{121} & 0 \\ R_{211} & R_{221} & 0 \\ 0 & 0 & R_{331} \end{bmatrix} + \frac{1}{s-a_2}\begin{bmatrix} R_{112} & R_{122} & 0 \\ R_{212} & R_{222} & 0 \\ 0 & 0 & R_{332} \end{bmatrix} + \frac{1}{s-\bar{a}_2}\begin{bmatrix} \bar{R}_{112} & \bar{R}_{122} & 0 \\ \bar{R}_{212} & \bar{R}_{222} & 0 \\ 0 & 0 & \bar{R}_{332} \end{bmatrix}. \end{aligned}$$

Note that (i) the dynamic modes are independent of the sparsity pattern[30] and (ii) the sparsity pattern is equally reflected into system coefficients and then naturally extended to its state-space realization[31]:

[29] Without any loss of generality, it is assumed three dynamic modes ($N = 3$) $\{a_1, a_2, \bar{a}_2\}$ for illustrative purposes, just as prensented in Subsection (2.4.1).

[30] This means the pair $\{\mathbf{A}, \mathbf{B}\}$ is kept from the original VF unconstrained estimation.

[31] This statement holds either for complex or real-only realizations.

$$\mathbf{C}_{\mathcal{E}}=\begin{bmatrix} R_{111} & \mathrm{Re}(R_{112}) & \mathrm{Im}(R_{112}) & R_{121} & \mathrm{Re}(R_{122}) & \mathrm{Im}(R_{122}) & 0 & 0 & 0 \\ R_{211} & \mathrm{Re}(R_{212}) & \mathrm{Im}(R_{212}) & R_{221} & \mathrm{Re}(R_{222}) & \mathrm{Im}(R_{222}) & 0 & 0 & 0 \\ 0 & 0 & 0 & 0 & 0 & 0 & R_{331} & \mathrm{Re}(R_{332}) & \mathrm{Im}(R_{332}) \end{bmatrix} \quad \mathbf{D}_{\mathcal{E}}=\begin{bmatrix} R_{110} & R_{120} & 0 \\ R_{210} & R_{220} & 0 \\ 0 & 0 & R_{330} \end{bmatrix}.$$

This partial realization along with $\mathbf{P} = \mathbf{I}$ translates into a completable cone with block-arrow pattern inherited from and intimately connected with the partial positive system. Therefore, the partial system and the associated completable cone are related as follows:

$$\begin{bmatrix} H_{11} & H_{12} & 0 \\ H_{21} & H_{22} & 0 \\ 0 & 0 & H_{33} \end{bmatrix} \Longleftrightarrow$$

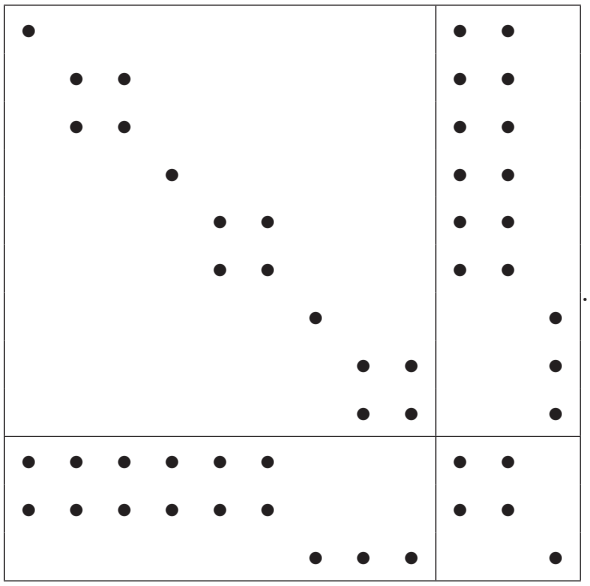

This chordality equivalence between the frequency and time domain descriptions holds for the classical Vector Fitting realization, discussed and illustrated in Section (2.4.1), in either complex or real-only form. Other realizations need not result in a chordal pattern *a priori* and chordality has to be verified by means of the MCS algorithm. A variant of the classical VF algorithm is the Orthogonal Vector Fitting (OVF) which employs orthonormal basis functions resulting in a different realization whose sparsity pattern is not chordal owing to the nearly triangular form of its dynamics matrix, in constrast with the block-diagonal form obtained with the VF realization. Even though the illustration used known chordal patterns discussed in Section (3.4), *i.e.* overlapping diagonal blocks and block-arrow patterns, more general chordal patterns could arise. Whichever pattern appears, its chordality can be either confirmed or refuted with the Maximum Cardinality Search (MCS) algorithm, which only requires the adjacency matrix[32] associated with the allegedly completable cone.

Building on these results, we have implemented in Matlab a customized Partial Positive Matrix Passivity Assessment Algorithm (PPMPAA) to solve the problem at hand, whereby the individual subsystems are assessed with the Half-size test, the positive

[32] See definition (40)

cliques are segregated and chordality is tested with the MCS algorithm. A summary of the PPMPAA is given in the pseudo-code Algorithm (1).

On exit, the algorithm delivers as output a partially specified positive $P \times P$ system, not necessarily chordal. If the system is sprinkled with violating subsystems in a complicated way, then at least the diagonal scalar subsystems are sure to be positive and they form a very simple chordal pattern, for this is a necessary condition for a completable cone to admit a completion. Obviously, this is not the most favourable scenario when it comes to algorithm performance but it must stressed that it may occur as well. By looking on the bright side and assuming an otherwise more general denser pattern, if the algorithm flags the partial positive system as chordal, then a completable cone is ready to be completed as will be discussed in the sequel.

Algorithm 1 Partial Positive Matrix Passivity Assessment Algorithm (PPMPAA)

function PPMPAA($\mathbf{H}(s) \not\succeq 0$) ▷ **Input**: Full $P \times P$ system.
  for $i = 1, \ldots, P$ **do**
    if $\{\mathbf{H}_{ii}(s) \not\succeq 0\}$ **then**
      Enforce $\{\mathbf{H}_{ii}(s) \succeq 0\}$ ▷ Scalar enforcement.
    end if
  end for
  Form $\mathcal{B} = [\beta_1, \ldots, \beta_{2^P-1}]$; ▷ Contains all indices of all principal submatrices.
  $\mathcal{T} = [\quad]$; ▷ Initialize empty clique tree.
  for $i = 2^P - 1, \ldots, 1$ **do** ▷ Search in reverse lexicographic order.
    If $\mathbf{H}_{\beta_i\beta_i} \succeq 0$ ▷ Dense Positive subsystem.
    $\mathcal{T} = [\mathcal{T}, \beta_i]$;
  end for
  $\mathcal{G} = (\mathcal{V}, \mathcal{E}) \leftarrow \bigcup_{\beta_i \in \mathcal{T}} \mathbf{H}_{\beta_i\beta_i}$; ▷ Assemble Partial Positive System
  Form $\mathbf{A}(\mathcal{G})$; ▷ Adjacency Matrix for the Sparsity Graph $\mathcal{G}$
  if $\mathcal{E}$ chordal pattern **then**
    return $\Pi_{\mathcal{E}}(\mathbb{S}^n_+)$ ▷ Completable Cone;
  elsereturn Partial Positive System ▷ Not necessarily completable
  end if
end function ▷ **Input**: Partial Positive System.

Note that the completable cone $\Pi_{\mathcal{E}}(\mathbb{S}^n_+)$ is associated with a partial positive system represented via either $\mathbf{H}_{\mathcal{E}}(s)$ or $\{\mathbf{A}, \mathbf{B}, \mathbf{C}_{\mathcal{E}}, \mathbf{D}_{\mathcal{E}}\}$[33]. The partial system has sparsity pattern denoted by $\mathcal{E}$ thus meaning $H_{ij} \neq 0$ whenever $\{i, j\} \in \mathcal{E}$ and $H_{ij} = 0$ otherwise[34].

5.4 Completion-Based Passivity Enforcement (CBPE)

In this section we outline the proposed algorithm (CBPE) to compute a positive definite completion for the completable cone specified by the novel assessment

[33] Note the subscript $\mathcal{E}$ is left out for the pair $\{\mathbf{A}, \mathbf{B}\}$ to emphasize that they are retained from the unconstrained VF realization and therefore unaffected by the sparsity pattern.

[34] Zero and non-zero entries are specified *mutatis mutandis* for the associated state-space realization.

described in the preceeding section. The underlying assumption for the forthcoming enforcement algorithm is that the passivity assessment summarized in Algorithm (1) has successfully specified a partial positive (semi-)definite system with a chodal sparsity pattern, an existence condition which gives a *carte blanche* to compute a completion[35].

5.4.1 Parameter Completion

As discussed in Subsection (2.4.1), the VF algorithm possesses no capability whatsoever to ensure its associated realization complies with the conditions imposed upon its parameters by dissipativity/passivity inequalities[36]. This major shortcoming has been extensively addressed in the literature and Chapter (4) illustrates many formulations to enforce compliance. In pursuit of improved precision relative to existing formulations, we begin describing a novel formulation.

The idea hinges on the following assumptions: (i) a VF realization with passivity violations exists, (ii) all realization parameters have been determined to sufficiently accurate precision and (iii) a completable positive (semi-)definite cone exists. The completion problem can be solved as convex optimization problem whereby the objective function to be minimized accounts for an approximation error while satisfying a set of inequality (passivity) and equality (projection) constraints. Let $\mathbf{H}(s)$ denote the measured data as well as $\mathbf{H}_{\mathcal{E}}(s)$[37] and $\hat{\mathbf{H}}(s)$ denote the partial system and the completed system with their respective associated realizations $\{\mathbf{A}, \mathbf{B}, \mathbf{C}_{\mathcal{E}}, \mathbf{D}_{\mathcal{E}}\}$ and $\{\mathbf{A}, \mathbf{B}, \hat{\mathbf{C}}, \hat{\mathbf{D}}\}$[38] the problem can be formulated as follows:

$$
\begin{aligned}
\text{minimize} \quad & \sum_{\{i,j\}\notin\mathcal{E}} \sum_{k=1}^{K} |\Xi_{ij}(s_k)| \|H_{ij}(s_k) - \hat{H}_{ij}(s_k)\|^2 \\
\text{subject to} \quad & \begin{bmatrix} -\mathbf{A}^T\mathbf{P} - \mathbf{P}\mathbf{A} & -\mathbf{P}\mathbf{B} + \hat{\mathbf{C}}^T \\ -\mathbf{B}^T\mathbf{P} + \hat{\mathbf{C}} & \hat{\mathbf{D}}^T + \hat{\mathbf{D}} \end{bmatrix} \succeq 0 \\
& \{\hat{\mathbf{C}}, \hat{\mathbf{D}}\}\Big|_{\gamma_i\in\mathcal{T}} = \{\mathbf{C}_{\mathcal{E}}, \mathbf{D}_{\mathcal{E}}\} \\
& \mathbf{P} \succeq 0
\end{aligned}
\tag{5.4}
$$

Applying suitable transformations to Equation (5.4), details can be found in

[35] If a partial positive system without a chordal pattern is specified, a completion may still exist.
[36] This can happen accidentally though.
[37] Recalling that $\mathbf{H}_{\mathcal{E}}(s) = \bigcup_{\gamma_i\in\mathcal{T}}\{\mathbf{H}_{\gamma_i\gamma_i}(s)\}$
[38] The pair $\{\mathbf{A}, \mathbf{B}\}$ has no hat superscript since it is problem data, inherited from the original unconstrained VF realization.

Section (3.1) and Subsection (4.3.1), the problem achieves the form:

$$
\begin{aligned}
\text{minimize} \quad & t(\hat{\mathbf{C}}, \hat{\mathbf{D}}, \mathbf{P}) \\
\text{subject to} \quad & \begin{bmatrix} -\mathbf{A}^T\mathbf{P} - \mathbf{P}\mathbf{A} & -\mathbf{P}\mathbf{B} + \hat{\mathbf{C}}^T \\ -\mathbf{B}^T\mathbf{P} + \hat{\mathbf{C}} & \hat{\mathbf{D}}^T + \hat{\mathbf{D}} \end{bmatrix} \succeq 0 \\
& \{\hat{\mathbf{C}}, \hat{\mathbf{D}}\}\Big|_{\gamma_i \in \mathcal{T}} = \{\mathbf{C}_\mathcal{E}, \mathbf{D}_\mathcal{E}\} \\
& \left.\begin{array}{c} \mathbf{E}_{ij}^T\mathbf{E}_{ij} - \delta_{ij}^2 \leq t_{ij} \\ t_{ij} \leq t \\ t \geq 0 \end{array}\right| _{\{i,j\} \notin \mathcal{E}} \\
& \mathbf{P} \succeq 0
\end{aligned}
\tag{5.5}
$$

Lumping all unknown state-space parameters into a single vector variable θ and writing this problem in standard epigraph form, we get:

$$
\begin{aligned}
\text{minimize} \quad & t(\theta, \mathbf{P}) \\
\text{subject to} \quad & \mathcal{M}(\theta, \mathbf{P}) \succeq 0 \\
& \hat{\mathbf{C}}(\theta) = \tilde{\mathbf{C}}, \qquad \{i,j\} \in \mathcal{E} \\
& \hat{\mathbf{D}}(\theta) = \tilde{\mathbf{D}}, \qquad \{i,j\} \in \mathcal{E} \\
& \|\mathbf{E}_{ij}\theta_{ij} + \delta_{ij}\|_2 \leq t_{ij}, \quad \{i,j\} \notin \mathcal{E} \\
& t_{ij} \leq t \\
& t \geq 0.
\end{aligned}
\tag{5.6}
$$

In equation (5.6), three kinds of convex cones constrain the search space, namely $\mathcal{M}(\theta, \mathbf{P})$ which is a SDP constraint to satisfy the Positive-Real Lemma LMI (passivity constraint), each $\|\mathbf{E}_{ij}\theta + \delta_{ij}\|_2$ is a SOCP constraint accounts for matching criterium (Error bounding constraints) for all unspecified entries ($\{i,j\} \notin \mathcal{E}$) and the non-negativity constraint t. Additionally, equality constraints to represent known parameters, *i.e.* those inherited from the VF realization. The problem variable $\theta \in \mathbb{R}^\mathcal{D}$ has dimension defined by $\mathcal{D} = |\mathcal{E}^c| \times (n+1)$, with $|\mathcal{E}^c|$ denoting the cardinality of the complement edge set (relaxed parameters) and n is the degree or dynamic order[39].

All transformations between the initial form Equation (5.4) and the final standard epigraph convex form Equation (5.6) do not entail any computation whatsoever, they simply change the form of the objective and constraint functions, the problem data for the problems are the same. Equation (5.6) comprises a constrained data fitting problem whereby variables correspond to unknown model parameters and the constraints correspond to prior information to be incorporated into the solution. This problem can be

[39] See Definition (16).

solved with CVX, a package for specifying and solving convex programs (RESEARCH, 2012),(GRANT; BOYD, 2008) with core solver SEDUMI (STURM, 1999).

5.5 Case Studies

This section is devoted to present numerical evidence that the proposed novel passivity enforcement strategy combining both the PPMPA and the CBPE algorithms presented in the preceeding sections yield results comparable to those obtained with other state-of-the-art algorithms commonly used in the specialized literature. All models are built on data *in puris naturalibus*, *i.e.* measured data from actual systems without any preprocessing. In summary, the objective is to test how the algorithms respond to a practical problem setting whereby varying dynamic orders, port numbers and clique distributions arise. Dynamic order and total port number dictate much of algorithmic performance, while the first is user-prescribed, the second is not[40]. As we shall also see, the clique distributions are completely determined by the vagaries of the system.

In what follows an Inductive Voltage Transformer (Subsection (5.5.1)) and a Power Transformer (Subsection (5.5.2)) are both modeled in a two-stage process in which a black-box frequency domain System Identification using the VF Algorithm (Subsection (2.4.1)) upon raw data is used as the first stage with a subsequent passive enforcement as the second. The former is assumed standard procedure whereas the latter is open to discussion and analysis. The analysis is tailored to underscore how the proposed method compares with other existing enforcement algorithms. To guide the comparison we use accuracy degradation[41] and computation time as indices, which is the standard performance analysis for passivity enforcement in the literature, *e.g.* (GRIVET-TALOCIA; UBOLLI, 2008). In order to pursue an imparcial performance analysis, all results are presented for models with order ranging from 10 to 40, such that the order is successively increased in equal order steps of 10. This order range encompasses low order and intermediate orders and should suffice to either illustrate the point without overfitting the data under analysis. Besides changing the order, other passivity enforcement algorithms are used to provide a data base for performance comparison, namely the RPD (Residue Perturbation Driver) and the PRL, as discussed at some length in Subsections (4.2.1) and (4.3.1), respectively.

The analysis is underpinned by Figures containing plots of errors, runtime and curve-fit versus dynamic order as well as Tables indicating scalar error, all measuring performance for the RPD, PRL and CBPE algorithms, *i.e.* a comparison between

[40] Sometimes terminals/windings can be ignored, *e.g.* by means of shorts and opens, depending on the purposes of the modeler to concentrate on parts more relevant to his analysis, the analysis herein taken however is committed to the full port number to avoid a potential confusion over subsystems.

[41] Degradation is meant to be relative to the unconstrained model, since it is always assumed the unconstrained model is always better then any constrained model.

the proposed algorithm versus existing consolidated ones. For the sake of clarity, the following notation is henceforth adopted: Y_{ij},$\hat{Y}_{ij}$ and $\tilde{Y}_{ij}$ indicate raw data, unconstrained model (VF) and constrained passive model (RPD,PRL,CBPE) respectively.

5.5.1 Inductive Voltage Transformer

In this first case study an Inductive Voltage Transformer (IVT) is considered as the system under analysis. The 525/0,116 [kV], 400 [VA], 60 [Hz] IVT (rated values) is part of the SF6 GIS within the Jirau hydroelectric power plant which possesses a 3,750 MW installed capacity, located on the Madeira River in Rondônia, northern Brazil. The IVT is measured as a 3-port system characterized by its admittance parameters:

$$\mathbf{Y}(s_k) = \begin{bmatrix} Y_{H1H1}(s_k) & Y_{L1H1}(s_k) & Y_{L2H1}(s_k) \\ Y_{L1H1}(s_k) & Y_{L1L1}(s_k) & Y_{L1L2}(s_k) \\ Y_{L2H1}(s_k) & Y_{L2L1}(s_k) & Y_{L2L2}(s_k) \end{bmatrix} = \begin{bmatrix} Y_{11}(s_k) & Y_{12}(s_k) & Y_{13}(s_k) \\ Y_{21}(s_k) & Y_{22}(s_k) & Y_{23}(s_k) \\ Y_{31}(s_k) & Y_{32}(s_k) & Y_{33}(s_k) \end{bmatrix},$$

with $s_k = j2\pi f_k$, such that each f_k is a discrete frequency taken out of the 1141 frequency samples logarithmically spaced in the interval 20Hz-10MHz. The IVT terminals are labelled with subscripts $H1$ for higher and $L1, L2$ for lower voltage terminals, but these voltage labels are dropped.

Table 2 – Magnitude and location of Most Negative Eigenvalue (MNE)

	MNE $\times 10^{-4}$	Freq. [Hz]$\times 10^{+6}$
data	-2.00	9.55
VF (10th)	-0.51	3.29
VF (20th)	-8.99	∞
VF (30th)	-17.00	9.55
VF (40th)	-14.00	9.58

Upon this data set four vector fitting realizations[42] are obtained such that their dynamic orders obey the increasing sequence $\{10, 20, 30, 40\}$. Neither the data nor any of the realizations for each different orders represent a passive system. Table (2) summarizes the largest violation and the frequency at which it occurs for each case. This table illustrates that models in the higher end of the order sequence (30th-40th) have accurately captured the frequency at which the largest violation manifests itself while amplifying the violation magnitude[43] relative to the original data. Order 20 created an oddity because of its peculiar largest violation occuring at a frequency being well beyond the measurement band and order 10 seems to have reduced the magnitude but missed the frequency for the most negative eigenvalue.

[42] Details of this realization are discussed in Subsection (2.4.1).

[43] This is a downside of these models indicating higher proneness to unstable time-domain simulation.

Since these VF models are not passive, they can be examined for embedded passive subsystems by means of the PPMPA Algorithm (1). These results are consolidated in Figure (39) whereby the positive clique distributions found for both the data and VF models are juxstaposed with the partial positive system obtained after enforcing violating diagonal subsystems to be passive on a scalar basis. Dashes have been used to indicate violating subsystems discarded as ineligible for completion whereas question marks indicate relaxed subsystems eligible for completion.

Data	VF 10th	Partial Positive
$\begin{bmatrix} - & - & - \\ - & Y_{22} & Y_{23} \\ - & Y_{32} & Y_{33} \end{bmatrix}$	$\begin{bmatrix} - & - & - \\ - & \hat{Y}_{22} & - \\ - & - & \hat{Y}_{33} \end{bmatrix}$	$\begin{bmatrix} \tilde{Y}_{11} & \hat{Y}_{12} & \hat{Y}_{13} \\ \hat{Y}_{21} & \hat{Y}_{22} & \hat{Y}_{23} \\ \hat{Y}_{31} & \hat{Y}_{32} & \hat{Y}_{33} \end{bmatrix}$
Data	**VF 20th**	**Partial Positive**
$\begin{bmatrix} - & - & - \\ - & Y_{22} & Y_{23} \\ - & Y_{32} & Y_{33} \end{bmatrix}$	$\begin{bmatrix} - & - & - \\ - & \hat{Y}_{22} & - \\ - & - & \hat{Y}_{33} \end{bmatrix}$	$\begin{bmatrix} \tilde{Y}_{11} & \hat{Y}_{12} & \hat{Y}_{13} \\ \hat{Y}_{21} & \hat{Y}_{22} & ? \\ \hat{Y}_{31} & ? & \hat{Y}_{33} \end{bmatrix}$
Data	**VF 30th**	**Partial Positive**
$\begin{bmatrix} - & - & - \\ - & Y_{22} & Y_{23} \\ - & Y_{32} & Y_{33} \end{bmatrix}$	$\begin{bmatrix} - & - & - \\ - & \hat{Y}_{22} & \hat{Y}_{23} \\ - & \hat{Y}_{32} & \hat{Y}_{33} \end{bmatrix}$	$\begin{bmatrix} \tilde{Y}_{11} & \hat{Y}_{12} & \hat{Y}_{13} \\ \hat{Y}_{21} & \hat{Y}_{22} & \hat{Y}_{23} \\ \hat{Y}_{31} & \hat{Y}_{32} & \hat{Y}_{33} \end{bmatrix}$
Data	**VF 40th**	**Partial Positive**
$\begin{bmatrix} - & - & - \\ - & Y_{22} & Y_{23} \\ - & Y_{32} & Y_{33} \end{bmatrix}$	$\begin{bmatrix} - & - & - \\ - & \hat{Y}_{22} & \hat{Y}_{23} \\ - & \hat{Y}_{32} & \hat{Y}_{33} \end{bmatrix}$	$\begin{bmatrix} \tilde{Y}_{11} & \hat{Y}_{12} & \hat{Y}_{13} \\ \hat{Y}_{21} & \hat{Y}_{22} & \hat{Y}_{23} \\ \hat{Y}_{31} & \hat{Y}_{32} & \hat{Y}_{33} \end{bmatrix}$

Figure 39 – Positive Clique Distributions for the raw data, the unconstrained VF models and the partial positive systems found with PPMPA.

What Figure (39) reveals is a novelty in terms of passivity assessment as one can better judge passivity violations from an individual, inside perspective as opposed to only a full-system view as it used to be the case before the PPMPAA. For instance, the left column depicted in the aforementioned figure demonstrates that something went wrong when the data for the Y_{11} entry was measured, since this admittance has negative real part thus not passive on a scalar basis and ultimately prompting a system-wise passivity violation. Another interesting pattern seen in the middle column is that the positive clique distributions for the VF models change as the dynamic order changes and also that these distributions are not necessarily inherited from the data as is the

case for lower orders. These results bear some resemblance to remarks made earlier about the largest violation and its location in the sense that higher behavioral variability has been found for lower order models.

The transition from the middle to the right column entails the scalar passivity enforcement only for the diagonal elements marked with a dash, recalling that dashes mean violating subsystem and that for completion problems the diagonal must be both especified and positive. Since all four VF realizations have at least one dash along the diagonal[44], none of them is originally passive. As the completion algorithm requires a partial positive matrix, the PPMPAA replaces violating subsystems along the diagonal with passive scalar systems, *i.e.* $\hat{Y}_{ii} \implies \tilde{Y}_{ii}$ whenever $\hat{Y}_{ii} < 0$. Without this scalar enforcement none of the models would qualify for completion. At first this may seem a bit contrived but in a completion problem one is free to choose the positive diagonal elements, as stated in the preceeding sections on the definition of the completion. Therefore, one is completely entitled to simply discard violating diagonals and replace them with any passive subsystem on an *ad hoc* basis. The PPMPAA was conceived to do so and find a replacement which approximates to the data. This capability coded into the PPMPAA guarantess that a necessary condition for completion be satisfied, otherwise it would be pointless to search for a partial positive system.

In the light of the foregoing discussion, it should then be clear that the scalar enforcement for diagonal elements can have favorable effects, *e.g.* the subsystems $\hat{Y}_{12}, \hat{Y}_{13}, \hat{Y}_{21}, \hat{Y}_{31}$ are marked as dashes in the middle column for all dynamic orders as a consequence of $\hat{Y}_{11} < 0$. There exists an interplay between the diagonal elements and all those along the same row and down the same column. The moment the violating condition ceases to exist[45] by means of the scalar enforcement, its effects propagate to associated elements denoting that passivity violations were not caused by the scalar subsystems $\hat{Y}_{12}, \hat{Y}_{13}, \hat{Y}_{21}, \hat{Y}_{31}$ [46].

The partial positive systems for orders $\{10, 30, 40\}$ identified by the PPMPAA are not only partial positive but also complete, *i.e.* a completion has been obtained in a single step and no further action is needed. This is not so for order $\{20\}$ as indicated by question marks corresponding to relaxed subsystems[47] eligible for completion. All subsystems marked as $[?]$ are replaced by zeros and the partial positive system is passed on to the CBPE algorithm which determines the remaining parameters. Figure (40) summarizes all passive models derived with the proposed algorithms, *viz.* PPMPAA and CBPE, and more importantly it shows whence each subsystem is derived: each $\hat{Y}_{ij}$ originated as a VF unconstrained estimate whereas each $\tilde{Y}_{ij}$ is a completion. Note on

[44] Recalling that diagonal dashes indicate $[-] \iff \hat{Y}_{ii} < 0$, then $\hat{Y}_{ii}$ has been discarded.
[45] $\hat{Y}_{11} < 0 \implies \tilde{Y}_{11} > 0$.
[46] This need not happen in general, though.
[47] Read: discarded.

the one hand that passive models having dynamic orders $\{10, 30, 40\}$ are essentially VF parameters, except for the $\tilde{Y}_{11}$ subsystem. On the other hand, order $\{20\}$ seems to be somewhat peculiar in behavior as it also required further passivity enforcement for subsystems $\tilde{Y}_{23}$ and $\tilde{Y}_{32}$.

Completion 10th	Completion 20th	Completion 30th	Completion 40th
$\begin{bmatrix} \tilde{Y}_{11} & \hat{Y}_{12} & \hat{Y}_{13} \\ \hat{Y}_{21} & \hat{Y}_{22} & \hat{Y}_{23} \\ \hat{Y}_{31} & \hat{Y}_{32} & \hat{Y}_{33} \end{bmatrix}$	$\begin{bmatrix} \tilde{Y}_{11} & \hat{Y}_{12} & \hat{Y}_{13} \\ \hat{Y}_{21} & \hat{Y}_{22} & \tilde{Y}_{23} \\ \hat{Y}_{31} & \tilde{Y}_{32} & \hat{Y}_{33} \end{bmatrix}$	$\begin{bmatrix} \tilde{Y}_{11} & \hat{Y}_{12} & \hat{Y}_{13} \\ \hat{Y}_{21} & \hat{Y}_{22} & \hat{Y}_{23} \\ \hat{Y}_{31} & \hat{Y}_{32} & \hat{Y}_{33} \end{bmatrix}$	$\begin{bmatrix} \tilde{Y}_{11} & \hat{Y}_{12} & \hat{Y}_{13} \\ \hat{Y}_{21} & \hat{Y}_{22} & \hat{Y}_{23} \\ \hat{Y}_{31} & \hat{Y}_{32} & \hat{Y}_{33} \end{bmatrix}$

Figure 40 – Passive models derived with PPMPAA and CBPE.

All passive models enumerated in Figure (40) have been derived in accordance with a completion strategy and shall therefore be compared with other competing enforcement algorithms, namely the RPD and PRL algorithms. Figure (41) displays the error performance relative to the unconstrained VF model recorded for the passivity enforcement methods labelled RPD, PRL and CBPE (completion): the left plot corresponds to the RMSE error while the right plot is the cost function objective value[48]. First and foremost the CBPE algorithm has performed unambiguously better considering the dynamic order sequence defined for the analysis. Furthermore, while the RPD and PRL algorithms have shown a somewhat erratic behavior as the order increases the CBPE algorithm has proved to be nearly monotonic in that respect. This improved performance delivered by the CBPE for this particular data set is not surprising given that nearly all parameters of the passive CBPE models were actually derived without any passivity compensation, *i.e.* they were originally derived by the pure unconstrained VF algorithm, as is clearly shown in Figure (40). This is where the completion strategy takes its advantage from. Obviously, no general conclusion is being herein drawn to endorse the completion method as better than both the RPD and PRL algorithms since the clique distributions can vary according to the data set and over the dynamic order assigned.

Despite having achieved an overall better fitting error one might ask how the errors on an entry-wise basis for the CBPE algorithm compare with other enforcement methods. Table (3) contains the individual errors for order 20 that add up to the cost function depicted in Figure (41). The errors attained by the CBPE relative to the unconstrained model are exactly zero except for the entries that required intervention, namely $\tilde{Y}_{11}$, $\tilde{Y}_{23}$ and $\tilde{Y}_{32}$, and any compensation to the model aimed at passive behavior befalls

[48] These errors have been defined back in Section (2.5), as Equations (2.30) and (2.31), respectively.

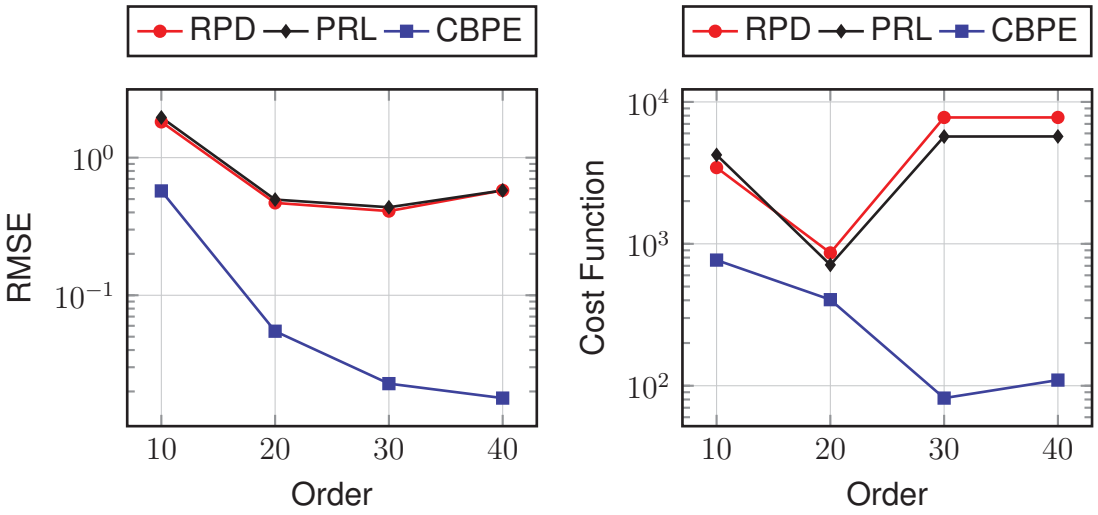

Figure 41 – Error relative to unconstrained VF: the RMSE and Cost Function.

them. Nevetheless, this does not mean that these entries are necessarily more penalized in terms of fit. For instance, the $\tilde{Y}_{11}$ diagonal subsystem derived by the completion approach has achieved the best fit among all passive models while at the same time the off-diagonal subsystems $\tilde{Y}_{23}$ and $\tilde{Y}_{32}$ were more penalized relative to other methods.

Table 3 – Entry-wise Cost Function for passive 20th order models.

Entry-wise Cost Function $\left(\times 10^{+2}\right)$									
	RPD 20th			PRL 20th			CBPE 20th		
	(H_1)	(L_1)	(L_2)	(H_1)	(L_1)	(L_2)	(H_1)	(L_1)	(L_2)
(H_1)	85.9175	0.0751	0.0094	2.4408	2.4272	0.9064	1.5516	0.0000	0.0000
(L_1)	0.0751	0.3142	0.0023	2.4272	0.6868	0.1831	0.0000	0.0000	2.4878
(L_2)	0.0094	0.0023	0.0014	0.9064	0.1831	0.4626	0.0000	2.4878	0.0000

It is not the actual numbers that matter most in Table (3) but rather the pattern: the CBPE achieves zero error[49] for those subsystems retained from the unconstrained estimate which is in striking contrast to what is achieved with the usual methods whereby passivity compensations are scattered over all subsystems. The CBPE algorithm concentrates passivity compensations precisely on those subsystems that cause violations whereas traditional methods amortize the cost of compensation across the entire system.

Besides recording the errors obtained for the three competing algorithms, the run time is also a measure of interest for algorithm performance. Consequently, Figure (42) includes the timing for each algorithm at each dynamic order. In this respect, there has been a more erratic response by the CBPE algorithm as it performed noticeably worse at order $\{20\}$. This poorer time performance is a consequence of the fact that precisely at this dynamic order the positive clique distribution required more entries

[49] Zero relative to the unconstrained model.

to be completed. Furthermore, even though both the PRL and the CBPE algorithms are convex formulations, the latter has additional constraints to ensure parameters are hold fixed. This alone does not necessarily demean the CBPE algorithm but it does underscore its sensitivity to the clique distributions which in turn are unpredictable until the passivity assessment with the PPMPAA reveals these patterns.

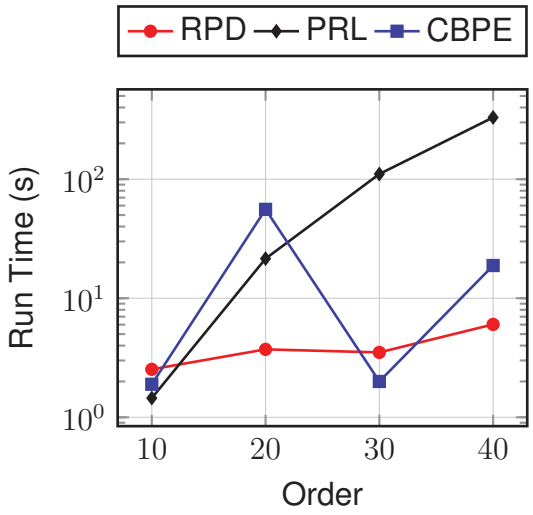

Figure 42 – Run Time for passivity enforcement.

In order to present the error pattern obtained with the CBPE algorithm in a pictorial form, Figures (43) and (44) display measured data, the unconstrained VF (20th) fit and the CBPE constrained (20th) fit as a function of frequency. The admittance magnitude curves for diagonal subsystems were overlaid onto a single graph (43) whereas the lower triangular[50] off-diagonal subsystems were overlaid onto a separate graph for improved visualization of results.

As expected, Figure (43) reveals that passivity compensations were necessary only for the $\hat{Y}_{11}$ subsystem in which case three distinct line types indicate the data (Y_{11}, dotted), the unconstrained VF model ($\hat{Y}_{11}$,dashed red) and the constrained CBPE model ($\tilde{Y}_{11}$, solid blue). Except for a gently softened resonance peak at about 200Hz, the three curves differ very little qualitatively. As for the remaining diagonal subsystems, there exists a perfect match between the unconstrained VF model and constrained CBPE model since the passive model inherited its parameters from the originally violating model. For this reason, the dashed red curves and the associated blue ones exactly overlay each other.

Figure (44) also confirms the pattern already verified in Table (3) as it becomes evident that the unconstrained and constrained models differ only for the Y_{32}[51] subsystem.

[50] System is symmetric/reciprocal.
[51] The same holds for the corresponding upper triangular subsystem.

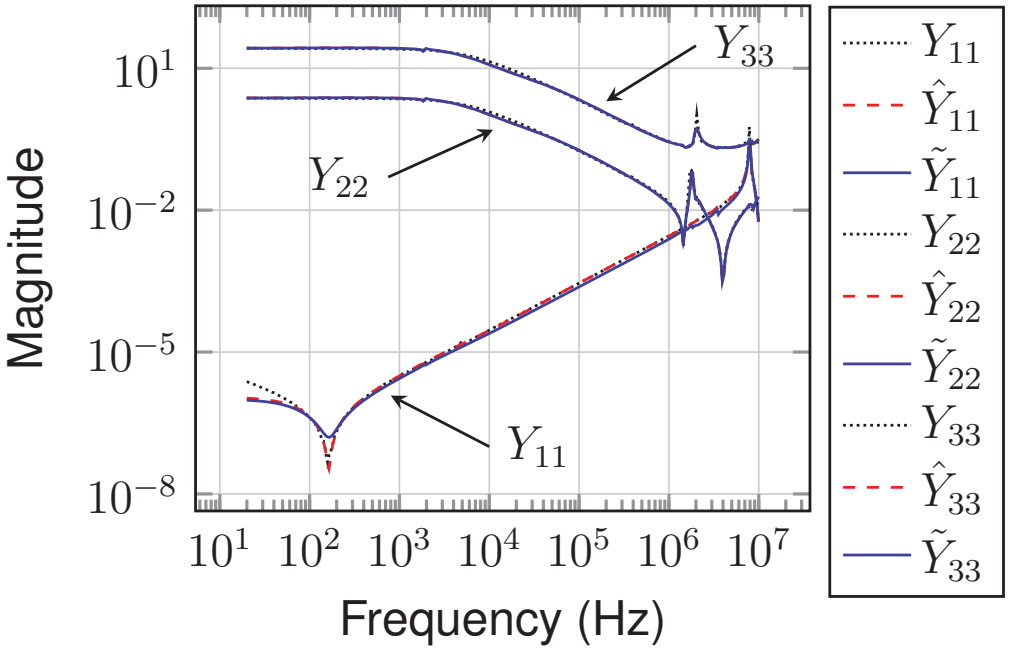

Figure 43 – Admittance Magnitude: diagonal subsystems.

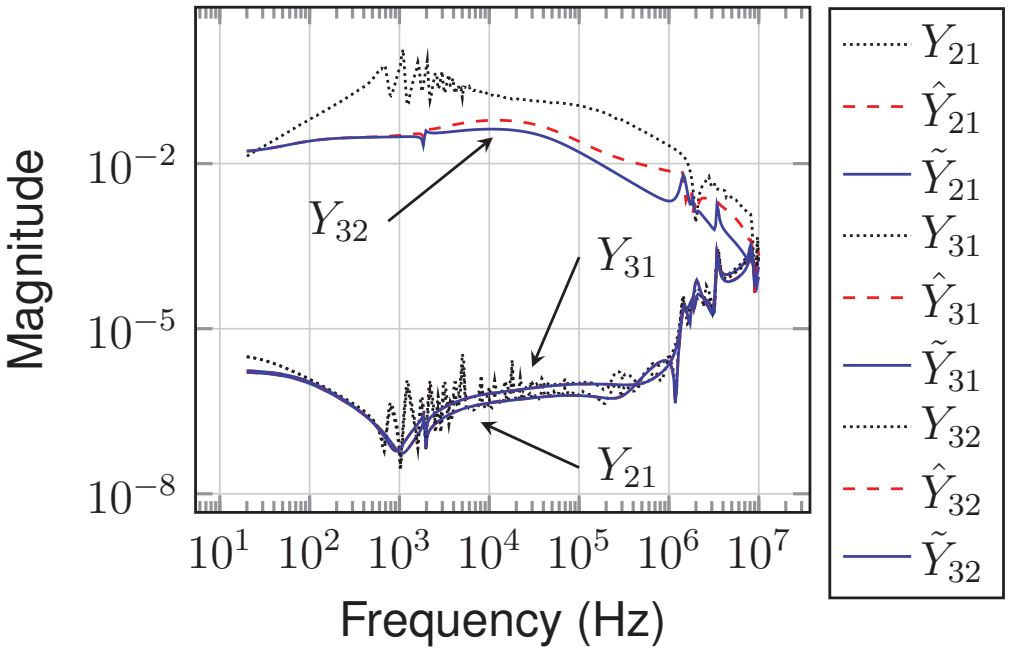

Figure 44 – Admittance Magnitude: off-diagonal subsystems.

The reason for a more detailed discussion on entry-wise results for order 20 is twofold: (i) the larger number of subsystems undergoing passivity compensations thus furnishing a richer discussion of what to expect in terms of results and (ii) to avoid a repetitive and voluminous account of each case. Nonetheless, the pattern for the remaining dynamic orders should be clear by now since only the diagonal subsystem Y_{11} required enforcement.

5.5.2 Power Transformer

In this second example the data set consists of the admittance parameters for a 500/230 [kV], 400 [MVA], Yd, three-phase power transformer (rated values) which is part of a transmission air insulated substation situated in Santana do Paraíso, a municipality in Minas Gerais, southeastern Brazil. The admittance matrix for the three-phase power transformer gives a 6-port system as follows:

$$\mathbf{Y}(s_k) = \begin{bmatrix} Y_{H1H1}(s_k) & Y_{H1H2}(s_k) & Y_{H1H3}(s_k) & Y_{H1L1}(s_k) & Y_{H1L2}(s_k) & Y_{H1L3}(s_k) \\ Y_{H2H1}(s_k) & Y_{H2H2}(s_k) & Y_{H2H3}(s_k) & Y_{H2L1}(s_k) & Y_{H2L2}(s_k) & Y_{H2L3}(s_k) \\ Y_{H3H1}(s_k) & Y_{H3H2}(s_k) & Y_{H3H3}(s_k) & Y_{H3L1}(s_k) & Y_{H3L2}(s_k) & Y_{H3L3}(s_k) \\ Y_{L1H1}(s_k) & Y_{L1H2}(s_k) & Y_{L1H3}(s_k) & Y_{L1L1}(s_k) & Y_{L1L2}(s_k) & Y_{L1L3}(s_k) \\ Y_{L2H1}(s_k) & Y_{L2H2}(s_k) & Y_{L2H3}(s_k) & Y_{L2L1}(s_k) & Y_{L2L2}(s_k) & Y_{L2L3}(s_k) \\ Y_{L3H1}(s_k) & Y_{L3H2}(s_k) & Y_{L3H3}(s_k) & Y_{L3L1}(s_k) & Y_{L3L2}(s_k) & Y_{L3L3}(s_k) \end{bmatrix}$$

$$= \begin{bmatrix} Y_{11}(s_k) & Y_{12}(s_k) & Y_{13}(s_k) & Y_{14}(s_k) & Y_{15}(s_k) & Y_{16}(s_k) \\ Y_{21}(s_k) & Y_{22}(s_k) & Y_{23}(s_k) & Y_{24}(s_k) & Y_{25}(s_k) & Y_{26}(s_k) \\ Y_{31}(s_k) & Y_{32}(s_k) & Y_{33}(s_k) & Y_{34}(s_k) & Y_{35}(s_k) & Y_{36}(s_k) \\ Y_{41}(s_k) & Y_{42}(s_k) & Y_{43}(s_k) & Y_{44}(s_k) & Y_{45}(s_k) & Y_{46}(s_k) \\ Y_{51}(s_k) & Y_{52}(s_k) & Y_{53}(s_k) & Y_{54}(s_k) & Y_{55}(s_k) & Y_{56}(s_k) \\ Y_{61}(s_k) & Y_{62}(s_k) & Y_{63}(s_k) & Y_{64}(s_k) & Y_{65}(s_k) & Y_{66}(s_k) \end{bmatrix},$$

with $s_k = j2\pi f_k$, such that each f_k is a discrete frequency taken out of the 600 frequency samples logarithmically spaced in the interval 10Hz-2MHz. The transformer terminals are labelled with subscripts $H1, H2, H3$ for higher voltage terminals and $L1, L2, L3$ for lower voltage terminals, but these voltage labels are dropped. Similarly to the previous example, four VF models are extracted for this data set with dynamic order in the same sequence $\{10, 20, 30, 40\}$.

Table 4 – Magnitude and location of Most Negative Eigenvalue (MNE)

	MNE $\times 10^{-2}$	Freq. [Hz]
data	—	—
VF (10th)	-2.71	0.00
VF (20th)	-1.70	0.00
VF (30th)	-0.70	0.00
VF (40th)	-0.28	0.00

Table (4) reveals that the data indicates a passive system whereas the models are tainted with passivity violations all occuring at DC frequency. Despite the contradiction between the data and the models with regard to passivity, the violations show diminished variability as a function of order both in terms of magnitude and frequency at which they occur.

VF 10th

$$\begin{bmatrix} - & - & - & - & - & - \\ - & - & - & - & - & - \\ - & - & - & - & - & - \\ - & - & - & \hat{Y}_{44} & \hat{Y}_{45} & - \\ - & - & - & \hat{Y}_{54} & \hat{Y}_{55} & \hat{Y}_{56} \\ - & - & - & - & \hat{Y}_{65} & \hat{Y}_{66} \end{bmatrix}$$

Partial Positive 10th

$$\begin{bmatrix} \tilde{Y}_{11} & \hat{Y}_{12} & \hat{Y}_{13} & ? & ? & ? \\ \hat{Y}_{21} & \tilde{Y}_{22} & \hat{Y}_{23} & \hat{Y}_{24} & ? & ? \\ \hat{Y}_{31} & \hat{Y}_{32} & \tilde{Y}_{33} & \hat{Y}_{34} & ? & ? \\ ? & \hat{Y}_{42} & \hat{Y}_{43} & \hat{Y}_{44} & ? & ? \\ ? & ? & ? & ? & \hat{Y}_{55} & \hat{Y}_{56} \\ ? & ? & ? & ? & \hat{Y}_{65} & \hat{Y}_{66} \end{bmatrix}$$

VF 20th

$$\begin{bmatrix} - & - & - & - & - & - \\ - & - & - & - & - & - \\ - & - & - & - & - & - \\ - & - & - & \hat{Y}_{44} & - & \hat{Y}_{46} \\ - & - & - & - & \hat{Y}_{55} & - \\ - & - & - & \hat{Y}_{64} & - & \hat{Y}_{66} \end{bmatrix}$$

Partial Positive 20th

$$\begin{bmatrix} \tilde{Y}_{11} & ? & ? & ? & ? & ? \\ ? & \tilde{Y}_{22} & ? & \hat{Y}_{24} & ? & ? \\ ? & ? & \tilde{Y}_{33} & \hat{Y}_{34} & \hat{Y}_{35} & ? \\ ? & \hat{Y}_{42} & \hat{Y}_{43} & \hat{Y}_{44} & ? & \hat{Y}_{46} \\ ? & ? & \hat{Y}_{53} & ? & \hat{Y}_{55} & ? \\ ? & ? & ? & \hat{Y}_{64} & ? & \hat{Y}_{66} \end{bmatrix}$$

VF 30th

$$\begin{bmatrix} - & - & - & - & - & - \\ - & - & - & - & - & - \\ - & - & - & - & - & - \\ - & - & - & \hat{Y}_{44} & - & \hat{Y}_{46} \\ - & - & - & - & \hat{Y}_{55} & \hat{Y}_{56} \\ - & - & - & \hat{Y}_{64} & \hat{Y}_{65} & \hat{Y}_{66} \end{bmatrix}$$

Partial Positive 30th

$$\begin{bmatrix} \tilde{Y}_{11} & \hat{Y}_{12} & \hat{Y}_{13} & ? & ? & ? \\ \hat{Y}_{21} & \tilde{Y}_{22} & \hat{Y}_{23} & ? & ? & ? \\ \hat{Y}_{31} & \hat{Y}_{32} & \tilde{Y}_{33} & \hat{Y}_{43} & ? & ? \\ ? & ? & \hat{Y}_{43} & \hat{Y}_{44} & ? & \hat{Y}_{46} \\ ? & ? & ? & ? & \hat{Y}_{55} & \hat{Y}_{56} \\ ? & ? & ? & \hat{Y}_{64} & \hat{Y}_{65} & \hat{Y}_{66} \end{bmatrix}$$

VF 40th

$$\begin{bmatrix} - & - & - & - & - & - \\ - & - & - & - & - & - \\ - & - & - & - & - & - \\ - & - & - & \hat{Y}_{44} & \hat{Y}_{45} & - \\ - & - & - & \hat{Y}_{54} & \hat{Y}_{55} & \hat{Y}_{56} \\ - & - & - & - & \hat{Y}_{65} & \hat{Y}_{66} \end{bmatrix}$$

Partial Positive 40th

$$\begin{bmatrix} \tilde{Y}_{11} & \hat{Y}_{12} & \hat{Y}_{13} & ? & ? & ? \\ \hat{Y}_{21} & \tilde{Y}_{22} & \hat{Y}_{23} & ? & ? & ? \\ \hat{Y}_{31} & \hat{Y}_{32} & \tilde{Y}_{33} & \hat{Y}_{43} & ? & ? \\ ? & ? & \hat{Y}_{43} & \hat{Y}_{44} & ? & ? \\ ? & ? & ? & ? & \hat{Y}_{55} & \hat{Y}_{56} \\ ? & ? & ? & ? & \hat{Y}_{65} & \hat{Y}_{66} \end{bmatrix}$$

Figure 45 – Positive Clique Distributions for the raw data, the unconstrained VF models and the completable systems found with PPMPA.

Figure (45) displays the positive clique distributions for the original unconstrained VF models in comparison with the distributions obtained after the diagonal subsystems are forced to be positive definite by the PPMPAA. All clique distributions vary with order for both the unconstrained and partial positive models, no distribution occurs twice and again the pattern for order 20 coincidentally departs the most from the others. Passing all partial positive models derived with the PPMPAA to the CBPE algorithm the unknown parameters are computed resulting in the passive models indicated in Figure (46). The smallest number of parameters that required a completion were those for orders 10 and 30, thus these models inherit the largest number of parameters from their associated unconstrained model.

Completion 10th

$$\begin{bmatrix} \tilde{Y}_{11} & \hat{Y}_{12} & \hat{Y}_{13} & \tilde{Y}_{14} & \tilde{Y}_{15} & \tilde{Y}_{16} \\ \hat{Y}_{21} & \tilde{Y}_{22} & \hat{Y}_{23} & \hat{Y}_{24} & \tilde{Y}_{25} & \tilde{Y}_{26} \\ \hat{Y}_{31} & \hat{Y}_{32} & \tilde{Y}_{33} & \hat{Y}_{34} & \tilde{Y}_{35} & \tilde{Y}_{36} \\ \tilde{Y}_{41} & \hat{Y}_{42} & \hat{Y}_{43} & \hat{Y}_{44} & \tilde{Y}_{45} & \tilde{Y}_{46} \\ \tilde{Y}_{51} & \tilde{Y}_{52} & \tilde{Y}_{53} & \tilde{Y}_{54} & \hat{Y}_{55} & \hat{Y}_{56} \\ \tilde{Y}_{61} & \tilde{Y}_{62} & \tilde{Y}_{63} & \tilde{Y}_{64} & \hat{Y}_{65} & \hat{Y}_{66} \end{bmatrix}$$

Completion 20th

$$\begin{bmatrix} \tilde{Y}_{11} & \tilde{Y}_{12} & \tilde{Y}_{13} & \tilde{Y}_{14} & \tilde{Y}_{15} & \tilde{Y}_{16} \\ \tilde{Y}_{21} & \tilde{Y}_{22} & \tilde{Y}_{23} & \hat{Y}_{24} & \tilde{Y}_{25} & \tilde{Y}_{26} \\ \tilde{Y}_{31} & \tilde{Y}_{32} & \tilde{Y}_{33} & \hat{Y}_{34} & \hat{Y}_{35} & \tilde{Y}_{36} \\ \tilde{Y}_{41} & \hat{Y}_{42} & \hat{Y}_{43} & \hat{Y}_{44} & \tilde{Y}_{45} & \hat{Y}_{46} \\ \tilde{Y}_{51} & \tilde{Y}_{52} & \tilde{Y}_{53} & \tilde{Y}_{54} & \hat{Y}_{55} & \tilde{Y}_{56} \\ \tilde{Y}_{61} & \tilde{Y}_{62} & \tilde{Y}_{63} & \hat{Y}_{64} & \tilde{Y}_{65} & \hat{Y}_{66} \end{bmatrix}$$

Completion 30th

$$\begin{bmatrix} \tilde{Y}_{11} & \hat{Y}_{12} & \hat{Y}_{13} & \tilde{Y}_{14} & \tilde{Y}_{15} & \tilde{Y}_{16} \\ \hat{Y}_{21} & \tilde{Y}_{22} & \hat{Y}_{23} & \tilde{Y}_{24} & \tilde{Y}_{25} & \tilde{Y}_{26} \\ \hat{Y}_{31} & \hat{Y}_{32} & \tilde{Y}_{33} & \hat{Y}_{43} & \tilde{Y}_{35} & \tilde{Y}_{36} \\ \tilde{Y}_{41} & \tilde{Y}_{42} & \hat{Y}_{43} & \hat{Y}_{44} & \tilde{Y}_{45} & \hat{Y}_{46} \\ \tilde{Y}_{51} & \tilde{Y}_{52} & \tilde{Y}_{53} & \tilde{Y}_{54} & \hat{Y}_{55} & \hat{Y}_{56} \\ \tilde{Y}_{61} & \tilde{Y}_{62} & \tilde{Y}_{63} & \hat{Y}_{64} & \hat{Y}_{65} & \hat{Y}_{66} \end{bmatrix}$$

Completion 40th

$$\begin{bmatrix} \tilde{Y}_{11} & \hat{Y}_{12} & \hat{Y}_{13} & \tilde{Y}_{14} & \tilde{Y}_{15} & \tilde{Y}_{16} \\ \hat{Y}_{21} & \tilde{Y}_{22} & \hat{Y}_{23} & \tilde{Y}_{24} & \tilde{Y}_{25} & \tilde{Y}_{26} \\ \hat{Y}_{31} & \hat{Y}_{32} & \tilde{Y}_{33} & \hat{Y}_{43} & \tilde{Y}_{35} & \tilde{Y}_{36} \\ \tilde{Y}_{41} & \tilde{Y}_{42} & \hat{Y}_{43} & \hat{Y}_{44} & \tilde{Y}_{45} & \tilde{Y}_{46} \\ \tilde{Y}_{51} & \tilde{Y}_{52} & \tilde{Y}_{53} & \tilde{Y}_{54} & \hat{Y}_{55} & \hat{Y}_{56} \\ \tilde{Y}_{61} & \tilde{Y}_{62} & \tilde{Y}_{63} & \tilde{Y}_{64} & \hat{Y}_{65} & \hat{Y}_{66} \end{bmatrix}$$

Figure 46 – Passive models derived with PPMPAA and CBPE.

These four models are then compared with the RPD and PRL algorithms and the errors achieved by each algorithm are summarized in Figure (47). Despite having been unambiguously better, the CBPE also demonstrated monotonic error decrease with increasing order.

The increased accuracy however has come at a cost: in terms of runtime the CBPE has been unambiguously worse than the competing algorithms as depicted in Figure (48). This should be no surprise given the combinatorial nature of the passivity assessment performed by the PPMPAA and also the convex problem solved by the CBPE algorithm which becomes increasingly constrained the higher the number of specified entries.

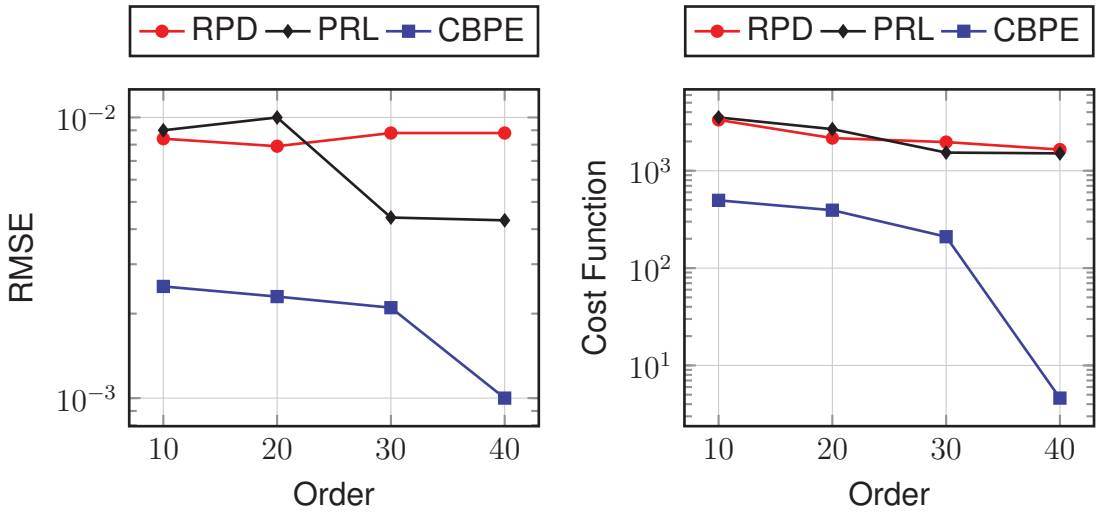

Figure 47 – Error relative to unconstrained VF: the RMSE and Cost Function.

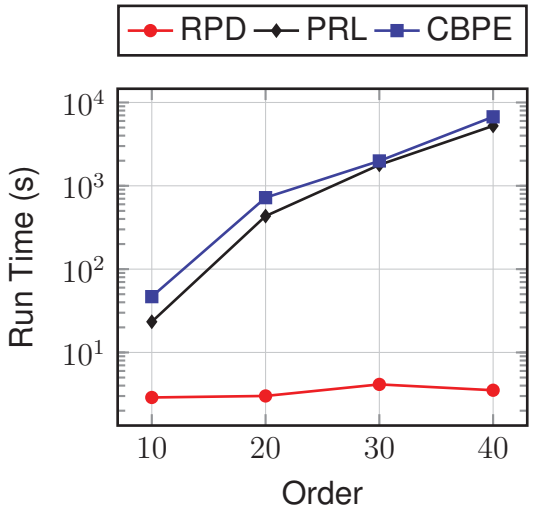

Figure 48 – Run Time for passivity enforcement.

The cost function error can be expanded out entry-wise as recorded in Table (5), for order 30 which resulted in the smallest number of subsystems requiring completion. Zero error entries indicate subsystems inherited from the original unconstrained model and kept as known parameters for the completion. This table not only confirms what the right panel in Figure (47) had already established for the overall error performance giving the CBPE unambiguously edge over competing algorithms but also showing that while algorithms RPD and PRL tend to spread the compensation across all subsystems somewhat uniformily, the CBPE concentrated compensations along the diagonal entries that required the initial scalar enforcement. The latter is preferable because compensations across off-diagonals cause larger distortions of the mutual inductances as they are smaller in magnitude, *i.e.* the diagonal subsystems corresponding to self-inductances can better absorb the impact of compensations. The RPD achieved the best fit only for the three higher voltage windings at cost degrading the mutuals.

Table 5 – Entry-wise Cost Function for passive 30th order models.

Entry-wise Cost Function $(\times 10^{+2})$												
	RPD 30th						CBPE 30th					
	(H_1)	(H_2)	(H_3)	(L_1)	(L_2)	(L_3)	(H_1)	(H_2)	(H_3)	(L_1)	(L_2)	(L_3)
(H_1)	0.1489	0.7532	0.7426	0.1548	1.5820	1.9129	0.6179	0	0	0.0351	0.0001	0.0002
(H_2)	0.7532	0.1572	0.4375	4.5349	0.1554	1.6184	0	0.5857	0	0.0004	0.0476	0.0003
(H_3)	0.7426	0.4375	0.1702	1.9791	2.6002	0.1746	0	0	0.7347	0	0.0002	0.0369
(L_1)	0.1548	4.5349	1.9791	0.1418	0.5252	1.1424	0.0351	0.0004	0	0	0.0413	0
(L_2)	1.5820	0.1554	2.6002	0.5252	0.1474	0.4670	0.0001	0.0476	0.0002	0.0413	0	0
(L_3)	1.9129	1.6184	0.1746	1.1424	0.4670	0.1597	0.0002	0.0003	0.0369	0	0	0
	PRL 30th						CBPE 30th					
	(H_1)	(H_2)	(H_3)	(L_1)	(L_2)	(L_3)	(H_1)	(H_2)	(H_3)	(L_1)	(L_2)	(L_3)
(H_1)	0.0630	2.2741	2.3880	0.1762	1.0266	1.0205	0.6179	0	0	0.0351	0.0001	0.0002
(H_2)	2.2741	0.0724	1.8036	0.9326	0.1973	1.1703	0	0.5857	0	0.0004	0.0476	0.0003
(H_3)	2.3880	1.8036	0.0794	1.0813	0.9093	0.1914	0	0	0.7347	0	0.0002	0.0369
(L_1)	0.1762	0.9326	1.0813	0.0669	0.4940	0.7953	0.0351	0.0004	0	0	0.0413	0
(L_2)	1.0266	0.1973	0.9093	0.4940	0.0892	0.4564	0.0001	0.0476	0.0002	0.0413	0	0
(L_3)	1.0205	1.1703	0.1914	0.7953	0.4564	0.0824	0.0002	0.0003	0.0369	0	0	0

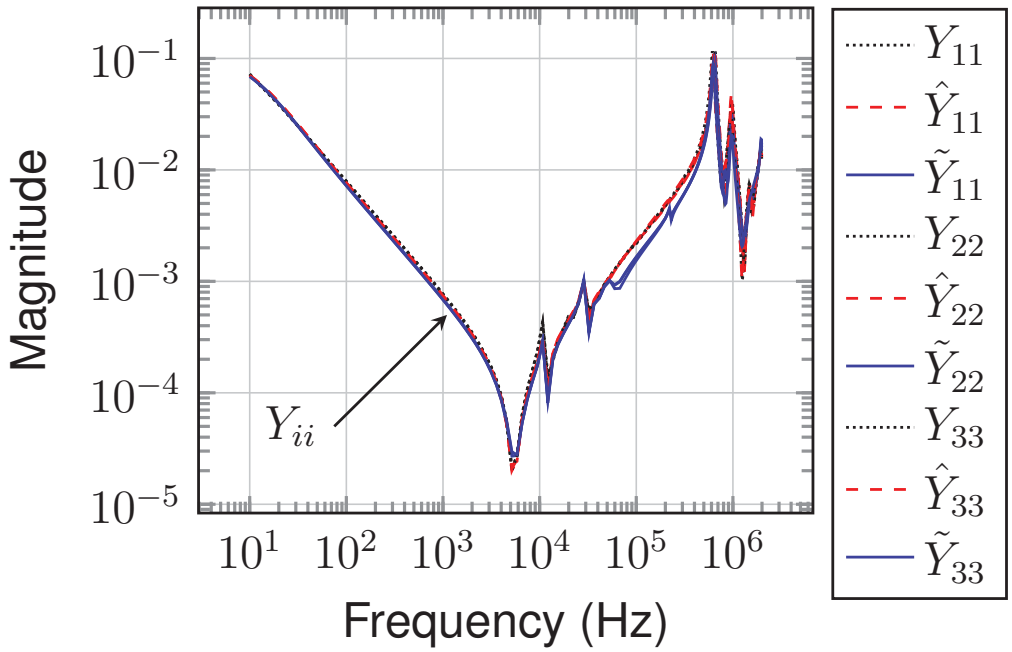

Figure 49 – Admittance Magnitude: diagonal subsystems.

A pictorial view of the data, VF model (30th) and passive CBPE model (30th) is given in Figures (49) and (50), for the first three diagonal subsystems[52] that required enforcement and the off-diagonal subsystems $\tilde{Y}_{41}$, $\tilde{Y}_{52}$ and $\tilde{Y}_{63}$[53], respectively. The notation Y_{ii} in Figure (49) and Y_{ij} in Figure (50) is meant to suggest that these curves differ by negligible[54] amount so that the difference between them is difficult to discern.

[52] Corresponding to the higher-voltage winding's self-inductances.

[53] These subsystems lie along the diagonal within the 2-1 block matrix coupling higher to lower voltages.

[54] Negligible refers to the fact the measurements Y_{11}, Y_{22} and Y_{33} almost exactly overlay a feature that is passed over to the models thus conveying the erroneous impression that some curves are missing, but they are not and each graph portrays nine curves just as the legend announces.

The pattern for the remaining subsystems not depicted in the plots should be clear: all subsystems whose positions in Table (5) hold a zero error have admittances exactly the same as the unconstrained VF model so that their curves would be simply repeated in the plots. The remaining non-zero errors omitted from the graphs have differences appearing only in the fourth decimal places, which is nearly indiscernible.

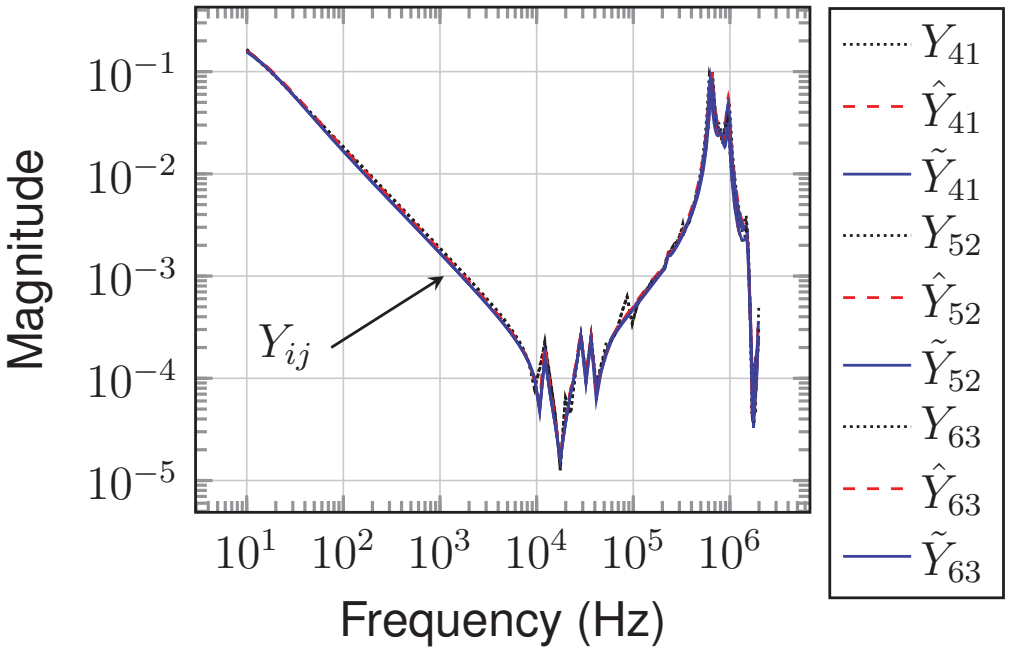

Figure 50 – Admittance Magnitude: off-diagonal subsystems.

5.6 Discussion

This chapter has essentially combined all theoretical developements presented earlier into two algorithms that together form the Passivity Enforcement using the positive (semi-)definite completion approach. Besides establishing the logical connections that constitute the mathematical underpinnings of the proposed algorithms two case studies were used to showcase them and illustrate how they compare with existing algorithms. The analysis revealed that fit is not the only measure for judging whether a model is appropriate since other intrinsic properties vary considerably with order, *e.g.* the location and magnitude of the most negative eigenvalue. These considerations should be taken into account.

The completion approach is philosophically different from other existing algorithms in the sense that it thrives whenever a large number of parameters from the original unconstrained VF realization can be kept and thus inherited to the ultimately passive realization. This is in contrast with other existing approaches which either take the unconstrained VF realization as a starting point to be perturbed or compute all

parameters anew, both under passivity constraints, amortizing the impact across the entire system.

The formulation adopted for the completion approach relies on automatic chordal correspondence between cones which are less general than the author had originally envisioned to the extent that it is realization-dependent: not all realizations result in a chordal pattern, *e.g.* the orthonormal vector fitting realization. Other realizations exist which must be tested by means of the MCS algorithm to verify chordality.

There are some perils the CBPE algorithm could potentially run into when trying to identify a partial positive matrix, *e.g.* both the data and unconstrained model could be sprinkled with violating subsystems, all containing large passivity violations. In particular, large passivity violations for the scalar diagonal subsystems can cause the algorithm to fail should these violations prove impossible to remove. Furthermore, positive clique distributions are also system-dependent and can happen unfavorably. An example of an unfavorable clique distribution is as follows:

$$\begin{bmatrix} \tilde{Y}_{11} & ? & ? & ? & ? & ? \\ ? & \tilde{Y}_{22} & ? & ? & ? & ? \\ ? & ? & \tilde{Y}_{33} & ? & ? & ? \\ ? & ? & ? & \tilde{Y}_{44} & ? & ? \\ ? & ? & ? & ? & \tilde{Y}_{55} & ? \\ ? & ? & ? & ? & ? & \tilde{Y}_{66} \end{bmatrix}.$$

This illustrates a system for which none of the subsystems along the diagonal were originally passive as derived by the VF algorithm thus requiring the enforcement. Contrary to examples presented earlier, the scalar enforcement has not caused any other $\hat{Y}_{ij}$ to build into larger positive cliques. Such factors can adversely affect the end result and success is ultimately determined by the vagaries of the system. Nevetheless, this also happens to be the case for other methods.

6 CHORDAL DECOMPOSITION PASSIVITY ENFORCEMENT

In this chapter a particular chordal sparsity pattern resurfaces under a trifle different purpose, namely computational efficiency. The idea is to reduce the number of problem variables by imposing a banded sparsity pattern on the Lyapunov Quadratic Function associated with the Positive-Real Lemma. This estructure is embedded in the Chordal Decomposition Passivity Enforcement algorithm and tested with empirical data.

6.1 Banded Matrices

This preliminary section introduces some basic terminology and notation for the Chordal Decomposition Passivity Enforcement Problem. The chief idea behind the proposed strategy entails the imposition of sparsity patterns to reduce the computational burden required by the auxiliary variables introduced with the Lyapunov Equation embedded in the Positive-Real Lemma passivity constraints. The particular kind of sparsity employed requires the notion of banded matrices. According to (GOLUB; LOAN, 2012; MEYER, 2000; HORN; JOHNSON, 2012):

Definition 47 *Let* ***P*** *be an* $n \times n$ *matrix*[1]*, then* ***P*** *is called a* ***band matrix, banded matrix*** *or a matrix with* ***banded sparsity pattern*** *whenever* $\mid i - j \mid > w$ *with* $w \in \mathbb{Z}^+$ *implies* $P_{ij} = 0$[2]*. Parameter* w *is denoted the bandwidth.*

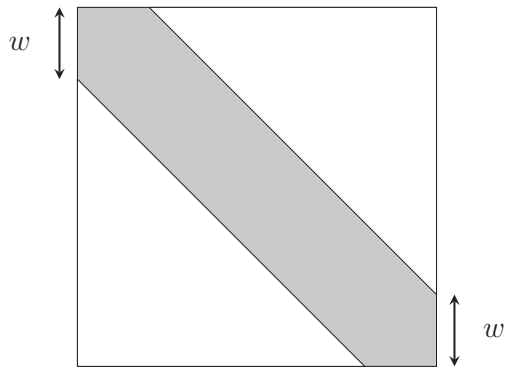

Figure 51 – Banded Matrix with bandwidth w.

According to Definition (47), all nonzero entries of **P** are constrained to reside along the *main diagonal*, the *upperdiagonals* and the *lowerdiagonals*[3]. Upperdiagonals and lowerdiagonals are all nonzero entries P_{ij} such that $i \neq j$[4] with $j - i \leq w$ and $i - j \leq w$

[1] The entries of this matrix could be real or complex numbers.
[2] These are syntatic zeros, *i.e.* these entries have zero value by fiat.
[3] Some authors apply the superdiagonal and subdiagonal terminologies.
[4] Excluding the entries along the main diagonal.

respectively[5]. Figure (51) exemplifies a general banded matrix with bandwidth w. Trivial examples are tridiagonal matrices and diagonal matrices for which the bandwidths are respectively $w = 1$ and $w = 0$. Below is a 6×6 banded matrix with bandwidth $w = 2$ whereby the upper and lower diagonals are denoted U_{ij}^k and L_{ij}^k such that subscripts are the indices for rows and columns while superscript $k \leq n - 1$ especifies the shift relative to the main diagonal:

$$\mathbf{P} = \begin{bmatrix} P_{11} & P_{12} & P_{13} & P_{14} & P_{15} & P_{16} \\ P_{21} & P_{22} & P_{23} & P_{24} & P_{25} & P_{26} \\ P_{31} & P_{32} & P_{33} & P_{34} & P_{35} & P_{36} \\ P_{41} & P_{42} & P_{43} & P_{44} & P_{45} & P_{46} \\ P_{51} & P_{52} & P_{53} & P_{54} & P_{55} & P_{56} \\ P_{61} & P_{62} & P_{63} & P_{64} & P_{65} & P_{66} \end{bmatrix} = \begin{bmatrix} D_{11} & U_{12}^1 & U_{13}^2 & 0 & 0 & 0 \\ L_{21}^1 & D_{22} & U_{23}^1 & U_{24}^2 & 0 & 0 \\ L_{31}^2 & L_{32}^1 & D_{33} & U_{34}^1 & U_{35}^2 & 0 \\ 0 & L_{42}^2 & L_{43}^1 & D_{44} & U_{45}^1 & U_{46}^2 \\ 0 & 0 & L_{53}^2 & L_{54}^1 & D_{55} & U_{56}^1 \\ 0 & 0 & 0 & L_{64}^2 & L_{65}^1 & D_{66} \end{bmatrix}.$$

The higher the bandwidth the less sparse the matrix and a full matrix P has at most $n - 1$ upper and $n - 1$ lower diagonals. The lowerdiagonals, main diagonal and upperdiagonals for the foregoing matrix **P** correspond to the following vectors:

$$L^2 = \begin{bmatrix} L_{31}^2 \\ L_{42}^2 \\ L_{53}^2 \\ L_{64}^2 \end{bmatrix}, \quad L^1 = \begin{bmatrix} L_{21}^1 \\ L_{32}^1 \\ L_{43}^1 \\ L_{54}^1 \\ L_{65}^1 \end{bmatrix}, \quad D = \begin{bmatrix} D_{11} \\ D_{22} \\ D_{33} \\ D_{44} \\ D_{55} \\ D_{66} \end{bmatrix}, \quad U^1 = \begin{bmatrix} U_{12}^1 \\ U_{23}^1 \\ U_{34}^1 \\ U_{45}^1 \\ U_{56}^1 \end{bmatrix}, \quad U^2 = \begin{bmatrix} U_{13}^2 \\ U_{24}^2 \\ U_{35}^2 \\ U_{46}^2 \end{bmatrix}.$$

Should the matrix **P** be endowed with additional properties, *e.g.* positive (semi)definiteness, further properties become immediately exploitable such as the fact that it must be diagonally dominant and symmetric. These features can be visualized in more detail using Figure (52) which reveals the expected pattern for the example banded matrix: (i) diagonally dominant, (ii) $\|L^1\|$=$\|U^1\|$, (iii) $\|L^2\|$=$\|U^2\|$ and (iv) $\|L^k\|$=$\|U^k\| = 0$ for $k > w$.

Even though the actual values[6] vary from problem to problem, the pattern is clear: a banded positive (semi-)definite matrix concentrates its meaningful values around the main diagonal which is normalized for convenience, the left and right panels illustrate a strictly monotonic and non-strictly monotonic decrease of norm values with respect to width. This can be used to approximate a full positive definite matrix to a banded one whenever norms vanish for some $k > w$, with w as the approximation parameter.

[5] Nonsquare matrices can have different lower and upper bandwidths. This research deals only with square matrices though.

[6] Values depicted in Figure (52) are arbitrary.

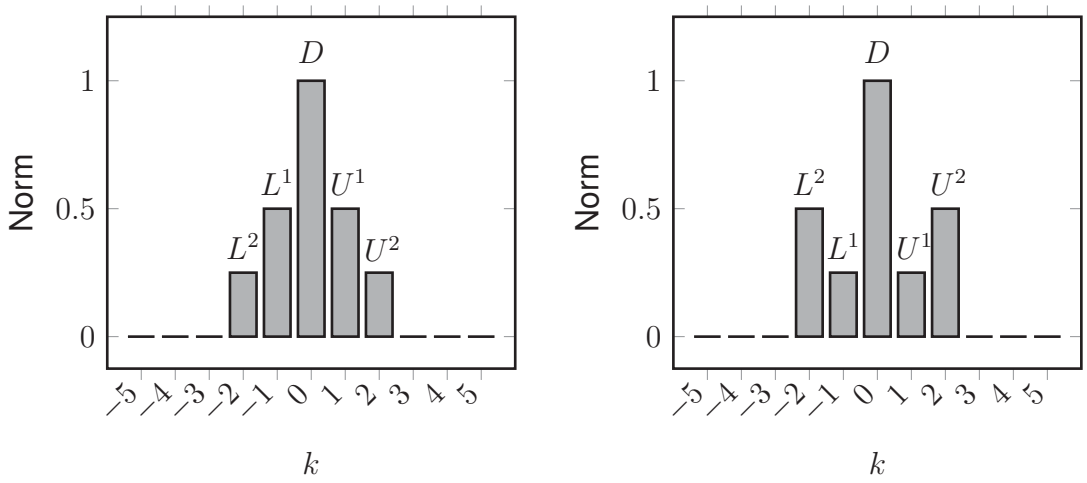

Figure 52 – Histogram of norm values for the banded $\mathbf{P}_{6\times6}$ example matrix as a function of parameter k, negative values were adopted as a convention for lowerdiagonals.

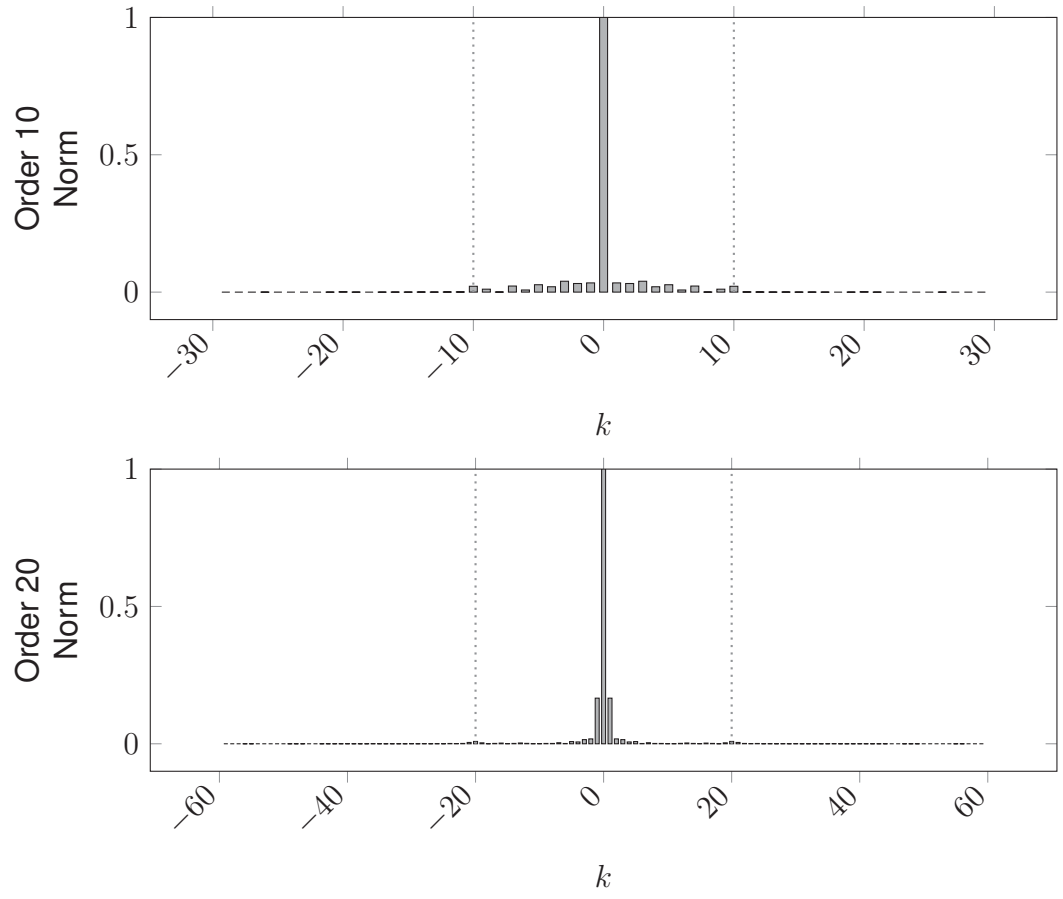

Figure 53 – IVT: Histogram of norm values as a function of k for the full matrix **P** associated with the Lyapunov function obtained as solution to the PRL LMI.

The logic behind that reasoning can be substantiated by empirical evidence derived from the Histogram of norm values for the solution **P** to linear quadratic storage function (LQ-Lyapunov) obtained with the PRL algorithm. The quadratic storage

function is parametrized by a coefficient matrix **P** with dimensions determined by the user-assigned dynamic order n and the number of ports p, therefore a $(np) \times (np)$ matrix. Figure (53) shows the underlying pattern of solutions for both orders 10 and 20 considering the IVT 3-port system presented in the preceeding chapter, Subsection (5.5.1).

The aforementioned figure demonstrates the matrix **P** to be nearly banded in the sense that norm values precipitously fall after a given width w. Such width can be understood as a measure of how the internal energy is exchanged between neighbouring ports and their associated dynamic modes. This particular pattern is a consequence of how the realization is built (2.4.1) and how the positive cliques are distributed. The vertical dotted lines mark the widths corresponding to the number of lower and upper diagonals accounting for most of the internal energy coupling associated with the Lyapunov storage function $V(\mathbf{x}(t)) = \mathbf{x}^T\mathbf{P}\mathbf{x}$.

Figure (54) contains the positive clique distributions for the unconstrained models before the PRL enforcement generated the storage function analyzed in the histogram. It indicates that the dynamic modes in disagreement with a dissipative behavior are precisely those associated with the diagonal subsystem corresponding to the first port[7] whose scalar localized[8] enforcement had caused the system to be passive using the completion approach, thus corroborating the pattern consisting of a highly concentrated solution for widths 10 and 20. Since the remaining ports[9] were already consistent with a dissipative behavior, the energy exchange among the states are progressively less coupled as the width increases. In this particular respect, Figures (53) and (54) are correlated. This correlation is the key to decide what width to assign as a good approximation for a faster passivity enforcement since the histograms requires the solution of traditional full-sized problem while the clique distributions can be readily obtained the PPMPAA, the earlier constitutes a hard enforcement problem whereas the latter a much simpler assessment problem.

VF 10th

$$\begin{bmatrix} - & - & - \\ - & \hat{Y}_{22} & - \\ - & - & \hat{Y}_{33} \end{bmatrix}$$

VF 20th

$$\begin{bmatrix} - & - & - \\ - & \hat{Y}_{22} & - \\ - & - & \hat{Y}_{33} \end{bmatrix}$$

Figure 54 – IVT: Positive Clique Distributions for the unconstrained VF models as determined by the PPMPA.

The same ideas also apply to the power transformer analyzed back in Subsection (5.5.2) which furnishes a more complex coupling structure given its higher port number.

[7] High-voltage port.
[8] This means uncoupled with neighbouring subsystems
[9] Lower-voltage ports.

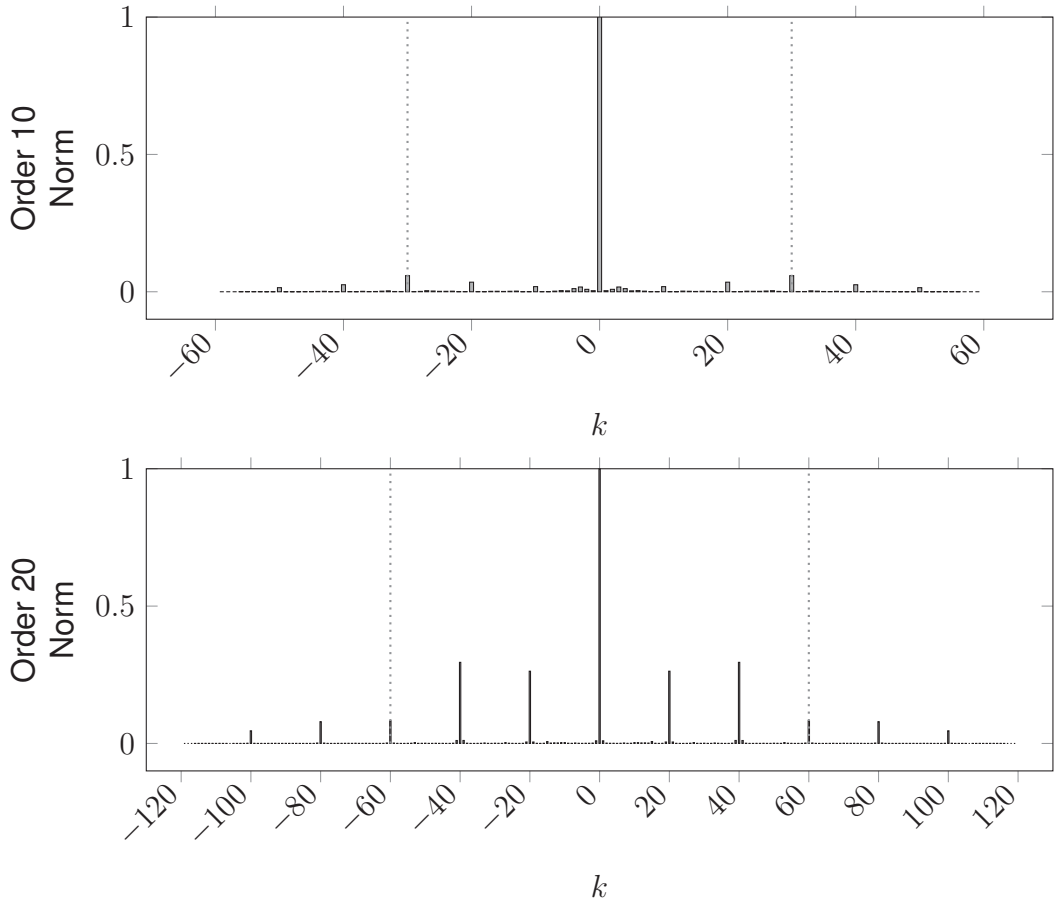

Figure 55 – Power Transformer: Histogram of norm values as a function of k for the full coefficient matrix **P** associated with the Lyapunov function obtained as a solution to the PRL passivity enforcement.

Recalling that this $6-$port power transformer had more violations interspersed with passive blocks, the histogram of norms shows a slightly more scattered pattern as seen in Figure (55). The dotted lines now advance away from the diagonal as far as three times the dynamic order in agreement with the first three violating diagonal subsystems, shown in Figure (56).

VF 10th

$$\begin{bmatrix} - & - & - & - & - & - \\ - & - & - & - & - & - \\ - & - & - & - & - & - \\ - & - & - & \hat{Y}_{44} & \hat{Y}_{45} & - \\ - & - & - & \hat{Y}_{54} & \hat{Y}_{55} & \hat{Y}_{56} \\ - & - & - & - & \hat{Y}_{65} & \hat{Y}_{66} \end{bmatrix}$$

VF 20th

$$\begin{bmatrix} - & - & - & - & - & - \\ - & - & - & - & - & - \\ - & - & - & - & - & - \\ - & - & - & \hat{Y}_{44} & - & \hat{Y}_{46} \\ - & - & - & - & \hat{Y}_{55} & - \\ - & - & - & \hat{Y}_{64} & - & \hat{Y}_{66} \end{bmatrix}$$

Figure 56 – Power Transformer: Positive Clique Distributions for the unconstrained VF models as determined by the PPMPA.

6.2 CDPE

The Positive-Real Lemma passivity constraints defined in Subsection (2.2.1) prompt its the convex formulation (see Subsection (4.3.1)) to scale rapidly with both dynamic order and port number since the Quadratic Lyapunov Function embedded into the PRL-LMI is treated as an auxiliary variable whose values are usually not retrieved after a passive solution is found. However worthy it is, the standard procedure is not to be concerned with what exact values the entries of matrix **P** have as long as **P** be positive-definite and the PRL thus satisfied. According to the analysis in the preceeding Section (6.1), there exists a concealed structure embedded in the coefficient matrix **P** which can be fruitfully exploited.

The strategy entails imposing a banded structure to the quadratic Lyapunov Coefficient matrix **P** by truncating the width number w. Instead of using a Linear Quadratic Lyapunov Function we proposed the use of banded LQ function. The rationale is to reduce the number of auxiliary variables by constraining most of the entries in **P** to be zero. Not only the number of variables is reduced but also the PRL-LMI acquires an arrow sparsity pattern which is chordal. The question of what the entries in the solution to the Lyapunov equation are and how they are distributed is subtle, but imposing an structure that nearly approximates what is found in practice has very important practical consequences, as we will be shown shortly.

According to (VANDENBERGHE; ANDERSEN, 2015), while standard LP and conic form convex problem have much in common, they differ significantly when it comes to exploiting sparsity. The first benefits largely from well-established methods from numerical linear algebra whereas the second does not, except when the sparsity pattern of the aggregate is chordal.

To achieve an aggregate chordal sparsity pattern we propose a reformulation of the PRL enforcement that results an overall chordal pattern for the problem coefficients. We begin by recapitulating a original formulation as presented in Subsection (4.3.1), the main optimization problem is a follows:

$$
\begin{aligned}
\text{minimize} \quad & t(\mathbf{C}, \mathbf{D}, \mathbf{P}) \\
\text{subject to} \quad & \begin{bmatrix} -\mathbf{A}^T\mathbf{P} - \mathbf{P}\mathbf{A} & -\mathbf{P}\mathbf{B} + \mathbf{C}^T \\ -\mathbf{B}^T\mathbf{P} + \mathbf{C} & \mathbf{D}^T + \mathbf{D} \end{bmatrix} \succeq 0 \\
& \mathbf{P} \succeq 0 \\
& \left.\begin{array}{c} \mathbf{E}_{ij}^T\mathbf{E}_{ij} + \delta_{ij}^2 \leq t_{ij} \\ t \geq 0 \\ t_{ij} \leq t \end{array}\right| 1 \leq i,j \leq n
\end{aligned}
$$

which is Equation (4.37) simply repeated for convinience. Careful parsing reveals that this problem consists of two SDP blocks and $\frac{P(P+1)}{2}$[10] SOCP blocks. The SDP blocks correspond to the PRL LMI and the LQ Lyapunov Storage Function, the SOCPs account for the cost function as applied to each individual subsystem $\mathbf{Y}_{ij}(s)$. By constraining the Lyapunov Variable to be banded with bandwidth w, both SDP blocks are chordal: the PRL-LMI becomes block-arrow and $\mathbf{P}$ banded.

Recalling Section (3.2), SDP encompasses LPs, QPs and SOCPs which can be embedded into SDP blocks, the so-called SDP-embeddeding, as follows:

SOCP		**Equivalent SDP**	
minimize	t	minimize	t
subject to	$\|\mathbf{E}_{ij}x + \delta_{ij}^2\|_2 \leq t$	subject to	$\begin{bmatrix} \mathbf{I} & \left(\mathbf{E}_{ij}x + \delta_{ij}^2\right) \\ \left(\mathbf{E}_{ij}x + \delta_{ij}^2\right)^T & t^2 \end{bmatrix} \succeq 0.$

This SDP embedding accounting the error for each $\mathbf{Y}_{ij}(s)$ also has a block-arrow sparsity pattern, they can then be stacked into a single larger arrow-block SDP. Therefore, the problem acquires the following form:

$$\begin{aligned} \text{minimize} \quad & t(\mathbf{C}, \mathbf{D}, \mathbf{P}) \\ \text{subject to} \quad & \begin{bmatrix} -\mathbf{A}^T\mathbf{P} - \mathbf{P}\mathbf{A} & -\mathbf{P}\mathbf{B} + \mathbf{C}^T \\ -\mathbf{B}^T\mathbf{P} + \mathbf{C} & \mathbf{D}^T + \mathbf{D} \end{bmatrix} \succeq 0 \\ & \mathbf{P} \succeq 0 \\ & \begin{bmatrix} \mathbf{I} & \left(\mathbf{E}(\mathbf{C}, \mathbf{D}) + \Delta\right) \\ \left(\mathbf{E}(\mathbf{C}, \mathbf{D}) + \Delta\right)^T & t^2\mathbf{I} \end{bmatrix} \succeq 0, \end{aligned} \tag{6.1}$$

with Δ a diagonal matrix containing each δ_{ij}^2. Equation (6.1) comprises three SDP blocks, all chordal and one is entitled to say the problem has an aggregate chordal sparsity pattern. Lumping all unknown state-space parameters into a single vector variable θ and writing this problem in standard epigraph form, we get:

$$\begin{aligned} \text{minimize} \quad & t(\theta, \mathbf{P}) \\ \text{subject to} \quad & \mathcal{M}_1(\theta, \mathbf{P}) \succeq 0 \\ & \mathcal{M}_2(\theta) \succeq 0 \\ & \mathbf{P} \succeq 0. \end{aligned} \tag{6.2}$$

This problem can be solved with SparseCoLO, a package for specifying and solving chordal conic linear convex programs (FUJISAWA et al., 2009) with core solver

[10] Assuming a symmetric transfer matrix.

SEDUMI (STURM, 1999). The reason for passing the problem (6.2) in conic form to SparseCoLO is precisely that exploiting sparsity for SOCPs and SDP is not as trivial as it is for LPs and QPs. SparseCoLO applies the chordal conversion method proposed by (FUKUDA et al., 2001) and implemented in (FUJISAWA et al., 2009), thus enabling the core solver to achieved increased performance by exploiting chordal sparsity.

6.3 Case Studies Revisited

The CDPE algorithm is now applied as a passivity enforcement method to the data sets used in the previous chapter to see how the proposed method performs in practice. The analysis aims at evaluating the impact the varying bandwidths can have on both run time and degree of accuracy and it should similar in presentation to the earlier version in which the completion algorithm was used.

6.3.1 Inductive Voltage Transformer - Revisited

The IVT consists of a three port device whose admittance parameters were collected over 1141 frequency samples logarithmically spaced in the interval 20Hz-10MHz. The dynamic modes were identified by means of standard VF algorithm for varying order within the range $\{10, 20, 30, 40\}$ in increasing steps of 10. Taking the histogram depicted in Figure (53) and concentrating the analysis on order 20, a passive model for this specific order is obtained with the CDPE for bandwidths in the sequence $\{1, 5, 10, 15, 20, 60\}$. The simplest case $w = 1$ corresponds to a tridiagonal positive-definite Lyapunov Function and the remaining widths account for higher bandwiths up to full width corresponding to the regular PRL solution.

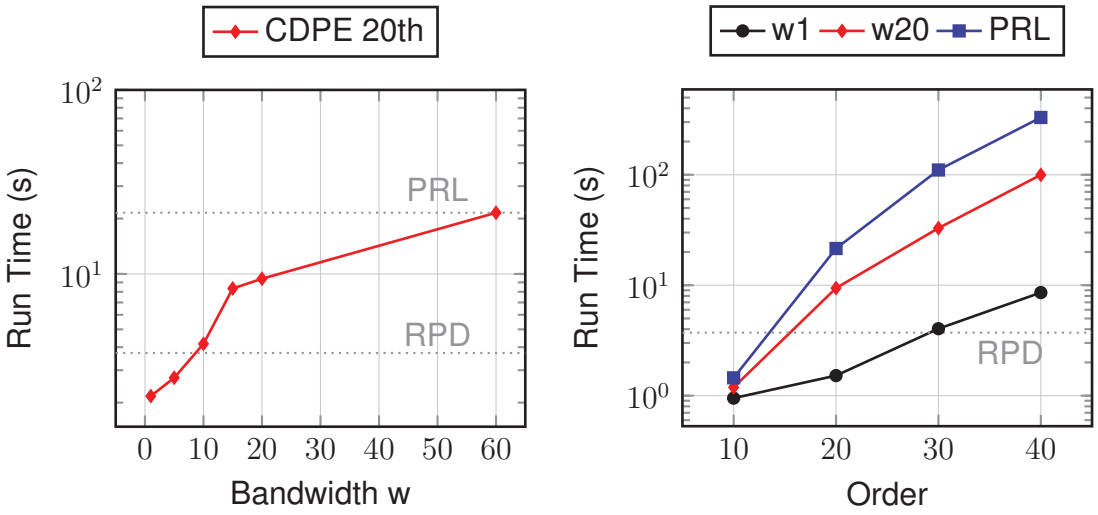

Figure 57 – IVT: Width effect over run time for fixed and varying orders.

The analysis in Section (6.1) reveals the threshold value for width to be 20[11]. The

[11] This might get confusing since the model order is also 20, thus this note of caution.

left panel in Figure (57) shows how the run time surge as parameter w increases from the tridiagonal case to the full width. Horizontal lines indicate the times obtained for the RPD and PRL algorithms. As expected the CDPE algorithm and PRL coincide for full width since the PRL-LMI is no longer sparse chordal. For width as low as 10 the CDPE has very competitive run times, similar to the RPD algorithm. Shifting the attention to the right panel in Figure (57), the plot contains both the width and order effect in the same picture to give a perspective on the combined effect of these two model parameters. The uppermost curve gives the run times for the PRL algorithmm the mid-height curve indicates the recommended threshold and the tridiagonal is represented as the lowest curve. Dotted horizontal lines give the average run time for the RPD in comparison. The bottom line is that the lower the width the faster a solution is found.

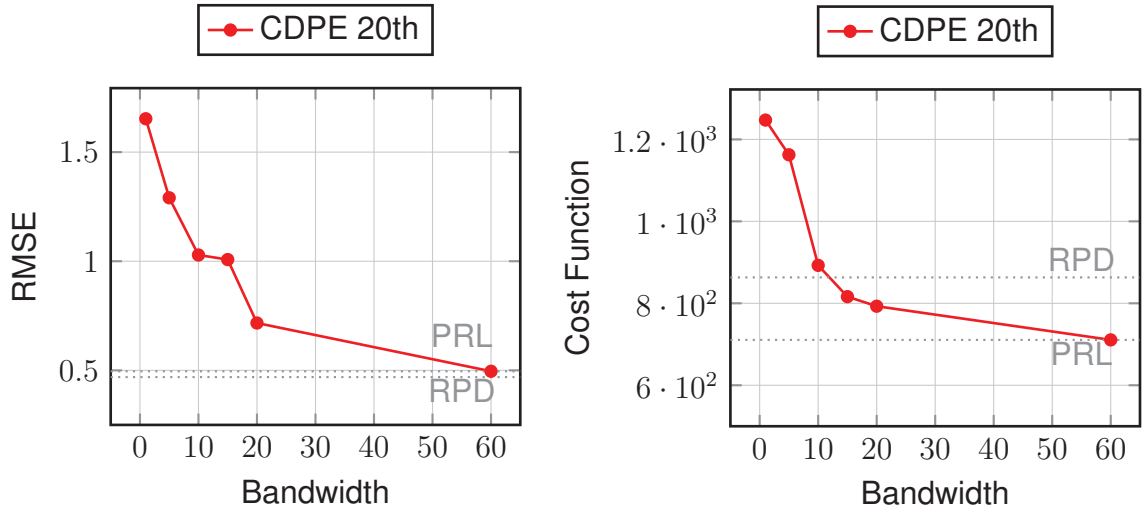

Figure 58 – IVT: RMSE and Cost Function values for varying widths.

On the other hand, the faster a solution is found the worst the approximation. This regrettable claim is substantiated by Figure (58). Nonetheless, this figure also indicates that the threshold width is a somewhat good compromise in terms accuracy loss and run time reduction in so long as they achieved competitive performance relative to the other algorithms.

A more qualitative perspective on the impact varying widths have on the approximation misfit can be visualized in Figure (59). This picture is a close-up of the main resonance for the Y_{11} subsystem and it reinforces the assumption about the threshold value for width given its nearly overlapping fit with the full width solution. The reason for adopting a close-up view to subsidize this qualitative discussion is that these nuances are hardly noticeable from a broader scale, *i.e.* even though the errors differ, the curves are all near each other.

As for the other widths, despite the approximation being evidently less accurate, the main outline has been preserved: the resonance frequency has not been displaced

but only slightly attenuated. This pattern is reproduced for dynamic orders other than 20. The threshold value 20 is a connected with the norm values obtained for the histogram for the full width solution and gives an approximation number by truncating the number of lower and upperdiagonals associated with the Lyapunov Storage Function.

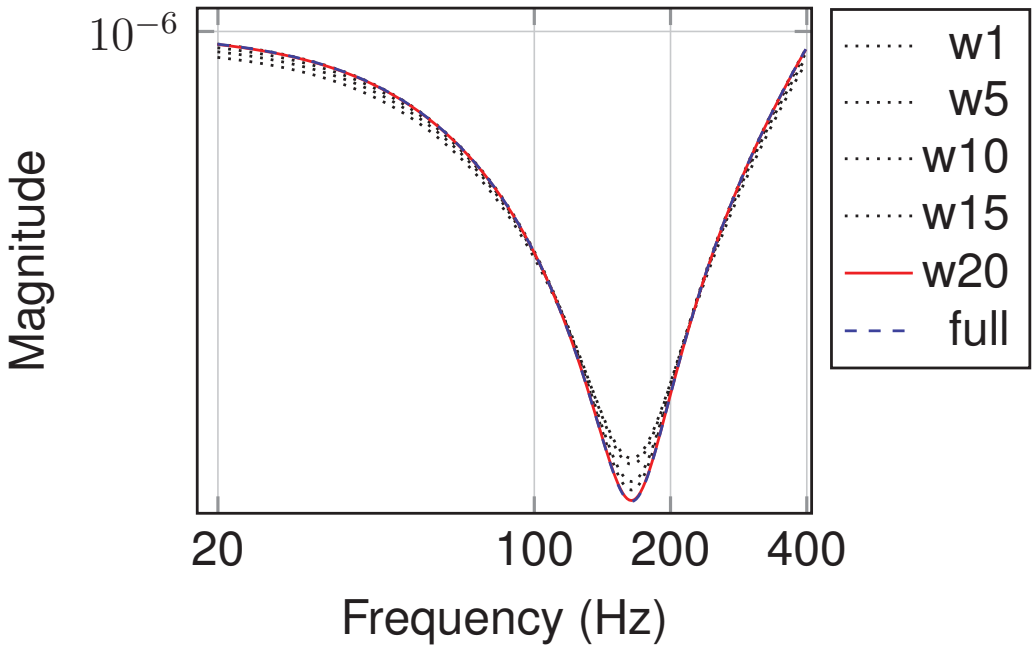

Figure 59 – Y_{11} main resonance as a function of w.

6.3.2 Power Transformer - Revisited

The power transformer consists of a six port device whose admittance parameters were collected over 600 frequency samples logarithmically spaced in the interval 10Hz-2MHz. The dynamic modes were identified by means of standard VF algorithm for varying order within the range $\{10, 20, 30, 40\}$ in increasing steps of 10. Taking the histogram depicted in Figure (55) and concentrating the analysis on order 20, a passive model for this specific order is obtained with the CDPE for bandwidths in the sequence $\{1, 20, 40, 60, 120\}$. Again, case $w = 1$ corresponds to a tridiagonal positive-definite Lyapunov Function and the remaining widths account for higher bandwiths up to full width corresponding to the regular PRL solution.

Recalling Section (6.1), specifically Figures (55) and (56), the threshold value for width was 60. Similarly, the left panel in Figure (60) shows how the run time surge as parameter w increases from the tridiagonal case to the full width. Horizontal lines indicate the times obtained for the RPD and PRL algorithms. As expected the CDPE algorithm and PRL coincide for full width since the PRL-LMI is no longer sparse chordal.

For this higher port system the width seems to have played a lesser role in dimisnishing the run times as compared to the preceeding example. Nevetheless, the

tridiagonal case, $w = 1$, still attains a competitive run tine relative the RPD algorithm. The threshold value however nearly approximates the full width PRL performance. The right panel confirms this trend by including the effect of varying orders. The uppermost curve gives the run times for the PRL algorithmm the mid-height curve indicates the recommended threshold and the tridiagonal is represented as the lowest curve, the latter obtaining similar results to the mean time for the RPD algorithm.

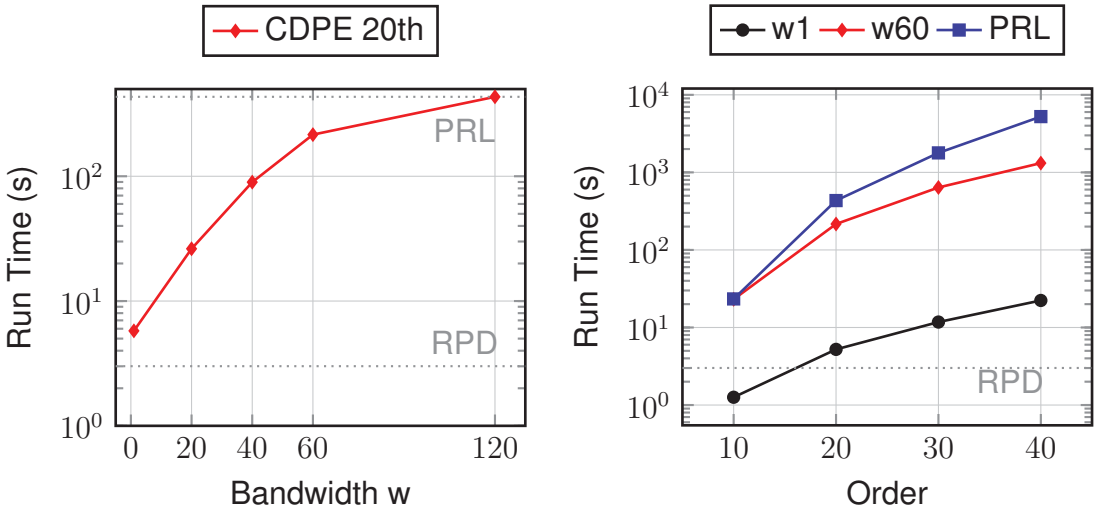

Figure 60 – Width effect over run time for fixed and varying orders.

As depicted in Figure (61), the error behavior shows a pattern equivalent to the one observed in the previous example: there exist a tendency towards increased accuracy as the width number increases. Something to be noted relative to the previous example is the higher trade-off between run time and approximation error for higher port number, since the threshold width has significantly increased the run time while nearly achieving the same error performance as the full width model.

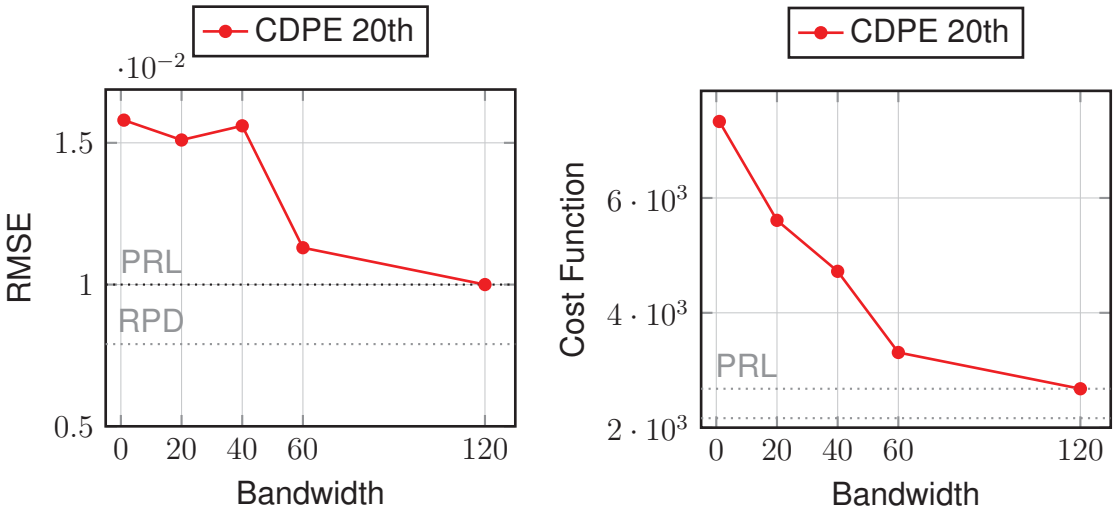

Figure 61 – Power Transformer: RMSE and Cost Function values for varying widths.

The qualitative impact of varying widths on the approximation misfit can be visualized in Figure (62), a close-up of the main resonance for the Y_{11} subsystem. Again, the main resonance frequency has been preserved while significantly attenuated for the lower widths.

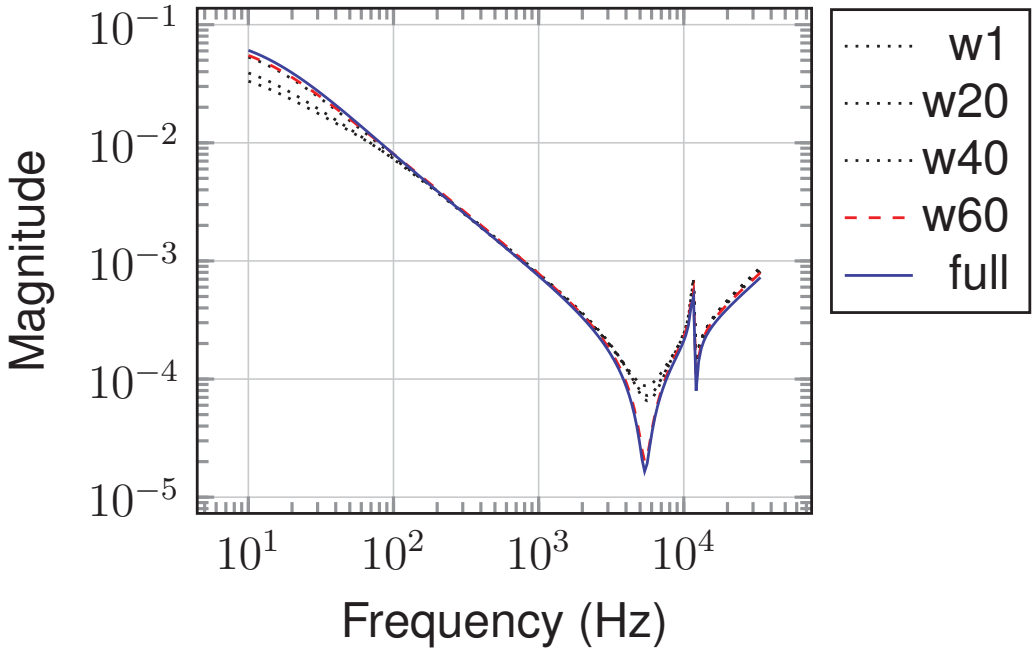

Figure 62 – Y_{11} main resonance as a function of w.

6.4 Discussion

The central idea behind the formulation of an algorithm such as the CDPE is to concentrate on methods that can exploit problem structure, such as sparsity, to gain efficiency. As it stands, the CDPE algorithm seems to be bounded by a trade-off between accuracy and efficiency the more efficient, the less accurate. Another possible cause for decreased accuracy due to the chordal conversion applied by (FUJISAWA et al., 2009) is pointed out in (RAGHUNATHAN; KNYAZEV, 2016): the SDP decomposition results in the schur-complement matrix of the Interior-Point Solvers achieving higher condition number as compared with the original SDP formulation.

Progress however might reside in optimizing over the lower and upper diagonals. Instead of choosing a fixed width for which all lower and upper diagonal are included, a better alternative might be to choose only the few pairs up to the width w that have relevance as measured by norm value, or perhaps some other criteria. The difficulty lies in deciding *a priori* without the histograms which diagonals to consider so as to optimally choose the diagonals to be retained as part of the Lyapunov Storage Function. This indicates a sparser solution with alternating diagonals is one possible strategy to break the stalemate.

7 CONCLUSIONS AND PERSPECTIVES

In summary, we have presented three algorithms, namely the PPMPA, the CBPE and the CDPE, for both the passivity assessment and enforcement of linear time-invariant dynamical systems. The assessment algorithm combines the Half-size test with Graph Theory to identify passivity violations within a given system: each principal subsystem is individually assessed and a partial positive system is assembled whenever the positive subsystems form a chordal pattern. This algorithm is applicable both to measured data and to model parameters. The fact that data can now be assessed in this manner allows for incorrect measurements to be spotted at an early data acquisition stage, not to mention further insights into what is causing passivity violations for specific scalar measurements to be latter assembled into a MIMO measured matrix. When applied to a given model as identified by the Vector Fitting algorithm with a real-only state-space realization the PPMPAA finds a partial positive system whose sets of specified parameters can be retained and held fixed during the passivity enforcement process for they do not contribute to passivity violations.

The CBPE algorithm is a natural continuation to the PPMPAA to the extent that the partial system is completed into a full system. The parameters determined by the CBPE algorithm are those found by the PPMPAA to wreak passivity violations. Therefore, it comprises a passivity enforcement by parts in which only the offending parts (subsystems) are replaced. This constitutes a real paradigm shift in terms of passivity enforcement. The downside of this completion approach can be felt whenever the system abounds in anomalous passivity violations in a way that the partial positive system has very few specified entries: the approach is designed to thrive on systems requiring few completions since otherwise its convex formulation leads to macroscopic solution times.

The CDPE comes as a response to mitigate those macroscopic times by using chordal graphs in a different manner. While the preceeding algorithm (CBPE) uses chordality as an existence condition, the CDPE enforces chordality to gain efficiency by reducing the number of problem variables and imposing sparse structure. Chordality is imposed by requiring the Lyapunov Function to be banded positive-definite. Regrettably, this can sometimes cause the solution to depart considerably from the optimal convex solution depending on the number of lower and upper diagonals aggregating into the banded pattern. A correlation between violating subsystems and the allegedly optimal width has been sketched but remains unproved. The author is firmly of the belief that this research contributed to both applied and theoretical standpoints: new mathematical methods were brought to fruition and the case studies recorded in earlier chapters

how the assessment algorithm can greatly strengthen the identification of incorrect measurements as they are taken *in situ*.

The author envisages that there remains untapped potential and the research herein initiated could evolve toward different directions:

- Extend the decomposition theorem to the bounded-real matrices (aiming for scattering parameters);
- Combine the PPMPAA, the CBPE and CDPE into a single algorithm which would benefit from the precision obtained by the CBPE and the efficiency gained with the CDPE;
- Verify, improve and prove the correlation between the optimal bandwidth and the positive clique assessment;
- Bring uncertainty from the measurement setup into the model to formulate robust passivity assessment and enforcement algorithms.

Hopefully, this research opens up new possibilities in terms of new methods being brought to system theory. Sparsity for more general problems like SOCPs and SDPs is only relatively recent and currently a very active research area. Our modest contributions serve as an unequivocal indication that theses methods definitely deserve further consideration by the scientific community and related researchers.

BIBLIOGRAPHY

AGUIRRE, L. A. *Introdução à Identificação de Sistemas*. 3a.. ed. [S.l.]: Editora UFMG, 2007. Cited 2 times on pages 18 and 19.

AKÇAY, H.; ISLAM, S. M.; NINNESS, B. Identification of power transformer models from frequency response data: A case study. *Signal Processing*, v. 68, n. 3, p. 307–315, 1998. Cited on page 19.

ALLEN, J. C. *H-infinity Engineering and Amplifier Optimization*. 1. ed. [S.l.]: Birkhauser, 2004. Cited 4 times on pages 38, 41, 43, and 88.

AMOIRALIS, E. I.; TSILI, M. A.; KLADAS, A. G. Transformer design and optimization: A literature survey. *IEEE Transactions on Power Delivery*, v. 24, n. 4, p. 1999–2024, 2009. Cited on page 18.

ANDERSON, B. D. O. Algebraic description of bounded real matrices. *Electronics Letters*, v. 2, n. 12, p. 464–465, 1967. Cited on page 92.

ANDERSON, B. D. O. A system theory criterion for positive real matrices. *SIAM Journal on Control*, v. 5, n. 2, p. 171–182, 1967. Cited 2 times on pages 31 and 92.

ANDERSON, B. D. O.; VONGPANITLERD, S. *Network Analysis and Synthesis: A Modern Systems Theory Approach*. [S.l.]: Dover Publications, 2006. Cited 2 times on pages 31 and 55.

ANNAKKAGE, U. D. et al. Dynamic system equivalents: A survey of available techniques. *IEEE Transactions on Power Delivery*, v. 27, n. 1, p. 411–420, 2012. Cited on page 18.

ANTOULAS, A. C. *Approximation of Large-Scale Dynamical Systems*. [S.l.]: Society for Industrial and Applied Mathematics - SIAM, 2010. Cited 3 times on pages 20, 27, and 28.

BAMBERG, P.; STERNBERG, S. *A course in mathematics for students of physics*. [S.l.]: Cambridge University Press, 1990. v. 2. Cited on page 37.

BARRETT, W.; JOHNSON, C.; LOEWY, R. The real positive definite completion problem cycle completability. *Memoirs of the American Mathematical Society*, v. 122, n. 584, p. 1–69, 1996. Cited 2 times on pages 121 and 122.

BARRETT, W. W.; JOHNSON, C. R.; LOEWY, R. The real positive definite completion problem : cycle completability. *Memoirs of the American Mathematical Society*, v. 122, n. 4, 1996. Cited on page 121.

BECHARA, R. *Analysis of power transformer failures (in portuguese)*. Dissertação (Mestrado) — USP/Escola Politécnica, 2010. Cited on page 18.

BEN-TAL, A.; NEMIROVSKI, A. *Lectures on Modern Convex Optimization: Analysis, Algorithms, and Engineering Applications*. 1. ed. [S.l.]: Society for Industrial and Applied Mathematics, 2001. Cited on page 60.

BERTSEKAS, D. P. *Convex Optimization Theory*. 1. ed. [S.l.]: Athena Scientific, 2009. Cited 3 times on pages 60, 62, and 68.

BEYGI, A.; DOUNAVIS, A. An instrumental variable vector-fitting approach for noisy frequency responses. *IEEE Transactions on Microwave Theory and Techniques*, v. 60, n. 9, p. 2702–2712, 2012. Cited on page 49.

BOYD, S. P.; BALAKRISHNAN, V.; KABAMBA, P. A bisection method for computing the H_∞ norm of a transfer matrix and related problems. *Mathematics of Control, Signals, and Systems*, v. 2, p. 207–219, 1989. Cited 2 times on pages 93 and 95.

BOYD, S. P.; CHUA, L. O. On the passivity criterion for LTI n-ports. *Circuit Theory and Applications*, v. 10, p. 323–333, 1982. Cited 3 times on pages 41, 43, and 88.

BOYD, S. P. et al. *Linear Matrix Inequalities in System and Control Theory*. [S.l.]: SIAM, 1994. Cited 2 times on pages 33 and 92.

BOYD, S. P.; VANDENBERGHE, L. *Convex Optimization*. [S.l.]: Cambridge University Press, 2004. Cited 5 times on pages 60, 62, 86, 99, and 113.

BRUNE, O. W. H. O. *Synthesis of a finite two-terminal network whose driving-point impedance is a prescribed function of frequency*. Tese (Doutorado) — MIT - Department of Electrical Engineering, 1931. Cited 3 times on pages 19, 36, and 87.

CALAFIORE, G. C.; CHINEA, A.; GRIVET-TALOCIA, S. Subgradient techniques for passivity enforcement of linear device and interconnect macromodels. *IEEE Transactions Microwave Theory Techniques*, v. 60, n. 10, p. 2990–3003, 2012. Cited on page 23.

CALAFIORE, G. C.; GHAOUI, L. E. *Optimization Models*. 1. ed. [S.l.]: Cambridge University Press, 2014. Cited on page 60.

CARLIN, H. J. The scattering matrix in network theory. *IRE Transactions on Circuit Theory*, v. 3, n. 2, p. 88–97, 1956. Cited 2 times on pages 49 and 57.

CHEN, C.-T. *Linear System Theory and Design*. 3. ed. [S.l.]: Oxford University Press, 1999. Cited 3 times on pages 20, 27, and 109.

CHIARIELLO, A. G. et al. Numerical validation of a procedure for direct identification of passive linear multiport with convex programming. In: *14th IEEE Workshop on Signal Propagation on Interconnects*. [S.l.: s.n.], 2010. p. 141–144. Cited on page 117.

CHUA, L. O.; LAM, Y.-F. A theory of algebraic n-ports. *IEEE Transactions on Circuit Theory*, v. 20, n. 4, p. 370–382, 1973. Cited 3 times on pages 38, 41, and 43.

CIPPARRONE, F. A. M.; GUSTAVSEN, B.; SEMLYEN, A. Discussion of enforcing passivity for admittance matrices approximated by rational functions. *IEEE Transactions on Power Systems*, v. 16, n. 4, p. 954–955, 2001. Cited on page 106.

COELHO, C. P.; PHILLIPS, J.; SILVEIRA, L. M. A convex programming approach to positive real rational approximation. In: *Proceedings of International Conference on Computer Aided Design*. Santa Clara CA, USA: [s.n.], 2001. p. 245–251. Cited 2 times on pages 111 and 114.

COELHO, C. P.; PHILLIPS, J.; SILVEIRA, L. M. A convex programming approach for generating guaranteed passive approximations to tabulated frequency data. *IEEE Transactions on Computer Aided Design of Integrated Circuits and Systems*, v. 23, n. 2, p. 293–301, 2004. Cited 8 times on pages 20, 21, 22, 111, 112, 113, 114, and 117.

COXSON, G. E. The P-matrix problem is co-NP-complete. *Mathematical Programming*, v. 64, n. 64, p. 173–178, 1994. Cited on page 120.

CRAVO, G. Matrix completion problems. *Linear Algebra and its Applications*, v. 430, p. 2511–2540, 2009. Cited 2 times on pages 121 and 122.

CRAVO, G. A note on matrix completion problems. *Algebra Colloquium*, v. 19, p. 1179–1186, 2012. Cited on page 121.

CRAVO, G.; SILVA, F. C. Eigenvalues of matrices with several prescribed blocks ii. *Linear Algebra and its Applications*, v. 364, p. 81–89, 2003. Cited on page 120.

CURTAIN, R. F. Old and new perspectives on the positive-real lemma in systems and control theory. *Zeitschrift für Angewandte Mathematik und Mechanik*, v. 79, n. 9, p. 579–590, 1999. Cited on page 92.

DEO, N. *Graph Theory*. Dover edition. [S.l.]: Dover, 2016. Cited on page 70.

DESCHRIJVER, D.; DHAENE, T. Modified half-size test matrix for robust passivity assessment of S-parameter macromodels. *IEEE Microwave and Wireless Components Letters*, v. 19, n. 5, p. 263–265, 2009. Cited on page 96.

DESCHRIJVER, D.; DHAENE, T.; HAEGEMAN, B. Orthonormal vector fitting: A robust macromodeling tool for rational approximation of frequency domain responses. *IEEE Transactions on Advanced Packaging*, v. 30, n. 2, p. 216–225, 2007. Cited 2 times on pages 19 and 49.

DESCHRIJVER, D. et al. Macromodeling of multiport systems using a fast implementation of the vector fitting method. *IEEE Transactions on Microwave and Wireless Components Letters*, v. 18, n. 6, p. 383–385, 2008. Cited on page 52.

DESOER, C. A.; KUH, E. S. *Basic Circuit Theory*. International student edition. [S.l.]: McGraw-Hill, 1969. Cited on page 43.

DOETSCH, G. *Introduction to the Theory and Application of the Laplace Transformation*. [S.l.]: Springer, 1974. Cited on page 34.

FONIOK, J. P-matrix recognition is co-np-complete. *CoRR*, abs/0710.3519, 2007. Disponível em: <http://arxiv.org/abs/0710.3519>. Cited on page 120.

FUJISAWA, K. et al. Technical Report B-453, *User's manual for SparseCoLO: Conversion methods for sparse conic-form linear optimization problems.* 2009. Cited 3 times on pages 156, 157, and 161.

FUKUDA, M. et al. Exploiting sparsity in semidefinite programming via matrix completion i: General framework. *SIAM Journal on Optimization*, v. 11, p. 647–674, 2001. Cited on page 157.

GAWTHROP, P. J.; BEVAN, G. P. Bond-graph modeling. *IEEE Control Systems Magazine*, v. 27, n. 2, p. 24–45, 2007. Cited 2 times on pages 38 and 40.

GHAOUI, L. E.; NICULESCU, S.-I. *Advances in Linear Matrix Inequality Methods in Control*. [S.l.]: Johns Hopkins University Press, 2000. Cited on page 33.

GLUNT, W. et al. Positive definite completions and determinant maximization. *Linear Algebra and its Applications*, v. 288, p. 1–10, 1999. Cited on page 123.

GOLUB, G. H.; LOAN, C. F. V. *Matrix Computations*. 4. ed. [S.l.]: Johns Hopkins University Press, 2012. Cited 4 times on pages 90, 91, 95, and 150.

GRANT, M.; BOYD, S. Graph implementations for nonsmooth convex programs. In: BLONDEL, V.; BOYD, S.; KIMURA, H. (Ed.). *Recent Advances in Learning and Control*. [S.l.]: Springer-Verlag Limited, 2008, (Lecture Notes in Control and Information Sciences). p. 95–110. Cited 3 times on pages 114, 115, and 135.

GRIEWANK, A.; TOINT, P. L. On the existence of convex decompositions of partially separable functions. *Mathematical Programming Springer-Verlag*, v. 28, n. 1, p. 25–49, 1984. Cited on page 124.

GRIFFIN, K.; TSATSOMEROS, M. J. Principal minors, part I: A method for computing all the principal minors of a matrix. *Linear Algebra and its Applications*, v. 419, p. 107–124, 2006. Cited on page 120.

GRIFFIN, K.; TSATSOMEROS, M. J. Principal minors, part II: The principal minor assignment problem. *Linear Algebra and its Applications*, v. 419, p. 125–171, 2006. Cited on page 120.

GRIVET-TALOCIA, S. Passivity enforcement via perturbation of hamiltonian matrices. *IEEE Transactions on Circuits and Systems*, v. 51, n. 9, p. 1755–1769, 2004. Cited 8 times on pages 22, 93, 94, 95, 99, 108, 109, and 110.

GRIVET-TALOCIA, S. On passivity characterization of symmetric rational macromodels. *IEEE Transactions on Microwave Theory and Techniques*, v. 58, n. 5, p. 1238–1247, 2010. Cited on page 96.

GRIVET-TALOCIA, S. A perturbation scheme for passivity verification and enforcement of parameterized macromodels. *IEEE Transactions on Components, Packaging and Manufacturing Technology*, v. 7, n. 11, p. 1869–1881, 2017. Cited on page 23.

GRIVET-TALOCIA, S.; GUSTAVSEN, B. *Passive Macromodeling*. [S.l.]: John Wiley & Sons, 2016. Cited 4 times on pages 17, 18, 50, and 55.

GRIVET-TALOCIA, S.; UBOLLI, A. A comparative study of passivity enforcement schemes for linear lumped macromodels. *IEEE Transactions on Advanced Packaging*, v. 31, n. 4, p. 673–683, 2008. Cited 6 times on pages 22, 94, 101, 110, 114, and 135.

GRONE, R. et al. Positive definite completions of partial hermitian matrices. *Linear Algebra and its Applications*, v. 58, p. 109–124, 1984. Cited on page 123.

GUSTAVSEN, B. Computer code for rational approximation of frequency dependent admittance matrices. *IEEE Transactions on Power Delivery*, v. 17, n. 4, p. 1093–1098, 2002. Cited on page 102.

GUSTAVSEN, B. Frequency-dependent modeling of power transformers with ungrounded windings. *IEEE Transactions on Power Delivery*, v. 19, p. 1328–1334, 2004. Cited on page 44.

GUSTAVSEN, B. Wide band modeling of power transformers. *IEEE Transactions on Power Delivery*, v. 19, p. 414–422, 2004. Cited 2 times on pages 18 and 44.

GUSTAVSEN, B. Improving the pole relocating properties of vector fitting. *IEEE Transactions on Power Delivery*, v. 21, n. 3, p. 1587–1592, 2006. Cited on page 49.

GUSTAVSEN, B. Computer code for passivity enforcement of rational macromodels by residue perturbation. *IEEE Transactions on Advanced Packing*, v. 30, n. 2, p. 209–215, 2007. Cited 2 times on pages 102 and 106.

GUSTAVSEN, B. Fast passivity enforcement for pole-residue models by perturbation of residue matrix eigenvalues. *IEEE Transactions on Power Delivery*, v. 23, n. 4, p. 2278–2285, 2008. Cited on page 108.

GUSTAVSEN, B. Passivity enforcement of rational models via modal perturbation. *IEEE Transactions on Power Delivery*, v. 23, n. 2, p. 768–775, 2008. Cited 2 times on pages 107 and 117.

GUSTAVSEN, B. Study of transformer resonant overvoltages caused by cable-transformer high-frequency interaction. *IEEE Transactions on Power Delivery*, v. 25, n. 2, p. 770–779, 2010. Cited on page 19.

GUSTAVSEN, B. Removing insertion impedance effects from transformer admittance measurements. *IEEE Transactions on Power Delivery*, v. 27, n. 2, p. 1027–1029, 2012. Cited on page 44.

GUSTAVSEN, B. Rational modeling of multiport systems via a symmetry and passivity preserving mode-revealing transformation. *IEEE Transactions on Power Delivery*, v. 29, n. 1, p. 199–206, 2014. Cited on page 58.

GUSTAVSEN, B.; HEITZ, C. Modal vector fitting: A tool for generating rational models of high accuracy with arbitrary terminal conditions. *IEEE Transactions on Advanced Packing*, v. 31, n. 4, p. 664–672, 2008. Cited on page 107.

GUSTAVSEN, B.; SEMLYEN, A. Application of vector fitting to state equation representation of transformers for simulation of electromagnetic transients. *IEEE Transactions on Power Delivery*, v. 13, n. 3, p. 834–842, 1998. Cited on page 19.

GUSTAVSEN, B.; SEMLYEN, A. Rational approximation of frequency domain responses by vector fitting. *IEEE Transactions on Power Delivery*, v. 14, n. 3, p. 1052–1061, 1999. Cited 5 times on pages 19, 20, 49, 100, and 102.

GUSTAVSEN, B.; SEMLYEN, A. Enforcing passivity for admittance matrices approximated by rational functions. *IEEE Transactions on Power Systems*, v. 16, n. 1, p. 97–104, 2001. Cited 6 times on pages 20, 21, 22, 101, 102, and 106.

GUSTAVSEN, B.; SEMLYEN, A. A robust approach for system identification in the frequency domain. *IEEE Transactions on Power Delivery*, v. 19, n. 3, p. 1167–1173, 2004. Cited 5 times on pages 52, 98, 100, 106, and 108.

GUSTAVSEN, B.; SEMLYEN, A. Fast passivity assessment for s-parameter rational models via a half-size test matrix. *IEEE Transactions on Microwave Theory and Techniques*, v. 56, n. 12, p. 2701–2708, 2008. Cited 3 times on pages 96, 99, and 100.

GUSTAVSEN, B.; SEMLYEN, A. A half-size singularity test matrix for fast and reliable passivity assessment of rational models. *IEEE Transactions on Power Delivery*, v. 24, n. 1, p. 345–351, 2009. Cited 6 times on pages 52, 96, 97, 99, 100, and 106.

GUSTAVSEN, B.; SEMLYEN, A. On passivity tests for unsymmetrical models. *IEEE Transactions on Power Delivery*, v. 24, n. 3, p. 1739–1741, 2009. Cited on page 96.

GUSTAVSEN, B.; SILVA, H. M. J. D. Inclusion of rational models in an electromagnetic transients program: Y-parameters, z-parameters, s-parameters, transfer functions. *IEEE Transactions on Power Delivery*, v. 28, n. 2, p. 1164–1174, 2013. Cited 2 times on pages 57 and 58.

HENDRICKX, W.; DESCHRIJVER, D.; DHAENE, T. Some remarks on the vector fitting iteration. In: ____. *Progress in Industrial Mathematics at ECMI 2004*. [S.l.: s.n.], 2006. p. 134–139. Cited on page 49.

HINRICHSEN, D.; PRITCHARD, A. J. *Mathematical Systems Theory I: Modelling, State Space Analysis, Stability and Robustness*. 1. ed. [S.l.]: Springer, 2013. Cited on page 20.

HOLBROOK, J. G. *Laplace Transform for Electronic Engineers*. 2. ed. [S.l.]: Pergamon Press, 1966. Cited on page 34.

HORI, M. et al. Observation and analysis of incident surge voltage waveforms in substations by winter lightning. *IEEE Transactions on Power Delivery*, v. 22, n. 1, 2007. Cited on page 18.

HORN, R. A.; JOHNSON, C. R. *Matrix Analysis*. 2. ed. [S.l.]: Cambridge University Press, 2012. Cited 5 times on pages 43, 90, 91, 118, and 150.

HU, Y. et al. A guaranteed and efficient method to enforce passivity of frequency-dependent network equivalents. *IEEE Transactions on Power Systems*, v. 32, n. 3, p. 2455–2463, 2017. Cited on page 23.

HUELSMAN, L. P. *Circuits, Matrices and Linear Vector Spaces*. [S.l.]: Dover Publications Inc, 2011. Cited 6 times on pages 38, 45, 46, 47, 48, and 58.

IHLENFELD, L. P. R. K.; OLIVEIRA, G. H. C. On the optimality of passive and symmetric high-frequency n-terminal transformer models. *IEEE Transactions on Power Delivery*, v. 34, n. 1, p. 129–136, 2019. Cited 2 times on pages 22 and 56.

IHLENFELD, L. P. R. K. et al. Modelagem em larga faixa de frequencias de TP indutivos para análise de falhas devido a VFTO. In: ERIAC. [S.l.], 2019. p. 1–8. ISBN 978-85-906780-1-4. Cited on page 58.

IHLENFELD, L. P. R. K.; OLIVEIRA, G. H. C.; SANS, M. R. A data passivity-enforcement preprocessing approach to multiport system modeling. *IEEE Transactions on Power Delivery*, v. 31, n. 3, p. 1351–1359, 2016. Cited on page 21.

JOHNSON, C. R. *Matrix Theory and Applications*. [S.l.]: American Mathematical Society - SIAM, 1990. Cited on page 23.

JOHNSON, C. R.; WOLKOWICZ, H. An interior-point method for approximate positive semidefinite completions. *Computational Optimization and Applications*, v. 9, p. 175–190, 1998. Cited on page 123.

JURISIC, B. et al. Difficulties in high frequency transformer modeling. *Electric Power Systems Research*, v. 138, p. 25–32, 2016. Cited on page 18.

JWG-A2/C4.39, C. *Electrical Transient Interaction Between Transformers and the Power System. Part 1: Expertise and Part 2: Case Studies*. [S.l.]: Cigre, 2014. Cited 2 times on pages 18 and 21.

KAKIMURA, N. A direct proof for the matrix decomposition of chordal structured positive semidefinite matrices. *Linear Algebra and its Applications*, v. 433, p. 819–823, 2010. Cited on page 124.

KALMAN, R. E. *On a new characterization of linear passive systems*. Baltimore, 1964. Cited on page 92.

KASSIS, M. T. et al. Passive reduced order macromodeling based on loewner matrix interpolation. *IEEE Transactions on Microwave Theory and Techniques*, v. 64, n. 8, p. 2423 – 2432, 2016. Cited on page 23.

KATSOULEAS, G.; MAROULAS, J. The imbeddability for hermitian and normal matrices. *Linear Algebra and its Applications*, v. 439, p. 552–564, 2013. Cited on page 121.

KUO, F. F. *Network Analysis and Synthesis*. Wiley international edition. [S.l.]: John Wiley and Sons, 1966. Cited 4 times on pages 38, 41, 42, and 47.

KUROKAWA, K. Power waves and the scattering matrix. *IEEE Transactions on Microwave Theory*, v. 13, n. 2, p. 194–202, 1965. Cited on page 49.

LEE, S.-G.; SEOL, H.-G. A survey on the matrix completion problem. *Trends in Mathematics*, v. 4, n. 1, p. 38–43, 2001. Cited on page 123.

LJUNG, L. *System Identification: Theory for the user*. 2a.. ed. [S.l.]: Prentice Hall, 1999. Cited on page 19.

LJUNG, L. Perspectives on system identification. *ELSEVIER Annual Reviews in Control*, v. 34, n. 1, p. 199–206, 2010. Cited on page 18.

LOAN, C. F. V. The ubiquitous kronecker product. *Journal of Computational and Applied Mathematics*, v. 123, p. 85–100, 2000. Cited on page 110.

LUNDQUIST, M. E.; JOHNSON, C. R. Linearly constrained positive definite completions. *Linear Algebra and its Applications*, v. 150, p. 195–207, 1991. Cited on page 121.

MAESTRELLI, R. *Funções Ortonormais em Tempo Contínuo com Seleção ótima das Dinâmicas do Modelo na Identificação de Sistemas no Domínio da Frequência*. Dissertação (Mestrado) — Pontifícia Universidade Católica do Paraná, 2010. Cited on page 19.

MAESTRELLI, R.; OLIVEIRA, G. H. C. Método para identificação de sistemas contínuos mal amortecidos no domínio da frequência usando funções ortonormais. In: *17 Congresso Brasileiro de Automática*. [S.l.: s.n.], 2010. Cited on page 19.

MAHANTA, P. K.; YAMIN, N.; ZADEHGOL, A. Passivity verification and enforcement a review paper. *International Journal of Numerical Modelling*, p. 1–16, 2017. Cited on page 23.

MAHMOOD, Z. et al. Efficient localization methods for passivity enforcement of linear dynamical models. *IEEE Transactions on Computer-aided Design of Integrated Circuits and Systems*, v. 33, n. 09, p. 1328–1341, 2014. Cited on page 23.

MAVADDAT, R. *Network Scattering Parameters*. [S.l.]: World Scientific Publishing Company, 1996. Cited on page 58.

MEYER, C. D. *Matrix analysis and applied linear algebra*. [S.l.]: SIAM, 2000. Cited 3 times on pages 91, 118, and 150.

MORALES, J. et al. Pole-selective residue perturbation technique for passivity enforcement of fdnes. *IEEE Transactions on Power Delivery*, v. 33, n. 6, p. 2746–2754, 2018. Cited on page 23.

NESTEROV, Y.; NEMEROVSKI, A. *Interior-point polynomial algorithms in convex programming*. 1. ed. [S.l.]: Society for industrial and applied mathematics, 1994. Cited 2 times on pages 60 and 68.

NEWCOMB, R. W. *Linear Multiport Synthesis*. [S.l.]: McGraw-Hill, 1966. Cited on page 38.

OLIVEIRA, G. H. C.; IHLENFELD, L. P. R. K.; RODRIGUES, L. F. M. Sobre o uso de parâmetros S para aprimorar modelos de TP indutivos presentes em GIS. In: *XXV Seminário Nacional de Produção e Transmissão de Energia Elétrica*. [S.l.: s.n.], 2019. Cited on page 58.

OLIVEIRA, G. H. C.; MAESTRELLI, R.; ROCHA, A. C. O. An application of orthonormal basis functions in power transformers wide band modeling. In: *7th IEEE International Conference on Control and Automation*. [S.l.: s.n.], 2009. Cited on page 19.

OLIVEIRA, G. H. C.; MITCHELL, S. D. Comparison of black-box modeling approaches for transient analysis: A gis case study. In: *Proceeding of the International Conference on Power System Transients*. Vancouver, CA: [s.n.], 2013. Cited on page 19.

OLIVEIRA, G. H. C.; RODIER, C.; IHLENFELD, L. P. R. K. LMI-based method for estimating passive black-box models in power systems transient analysis. *IEEE Transactions on Power Delivery*, 2016. Cited 3 times on pages 22, 112, and 114.

PORDANJANI, I. R. et al. A method to construct equivalent circuit model from frequency responses with guaranteed passivity. *IEEE Transactions on Power Delivery*, v. 26, n. 1, p. 400–409, 2011. Cited on page 23.

PORDANJANI, I. R.; MAZIN, H. E.; XU, W. A novel genetic programming approach for frequency-dependent modeling. *IEEE Transactions on Evolutionary Computation*, v. 17, n. 3, p. 353–367, 2013. Cited on page 23.

QUEIRO, J. F.; DUARTE, A. L. Imbedding conditions for normal matrices. *Linear Algebra and its Applications*, v. 430, p. 1806–1811, 2009. Cited on page 121.

RAGHUNATHAN, A. U.; KNYAZEV, A. V. Degeneracy in maximal clique decomposition for semidefinite programs. In: *American Control Conference (ACC)*. Boston, MA: [s.n.], 2016. p. 5605–5611. Cited on page 161.

RAISBECK, G. A definition of passive linear networks in terms of time and energy. *Journal of Applied Physics*, v. 25, n. 12, p. 1510–1514, 1954. Cited on page 87.

REGINATO, B. C. *Ambiente Computacional para Identificação no Domínio do Tempo e da Frequência usando Bases de Funções Ortonormais*. Dissertação (Mestrado) — Pontifícia Universidade Católica do Paraná, 2008. Cited on page 19.

REGINATO, B. C.; OLIVEIRA, G. H. C. On selecting the mimo generalized orthonormal basis functions poles by using particle swarm optimization. In: *Proc. of the European Control Conference*. [S.l.: s.n.], 2007. p. 1–6. Cited on page 19.

REGINATO, B. C.; OLIVEIRA, G. H. C. Algoritmo híbrido para seleção de pólos em modelos formados por bases de funções ortonormais generalizadas. In: *17 Congresso Brasileiro de Automática*. [S.l.: s.n.], 2008. Cited on page 19.

RESEARCH, I. C. *CVX: Matlab Software for Disciplined Convex Programming, version 2.0*. 2012. Http://cvxr.com/cvx. Cited 3 times on pages 114, 115, and 135.

SANATHANN, C. K.; KOERNER, J. Transfer function synthesis as a ratio of two complex polynomials. *IEEE Transactions Automatic Control*, v. 9, n. 1, p. 56–58, 1963. Cited 2 times on pages 19 and 49.

SANS, M. R. *Análise de Métodos de Medição da Matriz Admitância em Transformadores de Potência*. Dissertação (Mestrado) — UFPR/Electrical Engineering Department, 2013. Cited on page 44.

SANS, M. R.; OLIVEIRA, G. H. C.; JUNIOR, J. A. T. Sobre métodos de medição da matriz de admitância para simulação de transitórios elétricos envolvendo transformadores de potência. In: *XIX Congresso Brasileiro de Automática*. [S.l.: s.n.], 2012. Cited on page 44.

SARASWAT, D.; ACHAR, R.; NAKHLA, M. S. A fast algorithm and practical considerations for passive macromodeling of measured/simulated data. *IEEE Transactions on Advanced Packaging*, v. 27, n. 1, p. 57–70, 2004. Cited 2 times on pages 22 and 101.

SCHUMACHER, R.; OLIVEIRA, G. H. C. An optimal vector fitting method for estimating frequency-dependent network equivalents in power systems. *Electric Power Systems Research*, v. 150, p. 96–104, 2017. Cited 2 times on pages 19 and 49.

SCHUMACHER, R.; OLIVEIRA, G. H. C. A unifying method to construct rational basis functions for linear and nonlinear systems. *Circuits, Systems, and Signal Processing*, v. 37, p. 2394–2412, 2018. Cited on page 50.

SHIPP, D. D. et al. Transformer failure due to circuit-breaker-induced switching transients. *IEEE Transactions on Industry Applications*, v. 47, n. 2, p. 707–717, 2011. Cited on page 18.

SMITH, R. L. The positive definite completion problem revisited. *Linear Algebra and its Applications*, v. 429, p. 1442–1452, 2008. Cited on page 123.

SPIEGEL, M. R. *Laplace Transforms*. [S.l.]: McGraw-Hill, 1965. Cited on page 34.

STURM, J. F. Using sedumi 1.02, a matlab toolbox for optimization over symmetric cones. *Optimization Methods and Software*, p. 625–653, 1999. Cited 3 times on pages 114, 135, and 157.

SU, D. et al. Passivity enforced circuit model of frequency-domain responses with source elements. *International Journal of Numerical Modelling*, p. 1–11, 2016. Cited on page 23.

TARJAN, R. E.; YANNAKAKIS, M. Simple linear-time algorithms to test chordality of graphs, test acyclicity of hypergraphs, and selectively reduce acyclic hypergraphs. *SIAM Journal on Computing*, v. 13, n. 3, p. 566–579, 1963. Cited on page 80.

THOMPSON, R. C. Principal submatrices III: Linear inequalities. *Journal of Research of the Nationol Bureau of Standards*, v. 72, n. 1, p. 7–22, 1968. Cited on page 121.

THOMPSON, R. C. Principal submatrices V: Some results concerning principal submatrices of arbitrary matrices. *Journal of Research of the Nationol Bureau of Standards*, n. 2, p. 115–125, 1968. Cited on page 121.

THOMPSON, R. C. Principal submatrices VII: Further results concerning matrices with equal principal minors. *Journal of Research of the Nationol Bureau of Standards*, v. 72, n. 4, p. 249–252, 1968. Cited on page 121.

THOMPSON, R. C. Principal submatrices IV: Principal submatrices iv. on the independence of the eigenvalues of different principal submatrices. *Linear Algebra and its Applications*, n. 2, p. 355–374, 1969. Cited on page 121.

THOMPSON, R. C. Principal submatrices VI: On the independence of the eigenvalues of different principal submatrices. *Linear Algebra and its Applications*, n. 2, p. 375–379, 1969. Cited on page 121.

THOMPSON, R. C. Principal submatrices IX: Interlacing inequalities for singular values of submatrices. *Linear Algebra and its Applications*, n. 5, p. 1–12, 1972. Cited on page 121.

THOMPSON, R. C. Principal submatrices VIII: Principal sections of a pair of forms. *Rocky Mountain Journal of Mathematics*, v. 2, n. 1, p. 97–110, 1972. Cited on page 121.

THOMPSON, R. C. Prlnclpal minors of complex symmetric and skew matrices. *Linear Algebra and its Applications*, n. 28, p. 249–255, 1972. Cited on page 121.

THOMPSON, R. C.; MCENTEGGERT, P. Principal submatrices II: The upper and lower quadratic inequalities. *Linear Algebra and its Applications*, n. 1, p. 211–243, 1968. Cited 2 times on pages 120 and 121.

TOMMASI, L. D.; DESCHRIJVER, D.; DHAENE, T. Single-input-single-output-passive macromodeling via positive fractions vector fitting. *Twelfth IEEE Workshop on Signal Propagation on Interconnects*, 2008. Cited on page 114.

TOMMASI, L. D. et al. An algorithm for direct identification of passive transfer matrices with positive real fractions via convex programming. *International Journal of Numerical Modelling: Electronic Networks, Devices and Fields*, v. 24, n. 10, p. 375–386, 2011. Cited 3 times on pages 22, 114, and 115.

TOMMASI, L. D.; MAGNANI, A.; MAGISTRIS, M. de. Advancements in the identification of passive RC networks for compact modeling of thermal effects in electronic devices and systems. *International Journal of Numerical Modelling*, p. 1–13, 2017. Cited on page 23.

TRANSFORMERS-SWITCHGEAR-COMMITTEE. *IEEE Guide to Describe the Occurrence and Mitigation of Switching Transients Induced by Transformers, Switching Device, and System Interaction*. [S.l.]: IEEE Power & Energy Society, 2010. Cited on page 21.

TRIVERIO, P. et al. Stability, causality, and passivity in electrical interconnect models. *IEEE Transactions on Advanced Packaging*, v. 30, n. 4, p. 795–808, 2007. Cited 6 times on pages 20, 21, 27, 88, 89, and 90.

TRUDEAU, R. J. *Introduction to Graph Theory*. Dover edition. [S.l.]: Dover, 1993. Cited on page 70.

TSATSOMEROS, M. J.; LI, L. A recursive test for p-matrices. *BIT*, v. 40, p. 404–408, 2000. Cited on page 120.

VANDENBERGHE, L.; ANDERSEN, M. S. *Chordal Graphs and Semidefinite Optimization*. [S.l.]: Now Publishers, 2015. Cited 3 times on pages 23, 70, and 155.

VARRICCHIO, S. L. et al. Transient short-circuit calculations using time shifts and rational models. In: *VII SBSE - Simpósio Brasilerio de Sistemas Elétricos*. [S.l.: s.n.], 2018. Cited on page 46.

VéLIZ, F. C.; VARRICCHIO, S. L.; JR., S. G. Equivalentes dinâmicos para estudos de harmônicos usando análise modal. In: *X SEPOPE - Simpósio de Especialistas em Planejamento da Operação e Expansão Elétrica*. [S.l.: s.n.], 2006. Cited on page 46.

WILLEMS, J. C. Willems least squares stationary optimal control and the algebraic riccati equation. *IEEE Transactions on Automatic Control*, v. 16, n. 6, p. 621–634, 1971. Cited 3 times on pages 20, 30, and 35.

WILLEMS, J. C. Dissipative dynamical systems : Part I general theory. *Archive for Rational Mechanics and Analysis*, v. 45, p. 321–351, 1972. Cited 4 times on pages 20, 30, 67, and 87.

WILLEMS, J. C. Dissipative dynamical systems : Part II linear systems with quadratic supply rates. *Archive for Rational Mechanics and Analysis*, v. 45, p. 352–393, 1972. Cited 2 times on pages 20 and 30.

WILLEMS, J. C. The behavioral approach to open and interconnected systems. *IEEE Control Systems Magazine*, v. 27, n. 6, p. 46–99, 2007. Cited 2 times on pages 20 and 30.

WILLEMS, J. C. Dissipative dynamical systems. *European Journal of Control*, v. 13, p. 134–51, 2007. Cited on page 30.

WILLEMS, J. C. *Introduction to Mathematical Systems Theory: A Behavioral Approach*. 2. ed. [S.l.]: Springer, 2008. Cited 3 times on pages 20, 27, and 30.

WILLEMS, J. C. The behavior of resistive circuits. In: *Joint 48th IEEE Conference on Decision and Control and 28th Chinese Control Conference*. Shanghai, China: [s.n.], 2009. p. 8124–8129. Cited on page 38.

WILLEMS, J. C. Terminals and ports. In: *Proceedings of 2010 IEEE International Symposium on Circuits and Systems*. Paris, France: [s.n.], 2010. p. 8–26. Cited 3 times on pages 38, 39, and 41.

WILLEMS, J. C.; TAKABA, K. Dissipativity and stability of interconnections. *International Journal Of Robust And Nonlinear Control*, n. 17, p. 563–586, 2007. Cited on page 30.

WOHLERS, M. R. *Lumped and distributed passive networks*. 1. ed. [S.l.]: Academic Press, 1969. Cited 4 times on pages 41, 43, 88, and 89.

WOLKOWICZ, H.; ANJOS, M. F. Semidefnite programming for discrete optimization and matrix completion problems. *Discrete Applied Mathematics*, v. 123, p. 513–577, 2002. Cited on page 123.

WONG, N.; ZHANG, Z. Discussion of a half-size singularity test matrix for fast and reliable passivity assessment of rational models. *IEEE Transactions on Power Delivery*, v. 25, n. 2, p. 1212–1213, 2010. Cited 2 times on pages 96 and 100.

XIAO, Y. Q.; KABIR, M.; KHAZAKA, R. Passivity enforcement using incomplete complex frequency hopping. In: *IEEE 25th Conference on Electrical Performance Of Electronic Packaging And Systems*. San Diego, CA, USA: [s.n.], 2016. Cited on page 23.

YAMIN, N.; ZADEHGOL, A. Verification and enforcement of passivity through direct minimal modification of equivalent circuits. In: *IEEE Proc. of the 2016 International Symposium on Electromagnetic Compatibility*. Wroclaw, Poland: [s.n.], 2016. Cited on page 23.

YANNAKAKIS, M. Computing the minimum fill-in is np-complete. *SIAM Journal on Algebraic Discrete Methods*, v. 2, n. 1, p. 77–79, 1981. Cited on page 80.

YOULA, L. J. C. D. C.; CARLIN, H. J. Bounded real scattering matrices and the foundations of linear passive network theory. *IRE Transactions on Circuit Theory*, v. 12, p. 102–124, 1959. Cited on page 88.

ZANCO, A. et al. Enforcing passivity of parameterized lti macromodels via hamiltonian-driven multivariate adaptive sampling (early access). *IEEE Transactions on Computer-Aided Design of Integrated Circuits and Systems*, 2018. Cited on page 23.

ZEMANIAN, A. H. An n-port realizability theory based on the theory of distributions. *IEEE Transactions on Circuit Theory*, p. 265–274, 1963. Cited on page 88.

ZHONGYUAN, Z.; FANGCHENG, L.; GUISHU, L. High-frequency circuit model of a potential transformer for the very fast transient simulation in GIS. *IEEE Transactions on Power Delivery*, v. 23, n. 4, p. 1995–1999, 2013. Cited on page 57.